

MODERN DEVELOPMENT OF MAGNETIC RESONANCE

abstracts

2018

KAZAN * RUSSIA





MODERN DEVELOPMENT OF MAGNETIC RESONANCE

ABSTRACTS OF THE
INTERNATIONAL CONFERENCE

Editor:
KEV M. SALIKHOV

KAZAN, SEPTEMBER 24–28, 2018

This work is subject to copyright.

All rights are reserved, whether the whole or part of the material is concerned, specifically those of translation, reprinting, re-use of illustrations, broadcasting, reproduction by photocopying machines or similar means, and storage in data banks.

© 2018 Zavoisky Physical-Technical Institute, FRC Kazan Scientific Center of RAS, Kazan

© 2018 Igor A. Aksenov, graphic design

Printed in Russian Federation

Published by Zavoisky Physical-Technical Institute, FRC Kazan Scientific Center of RAS, Kazan

www.kfti.knc.ru

CHAIRMEN

Alexey A. Kalachev

Kev M. Salikhov

PROGRAM COMMITTEE

Kev Salikhov, chairman (Russia)

Albert Aganov (Russia)

Vadim Atsarkin (Russia)

Pavel Baranov (Russia)

Marina Bennati (Germany)

Bernhard Blümich (Germany)

Michael Bowman (USA)

Sabine Van Doorslaer (Belgium)

Rushana Eremina (Russia)

Jack Freed (USA)

Ilgiz Garifullin (Russia)

Alexey Kalachev (Russia)

Walter Kockenberger (Great Britain)

Wolfgang Lubitz (Germany)

Klaus Möbius (Germany)

Hitoshi Ohta (Japan)

Igor Ovchinnikov (Russia)

Vladimir Skirda (Russia)

Murat Tagirov (Russia)

Takeji Takui (Japan)

Valery Tarasov (Russia)

Yurii Tsvetkov (Russia)

Violeta Voronkova (Russia)

LOCAL ORGANIZING COMMITTEE

Kalachev A.A., chairman	Kupriyanova O.O.
Mamin R.F., vice-chairman	Kurkina N.G.
Voronkova V.K., scientific secretary	Latypov V.A.
Akhmin S.M.	Mosina L.V.
Falin M.L.	Oladoshkin Yu.V.
Galeev R.T.	Salikhov K.M.
Gavrilova T.P.	Siafetdinova A.Z.
Goleneva V.M.	Tarasov V.F.
Gubaidulina A.Z.	Yanduganova O.B.
Guseva R.R.	Yurtaeva S.V.

SCIENTIFIC SECRETARIAT

Violeta K. Voronkova
Laila V. Mosina
Vlad A. Latypov

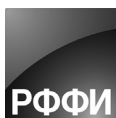
The conference is organized under the auspices of the AMPERE Society

ORGANIZERS

Zavoisky Physical-Technical Institute, FRC Kazan Scientific Center of RAS
The Academy of Sciences of the Republic of Tatarstan
Kazan Federal University

SUPPORTED BY

The Government of the Republic of Tatarstan
The Russian Foundation for Basic Research, no. 18-02-20117
Bruker BioSpin
ADANI Ltd.
PROMENERGOLAB Ltd.



ADANI
from ideas to solutions



CONTENTS

ZAVOISKY AWARD LECTURE

Solar Fuels: Nature's Approach

R. D. Britt

2

PLENARY LECTURES

ESR in Strongly Correlated Topological Insulator SmB_6 :

Built-in Mechanism of Time Reversal Symmetry

Breaking and Anomalous Spin Relaxation

S. V. Demishev, M. I. Gilmanov, A. N. Samarin, A. V. Semeno,

N. E. Sluchanko, N. A. Samarin, A. V. Bogach, N. Yu. Shitsevalova,

V. B. Filipov, V. V. Glushkov

4

Resolving Protein – Paramagnetic Intermediate Interactions

by Two-Dimensional Pulsed EPR Spectroscopy

S. A. Dikanov

6

High-Field EPR Studies of Water-Protein Hydrogen Bond

Interactions and Their Role For Biological Function

K. Möbius

7

Studying Isotopically Purified Rare-Earth Doped Crystals

for Raman Quantum Memories

A. A. Kalachev

8

Development and Application of THz ESR in Kobe University

S. Okubo, Y. Kitahara, S. Ikeda, S. Hara, T. Sakurai, H. Ohta,

D. Yoshizawa, M. Hagiwara, F. Kimura, T. Kimura, Y. Sakurai,

K. Nawa, Y. Okamoto, Z. Hiroi

9

Pseudo Jahn-Teller Effect in Spin-Orbit Entangled Mott Insulators

G. Khaliullin

11

Biological Hydrogen Conversion Studied by EPR and NMR

Techniques

W. Lubitz

12

Structure and Dynamics of Micro- and Macromolecules by NMR

Ch. Griesinger

14

Optical Orientation of Magnetic Polarons in Diluted Magnetic

Semiconductors

Yu. G. Kusrayev

15

Light-Induced Nuclear Hyperpolarization as a Sensitive Tool for Detection of Illusive Radicals of Biomolecules <i>A. Yurkovskaya, O. Morozova, A. Kiryutin, H.-M. Vieth, R. Z. Sagdeev, K. Ivanov</i>	17
 SECTION 1 SPIN-BASED INFORMATION PROCESSING	
Cross-Relaxation Magnetometry in Diamond NV-Centers with Polycrystalline Samples <i>R. A. Akhmedzhanov, L. A. Gushchin, N. A. Nizov, V. A. Nizov, D. A. Sobgayda, I. V. Zelensky</i>	20
Investigation of Neodymium Doped YVO ₄ by EPR Method <i>R. M. Eremina, I.V. Yatsyk, V. F. Tarasov, K. B. Konov, Y. D. Zavartsev, S. A. Kutovoi, R. F. Likero</i>	21
EPR Study of the Neutral Germanium-Vacancy Center in Diamond <i>A. Komarovskikh, V. Nadolinny, Y. Palyanov, I. Kupriyanov</i>	23
 SECTION 2 THEORY OF MAGNETIC RESONANCE	
Experimental and Theoretical Investigations of Multiple-Quantum NMR Coherences in One-Dimensional Systems <i>G. Bochkina, E. Fel'dman, I. Lazarev, S. Vasil'ev, V. Volkov</i>	26
Low Symmetry Orienting Potentials and Efficient Computation of ESR Line Shapes <i>K. A. Earle, T. Broderick</i>	27
Hybrid Quantum-Classical Method for Simulating High-Temperature Dynamics of Nuclear Spins in Solids <i>B. V. Fine</i>	28
 SECTION 3 CHEMICAL AND BIOLOGICAL SYSTEMS	
Nitroxides in Cotton and Cellulose. Physicochemistry and Technology. 42 Years of History <i>G. Likhtenshtein</i>	30
Trehalose Effect on the Forward and Backward Electron Transfer in Photosystem I <i>V. Kurashov, G. E. Milanovsky, M. Gorka, D. A. Cherepanov, J. H. Golbeck, A. Yu. Semenov</i>	31
New Methods in Singlet-State NMR <i>B. A. Rodin, K. F. Sheberstov, A. S. Kiryutin, A. V. Yurkovskaya, K. L. Ivanov</i>	32

Triptyl Biradicals in Solution: Conformations and Dynamics <i>M. K. Bowman, B. Fowler, M. Lockart, J. A. Lecaroz, A. G. Maryasov, A. G. Matveeva, V. M. Tormyshev</i>	33
EPR Probe-Based Approach for Acid Base Characterization of Mesoporous Silicas with Different Functionalities <i>E. Kovaleva, L. Molochnikov, D. Tamasova, D. Antonov</i>	34
EPR Studies of the Reactive Oxygen Species on Powder TiO ₂ <i>R. I. Samoilova</i>	37
ESEEM Observation and Localization of Bound Deuterated Substrate Histidine-d5 in Spin Labeled ABC Transporter HisQMP ₂ <i>N. Isaev, J. Heuveling, N. Ivanisenko, E. Schneider, H.-J. Steinhoff</i>	38
 SECTION 4 MOLECULAR MAGNETS AND LIQUID CRYSTALS	
Experimental Strategies for ¹³ C- ¹⁵ N Dipolar Spectroscopy in Liquid Crystals with Natural Isotopic Abundance <i>S. V. Dvinskikh</i>	42
 SECTION 5 STRONGLY CORRELATED ELECTRON SYSTEMS	
Magnetic Quantum Oscillations in Doped Antiferromagnetic Insulators <i>V. V. Kabanov</i>	44
Coherent Spin Dynamics of Solitons in the Organic Spin Chain Compounds (<i>o</i> -DMTTF) ₂ X (X = Cl, Br) <i>J. Zeisner, O. Pilone, H. Vezin, O. Jeannin, M. Fourmigué, B. Büchner, V. Kataev, S. Bertaina</i>	45
Spin Dynamics in the System with Honeycomb Lattice with Defects and Frustration Probed by Nuclear Magnetic Resonance Technique <i>E. Vavilova, M. Iakovleva, T. Salikhov, H.-J. Grafe, E. Zvereva, V. Nalbandyan, A. Vasiliev, A. Möller, B. Büchner, V. Kataev</i>	46
New State of Matter <i>V. R. Shaginyan</i>	47
Microwave Absorption Study of Charge Density Waves in La _{2-x} Sr _x CuO ₄ Crystals <i>I. Gimazov, Yu. Talanov, T. Adachi</i>	48
Anomalous Features of Antiferromagnetic Resonance in GdB ₆ <i>A. V. Semeno, M. I. Gilmanov, N. E. Sluchanko, N. Yu. Shitsevalova, V. B. Filipov, S. V. Demishev</i>	50

SECTION 6
MODERN METHODS OF MAGNETIC
RESONANCE

- X band CW EPR Studies of Chemical Reactions of Relevance
to Renewable Fuels
R. D. Britt 52
- Peculiar Features of the Spectrum Saturation Effect
When the Spectral Diffusion Operates
*K. M. Salikhov, M. M. Bakirov, B. Bales, R. T. Galeev,
I. T. Khairuzhdinov* 53
- Kinetics of the Polarization Transfer in the Disordered Spin System
 ^8Li - ^6Li of LiF Single Crystal
A. D. Gulko, F. S. Dzheparov, D. V. Lvov, A. N. Tyulyusov 54

SECTION 7
LOW-DIMENSIONAL SYSTEMS AND NANO-SYSTEMS

- High-Frequency Magnetic Resonance and Cross-Relaxation Effects
in Rare Earth Doped YAG
N. G. Romanov, R. A. Babunts, A. G. Badalyan, P. G. Baranov 56
- ESR Study of a Spin Ladder Magnet with Defects
*V. Glazkov, Y. Krasnikova, A. Pomomaryov, S. Zvyagin,
D. Schmidiger, K. Povarov, S. Galeski, A. Zheludev* 58
- Microwave Dielectric Anomaly in $S = 1$ Quantum Antiferromagnet
at Spin Gap Closing
*A. I. Smirnov, T. A. Soldatov, K. Yu. Povarov, E. Wulf, A. Mannig,
A. Zheludev* 60
- Electron Spin Resonance in 2D Systems Formed
in [001] AlAs Quantum Wells
*A. V. Shchepetilnikov, D. D. Frolov, Yu. A. Nefyodov, I. V. Kukushkin,
L. Tiemann, C. Reichl, W. Dietsche, W. Wegscheider* 61
- Magnetic Resonance Force Spectroscopy of Permalloy Microstrips
E. Skorokhodov, M. Sapozhnikov, R. Gorev, V. Mironov 62
- Defining the Interlayer Interaction in Magnetic Multilayer Structures
on the Base of the FMR Peaks Asymmetry
*O. G. Udalov, E. S. Demidov, S. N. Vdovichev, N. S. Gusev,
S. A. Gusev, V. V. Rogov, D. A. Tatarsky, I. S. Beloborodov,
O. L. Ermolaeva, A. A. Fraerman* 63

SECTION 8

PERSPECTIVE OF MAGNETIC RESONANCE IN
SCIENCE AND SPIN-TECHNOLOGY

- In situ* Irradiation in NMR, Some Concepts and Applications
G. Gescheidt 66
- Excited Coherent Quantum States
Yu. M. Bunkov 67
- Magnetic Moments in Topological Insulators Studied by EPR
V. Sakhin, A. Kiyamov, E. Kukovitsky, N. Garifyanov, R. Khasanov, Yu. Talanov, G. Teitel'baum 69

SECTION 9

ELECTRON SPIN BASED METHODS FOR ELECTRONIC AND
SPATIAL STRUCTURE DETERMINATION IN PHYSICS,
CHEMISTRY AND BIOLOGY

- Cu^{2+} -Ion as an ESR Probe of Protein Structure
S. K. Saxena 72
- Analytical Solution of the PELDOR Inverse Problem
Using the Integral Mellin Transform
A. G. Matveeva, V. M. Nekrasov, A. G. Maryasov 73
- Effective Method of Level Anti-Crossing Spectra
of NV Centers in Diamond Calculation
S. V. Anishchik, K. L. Ivanov 75
- Interaction of Native Protons with the Intrinsic Stable
Radicals in Crude Oil as Revealed by ENDOR and
DNP Measurements
M. Gafurov, B. Gizatullin, A. Rodionov, G. Mamin, C. Mattea, S. Stapf, S. Orlinskii 79
- Microwave-Assisted Cross-Polarization of Nuclear Spin Ensembles
from Optically-Pumped Nitrogen-Vacancy Centers
in Diamond
F. Shagieva, S. Zaiser, P. Neumann, D. B. R. Dasari, R. Stöhr, A. Denisenko, R. Reuter, C. A. Meriles, J. Wrachtrup 80

SECTION 10

OTHER APPLICATIONS OF MAGNETIC
RESONANCE

- Ionic and Molecular Transport in Solid Electrolytes
on Magnetic Resonance Data
V. I. Volkov 82

Electrodynamics of Superconductor/Ferromagnet Hybrids <i>S. V. Mironov</i>	84
Applications of Magnetic Resonance and Microwave Techniques for Identification of Liquid Materials <i>B. Z. Rameev</i>	85
Magnetic Resonance Study of BaAg ₂ Cu[VO ₄] ₂ Quantum Magnet <i>Y. Krupskaya, M. Schäpers, A. U. B. Wolter, H.-J. Grafe, E. Vavilova, A. Möller, B. Büchner, V. Kataev</i>	86
NMR Investigation of ¹⁴ N Quadrupole Coupling Interactions in Liquids <i>G. V. Mozzhukhin, G. S. Kupriyanova, A. Maraşlı, S. Mamadazizov, B. Z. Rameev</i>	87
Ferromagnet/Superconductor Hybridization for Magnonic Applications <i>I. A. Golovchanskiy, N. N. Abramov, V. S. Stolyarov, V. V. Bolginov, V. V. Ryazanov, A. A. Golubov, A. V. Ustinov</i>	89
EPR of Gd ³⁺ Centers in Pb _{1-x} Gd _x S Narrow Gap Semiconductor Crystals: Observation of “Reversed” Dyson Profiles of the EPR Lines <i>V. A. Ulanov, I. V. Yatsyk, R. R. Zainullin, A. M. Sinicin</i>	92
Spectral Hole Burning Spectroscopy of Silicon Vacancy-Related Centers in SiC <i>V. Soltamov, C. Kasper, G. V. Astakhov, S. A. Tarasenko, A. V. Poshakinskiy, A. N. Anisimov, P. G. Baranov, V. Dyakonov</i>	94
 SECTION 11 MEDICAL PHYSICS	
Interaction of Statins with Different Model Membranes Studied by NMR Spectroscopy <i>L. Galiullina, G. Musabirova, A. Aganov, V. Klochkov, H. A. Scheidt, D. Huster</i>	96
Spectra Convolution for Quantitative Analysis in EPR Spectroscopy <i>S. V. Kuzin, N. A. Chumakova, E. N. Golubeva, A. A. Korotkevich</i>	97
Living Systems Can Produce Magnetic Iron Oxide Crystals. EPR Spectroscopy Data <i>S. Yurtaeva</i>	98

POSTERS

NMR Investigation of Sodium Gluconate <i>M. M. Akhmetov, G. G. Gumarov, V. Yu. Petukhov, M. Yu. Volkov</i>	102
³ He NMR in Contact with Nanoparticles <i>E. M. Alakshin, E. I. Kondratyeva, V. V. Kuzmin, K. R. Safullin, A. A. Stanislavovas, A. V. Savinkov, A. V. Klochkov, M. S. Tagirov</i>	104
Low-Frequency RYDMR in Mechanical Properties of Crystals <i>V. I. Alshits, E. V. Darinskaya, M. V. Koldaeva, E. A. Petrzhik</i>	105
EPR Spectra in CaF ₂ Crystals Doped with CeO ₂ <i>L. K. Aminov, I. N. Kurkin, A. V. Lovchev, R. M. Rakhmatullin</i>	107
Influence of Magnetic Field on the Luminescence from X-irradiated Diamonds <i>S. V. Anishchik, V. I. Borovkov, A. R. Melnikov, V. G. Vins, D. G. Bagryantsev, A. P. Yelisseyev</i>	109
The Application of the Clinical MR Scanner for Multinuclear Research <i>N. V. Anisimov, A. G. Agafonnikova</i>	111
NMR Study of Magnetic Properties of New Triangle-Lattice Compound A ₂ MnTeO ₆ <i>E. Anisimova, D. Gafurov, G. Raganyan, E. Zvereva, V. Nalbandyan, A. Vasiliev, E. Vavilova</i>	113
CW Saturation of Nitroxyl Radicals in Liquids <i>M. M. Bakirov, K. M. Salikhov, R. T. Galeev, I. T. Khairuzhdinov, B. Bales</i>	114
Receiving and Transmitting System for a Specialized Small-Sized Magnetic Resonance Scanner with a 0.4 Tesla Field <i>A. A. Bayazitov, Ya. V. Fattakhov, V. E. Khundiryakov, A. R. Fakhrutdinov, V. A. Shagalov, R. Sh. Khabipov</i>	115
Spatial Structure of YRFK Peptides with Triphenylphosphonium Moiety by NMR Spectroscopy <i>D. S. Blokhin, R. Garifullin, T. I. Abdullin, V. V. Klochkov</i>	116
Peculiarities of Low Temperature FMR in Ion Beam Synthesized Co Silicide Films <i>V. V. Chirkov, G. G. Gumarov, V. Yu. Petukhov, M. M. Bakirov</i>	118
Fe ³⁺ -Cytochromes Signals in EPR Spectra of Sportsmen's Serum Blood <i>A. I. Chushnikov, M. I. Ibragimova, G. V. Cherepnev, V. Yu. Petukhov, I. V. Yatsyk</i>	119
The Study of Protein Ligand Interaction by Water LOGSY NMR <i>A. G. Danilova, A. N. Turanov, B. I. Khairutdinov, Yu. F. Zuev</i>	121

Electron Spin Resonance Study of $\text{Sm}_{1-x}\text{Eu}_x\text{B}_6$ Solid Solutions <i>S. V. Demishev, M. I. Gilmanov, A. N. Samarin, A. V. Semeno, N. E. Sluchanko, N. Yu. Shitsevalova, V. B. Filipov, V. V. Glushkov</i>	122
The Nature of Electron Spin Resonance in CeB_6 <i>S. V. Demishev, M. I. Gilmanov, A. N. Samarin, A. V. Semeno, N. E. Sluchanko, N. Yu. Shitsevalova, V. B. Filipov, V. V. Glushkov</i>	124
Structural Model of the Yb^{3+} Ion in the LiCaAlF_6 Single Crystal <i>M. L. Falin, V. A. Latypov, A. M. Leushin, G. M. Safiullin, A. A. Shakirov, A. A. Shavelev</i>	125
New Fe(III) Complexes with Tetradentate Schiff Bases and Photosensitive Ligands <i>E. Frolova, O. Turanova, M. Volkov, L. Mingalieva, L. Gafiyatullin, I. Ovchinnikov, A. Turanov</i>	127
Study of the Conformation of γ -Irradiated Calcium Gluconate by the ESR Method <i>A. R. Gafarova, G. G. Gumarov, I. A. Goenko</i>	128
Study of γ -Irradiated Calcium Gluconate by X- and Q-EPR <i>A. R. Gafarova, G. G. Gumarov, I. A. Goenko, M. M. Bakirov, R. B. Zaripov, V. Yu. Petukhov</i>	129
Proximity Effect in Superconducting Triplet Spin-Valve F2/S2/F1/S1 Structure <i>R. R. Gaifullin, V. N. Kushnir, R. G. Deminov, L. R. Tagirov, M. Yu. Kupriyanov, A. A. Golubov</i>	130
Nitric Oxide Production in the Rat Hippocampus in Acute Phase of Ischemic and Hemorrhagic Insult: Participation of NO-synthase <i>Kh. L. Gainutdinov, V. V. Andrianov, G. G. Yafarova, S. G. Pashkevich, M. O. Dosina, Y. P. Stukach, T. Kh. Bogodvid, V. S. Iyudin, A. A. Denisov, V. A. Kulchitchky</i>	131
Spin-Spin Interactions in AFM Dirac Semimetals: Diluted and Enriched Cases <i>Yu. V. Goryunov, A. N. Nateprov</i>	133
Magnetic Proximity Effects in $\text{CaCu}_3\text{Ti}_4\text{O}_{12}$ -Based Composites <i>T. Gavrilova, A. Yagfarova, I. Gilmudtinov, J. A. Deeva, I. Yatsyk, N. Lyadov, Y. Kabirov, T. Chupakhina, R. Eremina</i>	135
Magnetoresistance of Magnetic NanoContact with Taking Account Gradients of Chemical Potentials <i>L. Gerasimova, N. Useinov</i>	137
FMR Studies of Epitaxial Pd Films Implanted with Iron Ions <i>A. I. Gumarov, I. V. Yanilkin, I. R. Vakhitov, B. M. Khaliulin, A. A. Rodionov, R. V. Yusupov, M. N. Aliyev, L. R. Tagirov, V. I. Nuzhdin, R. I. Khaibullin</i>	139

Signature of the Field Induced Quantum Phase Transition in the Low-Dimensional Magnet BiCoPO ₅ <i>M. Iakovleva, E. Vavilova, H.-J. Grafe, A. Alfonsov, B. Büchner, Y. Skourski, R. Nath, V. Kataev</i>	140
Time Features of the Magnetic Effect on the Luminescence of Poly(9,9-di-n-octylfluorenyl-2,7-diyl) Films with Additive of KI Salt <i>N. Ibrayev, D. Afanasyev</i>	141
Effect of Magnetic Field on the Recombination Luminescence of Polymer Semiconductor Composites <i>N. Ibrayev, D. Afanasyev, A. Nurmakhanova</i>	142
Study of Synthetic Hydroxyapatites by EPR <i>K. Iskhakova, A. Sorokina, A. Starshova</i>	144
Resinous-Asphaltene Aggregates by NMR Analysis <i>D. Ivanov, V. Scirda</i>	145
Intramolecular Dynamic of Pillar[5]arene by NMR Spectroscopy Data and Computer Modeling <i>A. V. Ivanova, D. N. Shurpik, D. A. Sevastyanov, A. N. Turanov, E. A. Ermakova, I. I. Stoykov, Yu. F. Zuev, B. I. Khayrutdinov</i>	146
Heterointerfaces Composed of Complex Ferroelectric Oxides: an Experimental Insight <i>A. Kamashev, R. Zagidullin, D. Pavlov, I. Piyanzina, D. Tayurskii, R. Mamin</i>	148
Rescaling of 2D ESEEM Data for Inverse Problem Solving <i>Yu. E. Kandrashkin, A. A. Sukhanov, V. F. Tarasov</i>	149
New Approach of Determination T_1 and T_2 Relaxation Times by Using the CPMG Pulse Sequence <i>I. Khairuzhdinov, R. Zariyov, K. Salikhov</i>	150
Strain-Induced Rotation of Magnetic Easy Axis in Permalloy Microparticles Studied by Ferromagnetic Resonance <i>T. Khanipov, N. Nurgazizov, A. Zagitova, A. Bukharaev, L. R. Tagirov</i>	151
Magnetic Properties of Antiferromagnetic Chain Ternary Chalcogenides TlFeS ₂ and RbFeSe ₂ <i>A. Kiiamov, F. Vagizov, L. R. Tagirov, T. P. Gavrilova, Z. Seidov, V. Tsurkan, I. Filipova, D. Croitoro, H.-A. Krug von Nidda, A. Günther, A. Loidl</i>	153
Low Temperature Mössbauer Study and Magnetic State of Fe _{1.05} Se _{0.3} Te _{0.7} <i>A. G. Kiiamov, F. G. Vagizov, D. A. Tayurskii, L. R. Tagirov, V. Tsurkan, A. Loidl</i>	154

NMR Structural Elucidation of Indole-3-Carbaldehyde Phenylhydrazones <i>M. I. Kodess, M. A. Ezhikova, O. S. Ermakova, Y. A. Azev</i>	156
Contrast Agents for Magnetic Resonance Imaging Based on Nanosized Rare Earth Fluorides <i>E. I. Kondratyeva, E. M. Alakshin, A. V. Bogaychuk, A. V. Klochkov, V. V. Kuzmin, M. S. Tagirov</i>	158
Self-Association of Disordered Protein Alpha-Casein According to PFG NMR Spectroscopy <i>A. M. Kusova, A. E. Sitnitsky, Yu. F. Zuev</i>	160
Narrowing Behavior of Hyperfine Coupling Structure in CuEr Alloys <i>S. Lvov, E. Kukovitsky</i>	161
Nuclear Quadrupole Resonance Study of Polymorphic Forms of Piracetam <i>S. Mamadazizov, G. Kupriyanova</i>	162
Modelling NMR Spectra of Galium Borate Glasses <i>D. Materka, M. Olszewski</i>	164
Towards an Alpha-Casein Translational Mobility by NMR <i>D. L. Melnikova, I. V. Nesmelova, V. D. Skirda</i>	165
Optimization of Pulse RF Sequences Parameters for Contrast Enhancement of MR Images in the Presence of Magnetic Nanoparticles <i>A. V. Nikitina, Yu. V. Bogachev</i>	166
Experimental Investigation of Magnetostriction in LiRF_4 (R = Ho, Dy) in Strong Magnetic Fields <i>D. S. Nuzhina, S. Abe, A. G. Kiiamov, S. L. Korableva, K. Matsumoto, I. V. Romanova, A. C. Semakin, M. S. Tagirov, K. Ubukata</i>	168
Soviet Serial EPR and NMR Spectrometers by the Mid-1980s <i>V. V. Ptushenko</i>	170
EPR of Calixarenes Dopped by Rare-Earth Metals Ions <i>E. A. Razina, A. S. Ovsyannikov, S. E. Solovieva, I. S. Antipin, A. I. Konovalov, G. V. Mamin, M. R. Gafurov, M. S. Tagirov, S. B. Orlinskii</i>	171
ESR and Luminescence Investigations on Quantum Dots Doped with Various Paramagnetic Ions <i>D. O. Sagdeev, R. R. Shamilov, V. K. Voronkova, A. A. Sukhanov, Yu. G. Galyametdinov</i>	173
Excessive Oscillating Magnetization in CeD_6 and ESR Line Shape Analysis in Wölfle-Abrahams Theory <i>A. N. Samarin, M. I. Gilmanov, A. V. Semeno, S. V. Demishev</i>	174

Peculiar Features of the Spectrum Saturation Effect When the Spectral Diffusion Operates. System with Two Frequencies <i>K. M. Salikhov</i>	176
Theoretical Study of the EPR Spectrum Saturation Effect Taking Into Account Spectral Diffusion in a System with Gaussian Distribution of Resonance Frequencies of Spins <i>K. M. Salikhov, I. T. Khayruzhdinov</i>	177
NMR Study of Influence of the Defects to the Magnetic Interactions and Ground State of Honeycomb Compound $\text{Li}_3\text{M}_2\text{SbO}_6$ (where M is Cu and Ni) <i>T. Salikhov, E. Zvereva, V. Nalbandyan, A. Vasiliev, E. Vavilova</i>	178
Anomalous Features of Antiferromagnetic Resonance in GdB_6 <i>A. V. Semeno, M. I. Gilmanov, N. E. Sluchanko, N. Yu. Shitsevalova, V. B. Filipov, S. V. Demishev</i>	179
Influence of the Substrate Bias Voltage on the Structure $\text{Pd}_{1-x}\text{Fe}_x$ Thin Films by Magnetron Sputtering <i>Sh. M. Shabakaev, I. V. Yanilkin, A. M. Rogov, R. V. Yusupov</i>	180
EPR Spectroscopy of Impurity Centers in Mixed Crystals $\text{LiSr}_x\text{Ca}_{1-x}\text{AlF}_6:\text{Ce}^{3+}$ <i>A. A. Shakirov, A. A. Shavelev, S. B. Orlinsky, D. G. Zverev, A. A. Rodionov, A. S. Nizamutdinov, V. V. Semashko</i>	182
EPR-Spectroscopy and Spin-Lattice Relaxation NO_3^{2-} Complex and Mn^{2+} Ions in Synthetic Hydroxyapatite <i>D. V. Shurtakova, G. V. Mamin, M. R. Gafurov, S. B. Orlinskii</i>	183
The Study of the Receptor Properties of Pillar[5]arene Binding to DNA by NMR Spectroscopy <i>P. Skvortsova, D. Shurpik, I. Stoykov, Yu. Zuev, B. Khairutdinov</i>	184
Effect of Dimerization on the Photophysical Properties of Zinc Coproporphyrin I <i>A. A. Sukhanov, V. S. Tyurin, V. K. Voronkova</i>	185
TR EPR of Compact Naphthalimide-Phenothiazine Dyads for Understanding of Photophysics of Thermally Activated Delayed Fluorescence <i>B. G. Tang, A. A. Sukhanov, X. Li, W. Yang, Zh. Wang, F. Zhong, J. Zhao, V. K. Voronkova, G. Gurzadyan</i>	186
Influence of the Tetradentate Schiff Base on the Spin-Variable Properties of $[\text{FeL}(\text{tvp})]$ BPh_4 Complexes According to EPR Data <i>O. Turanova, E. Milordova, T. Ivanova, L. Mingalieva, V. Shustov, L. Gafiyatullin, I. Ovchinnikov</i>	187

The Study of Magnetic Properties of Fe(III) Complexes with Multidentate Schiff Bases in Dichloromethane by NMR, EPR, and UV-Spectroscopy <i>M. Volkoy, E. Frolova, L. Mingalieva, L. Gafiyatullin, O. Turanova, E. Milordova, I. Ovchinnikov, A. Turanov</i>	188
Magnetic Properties of High-Spin Fe(III) Complexes with Schiff Based Photoactive Ligands <i>V. Vorobyeva, N. Domracheva, E. Zueva, M. Gruzdev</i>	189
Time-Resolved EPR Study of TEMPO-Bodipy Dyad <i>K. Xu, J. Zhao, A. A. Sukhanov, V. K. Voronkova</i>	190
EPR Investigation of Antioxidant Protection and Production of Nitric Oxide in Rat after Spinal Cord Injury <i>G. G. Yafarova, I. I. Shaikhutdinov, V. V. Andrianov, V. S. Iyudin, Kh. L. Gainutdinov</i>	191
Magnetic Properties of $\text{CaCu}_3\text{Ti}_4\text{O}_{12}:\text{Fe}$ Solid Solutions <i>A. Yagfarova, T. Gavrilova, I. Gilmudtinov, I. Yatsyk, J. A. Deeva, A. L. Zinnatullin, F. G. Vagizov, T. I. Chupakhina, R. Eremina</i>	193
EPR, Magnetic Susceptibility Measurements, and Quantum-Chemical Calculations of Trinuclear Copper(II) Complexes Embedded in Functionalized Hyperbranched Polymer Boltorn H30 <i>S. Yurtaeva, R. Galeev, M. Kutyreva, N. Khafizov, I. Gilmudtinov, A. Rodionov, R. Zaripov, O. Kadkin</i>	195
Heterointerfaces Composed of Complex Ferroelectric Oxides <i>R. Zagidullin, I. Piyanzina, D. Tayurskii, R. Mamin</i>	197
Study of Substituent R^1 Influence on Photoisomerization $\text{R}^1\text{-N}=\text{N-R}^1$ and $\text{R}^2\text{-CH}=\text{CH-R}^3$ by UV and 2D NMR Spectroscopy <i>H. Zuhayri, L. G. Gafiyatullin, O. A. Turanova, A. N. Turanov</i>	198
Influence of Temperature on the EPR Parameters of Electrically Conductive Compounds <i>A. M. Zyuzin, M. A. Bakulin, N. V. Yantsen, A. V. Ishaev</i>	199
AUTHOR INDEX	201

ZAVOISKY AWARD LECTURE

Solar Fuels: Nature's Approach

R. D. Britt

Department of Chemistry, University of California, Davis 95616, CA USA

Virtually all of the energy available to earth's biological organisms derives from solar energy converted to chemical energy by photosynthesis. In cyanobacteria and higher plants, a mineral-like cluster, composed of manganese, calcium, and oxygen, uses solar energy harvested by chlorophyll to split water, generating bioavailable electrons and protons, with molecular oxygen formed as a fortunate bioproduct. After this light driven enzyme evolved some billions of years ago, the resultant oxygen transformed our atmosphere from an anaerobic one to the oxygen rich atmosphere that supports higher life. The electrons and protons liberated from water are ultimately used to convert atmospheric carbon dioxide into sugar, the product "fuel" of natural photosynthesis. These efficient reactions have inspired chemists to build synthetic complexes to mimic these solar fuel reactions, a research field often referred to as artificial photosynthesis. Other crucial energy relevant enzymes incorporate other complex metal-based clusters. For example, the conversion of gaseous N_2 to bioavailable nitrogen in the form of ammonia is carried about by a molybdenum/iron/sulfur cluster in the nitrogenase enzyme. Molecular hydrogen is produced from protons by the iron/sulfur containing catalytic clusters of hydrogenase enzymes. Research is ongoing in labs around the world to couple the hydrogenase reaction to the photosynthetic water splitting reaction, providing a biological route to making hydrogen fuel directly from water and sunlight. In addition to the mechanisms carried out by these metalloenzyme clusters, it is interesting to learn how nature assembles these complex clusters to efficiently carry out these important reactions.

The Britt laboratory characterizes such solar fuel reactions and their underpinning catalytic cluster biosynthesis via spectroscopic interrogation of reaction intermediates, mostly using electron paramagnetic resonance (EPR) methods to probe interactions between unpaired electrons in such intermediates with nuclear spins intrinsic to nuclei such as $^1H/^2H$, $^{14}N/^{15}N$, ^{13}C , ^{55}Mn and ^{57}Fe incorporated into the catalytic clusters, the surrounding protein, and the substrate molecules which they transform. It is of course a great honor to speak about our recent work in Kazan, the birthplace of EPR as established by the pioneering work of Yevgeny Zavoisky.

PLENARY LECTURES

ESR in Strongly Correlated Topological Insulator SmB_6 : Built-in Mechanism of Time Reversal Symmetry Breaking and Anomalous Spin Relaxation

**S. V. Demishev^{1,2,3}, M. I. Gilmanov^{1,2}, A. N. Samarin^{1,2}, A. V. Semeno^{1,2},
N. E. Sluchanko^{1,2}, N. A. Samarin¹, A. V. Bogach¹, N. Yu. Shitsevalova⁴,
V. B. Filipov⁴, V. V. Glushkov^{1,2,3}**

¹ Prokhorov General Physics Institute of RAS, Moscow 119991, Russian Federation, demis@lt.gpi.ru

² Moscow Institute of Physics and Technology, Dolgoprudny 141700 Moscow region,
Russian Federation

³ National Research University Higher School of Economics, Moscow 101000, Russian Federation

⁴ Institute for Problems of Materials Science of NASU, Kiev 03680, Ukraine

Introducing of topological Kondo insulator (TKI) concept for fluctuating valence compound – samarium hexaboride, SmB_6 , – has recently initiated a new round of studies aimed to clarify the nature of the ground state in this extraordinary system with strong electron correlations. Here we discuss the data of magnetic resonance in pristine single crystals of SmB_6 measured in 60 GHz cavity experiments at temperatures 1.8–300 K [1]. Our estimates of absorption of microwave radiation at the sample surface and in the bulk show that in experimental conditions the main part of the microwave losses for $T < 5$ K is due to the metallic surface layer of TKI SmB_6 . The microwave study as well as the *dc* resistivity and Hall effect measurements performed for the different states of SmB_6 [110] surface prove definitely the existence of the layer with metallic conductivity increasing under lowering temperature below 5 K. Four lines with the *g*-factors $g \approx 2$ are found to contribute to the ESR-like absorption spectrum that may be attributed to intrinsic paramagnetic centers on the sample's surface, which are robust with respect to the surface treatment. We argue that some magnetic Sm^{3+} ions $J = 5/2$ with the ground state Γ_8 may act as a source of intrinsic localized magnetic moments (LMM) visible in the ESR experiments. These LMM may appear at the sample surface as a consequence of anomalous spin relaxation rate, characterized by the frequency, which 3-4 orders of magnitude less than the $\text{Sm}^{3+} \leftrightarrow \text{Sm}^{2+}$ charge/spin fluctuation frequency assumed for the mixed valence state. The temperature dependence of integrated intensity $I(T)$ for main paramagnetic signal is found to demonstrate anomalous critical behavior $I(T) \sim (T^* - T)^\nu$ with characteristic temperature $T^* = 5.34 \pm 0.05$ K and exponent $\nu = 0.38 \pm 0.03$ indicating possible magnetic transition at the SmB_6 [110] surface. We wish to mark that these magnetic centers should break time-reversal symmetry removing the topological protection of the surface states. As a result, the initial 2D massless Dirac spectrum should evolve to a gapped one so that the quasiparticles in the surface layer acquire a finite effective mass. Additional resonant magnetoabsorption line,

which may be associated with either donor-like defects or cyclotron resonance mode corresponding to the mass $m_c \sim 1.2m_0$, is reported.

This work was supported by RFBR grant 17-02-00127-a and Programs of Russian Academy of Sciences “Electron spin resonance, spin-dependent electronic effects and spin technologies” and “Electron correlations in strongly interacting systems”.

1. Demishev S.V. *et al.*: Scientific Reports **8**, 7125 (2018)

Resolving Protein – Paramagnetic Intermediate Interactions by Two-Dimensional Pulsed EPR Spectroscopy

S. A. Dikanov

University of Illinois, Urbana 61801, USA, dikanov@illinois.edu

All major electron transfer pathways involve redox enzymes using a variety of metal cofactors, linked through diffusional steps. The flux in the membrane is carried by quinones. The chemistries catalyzed are proton-coupled electron transfer (PCET) reactions, which proceed through two one-electron steps, and lead to release or uptake of two protons, essential for completion of the redox reactions and a coupled H⁺-pumping function. Electron transfers from QH₂ or to Q are accompanied by the formation of reactive paramagnetic intermediates. Direct intermediates of quinone chemistry are semiquinones (SQs), whose properties define parameters for partial processes in PCET with electron-carrying metal centers such as iron-sulfur (Fe-S) clusters and hemes. Quinones and metal centers of the same structure possess diverse redox characteristics in different protein environments, showing that the redox-chemistry is protein-controlled, but the question of how specificity is determined at the molecular and atomic levels continues to present a challenge. The importance of pulsed EPR in addressing such problems comes from the specificity of information available about the electronic structure of redox cofactors, and the reaction environment provided by the protein and solvent, all of interest in understanding mechanistic detail.

This presentation is devoted to our applications of 2D ESEEM in conjunction with different ²H, ¹³C, ¹⁵N isotope labeling schemes directed at understanding the electronic structure of the paramagnetic intermediates, and their interactions with local environment and how these are modified in mutants. The intermediates focused on are SQs in the Q_A and Q_B sites of the bacterial Reaction Center from *Rhodobacter sphaeroides*, the Q_H site of the cytochrome *bo*₃ ubiquinol oxidase from *Escherichia coli*, and the three major classes of the protein-bound, reduced [2Fe-2S](His)_{*n*}(Cys)_{4-*n*} (*n* = 0, 1, 2) clusters.

Pulsed EPR part of this work is currently supported by the DE-FG0208ER15960 Grant from the Chemical Sciences, Geosciences and Biosciences Division, Office of Basic Energy Sciences, Office of Sciences, U.S. DOE.

High-Field EPR Studies of Water-Protein Hydrogen Bond Interactions and Their Role For Biological Function

K. Möbius^{1,2}

¹ Department of Physics, Free University Berlin, D-14195 Berlin, Germany,
moebius@physik.fu-berlin.de

² Max Planck Institute for Chemical Energy Conversion, D-45470 Mülheim (Ruhr), Germany

Some organisms in the kingdoms of micro-organisms, plants and animals can survive long periods of extreme environmental stress like complete dehydration and high temperatures. When providing some water they resume their metabolism and return to normal life (e.g., “resurrection plants” in deserts after a shower of rain). Under dehydration these organisms adapt to an “anhydrobiotic” state, in which the intracellular medium accumulates large amounts of non-reducing disaccharides such as trehalose or sucrose. Trehalose is known to be most effective in protecting isolated *in vitro* biostructures, and is exploited for *in vivo* food preservation. Until now, the molecular mechanism of the anhydrobiotic biostabilization in disaccharide sugar matrices is unclear and still controversially discussed.

To contribute to a clarification of this issue, we thoroughly studied structure and dynamics of light-induced cofactor ion radicals of photosynthetic reaction center complexes in disaccharide matrices as well as neutral nitroxide radicals as spin-probes. Different protein concentrations and hydration levels were probed by various cw and pulse high-field EPR techniques (95 and 244 GHz) [1]. From the results we conclude that the anhydrobiotic state of the protein-disaccharide system is NOT the result of matrix-induced changes of the local structure and dynamics of the charge-separated radical-pair cofactors. Rather, it originates in the high rigidity of the dry disaccharide glass matrix coating the protein surface already at RT by H-bond networks including local water molecules. This shifts the correlation time of thermal conformational fluctuations, which are essential for protein function, into the non-biological time regime.

This work has been done in collaboration with A. Savitsky, A. Nalepa, W. Lubitz (Max Planck Institute in Mülheim (Ruhr), Germany), M. Malferrari, F. Francia, G. Venturoli (University of Bologna, Italy), and A. Semenov (Moscow State University, Russia).

1. Nalepa A., Malferrari M., Lubitz W., Venturoli G., Möbius K., Savitsky A.: *Phys. Chem. Chem. Phys.* **19**, 28388 (2017)

Studying Isotopically Purified Rare-Earth Doped Crystals for Raman Quantum Memories

A. A. Kalachev

Zavoisky Physical-Technical Institute, FRC Kazan Scientific Center of RAS, Kazan 420029, Russian Federation, a.a.kalachev@mail.ru

Rare-earth (RE) doped solids have raised a strong interest in the field of quantum information storage, signal processing and communication. Among them, isotopically purified crystals are of particular interest. They can demonstrate very small inhomogeneous broadening of optical transitions (~ 10 MHz), which proves to be smaller than the hyperfine splitting of the energy levels of impurity ions, and provide high optical densities. As a result, these crystals are promising candidates for implementing quantum storage via off-resonant Raman absorption/emission of single photons.

In the present work, the recent progress in experimental and theoretical studying these materials is discussed [1–3]. In particular, the possibility of growing high-quality fluoride crystals with an inhomogeneous width of optical transitions as small as 13 MHz has been demonstrated [2]. An increase in the optical coherence time by an order of magnitude (from several μs to 300 μs) has been demonstrated for the first time in the crystals doped with Er-167 ions by using optical clock transitions and cooling the crystals down to ~ 100 mK [1]. In crystals doped with Nd-143 ions, the effect of electromagnetically induced transparency was observed [3] with the use of hyperfine ZEFOZ transitions, which directly confirms the possibility of realizing Raman quantum memory schemes in the materials under study.

The work is supported by RSF (project No. 14-12-00806).

1. Kukharchyk N., Sholokhov D., Morozov O., Korableva S.L., Kalachev A.A., Bushev P.A.: *New J. Phys.* **20**, 023044 (2018)
2. Kukharchyk N., Sholokhov D., Morozov O., Korableva S.L., Cole J.H., Kalachev A.A., Bushev P.A.: *Opt. Lett.* **43**, 935 (2018)
3. Akhmedzhanov R., Gushchin L., Nizov N., Nizov V., Sobgayda D., Zelensky I., Kalachev A.: *Phys. Rev. B* **97**, 245123 (2018)

Development and Application of THz ESR in Kobe University

**S. Okubo^{1,2}, Y. Kitahara², S. Ikeda², S. Hara³, T. Sakurai³, H. Ohta^{1,2},
D. Yoshizawa⁴, M. Hagiwara⁴, F. Kimura⁵, T. Kimura⁵, Y. Sakurai⁶,
K. Nawa⁷, Y. Okamoto⁸, Z. Hiroi⁹**

¹ Molecular Photoscience Research Center, Kobe University, Kobe 657-8501, Japan,
sokubo@kobe-u.ac.jp

² Graduate School of Science, Kobe University, Kobe 657-8501, Japan

³ Research Facility Center for Science and Technology, Kobe University, Kobe 657-8501, Japan

⁴ Center for Advanced High Magnetic Field Science, Graduate School of Science, Osaka University,
Osaka 560-0043, Japan

⁵ Division of Forest and Biomaterials Science, Kyoto University, Kyoto 606-8502, Japan

⁶ Institute of Multidisciplinary Research for Advanced Materials, Tohoku University,
Sendai 980-8577, Japan

⁷ Department of Applied Physics, Nagoya University, Nagoya 464-8603, Japan

⁸ Institute for Solid State Physics, University of Tokyo, Kashiwa 277-8581, Japan

⁹ National Institute for Materials Science, Tsukuba 305-0047, Japan

THz ESR system in Kobe University has been developed continuously for extending the frequency range, the magnetic fields and the high-pressure environments [1–4]. Our THz ESR system can cover the frequency region from 0.03 THz to 7 THz [1], the magnetic field region up to 55 T [2], the temperature region from 1.8 to 300 K [3], and the pressure region up to 2.15 GPa [4]. We have performed the THz ESR measurements of the spin frustration systems, multiferroic relate perovskite systems, and one-dimensional quantum spin systems. THz ESR measurements of Cr-jarosite ($\text{KCr}_3(\text{OH})_6(\text{SO}_4)_2$), which is model substance for $S = 3/2$ perfect kagome lattice antiferromagnet, revealed the D-vector of Dzyloshinski-Moriya interaction as an essential magnetic anisotropy of kagome antiferromagnets [5]. Perovskite compound YCrO_3 shows ferroelectricity and antiferromagnetism at room temperature. We observed THz gap and its anisotropy [6]. Spin nematic state is expected theoretically in $S = 1/2$ one-dimensional antiferromagnet with staggered D-vector. $\text{NaCuMoO}_4(\text{OH})$ is one of model of spin nematic system [7]. To obtain magnetic anisotropy of $\text{NaCuMoO}_4(\text{OH})$, THz ESR measurements of magnetically aligned powder sample has been performed [8]. Fig. 1 shows frequency dependence of THz ESR spectra for magnetically aligned powder sample of $\text{NaCuMoO}_4(\text{OH})$ for $B \parallel b$ at 1.8 K. Although number of spins of sample is essentially low due to dilution by epoxy resin, our THz ESR system succeeded in detecting ESR signals in broad frequency range. We will discuss the applications of THz ESR.

This work was supported by JSPS KAKENHI Grant-in-Aid for Challenging Exploratory Research Grant Number JP17K18760, and Grant-in-Aid for Scientific Research (C) Grant Number JP26400335.

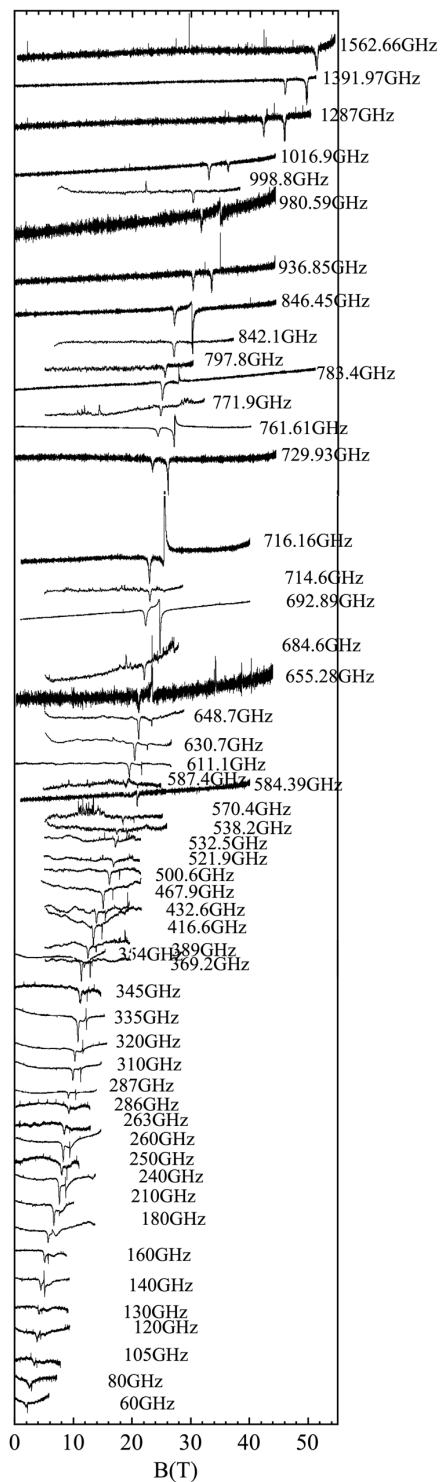


Fig. 1. Frequency dependence of THz ESR spectra for NaCuMoO₄(OH) $B||b$ at 1.8 K.

1. Okubo S. *et al.*: Physica B **346-347**, 627–632 (2004)
2. Ohta H. *et al.*: J. Phys. Conf. Series **51**, 611 (2006)
3. Nakagawa N. *et al.*: Int. J. Infrared Millimeter Waves **17**, 833 (1996)
4. Sakurai T. *et al.*: J. Phys. Soc. Jpn. **87**, 033701 (2018)
5. Okubo S. *et al.*: J. Phys. Soc. Jpn. **86**, 024703 (2017)
6. Ikeda S. *et al.*: Appl. Magn. Reson. **46**, 1053 (2015)
7. Nawa K. *et al.*: J. Phys. Soc. Jpn. **83**, 103702 (2014)
8. Kitahara Y. *et al.*: J. Jpn. Soc. Infrared Science & Technology **26**, 56 (2016)

Pseudo Jahn-Teller Effect in Spin-Orbit Entangled Mott Insulators

G. Khaliullin

Max Planck Institute for Solid State Research, Stuttgart, Germany

The consequences of Jahn-Teller (JT) orbital-lattice coupling for magnetism of pseudospin $S_{\text{eff}} = 1/2$ and $S_{\text{eff}} = 0$ compounds are addressed. In the former case, represented by iridium oxide Sr_2IrO_4 , this coupling generates, through the so-called pseudo-JT effect, the orthorhombic deformations of a crystal concomitant with magnetic ordering. The orthorhombicity axis is tied to the magnetization and rotates with it under magnetic field. Theory resolves a number of hitherto unexplained puzzles in Sr_2IrO_4 such as metamagnetic behavior, field dependence of the magnon gaps, etc. In case of pseudospin $S_{\text{eff}} = 0$ systems, the pseudo-JT effect leads to a spin-nematic transition well above magnetic ordering, which may explain the origin of "orbital order" in Ca_2RuO_4 .

Biological Hydrogen Conversion Studied by EPR and NMR Techniques

W. Lubitz

Max Planck Institute for Chemical Energy Conversion, Mülheim/Ruhr 45470,
Germany, wolfgang.lubitz@cec.mpg.de

Hydrogenases catalyze the reversible heterolytic splitting of H₂ at binuclear (NiFe or FeFe) metal centers [1]. Understanding how these enzymes achieve their high efficiencies is key to developing molecular catalysts for H₂ conversion and production. To shed light on the catalytic cycles of these enzymes intermediates are trapped and characterized by electrochemical and spectroscopic methods, especially magnetic resonance techniques [2]. The obtained parameters are verified by DFT calculations. It is demonstrated how this has led to a profound understanding of the catalytic cycle of the hydrogenases [1].

The field of [FeFe] hydrogenases has recently been revolutionized by the discovery of artificial maturation [3, 4]. The active site of [FeFe] hydrogenases (the “H-cluster”) is composed of a classical [4Fe-4S] cluster linked via a cysteine to a [2Fe] center that carries CO and CN⁻ ligands, and a bridging aza-propane-1,3-dithiolate (adt) ligand [1]. For [FeFe] hydrogenases from several organisms artificial maturation of the enzymes has been described [4], where the apo-protein carrying only the [4Fe-4S] cluster is reacted with chemically synthesized [2Fe] clusters. Such clusters with different substituents, different atomic compositions, and even different metals have been incorporated. The technique also allows specific isotope labelling for various spectroscopic experiments. This approach enabled for example the first detection of ¹H NMR on a hydrogenase in solution under physiological conditions [5]. The obtained paramagnetic shifts of the ¹H resonance lines have been explained based on the electron spin coupling model of the active site (H-cluster) that was developed earlier using EPR/ENDOR spectroscopies [6]. Recently, an iron-bound terminal hydride in the reduced state of the enzyme could be detected by NMR [7] that is considered the key intermediate in the catalytic cycle. Based on these and other spectroscopic results a model of the catalytic cycle for the [FeFe] hydrogenases could be developed.

The oxygen sensitivity of these enzymes is discussed that can significantly be improved by embedding the [FeFe] hydrogenase in a tailor-made polymer matrix [8]. It is demonstrated that hydrogenases and related model catalysts can successfully be attached to electrodes and used in devices [9].

1. Lubitz W., Ogata H., Rüdiger O., Reijerse E.: *Chem. Rev.* **114**, 4081 (2014)
2. Lubitz W., Reijerse E., van Gastel M.: *Chem. Rev.* **107**, 4331 (2007)
3. a) Berggren G., Adamska A., Lambert C., Simmons T.R., Esselborn J., Atta M., Gambarelli S., Muesca J.M., Reijerse E., Lubitz W., Happe T., Artero V., Fontecave M.: *Nature* **499**, 66 (2013); b) Esselborn J.,

- Lambertz C., Adamska-Venkatesh A., Simmons T., Berggren G., Noth J., Siebel J., Hemschemeier A., Artero V., Reijerse E., Fontecave M., Lubitz W., Happe T.: *Nat. Chem. Biol.* **9**, 607 (2013)
4. Birrell J., Rüdiger O., Reijerse E., Lubitz W.: *Joule* **1**, 61 (2017)
 5. Rumpel S., Ravera E., Sommer C., Reijerse E., Farès Ch., Luchinat C., Lubitz W.: *J. Am. Chem. Soc.* **140**, 131 (2018)
 6. Silakov A., Reijerse E., Albracht S., Hatchikian E.C., Lubitz W.: *J. Am. Chem. Soc.* **129**, 11447 (2007)
 7. Rumpel S., Sommer C., Reijerse E., Farès Ch., Lubitz W.: *J. Am. Chem. Soc.* **140**, 3863 (2018)
 8. a) Plumeré N., Rüdiger O., Oughli A.A., Williams R., Vivekananthan J., Pöller S., Schuhmann W., Lubitz W.: *Nat. Chem.* **6**, 822 (2014) b) Oughli A.A., Conzuelo F., Winkler M., Happe T., Lubitz W., Schuhmann W., Rüdiger O., Plumeré N.: *Angew. Chem., Int. Ed.* **54**, 12329 (2015)
 9. a) Rodríguez-Maciá P., Priyadarshani N., Dutta A., Weidenthaler C., Lubitz W., Shaw W., Rüdiger O. *Electroanalysis* **28**, 2452 (2016); b) Rodríguez-Maciá P., Dutta A., Lubitz W., Shaw W., Rüdiger O. *Angew. Chem., Int. Ed.* **54**, 12303 (2015)

Structure and Dynamics of Micro- and Macromolecules by NMR

Ch. Griesinger

Max Planck Institute for Biophysical Chemistry, Göttingen 37077, Germany,
cigr@nmr.mpibpc.mpg.de

Optical Orientation of Magnetic Polarons in Diluted Magnetic Semiconductors

Yu. G. Kusrayev

Ioffe Institute, Russian Academy of Sciences, St. Petersburg 194021, Russian Federation

Diluted magnetic semiconductors (DMS) attract enormous interest for a long time owing to their unusual extraordinary magneto-optical and magnetotransport phenomena such as giant spin splitting and Faraday effect, magnetopolaron effect, etc.

In this report we discuss the peculiarities of optical orientation of excitons and magnetic polarons in DMS and nanostructures based on A_2MnB_6 compounds. Magnetic polaron is a region of local magnetization of magnetic ions arising due to the exchange interaction with a localized carrier. Such a region of local

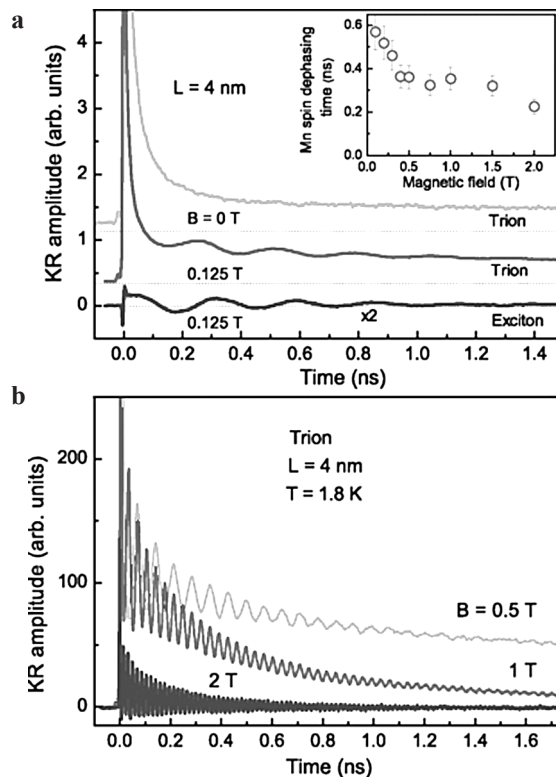


Fig. 1. Kerr rotation signals of the 4 nm-thick $Cd_{0.96}Mn_{0.04}Te/Cd_{0.76}Mn_{0.04}Mg_{0.20}Te$ QW. (a) Curves measured on the trion at $B = 0$ and on the trion as well as exciton at $B = 0.125$ T are shifted vertically for clarity. Inset: Spin dephasing time of the Mn spins as function of magnetic field. (b) KR signals measured on the trion at different magnetic fields.

magnetic ordering can be created by the excess equilibrium carriers or by photoexcited carriers and excitons. Under nonresonant optical excitation by circular polarized light the spin aligned carriers (excitons) in DMS quickly relax (lose) their spins followed by the emission of nonpolarized light. However under resonant optical excitation of localized states excitons the predominant spin orientation can be conserved till recombination. This effect is due to the existence of magnetization fluctuations resulting in the splitting of energy levels of localized states. The exchange field of magnetization fluctuation stabilizes carrier (exciton) spins and furthermore results in formation of magnetic polaron with the same direction of magnetization. The number of spin aligned magnetic moments in a polaron can be as large as 100 ($250 \mu_B$) so that one circular polarized photon can generate about 200 Bohr magnetons. Recombination of the exciton in spin aligned polarons results in the emission of circularly polarized light. Such a scenario has been realized in bulk CdMnSe CdMnTe crystals [1, 2].

Another type of optical orientation of magnetic polarons has been observed in CdMnTe/CdMgTe QW with resident holes. By means of picosecond pump-probe Kerr rotation it has been found that in addition to the relatively slow oscillatory signals from manganese spins ($g_{Mn} = 2.0$) and fast precessing of photoexcited electron spins (with effective g -factor $g_e = 90$) about an external magnetic field, there occurs a surprisingly long-lived (up to 60 ns) nonoscillating spin polarization (see Fig. 1). This polarization is ascribed to optical orientation of equilibrium magnetic polarons involving resident holes [3]. Resonant excitation creates either the neutral exciton X that quickly captures into the X^+ trion state (exciton+resident hole) either directly X^+ trion. This process is spin selective (total spin of two holes in the X^+ trion is zero). Optical excitation by σ^+ circularly polarized light produces imbalance between hole polaron states $-3/2$ ($-M_p$) and $+3/2$ ($+M_p$). This imbalance results in the nonoscillating long-living signal.

The lowest heavy-hole has strongly anisotropic of g -tensor: $g_{xx}, g_{yy} \ll g_{zz}$. A magnetic polaron, which is formed by a heavy hole, therefore also exhibits a strong anisotropy. For spin relaxation, the HMP should flip its magnetic moment: this requires overcoming the energy barrier equal to E_{MP} between two stable states $-M_p$ and $+M_p$. Therefore polaron spin dynamics is controlled by the anisotropic spin structure of the heavy hole. The magnetic polaron relaxation is accelerated with increasing temperature and magnetic field. The lack of oscillations in transverse magnetic field can also be ascribed to the potential barrier between two heavy-hole polaron states. The strong temperature dependence of the HMP spin-relaxation time observed in the experiment suggests that it occurs due to an activation process, which can be described by $\tau_{MP} \approx \tau_0 \exp(E_a(B, T)/k_B T)$, $E_a(B, T)$ is activation energy which depends on the hole exchange field B_{ex} and hole g -factor anisotropy g_{\perp}/g_{zz} , τ_0 is a pre-factor of the order of the hole spin-flip time.

The work was supported by Russian Science Foundation (grant 18-12-00352).

1. Warnock J., Kershaw R.N., Ridgely D., Dwight K., Wold A., Galazka R.R.: J. of Luminescence **34**, iss. 1–2, 25–35 (1985)
2. Zakharchenya B.P., Kusrayev Yu.G.: Zh. Eksp. Teor. Fiz. **50**, 199 (1989) [JETP Lett. **50**, 225 (1989)]
3. Zhukov E.A., Kusrayev Yu.G., Kavokin K.V., Yakovlev D.R., Debus J., Schwan A., Akimov I.A., Karczewski G., Wojtowicz T., Kossut J., Bayer M.: Phys. Rev. B **93**, 245305 (2016)

Light-Induced Nuclear Hyperpolarization as a Sensitive Tool for Detection of Illusive Radicals of Biomolecules

**A. Yurkovskaya¹, O. Morozova¹, A. Kiryutin¹, H.-M. Vieth²,
R. Z. Sagdeev¹, K. Ivanov¹**

¹ International Tomography Center SB RAS, Novosibirsk, Russian Federation,
alexandra.yurkovskaya@tomo.nsc.ru

² Freie Universitat Berlin, Berlin, Germany

During last decade we developed very efficient methods for creating light-induced spin hyperpolarization termed chemically induced dynamic nuclear polarization (CIDNP)[1] that can provide valuable data on the structure and reactivity of short lived radicals in biological systems at ambient conditions not obtainable by standard EPR techniques.

The talk describes significant progress in three directions:

(i) development of hardware and new techniques for investigating hyperpolarization over a wide range of magnetic fields from 5 nT to 16 T and microsecond time resolution at high field;

(ii) development of theory and methodology of spin hyperpolarization in condensed media;

(iii) application of spin hyperpolarization to the study of various chemical processes of biologically important molecules.

We continued with the development and application of methods of photo-induced nuclear spin hyperpolarization and relaxation in condensed media extending over a magnetic field range from 5 nT to 10 T [2] According to our methodological developments, the studies are largely devoted to the application of spin-hyperpolarization methods to the study of reactions and processes involving short-lived radical species. New results were obtained on the study of fast radical reactions involving biologically important molecules, in particular on the structure and reactivity of such radicals. Photoreactions of various benzophenones with biomolecules were studied in detail focused on intra- and intermolecular electron transfer.

CIDNP of the pyrimidine bases of thymine and thymidine DNA was studied in detail. Results on formation and decay of a newly discovered unusual guanosine radical cation including its pH dependence will be presented [3]. An oxidation reaction with the DNA base thymine in the presence of photosensitizers produces other short-lived nucleotide radicals. Here the abovementioned advantages of the CIDNP method will be amplified.

The magnetic field dependence of CIDNP as a source of information about electronic exchange interaction will be shown for a number of promising molecular systems: in recently synthesized dyads, which can be used in photovoltaics, and in biradicals [4].

1. Morozova O., Yurkovskaya A., Vieth H.-M., Sosnovsky D., Ivanov K., Mol. Phys. **115**, 2907 (2017)
2. Zhukov I., Kiryutin A., Yurkovskaya A., Grishin Yu., Vieth H.-M., Ivanov K.: Phys. Chem. Chem. Phys. **20**, 12396 (2018)
3. Morozova O., Fishman N., Yurkovskaya A.: Phys. Chem. Chem. Phys. **19**, 21262 (2017)
4. Paul S., Kiryutin A., Guo J., Ivanov K., Matysik J., Yurkovskaya A., Wang X.: Sci. Rep. **7**, 11892 (2017)

SECTION 1

SPIN-BASED INFORMATION PROCESSING

Cross-Relaxation Magnetometry in Diamond NV-Centers with Polycrystalline Samples

**R. A. Akhmedzhanov, L. A. Gushchin, N. A. Nizov, V. A. Nizov,
D. A. Sobgayda, I. V. Zelensky**

Institute of Applied Physics of the RAS, Nizhny Novgorod 603950, Russian Federation,
zelensky@appl.sci-nnov.ru

NV-center magnetometers have a special place among the modern methods of magnetometry. Depending on the task, such magnetometers are capable of providing high sensitivity, spatial resolution, compactness, and the ability to work under a variety of external conditions [1]. One of the main disadvantages of the “classic” NV center magnetometry is the necessity to use microwave radiation, which limits its potential applications. In our recent work [2] we suggest microwave free magnetometry scheme based on observation of cross-relaxation resonances between nonequivalently oriented NV-center groups in scanning magnetic field. The number and positions of these resonances depend on the magnitude and orientation of additional magnetic field and therefore provide a way to measure it.

In this work we study theoretically and experimentally the possibility of using polycrystalline diamond for implementing NV-center cross-relaxation magnetometry. The use of polycrystalline samples with arbitrary oriented axes instead of diamond single crystals simplifies the measurement procedure. In particular, the precise orientation of the sample is not required and only a single cross-relaxation resonance is observed. The projection of an unknown magnetic field on a given axis is directly determined by the position of the resonance. Note that the use of polycrystalline diamonds, as well as diamond powders, can significantly reduce the cost of magnetometer. The proposed technique can be applied to measure magnetic fields up to several gauss.

The reported research was funded by Russian Foundation for Basic Research and the government of Nizhny Novgorod region of the Russian Federation, grant № 18-42-520017.

1. Rondin L., Tetienne J-P., Hingant T., Roch J-F., Maletinsky P., Jacques V.: Rep. Prog. Phys. **77**, 056503 (2014)
2. Akhmedzhanov R., Gushchin L., Nizov N., Nizov V., Sobgayda D., Zelensky I.: Phys. Rev. A **96**, 013806 (2017)

Investigation of Neodymium Doped YVO_4 by EPR Method

**R. M. Eremina^{1,2}, I. V. Yatsyk^{1,2}, V. F. Tarasov¹, K. B. Konov¹,
Y. D. Zavartsev^{1,3}, S. A. Kutovoi^{1,3}, R. F. Likеров²**

¹Zavoisky Physical-Technical Institute, FRC Kazan Scientific Center of RAS, Kazan 420029, Russian Federation, REremina@yandex.ru

²Institute of Physics, Kazan Federal University, Kazan 420008, Russian Federation

³Prokhorov General Physics Institute, Moscow 119991, Russian Federation

Yttrium orthovanadate single crystals doped with rare earth elements are very attractive laser material currently used for microlaser and diode laser pumped solid-state lasers. Electron paramagnetic resonance (EPR) is a convenient method to study paramagnetic centers in these materials. Neodymium doped YVO_4 crystals were grown by the Czochralski method. We studied two YVO_4 monocrystals doped with 0.005 at.% $^{143}\text{Nd}^{3+}$ and 0.005 at.% $^{145}\text{Nd}^{3+}$. The first crystal contains only the ^{143}Nd isotope (sample I), the second crystal (sample II) contains only the ^{145}Nd isotope. The YVO_4 belongs to the $I4_1/amd$ space group with unit cell parameters $a = b = 7.118(0)$ Å, $c = 6.289(0)$ Å, which [1]. Typical EPR spectrum for $^{143}\text{Nd}^{3+}$ ions in YVO_4 with 8 lines ($2I + 1$) of hyperfine structure of ^{143}Nd and ^{145}Nd ions was observed. Angular dependencies of resonance magnetic fields, rotated in (ac)- and (ab)-planes of the monocrystal $\text{YVO}_4:^{143}\text{Nd}^{3+}$ was obtained on X-band EPR spectrometer Bruker EMX+ at $T = 15$ K. Temperature dependences of spin-lattice and spin-spin relaxation times were measured for both samples. The spin-lattice relaxation times were described according expression: $T_1^{-1} = AT + BT^9 + C\exp(-\Delta/kT)$.

The first term describes the process involving one phonon with the frequency equal to the frequency of the EPR transition. The second term is due

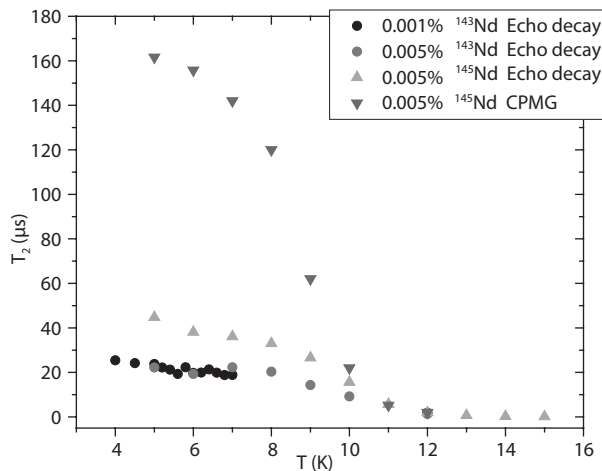


Fig. 1. Temperature dependences of spin-spin relaxation times for $^{143/145}\text{Nd}^{3+}:\text{YVO}_4$.

to the Raman two-phonon process; the third term describes the processes of the two-phonon Orbach-Aminov relaxation involving the excited low-lying electron level which lies at Δ above the ground level. Fitting parameters for spin-lattice relaxation times are equal for two samples: $A = 0.254 \text{ c}^{-1}\text{K}^{-1}$, $B = 2.03 \cdot 10^{-6} \text{ c}^{-1}\text{K}^{-9}$, $C = 1.9118 \cdot 10^{11} \text{ c}^{-1}$, $\Delta = 163.5 \text{ K}$. The value of the parameter $\Delta = 163.5 \text{ K}$ is in reasonable agreement with the value of $\Delta = 108 \text{ cm}^{-1}$ (155.5 K) which obtained from optical measurements [2]. The relaxation time T_2 was measured by the primary echo decay (see Fig. 1). The spin-spin relaxation times for the ^{145}Nd isotope are larger for as one the ^{143}Nd isotope in YVO_4 single crystals. Presumably, this is due to the difference of nuclear magnetic properties of Nd isotopes, e.g., the gyromagnetic ratio is $-1.47 \cdot 10^7$ and $-0.91 \cdot 10^7 \text{ rad} \cdot \text{s}^{-1} \cdot \text{T}^{-1}$ for ^{143}Nd and ^{145}Nd , respectively. The spin-spin relaxation times are same for two samples YVO_4 with 0.005% at. or 0.001% at. ^{143}Nd isotope. The strong temperature dependence of the T_2 value was attributed to the effect of the spectral diffusion caused by the hyperfine interaction with magnetic nuclei of the crystal matrix. This spectral diffusion can be efficiently eliminated in the Carr-Purcell-Meiboom-Gill (CPMG) pulse protocol.

We used principal values of g -tensor and energies of electron levels of the ground multiplets of the Nd^{3+} ions in YVO_4 known from the optic measurements [2] to determine crystal field parameters.

This work was supported by the Russian Science Foundation (project no. 16-12-00041).

1. Guillot-Noel O., Kahn-Harari A., Viana B. *et al.*: J. Phys. Cond. Matter **10**, 6491 (1998)
2. Bagdasarov Kh.S., Bogomolova G.A., Kaminskii A.A., Popov V.I.: Dokl. Akad. Nauk SSSR **180**, 1347 (1968)

EPR Study of the Neutral Germanium-Vacancy Center in Diamond

A. Komarovskikh^{1,2}, V. Nadolinny^{1,2}, Y. Palyanov^{2,3}, I. Kupriyanov^{2,3}

¹ Nikolaev Institute of Inorganic Chemistry SBRAS, Novosibirsk 630090, Russian Federation, komarovskikh@niic.nsc.ru

² Sobolev Institute of Geology and Mineralogy SBRAS, Novosibirsk 630090, Russian Federation

³ Novosibirsk State University, Novosibirsk, 630090, Russian Federation

Defects in diamond which electronic state can be affected by electromagnetic fields attract great attention nowadays. The nitrogen-vacancy ($\text{NV}^{0/-}$) and silicon-vacancy ($\text{SiV}^{0/-}$) centers are the most studied centers, they have narrow zero-phonon lines and can be used in different applications in quantum optics. Also, the negatively charged germanium-vacancy (GeV^-) and tin-vacancy (SnV^-) centers have been detected recently by optical spectroscopy, these defects can be considered as the analogs of the silicon-vacancy center.

Although no optical analog has been found for the neutral germanium-vacancy center yet the EPR spectrum of the GeV^0 center has been detected for the high-pressure high-temperature diamonds synthesized in the Mg-Ge-C system (Fig. 1) [1]. This EPR spectrum explicitly reveals the electron spin $S = 1$ and axial symmetry around the $\langle 111 \rangle$ direction. The following spin-Hamiltonian parameters were used to simulate the spectrum detected at room temperature: $g_{\parallel} = 2.0025$, $g_{\perp} = 2.0027$, and $D = 80.3$ mT, $E = 0$. The additional synthetic work was performed using germanium enriched with the ^{73}Ge isotope (nuclear spin $I = 9/2$). For the new center the hyperfine structure of one ^{73}Ge atom with approximately isotropic $A \approx 1.64$ mT was detected in EPR experiments. As the new germanium-containing paramagnetic center had the same symmetry and spin state as the neutral silicon-vacancy center SiV^0 , the new paramagnetic

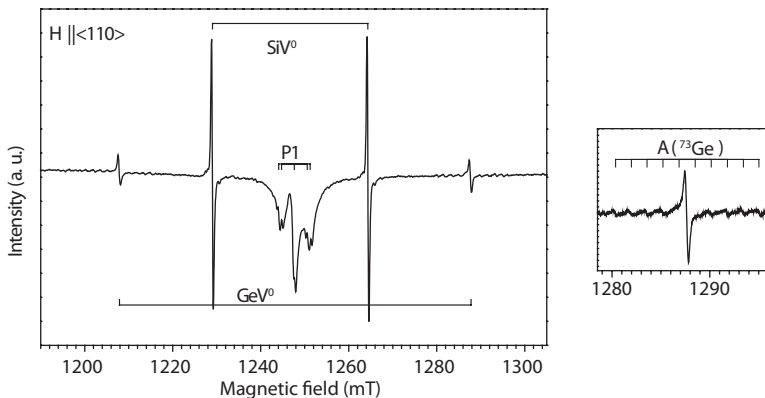


Fig. 1. The EPR spectrum of the ^{73}Ge ($I = 9/2$) enriched sample (room temperature, $\mathbf{H} \parallel \langle 110 \rangle$).

center was proposed to be the neutral germanium-vacancy center. The variation of intensity with temperature showed that the GeV^0 center was in the ground triplet state as well as the SiV^0 center. The zero-field splitting (ZFS) parameter D was surprisingly large for the GeV^0 center and the spin-orbit contribution was proposed to be the reason. It is known that Ge has a significantly larger spin-orbit coupling constant than Si ($\lambda(\text{Ge}) = 940 \text{ cm}^{-1}$, $\lambda(\text{Si}) = 149 \text{ cm}^{-1}$) giving a significantly larger D ($D(\text{GeV}^0) = 80.3 \text{ mT}$, $D(\text{SiV}^0) = 35.7 \text{ mT}$).

The GeV^0 in diamond has been investigated using the density functional theory (DFT) cluster method [2]. The g -tensor, hyperfine interaction constants, and ZFS parameter have been calculated and compared with experimental data. There is good agreement between the experimentally obtained and calculated spin-Hamiltonian parameters (for instance, the calculated $A_{\parallel} = 1.47 \text{ mT}$, $A_{\perp} = 1.55 \text{ mT}$, $D = 70.9 \text{ mT}$, $E = 0$). Thus, the performed DFT calculations confirm the assignment of the experimental EPR spectrum to the paramagnetic GeV^0 ($S = 1$) defect. Additionally, it has been demonstrated that the spin-orbit coupling interaction actually gives a dominant contribution to the total D parameter.

The spin relaxation process has been investigated for the GeV^0 center in the temperature range 80–110 K [3]. It has been shown that spin-lattice and spin-spin relaxation times for the GeV^0 are shorter than corresponding times for the SiV^0 center. Thereby, it can be suggested that GeV^0 center is less prospective in quantum applications. The spin-lattice relaxation of the GeV^0 center can be described by Orbach relaxation mechanism with the activation energy $\sim 39 \text{ meV}$ at temperatures 80–110 K.

This research was supported by Russian Science Foundation under Grant No. 14-27-00054.

1. Nadolinny V., Komarovskikh A., Palyanov Y., Kupriyanov I., Borzdov Y., Rakhmanova M., Yuryeva O., Veber S.: *Phys. Status Solidi A* **213**, 2623 (2016)
2. Komarovskikh A., Dmitriev A., Nadolinny V., Palyanov Y.: *Diamond Relat. Mater.* **76**, 86 (2017)
3. Komarovskikh A., Uvarov M., Nadolinny V., Palyanov Y.: *Phys. Status Solidi A*, DOI: 10.1002/pssa.201800193

SECTION 2

THEORY OF MAGNETIC RESONANCE

Experimental and Theoretical Investigations of Multiple-Quantum NMR Coherences in One-Dimensional Systems

G. Bochkin¹, E. Fel'dman¹, I. Lazarev¹, S. Vasil'ev¹, V. Volkov¹

¹Theoretical Department and NMR Laboratory, Institute of Problems of Chemical Physics of RAS, Chernogolovka 142432, Russian Federation, efeldman@icp.ac.ru

We investigate multiple quantum (MQ) NMR dynamics and relaxation of one-dimensional systems both experimentally and theoretically. The experimental study is performed on a single crystal of calcium fluorapatite. This compound has a hexagonal system of parallel chains of F ions along the *c*-axis of the crystal. The distance between neighboring chains is about three times larger than the distance between nearest ions in a chain. In fact, we can consider an isolated quasi-one-dimensional chain for describing MQ NMR dynamics and relaxation.

We obtained an exact solution for MQ NMR dynamics on the preparation period of the MQ NMR experiment [1] in the approximation of the nearest neighbor interactions using a fermion representation of the Hamiltonian describing MQ NMR dynamics [2]. In particular, we have found that only MQ NMR coherences of the zeroth and plus/minus second orders emerge on the preparation period. The obtained density matrix at the end of the preparation period was used as the initial condition for the relaxation process which occurs on the evolution period of the MQ NMR experiment.

Using the ZZ-model we obtained [3] the dependencies of the intensities of the MQ NMR coherences of the zeroth and second orders on the time of the evolution period for different lengths of the preparation period. We calculated the second moments of the line shapes of the intensities of MQ NMR coherences of the zeroth and second orders. We showed that the flip-flop part of the dipolar Hamiltonian does not contribute to the second moment of the line shape of the intensity of the MQ NMR coherence of the zeroth order. Using the obtained second moments we found semi-phenomenological formulae which allow us to describe the experimental data.

This work is supported by the RFBR (project no. 16-03-00056) and the Program of the Presidium of the Russian Academy of Sciences No. 5 "Electron spin resonance, spin-dependent electron effects and spin technologies".

1. Baum J., Munowitz M., Garrowsay A.N., Pines A.: J. Chem. Phys. **83**, 5, 2015–2025 (1985)
2. Fel'dman E.B.: Appl. Magn. Reson. **45**, 797–806 (2014)
3. Bochkin G.A., Fel'dman E.B., Vasil'ev S.G., Volkov V.I.: Chem. Phys. Lett. **680**, 56 (2017)

Low Symmetry Orienting Potentials and Efficient Computation of ESR Line Shapes

K. A. Earle¹, T. Broderick²

¹ University at Albany, Albany, NY 12222, USA

² Regeneron Pharmaceuticals Inc., Rensselaer, NY 12144, USA

ESR line shape simulation is an important tool to elucidate details of structure and dynamics, particularly when performed in the context of model parameter fitting. In systems where an ESR active spin label is covalently attached to a macromolecule, one can model probe ordering effects by a suitably chosen orienting potential. Conventional line shape analysis is restricted to orienting potentials of fairly high symmetry, typically possessing a center of inversion, e.g., D_{2h} , which may not be a faithful representation of the environment in which the spin label is diffusing. Regardless of the symmetry of the orienting potential, a key ingredient for generating a line shape simulation is the starting vector, which is typically computed from projections of diffusion operator eigenfunctions onto the equilibrium distribution modeled by the orienting potential [1]. This is often the most time-consuming part of line shape calculations, as it relies on numerical integration of highly oscillatory integrands. In order to improve the efficiency of the starting vector calculation, we have developed a vector recurrence relation with no restrictions on the form of the potential. As it is a homogeneous recurrence relation, the starting vector may be evaluated by standard methods, e.g., singular value decomposition. The vector recurrence relation can also be extended to the Slowly Relaxing Local Structure model [2], and this is work in progress. We will present illustrative simulations demonstrating the effects of low symmetry orienting potentials on the ESR line shape and discuss what modifications are necessary to line shape simulation software to accommodate orienting potentials of low symmetry. This work was partially supported by a Faculty Research Award Program grant from the University at Albany.

1. Meirovitch *et al.*: J. Chem. Phys. **77**, 3915 (1982)
2. Polimeno and Freed: J. Chem. Phys. **99**, 10995 (1997)

Hybrid Quantum-Classical Method for Simulating High-Temperature Dynamics of Nuclear Spins in Solids

B. V. Fine

Skolkovo Institute of Science and Technology, Moscow, Russian Federation,
University of Heidelberg, Germany, b.fine@skoltech.ru

We propose a new hybrid quantum-classical method for computing NMR free induction decay(FID) for spin 1/2 lattices. The method is based on the simulations of a finite cluster of spins 1/2 coupled to an environment of interacting classical spins via a correlation-preserving scheme. Such simulations are shown to lead to accurate FID predictions for one-, two- and three-dimensional lattices with a broad variety of interactions. The accuracy of these predictions can be efficiently estimated by varying the size of quantum clusters used in the simulations.

Reference

Starkov G.A., Fine B.V.: [arXiv:1806.09355](https://arxiv.org/abs/1806.09355)

SECTION 3

CHEMICAL AND BIOLOGICAL SYSTEMS

Nitroxides in Cotton and Cellulose. Physicochemistry and Technology. 42 Years of History

G. Likhtenshtein

Department of Chemistry, Ben-Gurion University of the Negev, Beer-Sheva, Israel;
Institute of Problems of Chemical Physics, Russian Academy of Science, Chernogolovka,
Moscow region, Russian Federation, gertz@bgu.ac.il

Since pioneering works of Marupov and Likhtenshtein groups [1, 2], nitroxides are widely used in solving a number of challenging problems of structure and functions of cotton fibres and cellulose. Methods of nitroxide spin luminescence labelling have been proved to be a powerful tool in this area. Covalent modification cotton fibres and cellulose by the labels and the use electron Spin Resonance (ESR) allow to establish the label location and motion the labelled samples which in turn is modulated by the polymers local molecular dynamics and its distribution. Data on dependencies of the fibres' molecular dynamics on origin, temperature, water and other plasticizing agents, nutrition, period of maturing, virus infection and radiation of seeds have been presented. Combination of ESR experiments and Zhurkov technique have revealed a strong dependence of fibres' resistance to stress (durability) on microscopic structural defects (n). Suggested modification of the Zhurkov equation allows to predict durability of cotton materials using values of n derived by the spinlabelling method. In the cotton fibres, the distribution of the molecular dynamics correlation time within 10^{-4} – 10^{-9} s temporal range was established. At ambient temperature the fibres molecular dynamics can occur in both the submillisecond and nanosecond scales indicating broad distribution of dynamic correlation times. The free activation energy distribution of mobility of the chromophore label were found to be 10.5 kJ/mole (data on fluorescence) and 6.7 kJ/mole (data on phosphorescence).

1. Marupov R.M., Bobodzhanov P.Kh., Kostina N.V., Shapiro A.B.: Spin label study of the structure and conformational properties of cotton filament grown from γ -irradiated seeds. *Biofizika* **21**, 825–828 (1976)
2. Marupov R., Bobodzhanov P.Kh., Yusupov I.Kh., Frolov E.N., Likhtenshtein G.I.: Study of temperature stability of cotton fibers by spin labeling. *Biofizika* **24**, 519–523 (1979)

Trehalose Effect on the Forward and Backward Electron Transfer in Photosystem I

V. Kurashov¹, G. E. Milanovsky², M. Gorka¹, D. A. Cherepanov^{2,3},
J. H. Golbeck¹, A. Yu. Semenov^{2,3}

¹ Department of Biochemistry and Molecular Biology, The Pennsylvania State University,
University Park, PA, USA

² A. N. Belozersky Institute of Physical-Chemical Biology, Moscow State University, Moscow,
Russian Federation

³ N. N. Semenov Institute of Chemical Physics Russian Academy of Sciences, Moscow,
Russian Federation

The forward and backward electron transfer (ET) kinetics were measured in the intact P_{700} - F_A/F_B Photosystem I (PS I) complexes, P_{700} - F_X cores, lacking terminal F_A/F_B iron-sulfur clusters and P_{700} - A_1 cores, lacking F_X , F_A and F_B iron-sulfur clusters, both in liquid and in trehalose glass at 11% humidity. By comparing kinetic events in increasingly simplified versions of PS I at 480 nm, a wavelength that reports primarily oxidation of phylloquinone molecules A_{1A}/A_{1B} in the A and B symmetrical branches of cofactors, and at 830 nm, a wavelength that reports the chlorophyll dimer P_{700}^+ reduction, assignments could be made for nearly all of the resolved kinetic phases. The recombination between the primary chlorophyll acceptor A_0^- and P_{700}^+ occurs in ~40% of trehalose-embedded P_{700} - F_A/F_B complexes, P_{700} - F_X cores, and P_{700} - A_1 cores, indicating inefficiency in forward ET beyond A_0 in a fraction of PS I. The forward ET from A_{1A} to F_X in trehalose-embedded PS I is slowed from 200 ns to 13 μ s. The ~10 μ s and ~150 μ s components were assigned to recombination between A_{1B} and P_{700}^+ and between A_{1A} and P_{700}^+ , respectively. The ~1.5 ms recombination between F_X^- and P_{700}^+ in trehalose-embedded PS I becomes heterogeneous and splits into lifetimes of ~550 μ s/4.5 ms, whereas the ~100 ms recombination reaction between $[F_A/F_B]^-$ and P_{700}^+ becomes heterogeneously distributed between 39 ms and ~2 s. The kinetics and amplitudes of all ET reactions can be well-fitted by a kinetic model that allowed calculation of the asymmetrical contribution of the A_{1A} and A_{1B} quinones to the electrochromic signal at 480 nm. The relative contributions of trehalose-embedded PS I with partially arrested forward ET were determined to be 0.53, 0.16, 0.22 and 0.10 for P_{700} - A_0 cores, P_{700} - A_1 cores, P_{700} - F_X -cores, and P_{700} - F_A/F_B complexes, respectively. The amplitude of the signal at 480 nm attributed to A_{1A} should be multiplied by a factor of 2.33 to obtain the true relative contribution of ET from P_{700} to A_{1A} at this wavelength. Low temperature X-band EPR studies of the PS I complexes in dry trehalose matrix showed that the redox potential of the terminal F_B cluster may be altered by dehydration to become more oxidizing than in the control PS I.

This work was supported by the Russian Foundation for Basic Research (Grant 17-00-00201).

New Methods in Singlet-State NMR

**B. A. Rodin^{1,2}, K. F. Sheberstov^{1,3}, A. S. Kiryutin^{1,2},
A. V. Yurkovskaya^{1,2}, K. L. Ivanov^{1,2}**

¹ International Tomography Center, Siberian Branch of the Russian Academy of Science, Novosibirsk 630090, Russian Federation, ivanov@tomo.nsc.ru

² Novosibirsk State University, Novosibirsk 630090, Russian Federation

³ The State Scientific Center of the Russian Federation “State Research Institute for Chemistry and Technology of Organoelement Compounds”, Moscow 111123, Russian Federation

Singlet-state NMR [1] is an important emerging concept potentially allowing one to overcome limitations imposed by finite relaxation times of nuclear spins. Experiments with nuclear singlet states allow one to exploit advantages of long-lived spin order, e.g., of long-lived spin states (LLSs). LLSs exist when the symmetry of the static Hamiltonian and that of the fluctuating Hamiltonian (which causes relaxation) coincide with a consequence that such states become immune to particular kinds of relaxation and becomes “long-lived” [1].

In this work, we present methods for generating and observing singlet LLSs by using adiabatically ramped RF-fields of a carefully chosen frequency; we name this method APSOC (Adiabatic-Passage Spin Order Conversion). This technique turns out to be very powerful, as it provides the maximal theoretically allowed conversion of magnetization to the singlet spin order, being applicable to weakly-coupled as well as strongly-coupled spin pairs. Furthermore, this technique is compatible with a filtering methods, which allows one to suppress background signals. In recent works, we provide methods, which further improve the performance of the APSOC method by using “fast” adiabatic variation of the Hamiltonian. The optimization utilizes optimal control methods and constant-adiabaticity RF-pulses [2], which significantly reduce the conversion time. Both schemes have been implemented and tested by running experiments with a strongly-coupled spin pairs.

Financial support from the Russian Science Foundation (grant No. 14-13-01053) and Russian Foundation for Basic Research (grant No. 17-33-50077) is gratefully acknowledged.

1. Levitt M.H.: *Annu. Rev. Phys. Chem.* **63**, 89–105 (2012)
2. Rodin B.A., Kiryutin A.S., Yurkovskaya A.V., Ivanov K.L., Yamamoto S., Sato K., Takui T.: *J. Magn. Reson.* **291**, 14–22 (2018)

Triptyl Biradicals in Solution: Conformations and Dynamics

**M. K. Bowman^{1,2}, B. Fowler¹, M. Lockart¹, J. A. Lecaroz¹,
A. G. Maryasov³, A. G. Matveeva³, V. M. Tormyshev²**

¹ Department of Chemistry & Biochemistry, University of Alabama, Box 870336, Tuscaloosa, Alabama 35487, USA, mkbowman@ua.edu

² N. N. Vorozhtsov Novosibirsk Institute of Organic Chemistry SB RAS, Novosibirsk 630090; Novosibirsk State University, Novosibirsk 630090, Russian Federation

³ V. V. Voevodsky Institute of Chemical Kinetics and Combustion SB RAS, Novosibirsk 630090, Russian Federation

Triptyl biradicals, connected by a flexible linker, allow the study of triptyl-triptyl interactions in dilute solutions as liquids or frozen solids. In liquid solution the flexible linker allows the two triptyl groups to come into contact and interact, or to separate with minimal interaction. Large exchange interactions in contact pairs decrease hyperfine couplings by a factor of two and increase the number of hyperfine lines. The modulation of the exchange interaction by the changing conformations of the biradical lead to classical alternating linewidth effects. The intensity and widths of the lines provide the magnitude of the exchange interaction and the relative energies of the conformations.

Triptyl biradicals were designed with a pair of ¹H on each triptyl group, giving a 1:2:1 triplet hyperfine structure when the triptyls were not interacting, but a pentet when they were strongly exchange coupled. The biradical spectra changed from a triplet to a pentet as the temperature was lowered, allowing measurement of the exchange interaction and the enthalpy and entropy of folding. A spectrum with a single broad line grew in at low temperature which seems to be caused by formation of small aggregates of the triptyl dimer molecules.

In frozen solution, pulsed ENDOR spectra revealed that the ¹H was half that of noninteracting radicals and the CW EPR spectrum showed indications of dipolar couplings. Long-pulse EDEPR spectra at different pulse turning angles showed that the EPR spectrum of this and several other triptyl biradicals was mainly from a strongly interacting triplet state. The distribution of zero field splittings, *D*, were determined from the EDEPR spectra by a new Mellin transform procedure. Fairly broad bimodal distributions were found for several of the biradicals. These two major conformations have similar energies and both are lower in energy than elongated conformations that leave the triptyl radicals as a pair of non-interacting doublets. This result is in agreement with the tendency of triptyl radicals to aggregate in frozen samples with multi-millimolar concentrations of triptyls.

This work was supported by the Ministry of Education and Science of the Russian Federation (state contract no. 2017-220-06-7355); the US National Science Foundation (grant 1416238); and the Russian Foundation for Basic Research (grant 14-03-93180).

EPR Probe-Based Approach for Acid Base Characterization of Mesoporous Silicas with Different Functionalities

E. Kovaleva¹, L. Molochnikov², D. Tambasova¹, D. Antonov^{1,2}

¹ Department of Technology for Organic Synthesis, Ural Federal University, Yekaterinburg 620002, Russian Federation, e.g.kovaleva@urfu.ru, d.p.tambasova@urfu.ru

² Department of Chemistry, Ural State Forest Engineering University, Yekaterinburg 620100, Russian Federation, lsmolochnikov@gmail.com

Although pure silicates used as mesoporous molecular sieves (MMS) manifest good adsorption properties and can be used as reactors for in situ synthesis [1], it is often required that the materials have a number of additional properties (high catalytic activity, thermostability etc.). For these purposes they are modified with organic, inorganic, metal complex and other compounds. The introduction of different amounts of a substituent affects different properties of mesoporous materials, i.e. acid base ones including their intraporous acidity as well as functional groups ionization characteristics and surface electrical potential (SEP). Therefore, the substituted materials are nowadays of great interest in terms of developing for them a technique for a complex characterization of their acid-base properties. Thus, the purpose of this research was to develop a new method for measuring local pH (pH^{loc}) and functional groups pK_a for mesoporous molecular sieves (MMS) substituted with heteroatoms by EPR of pH-sensitive nitroxide radicals (NR) as molecular probes.

C_{12} MCM-41, C_{16} MCM-41 and SBA-15 ($d_{channel} = 2.3\text{--}8.1$ nm) substituted with Al and B heteroatoms at Si:Al(B) ratios from 92 to 23 and a nitroxyl radical 4-dimethylamine-2-ethyl-5.5-dimethyl-2-(4-pyridyl)-2.5-dihydro-1*H*-imidazole-

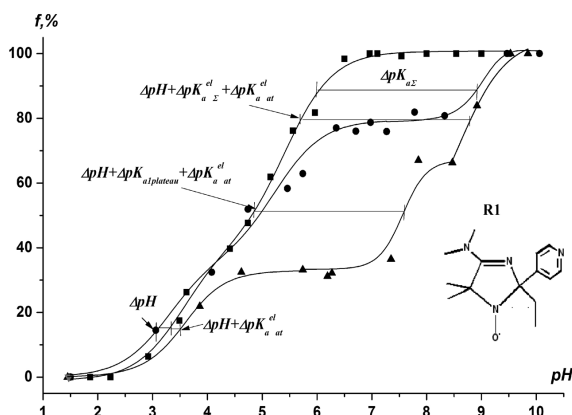


Fig. 1. The parameter f vs. pH for MMS.

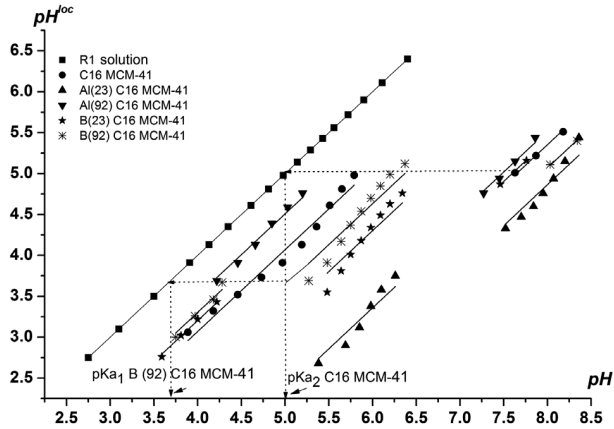


Fig. 2. pH^{loc} vs. pH for MMS.

1-oxyl with a range of pH -sensitivity from 2.5 to 6.5 pH units were used for this research.

For pure silica MMS [2] and Al (B)-substituted SBA-15 pH^{loc} and pK_a of silanol functional groups were determined from the dependences $f = F(pH)$ (curves of NR EPR titration, where f is a fraction of unprotonated NR form) for MMS by projecting a pH value in these curves to the same dependence plotted for the bulk water solution with ionic strength (μ) equal to 0.1M (calibration curve) (Fig. 1). It should be noted that pK_a of silanol functional groups were measured, in particular, from horizontal plateaus in the MMS curves, which reflected a process of their titration. In the modified MMS there were observed two horizontal plateaus, which correspond to the titration of silanol functional groups with two pK_a (Fig. 1).

Due to a total SEP arising as a result of all active centers titration in the modified MCM-41 is unequal to zero, the previously technique developed for measuring acid-base characteristics for pure silicates, can not be applied. Taking into account the shifts in pK_a of titration curves (ΔpK_a) 1) induced by heteroatoms incorporation as well as 2) by titration of functional groups which located close to and far from heteroatoms and 3) an electrical potential of a positively charged surface, we used the following formulas. For pure-silica MMS at the pH range upto the horizontal plateau getting started, $pH^{loc} = pH - \Delta pH$, whereas that after its ending $pH^{loc} = pH - \Delta pH - \Delta pK_a^{el} S$, for the MCM-41 with heteroatoms: at the pH range upto the first horizontal plateau (a heteroatom incorporation induced shift of titration curves) $pH^{loc} = pH - \Delta pH - \Delta pK_a^{el} at$, whereas that after its ending (both a heteroatom incorporation induced shift and a shift caused by the titration of the functional groups located in heteroatoms nearby surrounding) $pH^{loc} = pH - \Delta pH - \Delta pK_a^{el} plateau - \Delta pK_a^{el} at$. In case of the pH range after the second plateau ending (total a heteroatom incorporation induced shift

and the shifts resulted from by the titration of the functional groups located in heteroatoms nearby surrounding as well as far from them) $pH^{loc} = pH - \Delta pH - \Delta pK_a^{el} - \Delta pK_a^{at}$. According to a new approach from the dependences $pH^{loc} = f(pH)$ (Fig. 2) for both pure-silica and MMS substituted with heteroatoms can be directly measured pH^{loc} , whereas pK_a of different silanol groups are determined by pH^{loc} which correspond to the terminals parts of the same dependences.

This work was supported by the Program 211 of the Government of the Russian Federation № 02.A03.21.0006, RFBR grant 17-03-00641 & № 4.9514.2017/8.9 and 4.7772.2017/8.9.

1. Zhao X.S., Lu G.Q., Miller G.J.: *Ind. & Eng. Chem. Res.* **35**, 2075 (1996)
2. Kovaleva E.G., Molochnikov L.S., Antonov D.O. *et al.*: *J. Phys. Chem. B* (accepted) (2018)

EPR Studies of the Reactive Oxygen Species on Powder TiO₂

R. I. Samoilova

Institute of Chemical Kinetics and Combustion, Russian Academy of Sciences,
Novosibirsk 630090, Russian Federation, samoilov@kinetics.nsk.ru

Reactive oxygen species play important roles in various diseases caused by oxygen toxicity. Investigations on the organic chemistry of superoxide radical (O₂⁻) have shown that it can behave as a base, as a nucleophile, and as an oxidizing or reducing agent. Therefore, it is of interest to study the reactions of O₂⁻ with simple organic molecules to build up a picture of its possible biological effects. The generation of O₂⁻ was achieved by electrolytic reduction, enzymes, or using a photoinduced electron-transfer process. A catalyst with matrix-bound superoxide radical anion, generated by treating Ti(OR)₄ (R = iPr, nBu) with H₂O₂ was also reported and used as a selective heterogeneous catalyst for the oxidation of organic compounds [1]. In this work the generation of paramagnetic intermediates during decomposition of hydrogen peroxide on the TiO₂ surface has been monitored using continuous-wave and pulsed EPR spectroscopy. Structure, location and stability of paramagnetic species were studied in the absence and in the presence of the organic (*L*-tyrosine) substrate.

A dried sample of TiO₂ treated with H₂O₂ shows characteristic rhombic EPR signal with *g*-tensor components: *g*₁ = 2.026, *g*₂ = 2.0074, and *g*₃ = 2.0010 measured from Q-band spectrum. This result strongly suggests the presence of the stable superoxide radical anion generated by the decomposition of H₂O₂ on the TiO₂ surface [1, 2]. In the presence of *L*-tyrosine the EPR spectrum displaying a single asymmetrical line with the width ~2 mT. This type of the spectrum is consistent with the peroxy type radical ROO[•] [2]. Additional information about a proton environment of the radicals in both types of samples has been obtained from pulsed ENDOR and HYSCORE spectra that allowed us to propose models of the stabilized radicals.

1. Dewkar G., Nikalje M., Sayyed Ali I., Paraskar A., Jagtap H., Sudalai A.: *Angew. Chem. Int. Ed. Engl.* **40**, 405 (2001)
2. Attwood A., John L., Edwards J., Rowlands C., Murphy D.: *J. Phys. Chem. A* **107**, 1779 (2003)

ESEEM Observation and Localization of Bound Deuterated Substrate Histidine-d5 in Spin Labeled ABC Transporter HisQMP₂

**N. Isaev¹, J. Heuveling², N. Ivanisenko^{3,4}, E. Schneider²,
H.-J. Steinhoff⁵**

¹ Voevodsky Institute of Chemical Kinetics and Combustion SBRAS, Novosibirsk, Russian Federation, isaev@kinetics.nsc.ru

² Institut für Biologie/Bakterienphysiologie, Humboldt Universität zu Berlin, Berlin, Germany

³ Institute of Cytology and Genetics SB RAS, Novosibirsk, Russian Federation

⁴ Novosibirsk State University, Novosibirsk, Russian Federation

⁵ Physics Department, University of Osnabrück, Osnabrück, Germany

More than 90% of drug targets are proteins and more than 80% of drugs are small molecules. The majority of targets are membrane proteins (MP), structure determination of which is challenging for modern biophysics. However, localization of small substrates inside of a MP is even harder. So new techniques to study MP's substrate location and orientation for reasonable costs seems quite relevant.

We applied site-directed spin labeling with electron spin echo envelope modulation (ESEEM) to observe the isotope labeled ligand, deuterated histidine-d5, bound to the ABC transporter HisQMP₂. A crystal structure is not available for HisQMP₂, but a structure of the close homolog Art(QN)₂ is available with bound histidines. This enabled us to make a homology models with attached spin labels and deuterated substrate (Fig. 1; deuterons are represented by spheres). Having distance distributions between electron and deuterons we simulated ESEEM spectra for several spin labeled sites, compared these simulations with experimental ESEEM spectra and for HisM(L169R1) we could see a coincidence. By

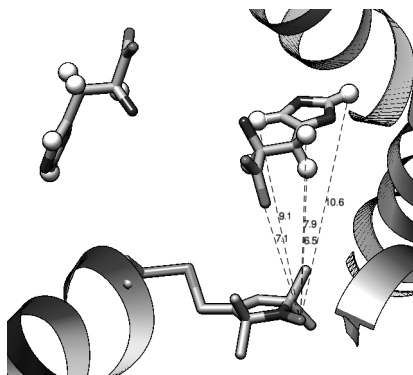


Fig. 1.

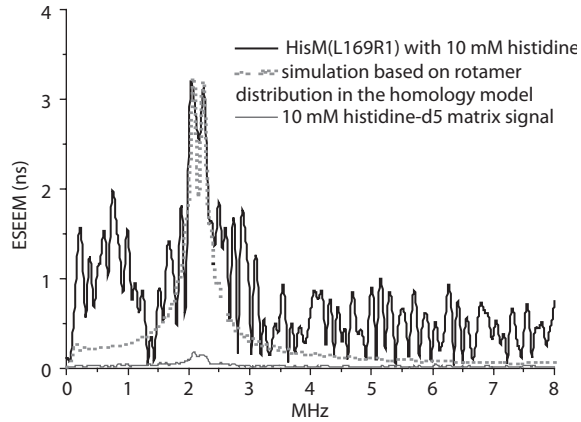


Fig. 2.

that we experimentally confirmed a histidine location in the homology model of HisQMP₂.

Thus ESEEM is applicable to study isotope substituted substrates in spin labeled membrane proteins.

This work was supported by Alexander von Humboldt Foundation. Computational modeling was funded by the Russian Science Foundation grant 14-44-00011.

SECTION 4

MOLECULAR MAGNETS AND LIQUID CRYSTALS

Experimental Strategies for ^{13}C - ^{15}N Dipolar Spectroscopy in Liquid Crystals with Natural Isotopic Abundance

S. V. Dvinskikh^{1,2}

¹ Department of Chemistry, KTH Royal Institute of Technology, Stockholm 10044, Sweden, sergeid@kth.se

² Laboratory of Bio-NMR, St. Petersburg State University, St. Petersburg 199034, Russian Federation

Direct dipolar spin couplings obtained from NMR spectra are among the most informative and sensitive probes for a wide range of dynamic processes and structural properties at the molecular level in liquid crystals and other anisotropic materials [1]. Typically, heteronuclear ^{13}C - ^1H dipolar couplings in liquid crystals with natural carbon-13 abundance and ^{15}N - ^1H couplings in ^{15}N -labelled samples are measured. Recording ^{13}C - ^{15}N dipolar NMR spectra in unlabelled materials is challenging because of the unfavourable combination of two rare isotopes; the fraction of the molecules containing ^{15}N - ^{13}C pairs is only $4 \cdot 10^{-5}$.

We describe and compare various experimental strategies to measure short- and long-range heteronuclear ^{13}C - ^{15}N dipolar couplings in highly ordered liquid crystalline samples with natural isotopic abundance [2, 3]. New techniques are introduced to selectively record ^{13}C and ^{15}N spectra of the naturally occurring ^{13}C - ^{15}N spin pairs while suppressing signals of the uncoupled isotopes. Due to relatively low demand on radio-frequency power, the experiments are easy to implement using conventional high-resolution solution state NMR probes. We demonstrate highly resolved ^{13}C - ^{15}N dipolar spectra in nematic and smectic mesophases. Coupling constants in the range 10–1000 Hz between spins separated by up to five chemical bonds and distances up to 5 Å are measured. Presented experimental methods to characterise the dipolar couplings in unlabelled materials provide novel routes to the investigations of molecular structure and dynamics in mesophases.

This work was supported by the Swedish Research Council VR and by the RFBR grant 17-03-00057.

1. Dvinskikh S.V. in: *Modern Methods in Solid-State NMR: A practitioners' Guide* (P. Hodgkinson, ed.), Abingdon: Royal Society of Chemistry 2018.
2. Jackalin L., Dvinskikh S.V.: *Z. Phys. Chem.* **231**, 795 (2017)
3. Cifelli M., Domenici V., Chizhik V.I., Dvinskikh S.V.: *Appl. Magn. Reson.* **49**, 553 (2018)

SECTION 5

STRONGLY CORRELATED ELECTRON SYSTEMS

Magnetic Quantum Oscillations in Doped Antiferromagnetic Insulators

V. V. Kabanov

Jozef Stefan Institute, Jamova 39, 1000 Ljubljana, Slovenia, viktor.kabanov@ijs.si

Energy spectrum of electrons (holes) doped into a two-dimensional antiferromagnetic insulator is quantized in an external magnetic field of arbitrary direction. A peculiar dependence of the de Haas-van Alphen or the Shubnikov-de Haas magneto-oscillation amplitudes on the azimuthal in-plane angle from the magnetization direction and on the polar angle from the out-of-plane direction is found, which can be used as a sensitive probe of the antiferromagnetic order in the doped Mott-Hubbard, spin-density wave, and conventional band structure insulators [1]. Experiments in which the predicted angular dependence is observed are discussed.

1. Kabanov V.V., Alexandrov A.S.: Phys. Rev. B **77**, 132403 (2008)

Coherent Spin Dynamics of Solitons in the Organic Spin Chain Compounds (*o*-DMTTF)₂X (X = Cl, Br)

**J. Zeisner^{1,2}, O. Pilone³, H. Vezin⁴, O. Jeannin⁵, M. Fourmigué⁵,
B. Büchner^{1,2}, V. Kataev¹, S. Bertaina³**

¹ Leibniz-Institute for Solid State and Materials Research IFW Dresden,
Dresden D-01069, Germany, j.zeisner@ifw-dresden.de

² Institute for Solid State and Materials Physics, TU Dresden, Dresden D-01069, Germany

³ IM2NP UMR7334, Aix-Marseille Université, CNRS, Marseille F-13397, France

⁴ LASIR UMR 8516, Université de Lille 1, CNRS, Villeneuve d'Ascq F-59655, France

⁵ Institut des Sciences Chimiques de Rennes, Université de Rennes 1, UMR-CNRS 6226,
Rennes, F-35042, France

Defects in one-dimensional spin systems continue to be an active field of modern solid state research as they are able to alter magnetic properties of the hosting materials drastically. In this work we studied the properties, in particular spin dynamics, of defects in the organic spin chain compounds (*o*-DMTTF)₂X (X = Br, Cl) by means of electron spin resonance (ESR) spectroscopy. Both materials exhibit spin-Peierls transitions at temperatures around 60 K [1], which allow a separation of the properties of defects inside the chains from the magnetic response of the spin chains. Indeed, continuous wave ESR measurements performed over a wide temperature range evidence the evolution of the spin dynamics from being governed by the spins in the chains at elevated temperatures to a low-temperature regime which is dominated by defects within the chains. Moreover, details of spin dynamics deep in the spin-Peierls phase were investigated by pulse ESR experiments which revealed, for instance, Rabi-oscillations as signatures of coherent spin dynamics. We discuss the results obtained from these complementary methods of ESR spectroscopy in terms of solitons localized at the defect sites.

1. Foury-Leylekian P., Auban-Senzier P., Coulon C., Jeannin O., Fourmigué M., Pasquier C., Pouget J.-P.: Phys. Rev. B **84**, 195134 (2011)

Spin Dynamics in the System with Honeycomb Lattice with Defects and Frustration Probed by Nuclear Magnetic Resonance Technique

**E. Vavilova¹, M. Iakovleva^{1,2}, T. Salikhov¹, H.-J. Grafe², E. Zvereva⁴,
V. Nalbandyan⁵, A. Vasiliev⁴, A. Möller³, B. Büchner², V. Kataev²**

¹ Zavoisky Physical-Technical Institute, FRC Kazan Scientific Center of RAS, Kazan 420029, Russian Federation, jenia.vavilova@gmail.com

² IFW Dresden, Dresden 01069, Germany

³ JGU Mainz, Mainz 55122, Germany

⁴ MSU, Moscow 119991, Russian Federation

⁵ SFU, Rostov-na-Donu 344090, Russian Federation

The spin-1/2 Heisenberg honeycomb lattice has a particular position among quasi-two-dimensional materials. Due to low coordination number ($z = 3$) quantum fluctuations are enhanced that causes a new interesting phenomena. Here we present two examples of materials with honeycomb magnetic lattice of copper ions with non-magnetic defects: $\text{InCu}_{2/3}\text{V}_{1/3}\text{O}_3$ and $\text{Li}_3\text{Cu}_2\text{SbO}_6$. Different kinds of magnetic frustration create different magnetic ground states. Moreover, the local resonance techniques like NMR and NQR gives us new information about interplay of competing phenomena during a process of slowing down of spin dynamics.

The work was supported by grant RFBR 18-02-00664.

New State of Matter

V. R. Shaginyan

Petersburg Nuclear Physics Institute, NRC Kurchatov Institute, Gatchina 188300, Russian Federation

We focus on the topological fermion condensation of quantum phase transition (FCQPT) that paves a new avenue in modern physics. Such a transition belongs to the unique type of quantum phase transitions the originators of the theory of instabilities omitted, and leads to the topological reconstruction of the Fermi surface. We discuss the modification of the systems under the action of FCQPT, representing the “missed” instability, which allows the development of an entirely new approach to or a “second edition” of condensed matter theory, presenting this physics as a completely new method for studying many-body objects [1, 2].

Further, it demonstrates that topological FCQPT takes place in many strongly correlated Fermi-systems like heavy fermion metals, high-temperature superconductors, new-type quantum spin liquids in insulators, quasicrystals and two-dimensional systems [1, 2].

FCQPT forms a new state of matter by making the behavior of strongly correlated Fermi systems universal, and in order to describe the new state of matter it is necessary to have a new version of the theory of condensed matter physics. The new state presents all the aspects of traditional condensed matter physics that have been significantly modified to offer a new avenue in modern physics.

1. Shaginyan V.R., Stephanovich V.A., Msezane A.Z., Schuck P., Clark J.W., Amusia M.Ya., Japaridze G.S., Popov K.G., Kirichenko E.V.: *J. Low Temp. Phys.* **189**, 410 (2017)
2. Shaginyan V.R., Amusia M.Ya., Msezane A.Z., Popov K.G.: *Phys. Rep.* **492**, 31 (2010)

Microwave Absorption Study of Charge Density Waves in $\text{La}_{2-x}\text{Sr}_x\text{CuO}_4$ Crystals

I. Gimazov¹, Yu. Talanov¹, T. Adachi²

¹ Zavoisky Physical-Technical Institute, FRC Kazan Scientific Center of RAS, Kazan 420029,
Russian Federation, ubvfp94@mail.ru

² Sophia University, Tokyo 102-8554, Japan

The charge ordering in the compound La_2CuO_4 doped with Ba, Sr and rare earth elements have been studied for a long time (see review [1] and references therein). In despite of this there are contradictions between different studies. For example, the X-ray diffraction measurements in $\text{La}_{2-x}\text{Sr}_x\text{CuO}_4$ have found well narrow range of the Sr concentrations with charge density waves (CDW) [2], while the transport study revealed their presence in a much broader area [3]. The reason of this discrepancy is a dynamic (or fluctuation) character of CDW on the most part of the “Sr-content – Temperature” phase diagram [4]. The use of the high-frequency investigation methods is a way to resolve the contradiction.

In this work, the state of $\text{La}_{2-x}\text{Sr}_x\text{CuO}_4$ at temperatures higher than superconducting transition was studied with the non-resonant microwave absorption (MWA) measurements upon varying the temperature at a fixed applied magnetic field. This method has shown itself as a good way to detect short-lived perturbations [5]. The superconducting transition temperature T_c was determined from the data of the high-frequency magnetic susceptibility measurements. The objects of the study were $\text{La}_{2-x}\text{Sr}_x\text{CuO}_4$ crystals with different strontium contents.

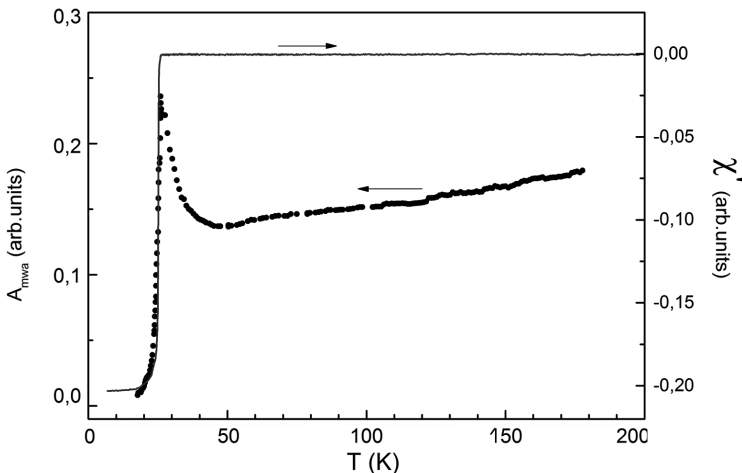


Fig. 1. Temperature dependence of the microwave absorption amplitude (points) and the AC-susceptibility (line) in the $\text{La}_{2-x}\text{Sr}_x\text{CuO}_4$ crystal with $x = 0.116$.

For all samples the temperature dependences of susceptibility and MWA were obtained. For example the dependences are shown in Fig. 1 for the underdoped crystal $\text{La}_{2-x}\text{Sr}_x\text{CuO}_4$ with $x = 0.116$. The amplitude of MWA falls abruptly at the superconducting transition temperature determined with the susceptibility measurement. Moreover, the temperature dependence of MWA sharply changes its slope at temperature T' far above T_c . This feature of the MWA behavior is detected for all samples, except optimally doped and overdoped ones. It denotes the appearance of the addition dissipation channel at T' . The latter may be due to the superconducting fluctuations or dynamic (fluctuating) charge density waves. The absence the magnetic field dependence and proximity to the CDW area determined from the X-rays diffraction study [2] allow us to conclude that namely the charge density waves are responsible for the change of the MWA temperature dependence at T' .

The results of the MWA and transport measurements allows us to plot the phase diagram of the $\text{La}_{2-x}\text{Sr}_x\text{CuO}_4$ compound with the boundaries of the superconductivity, superconducting fluctuation and CDW areas. The latter is in good agreement with the XRD data [2] and satisfies transport study [3] better than other data.

The financial support of the Russian Academy of Sciences (Program №5) is gratefully acknowledged.

1. Jie Q., Han S.J., Dimitrov I., Tranquada J.M., Li Q.: *Physica C* **481**, 46 (2012)
2. Croft T.P., Lester C., Senn M.S. *et al.*: *Phys. Rev. B* **89**, 144512 (2014)
3. Ando Y., Lavrov A.N., Komiya S., Segawa K., Sun X.F.: *Phys. Rev. Lett.* **87**, 017001 (2001)
4. Torchinsky D.H., Mahmood F., Bollinger A.T., Božovic I., Gedik N.: *Nature Mat.* **12**, 387 (2013)
5. Gimazov I.I., Sakhin V.O., Talanov Yu.I., Adachi T., Noji T., Koike Y.: *Appl. Magn. Reson.* **48**, 861 (2017)

Anomalous Features of Antiferromagnetic Resonance in GdB_6

**A. V. Semeno¹, M. I. Gilmanov^{1,2}, N. E. Sluchanko, N. Yu. Shitsevalova³,
V. B. Filipov³, S. V. Demishev¹**

¹ Prokhorov General Physics Institute of RAS, Moscow 119991, Russian Federation, semeno@lt.gpi.ru

² Moscow Institute of Physics and Technology, Dolgoprudny 141701, Russian Federation

³ Frantsevich Institute for Problems of Materials Science NASU, Kiev, Ukraine

We report first measurements of electron spin resonance (ESR) performed as in paramagnetic (PM) and in antiferromagnetic (AFM) phases of the metallic antiferromagnet GdB_6 ($T_N = 15.5$ K). Single resonance line is observed above T_N . It is found that strong line broadening starts in PM below $T^* \sim 70$ K accompanied by the shift of g -factor from its high temperature value $g \approx 2$. The relation between g -factor and the linewidth ΔW in this range is: $\Delta W(T) \sim \Delta g(T)$. Such behavior is not typical for AFM metals and may be caused by the motion of Gd^{3+} ions in oversized boron cages. The transition to AFM phase manifests itself by abrupt shift of the line position (from $B_0 \sim 1.9$ T до $B_0 \sim 3.9$ T at $\nu = 60$ GHz) with further smooth evolution characterized by four-line structure formation shifting to lower fields. The dependence $\omega(B_0)$ in AFM phase is well described by the model of easy axis antiferromagnet $\omega/\gamma = (H_A H_E + H_0^2)^{1/2}$, where H_E is the exchange field and H_A is the anisotropy field, which allows us estimating the latter parameter as $H_A \approx 800$ Oe. The origin of H_A may be explained by dipole-dipole interaction induced by mutual shift of Gd^{3+} ions. In this case the value of H_A gives the upper limit of this shift as $\sim 10\%$.

This work was supported by RSF Grant No. 17-12-01426.

SECTION 6

MODERN METHODS OF MAGNETIC RESONANCE

X band CW EPR Studies of Chemical Reactions of Relevance to Renewable Fuels

R. D. Britt

Department of Chemistry, University of California, Davis 95616, CA USA

In the modern EPR world with many pulse techniques at our disposal, carried out with instruments over an exceedingly wide range of microwave frequencies and magnetic fields, it is worth noting that the old standard X-band CW EPR spectrometer is still the source of many interesting scientific results. I will describe two such X band CW EPR projects currently underway in our laboratory, both of relevance to renewable energy research.

1) Cyanobacteria were the first organisms capable of oxygenic photosynthesis, and their evolution ultimately transformed the planet, converting an anaerobic biosphere to a largely aerobic one. Cyanobacteria are the simplest organisms known to possess a circadian clock, which provides a temporal basis for guiding gene expression on a 24 hr cycle, therefore allowing for increased photosynthetic efficiency by providing a mechanism for the organism to synchronize its metabolism to the light/dark cycle. The cyanobacterial clock is remarkably simple, with a set of three proteins, KaiA, KaiB, and KaiC, that can carry out the cycle *in vitro* via a biochemical mechanism involving sequential phosphorylation and dephosphorylation of two amino acids in KaiC. We are using site directed spin labeling and X-band CW EPR to monitor the mobility of selected residues over the 24 hour cycle to test and refine mechanistic models for the Kai clock function.

2) There is much interest in using metal oxide catalysts to split water to provide electrons and protons for solar fuel generations, following nature's example of using a manganese oxide cluster for this process in PSII. Relevant metals include Ir, Ru, and earth abundant metals such as Mn, Fe, Co, and Ni. Over the past few years a variety of metallo-oxide synthetic catalysts have been generated and have been the focus of much mechanistic study. We are interested in isotopic specific measurements to measure the $^{16}\text{O}/^{18}\text{O}$ ratios of the first O_2 molecules generated at the onset of electrochemical water oxidation catalysis. The EPR spectrum of O_2 discriminates the isotopic composition due to spin-rotational couplings, and X band CW EPR is sensitive enough to measure the reduced mass of the initial O_2 formed, allowing us to determine if oxygen is exclusively water-sourced (catalysis carried out in H_2^{18}O) or whether the initial O_2 includes ^{16}O sourced from the metal oxide catalyst itself. These results will provide useful constraints on mechanistic models of the various catalysts.

Peculiar Features of the Spectrum Saturation Effect When the Spectral Diffusion Operates

**K. M. Salikhov¹, M. M. Bakirov¹, B. Bales², R. T. Galeev¹,
I. T. Khairuzhdinov¹**

¹ Zavoisky Physical-Technical Institute, FRC Kazan Scientific Center of RAS, Kazan 420029,
Russian Federation

² Center for Biological Physics, California State University at Northridge, CA 91330, USA

An analysis of the saturation effect for model situations where the set of resonant frequencies of spin packets is described by the Gaussian distribution or there are only two frequencies will be presented. Spectral diffusion, which is a random process without correlation, is included in both models. The shape of the spectrum is obtained for arbitrary values of magnetic resonance parameters: relaxation times of the longitudinal and transverse components of the system magnetization vector, spectral diffusion rate and dispersion of the Gaussian distribution of resonance frequencies and magnetic induction of the microwave field. The results are compared with the solutions available in the literature for particular cases. The saturation curve of the spectrum is found. For the optimal case, when the frequency of the microwave field coincides with the average for the Gaussian distribution of resonant frequencies, a detailed analysis of the saturation curve of the spectrum is presented. An algorithm for finding the spin-lattice relaxation time is formulated using the experimental value of the microwave field induction at which the saturation curve passes through the maximum.

The saturation of the spins spectrum with two separated lines is theoretically analyzed in detail. Under the conditions of saturation of the spectrum, new effects associated with the interaction of spins with the microwave field appear: only in the presence of spectral diffusion new states appear, which were not in the original system. The resonance frequency associated with these new states depends on the splitting of the original resonant frequencies, on the speed of spectral diffusion and on the amplitude of the microwave field.

In this paper we present the results of an experimental study of the saturation effect in solutions of nitroxyl radicals (TEMPOL-15N-d17). To interpret the obtained experimental results, we used kinetic equations, which were discussed in detail in our work [1–3]. In these papers we have given General solutions for the case of linear response of systems. In this paper, we present the solution of these equations for solutions of nitroxyl radicals and use this solution to analyze the obtained experimental data.

1. Salikhov K.M.: Appl. Magn. Reson. **38**, 237 (2010)
2. Salikhov K.M., Bakirov M.M., Galeev R.T.: Appl. Magn. Reson. **47**, 1095 (2016)
3. Bales B.L. *et al.*: Appl. Magn. Reson. **48**, 1375 (2017)

Kinetics of the Polarization Transfer in the Disordered Spin System ^8Li - ^6Li of LiF Single Crystal

A. D. Gulko, F. S. Dzheparov, D. V. Lvov, A. N. Tyulyusov

National Research Center "Kurchatov Institute" (ITEP), Moscow 117258, Russian Federation,
dzheparov@itep.ru

The fundamental problem of random walks in disordered media is studied on the example of delocalization of the polarization of beta-active nuclei (beta-nuclei) ^8Li within impurity nuclei subsystem, formed by beta-nuclei and stable impurity ^6Li nuclei, which are present in the single crystal LiF with controlled concentration $c \leq 0.1$. The nuclei ^8Li were produced in the reaction $^7\text{Li}(\bar{n}, \gamma)^8\text{Li}$ on thermal polarized neutrons. The process is initiated by magnetic dipole-dipole interactions and consists in polarization transfer from initially polarized beta-nucleus ^8Li to nearest nuclei ^6Li and in the subsequent migration of the polarization among ^6Li nuclei with possible returning to the nucleus ^8Li . The kinetics of depolarization of the ^8Li nuclei was detected by measuring of the beta-decay asymmetry relative external magnetic field \mathbf{H}_0 . The process was studied until the diffusion asymptotics was achieved. The measurements were fulfilled for ^6Li concentrations $3\% < c < 10\%$, and for external fields $200 \text{ G} < H_0 < 1200 \text{ G}$.

Compared with previous study [1] new results contain more accurate numeric Monte-Carlo simulation of the process, and approximation of the results of the simulation (for subsequent comparison with the experiment) is fulfilled with very realistic analytical relations, which produce exact result in the main order of concentration (without application of continuum media approximation). It is shown, that the theory, constructed *ab initio*, is in reasonable agreement with the experimental results without using fitting parameters.

1. Abov Yu.G., Gulko A.D., Dzheparov F.S., Ermakov O.N., Lvov D.V., Lyubarev A.A.: Physics of Atomic Nuclei **77**, 682 (2014)

SECTION 7

LOW-DIMENSIONAL SYSTEMS AND NANO-SYSTEMS

High-Frequency Magnetic Resonance and Cross-Relaxation Effects in Rare Earth Doped YAG

N. G. Romanov, R. A. Babunts, A. G. Badalyan, P. G. Baranov

Ioffe Institute, St. Petersburg 194021, Russian Federation, nikolai.romanov@gmail.com

High-frequency electron paramagnetic resonance (EPR), electron spin echo (ESE) and optically detected magnetic resonance (ODMR) have been applied to study paramagnetic centers and cross-relaxation effects in garnet crystals doped with cerium and other rare earth ions.

In this study, we used a newly developed EPR-ESE-ODMR spectrometer with modern microwave bridges that operate in the near-terahertz region (0.094 THz and 0.130 THz) both in continuous wave and pulse modes and include extremely stable microwave generators and sensitive super heterodyne receivers with IQ detectors. A closed-circle magneto-optical cryostat with a split-coil superconducting magnet, which does not require cryogenic liquids and the corresponding infrastructure, made it possible to scan the magnetic field in a very wide range (up to 7 T) with the possibility of inversion of the field and a smooth transition through zero. The sample temperature could be varied from 1.5 to 300 K. Optical access to the sample was provided by four windows and allowed to measure photo-EPR and ODMR. ODMR was also studied using a 35 GHz ODMR spectrometer with an immersion-type cryostat.

We investigated cerium doped yttrium aluminum garnet (YAG) crystals grown from the melt by vertical directed crystallization. They were both gadolinium free and contained gadolinium in different concentrations. EPR, ESE and ODMR of non-Kramers Tb^{3+} ions have been found in these crystals in addition to Ce^{3+} and Gd^{3+} . Obviously Tb^{3+} entered YAG:Ce,Gd crystals as a contaminating impurity. EPR measurements were performed at 94 and 130 GHz both in cw and ESE modes. It was shown that the Tb^{3+} centers in YAG have nearly axial symmetry about $\{100\}$ axes and can be described by the spin Hamiltonian $\mathcal{H} = g_{\parallel}\mu(B\cos\theta)S_z + \Delta xS_x + \Delta yS_y + AS_zI_z$ with the following parameters: $g_{\parallel} = 15.8 \pm 0.2$, $\Delta = (\Delta x^2 + \Delta y^2)^{1/2} = 2.705 \pm 0.005 \text{ cm}^{-1}$, and $A = 0.197 \pm 0.005 \text{ cm}^{-1}$. Additional Tb^{3+} centers with slightly larger Δ were found and ascribed to Tb^{3+} ions with nearby defects. For one of them the zero-field splitting $\Delta = 3.1335 \text{ cm}^{-1}$ is very close to the energy of the 94 GHz microwave quantum and strong ESE signals were observed at zero magnetic field. Thus photon echo on hyperfine components of the Stark levels of Tb^{3+} at zero fields can be studied.

Direct evidence of the cross-relaxation effects in garnet crystals containing two electron spin systems, i.e., the simplest one of Ce^{3+} ions with the effective spin $S = 1/2$ and the system of Gd ions with the maximum spin $S = 7/2$, has been demonstrated by ODMR. Using ODMR technique that can be called “magnetic circular dichroism in luminescence excitation” it was possible to monitor the spin polarization of the Ce^{3+} ground state, which could be influenced directly by microwave-induced resonant EPR transitions between the spin sublevels of

Ce^{3+} , but also due to cross-relaxation of Ce^{3+} with another paramagnetic center [1]. EPR of Gd^{3+} was detected via PL of Ce^{3+} in YAG:Ce,Gd crystals that contained gadolinium in a concentration from the lowest (0.1%) to 100%. Specific behavior of cross-relaxation signals was studied.

A fundamental difference in the effect of magnetic field on the spin-dependent recombination in non-magnetic and magnetic matrices has been discovered. In preliminarily irradiated gadolinium garnet crystals doped with cerium, a giant increase of spin-dependent recombination afterglow in magnetic field has been found and ascribed to huge internal magnetic fields created by the magnetic moments of the unpaired electrons of the gadolinium ions. These fields suppress the recombination of radiation defects due to their spin alignment. Application of external magnetic field results in cross relaxation between the spin sublevels of Gd^{3+} ions and the levels of radiation-induced electron or hole centers and results in reorientation of their spins, which makes recombination allowed for a part of centers.

In YAG containing cerium and terbium ions, we have found ODMR of Tb^{3+} by monitoring PL intensity of Ce^{3+} , which cannot be explained by cross-relaxation but implies a connection between two spin systems. This result seems to be important since Ce^{3+} ions in garnets are considered as hardware for quantum information storage and processing [2].

1. Tolmachev D.O., Gurin A.S., Uspenskaya Yu.A., Asatryan G.R., Badalyan A.G., Romanov N.G., Petrosyan A.G., Baranov P.G., Wieczorek H., Ronda C.: Phys. Rev. B **95**, 224414 (2017)
2. Kolesov R., Xia K., Reuter R., Jamali M., Stohr R., Inal T., Siyushev P., Wrachtrup J.: Phys. Rev. Lett. **111**, 120502 (2013)

ESR Study of a Spin Ladder Magnet with Defects

**V. Glazkov^{1,2}, Y. Krasnikova^{1,2}, A. Pomomaryov³, S. Zvyagin³,
D. Schmidiger⁴, K. Povarov⁴, S. Galeski⁴, A. Zheludev⁴**

¹ P. Kapitza Institute for Physical Problems RAS, Moscow 119334, Russian Federation, glazkov@kapitza.ras.ru

² National Research University “Higher School of Economics”, Moscow, Russian Federation

³ Dresden High Magnetic Field Laboratory, Helmholtz-Zentrum, Dresden-Rosendorf D-01328, Dresden, Germany

⁴ Neutron Scattering and Magnetism, Laboratory for Solid State Physics, ETH Zurich, Zurich 8006, Switzerland

Spin ladder, a system of two coupled spin chains, is one of well studied toy models of magnetism. Excitation spectrum of spin ladder is gapped for arbitrary antiferromagnetic couplings along the leg and rung of the ladder (J_{leg} and J_{rung}). Due to this energy gap Δ , magnetic response of spin ladder at low temperatures $T \ll \Delta$ can be described as that of diluted gas of triplet ($S = 1$) quasiparticles. As the quasiparticles population numbers increase on heating, they began to interact and system enters strongly correlated “spin liquid” regime at $T \sim J_{\text{leg}}, J_{\text{rung}}$, which in turn cross to conventional paramagnetic regime at high temperatures. High energy resolution of ESR spectroscopy allows to follow through these regimes. In particular, ESR spectroscopy gives insight into relaxation processes and allows to resolve fine structure of triplet sublevels with accuracy unattainable by other experimental techniques.

Organometallic compound DIMPY (short for $(\text{C}_7\text{H}_{10}\text{N})_2\text{CuBr}_4$) is an example of strong-leg spin ladder with dominating exchange along the legs of the ladder: $J_{\text{leg}} = 1.42$ meV, $J_{\text{rung}} = 0.82$ meV and energy gap $\Delta = 0.33$ meV [1]. ESR of the pure DIMPY was studied in details earlier [2], these studies revealed presence of Dzyaloshinskii-Moriya (DM) interaction governing spin relaxation in DIMPY. Symmetry of DIMPY crystal fixes unusual pattern of DM interaction: it is uniform along the legs of the ladder and DM vectors on the neighboring legs are exactly opposite.

Here we report results of ESR study of diamagnetically diluted DIMPY with part (up to 6%) of $S = 1/2$ copper ions substituted by Zn. Zn doping breaks some of the rungs of the ladder leaving free spin $S = 1/2$ of the copper ion, which is “spread” over some distance (of the order of correlation length) along the ladder. These multispin objects (clusters) interact with triplet excitations and with each other, at low temperatures, as the population of excitations vanishes, they form correlated “spin islands” with non-zero net magnetization [3].

We have studied ESR of Zn-diluted DIMPY from 450 mK to 300 K. At low temperatures ESR response is dominated by multispin clusters. Analysis of ESR intensity and linewidth concentration dependences provides evidences of cluster-cluster interaction: ESR intensity increases nonlinearly with Zn content, indicating formation of cluster-cluster antiferromagnetic correlations), and ESR linewidth decreases with increasing Zn content, indicating that exchange nar-

rowing phenomenon enters the play as cluster-cluster mean distance decreases. At temperatures above 3...5 K collective gapped excitations dominate magnetic response of the Zn-doped DIMPY. However doping affects spin relaxation in this triplet-dominated regime: surprisingly, ESR linewidth (which is, essentially, inverse spin relaxation time) *decreases* with increasing Zn content. In the same time, scaling of linewidth angular dependences at different temperatures and for different doping levels (pure DIMPY including) proves, that *the same* anisotropic spin-spin interaction is responsible for spin relaxation in pure and Zn-doped samples. Thus, doping effectively “shortens” DM vector through some mechanism.

Thus, we observed different regimes of ESR response in pure and doped spin-ladder. These regimes are analyzed in terms of quasiparticles and spin clusters interaction. Effect of doping on quasiparticles relaxation in triplet-dominated regime is observed.

The work was supported by the Russian Foundation for Basic Research and by the RAS Presidium Program “Electron Spin Resonance, Spin Dependent Electronic Effects and Spin Technologies”.

1. Schmidiger D. *et al.*: Phys. Rev. Lett. **111**, 107202 (2013)
2. Glazkov V. *et al.*: Phys. Rev. B **92**, 184403 (2015)
3. Schmidiger D. *et al.*: Phys. Rev. Lett. **116**, 257203 (2016)

Microwave Dielectric Anomaly in $S = 1$ Quantum Antiferromagnet at Spin Gap Closing

**A. I. Smirnov¹, T. A. Soldatov¹, K. Yu. Povarov², E. Wulf², A. Mannig²,
A. Zheludev³**

¹ P. L. Kapitza Institute for Physical Problems RAS, Moscow 119334, Russian Federation

² ETH Zürich, Zürich 8093, Switzerland

$\text{NiCl}_2\text{-}4\text{SC}(\text{NH}_2)_2$, known as DTN, is a gapped $S = 1$ system with a single-ion anisotropy D dominating over the exchange interaction J : $D = 7.9$ K, $J = 2.2$ K. The exchange network is quasi one-dimensional with interchain exchange of about $0.1J$. The ground state is quantum-disordered and the spin-liquid behavior is provided mainly by the easy-plane type of the single ion anisotropy (positive D) which makes zero projection of the spin component preferable and stabilized by an energy gap [1]. Nevertheless, the spin gap of the collective triplet excitations propagating along the network of exchange bounds, may be closed in an external magnetic field of about 2 T, which causes the quantum phase transition from a spin liquid to 3D long range antiferromagnetic order [2]. This order is peculiar through a specific antiferromagnetic resonance [3], strong magnetostriction and electric polarization [4]. Now we report the observation of a nonresonant dynamic magnetic susceptibility in the ordered phase, which is measured by recording the shift of the frequency of the microwave resonator and its Q-factor vs magnetic field. The nature of the observed unconventional spin dynamics, resulting in a wide-range (7–90 GHz) strong nonresonant dynamic susceptibility of about 5 emu/mole, which exceeds the static susceptibility for about 10 times, will be discussed. This dynamic susceptibility indicates a low-frequency range of dynamic correlations which is probably associated with the Goldstone mode of the antiferromagnetic resonance of an easy-plane antiferromagnet in a magnetic field, modified by the mechanical stress due to magnetoelectric interaction or by the antiphase oscillations of two interpenetrating antiferromagnetic structures, which should occur in a body-centered tetragonal lattice carrying magnetic ions [5].

1. Wierschem K., Sengupta P.: *Mod. Phys. Lett. B* **28**, no. 32, 1430017 (2014)
2. Tsyrlin N. *et al.*: *J. Phys.: Condens. Matter* **25**, 216008 (2013)
3. Zvyagin S. *et al.*: *Phys. Rev. B* **77**, 092413 (2008)
4. Zapf V.S. *et al.*: *Phys. Rev. B* **83**, 140405(R) (2011)
5. Sizanov A.V., Syromyatnikov A.V.: *J. Phys.: Condens. Matter* **23**, 146002 (2011)

Electron Spin Resonance in 2D Systems Formed in [001] AIAs Quantum Wells

**A. V. Shchepetilnikov¹, D. D. Frolov¹, Yu. A. Nefyodov¹,
I. V. Kukushkin^{1,2}, L. Tiemann³, C. Reichl³,
W. Dietsche³, W. Wegscheider³**

¹ Institute of Solid State Physics RAS, Chernogolovka 142432, Moscow district, Russian Federation, shchepetilnikov@issp.ac.ru

² National Research University Higher School of Economics, Moscow 101000, Russian Federation

³ Solid State Physics Laboratory, ETH Zurich, Zurich 8093, Switzerland

The spin resonance of two dimensional electrons confined in the high quality [001] AIAs quantum wells was studied. Electron spin resonance (ESR) turned out to be detectable even if magnetic field was parallel to the plane of the two-dimensional system. As a result, the in-plane anisotropy of the electron g -factor could be measured with high accuracy. In case of the magnetic field aligned along [110] or $\bar{[110]}$ crystallographic axes only one ESR peak was observed, whereas it tended to split in two well-separated peaks when the in-plane component of the magnetic field was between these directions. This fact clearly indicates that two in-plane valleys at X-points of the Brillouin zone were occupied with electrons and each valley was characterized by the anisotropic g -factor with the [100], [010] and [001] principal axes. The principal g -factor values were extracted.

Spin dynamics of nuclei located in AIAs quantum well was studied with the aid of ESR. Dynamic polarization of nuclear spins due to the hyperfine interaction resulted in the so-called Overhauser shift of the ESR. Overhauser shift diminished resonantly when the RF-radiation of certain frequencies was applied to the sample. This effect served as an indirect, yet powerful method for nuclear magnetic resonance detection: NMR quadrupole splitting of ^{75}As nuclei was clearly resolved.

The nuclear spin-lattice relaxation rate extracted from the time decay of Overhauser shift was found to be dependent on the filling factor suggesting that nuclear spin relaxation is mostly due to the interaction between electron and nuclear spins. Formation of the fractional state at the filling of $2/3$ was revealed to slow down the nuclear spin relaxation rate. This observation suggests the enhancement of energy gap in the spin excitation spectrum of two-dimensional electrons at $2/3$ state.

Magnetic Resonance Force Spectroscopy of Permalloy Microstrips

E. Skorokhodov, M. Sapozhnikov, R. Gorev, V. Mironov

Institute for Physics of Microstructures RAS, Nizhny Novgorod, 603950, Russian Federation, Evgeny@ipmras.ru

We report on the magnetic resonance force microscopy (MRFM) investigations of the ferromagnetic resonance (FMR) in an individual permalloy microstrip [1]. The permalloy ($\text{Ni}_{80}\text{Fe}_{20}$) microstrips $3000 \times 500 \times 30 \text{ nm}^3$ were fabricated by e-beam lithography and lift-off technique. The MRFM spectra were investigated on a home-made magnetic resonance force microscope [1]. As a probe sensor we used standard NSG-1 cantilever (a resonant frequency of 9.2 kHz and a cantilever arm rigidity of 0.03 N/m) with a glued SmCo magnet particle. The sample was pumped at frequency 5.8 GHz by microwave generator using planar short-circuited strip line. The microwave field was modulated in amplitude with modulation depth of 100% at the cantilever resonant frequency. The pump power was 20 dBm. In the experiment the dependences of the cantilever oscillation amplitude on the external magnetizing field were recorded as FMR spectra. The typical MRFM spectra are presented in Fig. 1. The measurements were performed for different experimental geometries (different mutual orientation of external magnetic and microstrip, the different position of the probe above the sample). The features of the probe-sample interaction in magnetic resonance force microscope are demonstrated. For example it is shown that magnetic resonances can appear as peaks and dips. It depends on the position of the probe relative to the sample. The possibilities of using MRFM for studying the local microwave properties of magnetic nanostructures are discussed.

1. Скороходов Е.В., Сапожников М.В., Миронов В.Л.: Письма в ЖТФ **44**, № 5 (53), 49 (2018)

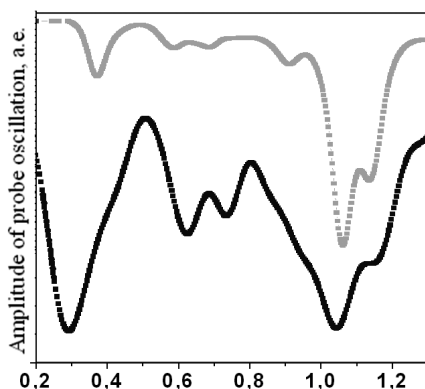


Fig. 1. MRFM spectra of NiFe microstrips. Numerical simulation (gray) and experiment (black).

Defining the Interlayer Interaction in Magnetic Multilayer Structures on the Base of the FMR Peaks Asymmetry

**O. G. Udalov^{1,3}, E. S. Demidov², S. N. Vdovichev¹, N. S. Gusev¹,
S. A. Gusev¹, V. V. Rogov¹, D. A. Tatarsky^{1,2}, I. S. Beloborodov³,
O. L. Ermolaeva¹, A. A. Fraerman¹**

¹ Institute for Physics of Microstructures RAS, Nizhny Novgorod 603950, Russian Federation

² Lobachevsky State University of Nizhny Novgorod, Nizhny Novgorod 603950, Russian Federation

³ California State University Northridge, Northridge 91331, CA, USA

Ferromagnetic resonance (FMR) is a powerful tool for studying of magnetic layered structures [1–5]. The FRM method allows obtaining the information on the magnetization magnitude and magnetic anisotropy of each layer. It also allows studying the interlayer coupling. Many efforts were spent on investigation of the coupling in the multilayer systems in which magnetic layers are separated by a non-magnetic metallic spacer [1]. In this case, the interlayer coupling is strong enough. This makes it relatively easy to determine the coupling sign and magnitude studying the shifts of the FMR peaks.

The situation is different for the case of magnetic tunnel junctions where ferromagnetic layers are separated by an insulator leading to a much weaker interlayer coupling [6]. Defining the interlayer interaction is a tricky issue in this case. The mutual shifts of FMR peaks is small comparing to the peak width [3, 4]. The situation becomes more complicated when resonant fields (frequencies) of the peaks are close to each other. In this case, a completely different approach is needed.

In the present work we propose to define the interlayer interaction sign and magnitude by studying the FMR peaks shape rather than the shift. We will

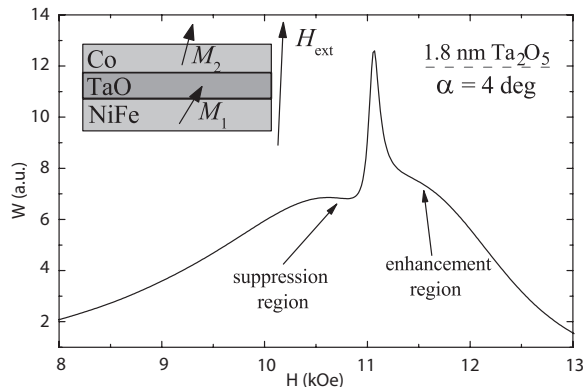


Fig. 1. FMR spectrum of NiFe/TaO (1.8 nm)/Co multilayer for perpendicular orientation of magnetic field. FMR peak asymmetry is clearly seen.

show that interaction induces FMR peaks asymmetry. Such an asymmetry can be considered as the Fano resonance in a magnetic multilayer [7]. We propose to use this asymmetry to define interaction sign and magnitude. Such a method is particularly useful when resonance frequencies of two interacting layers are close to each other.

Studying of interaction sign and magnitude with the conventional method based on the FMR peaks shift requires a reference sample without interaction. Only in this case one can define the peak shift. The method based on the peak shape does not have such a disadvantage. One can define the interaction sign and magnitude using a single sample.

In this work, we provide simple model demonstrating how such an asymmetry occurs. Numerical modeling of realistic FM1/I/FM2 system supports analytical results. We also demonstrate experimentally appearance of the asymmetric peak in FMR resonance of Ni/Ta₂O₅/Co multilayer. We fabricate such structures with different thickness of the insulating spacer. We measured FMR spectrums at different orientations of external magnetic field with respect to the multilayer surface. Fig. 1 shows the FMR peak of Ni/Ta₂O₅/Co multilayer. One can easily see the peak asymmetry. This asymmetry appears due to the FM interaction between magnetic layers. Fitting of the experimental data gives us the sign and the magnitude of the interaction. Existence of the interlayer coupling is confirmed with the magneto-optical Kerr effect measurements.

This research was supported by the Russian Science Foundation (Grant No. 16-12-10340).

1. Lindner J., Baberschke K.: *J. Phys.: Condens. Matter* **15**, S465 (2003)
2. Nascimento V.P., Saitovitch E.B., Pelegrinia F., Biondo A., Passamani E.: *J. Appl. Phys.* **99**, 08C108 (2006)
3. Popova E., Tiusan C., Schuhl A., Gendron F., Lesnik N.A.: *Phys. Rev. B* **74**, 224415 (2006)
4. Popova E., Keller N., Schuhl A., Lesnik N.A.: *Appl. Phys. Lett.* **91**, 112504 (2007)
5. Yang Q., Nan T., Zhang Y., Zhou Z., Peng B., Ren W., Ye Z.-G., Sun N.X., Liu: M.: *Phys. Rev. Appl.* **8**, 044006
6. Wong J.J.I., Ramirez L., Swartz A.G., Hoff A., Han W., Li Y., Kawakami R.K.: *Phys. Rev. B* **81**, 094406 (2010)
7. Joe Y.S., Satanin A.M., Kim C.S.: *Physica Scripta* **74**, 259 (2006)

SECTION 8

PERSPECTIVE OF MAGNETIC RESONANCE IN SCIENCE AND SPIN-TECHNOLOGY

In situ Irradiation in NMR, Some Concepts and Applications

G. Gescheidt

Institute of Physical and Theoretical Chemistry, Graz University of Technology,
Graz 8010, Austria

Photocatalysis presently experiences a renaissance in chemistry [1]. Several reactions have been tested in terms of being accessible to photo-induced procedures. The advantages of this synthetic method are that reactions can be precisely triggered, mostly proceed rapidly, and are energy-efficient. Moreover photo-induced reactions can be performed in microfluidic reaction vessels.

For the optimization and the understanding of photo-induced reactions, precise monitoring is crucial. We have been developing setups, which allow following light-triggered reactions *in situ* using magnetic resonance, particularly NMR.

The challenges are transferring appropriate light intensity into the NMR probehead and matching the optically-active and NMR-detectable volume (Fig. 1) [2].

I will present advantages of new experimental setups and highlight their application in NMR and, *e.g.*, for *in situ* “Photo-Induced Reversible Acceleration of T-1-Relaxation” (PIRAT) [3].

1. Corrigan N., Shanmugam S., Xu J.T., Boyer C.: *Chem. Soc. Rev.* **45**, 6165–6212 (2016)
2. Stadler E., Eibel A., Neshchadin D., Gescheidt G.: *Z. Phys. Chem.* **231**, 625–636 (2017)
3. Stadler E., Dommaschk M., Fruhwirt P., Herges R., Gescheidt G.: *Chemphyschem* **19**, 571–574 (2018)

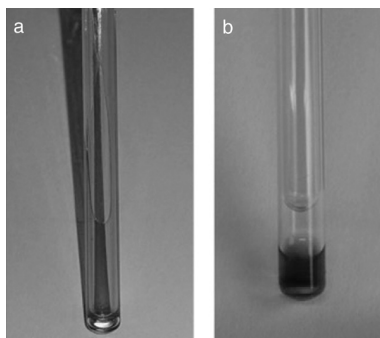


Fig. 1. Double-tube setup for matching the optically and NMR accessible volume of a sample tube.

Excited Coherent Quantum States

Yu. M. Bunkov

Institute of Physics, Kazan Federal University, Kazan 420008, Russian Federation,
Yury.bunkov@neel.cnrs.fr

The new state of matter has been discovered in 1984 in antiferromagnetic superfluid ^3He – the spontaneously self-organized phase-coherent precession of spins [1, 2]. This state has all the signatures of spin superfluidity, but it is radically different from the conventional ordered states in magnets. It is the quasi-equilibrium state, which emerges on the background of the ordered magnetic state, and which can be represented in terms of the Bose condensation of magnetic excitations – magnons. This discovery opened the new class of the systems, the Bose-Einstein condensates of quasiparticles and collective modes, whose number is not conserved. Representatives of this class in addition to BEC of magnons are the BEC of phonons, excitonpolaritons, photons, rotons and other possible bosonic modes. The life time of these condensates is finite, but can be very long, reaching minutes in antiferromagnetic superfluid $^3\text{He-B}$. There is no phenomenon of magnon BEC at thermodynamic equilibrium.

However, the density of magnons can be drastically increased by a magnetic resonance methods. The excited magnons can form the quasi-equilibrium state with a time scale of about few quasiparticles scattering time. Magnon-magnon scattering conserves the total number of quasiparticles and hold the distribution function with the effective temperature T and effective chemical potential μ . The critical density of magnons can be estimated from equation

$$T_{\text{BEC}} \approx 3.31(\hbar^2/k_B m)(N_c)^{2/3},$$

in which temperature is a given temperature of phonons (which determines the magnetization M and density of thermal magnons. N_c is the critical density for magnon BEC at given temperature. In difference with atomic BEC, in the case of magnon BEC we are able to increase the density of excited magnons at constant temperature. At the magnons excitation, at conditions, when $N_M > N_c$ the magnons should forms a BEC state, under certain conditions, which will be discussed in this presentation.

Our presentation is devoted to a detailed description of magnonic superfluid phenomena in magnetically ordered materials, from antiferromagnetic superfluid ^3He to Easy plain antiferromagnets with suhlnacamura interaction [3] and Yttrium Iron Garnet (YIG). We discuss different phases of magnon superfluidity, including those in magnetic trap; and the observed signatures of spin superfluidity of magnon BEC: (i) spin supercurrent, which transports the magnetization on a macroscopic distance (as long as 1 cm); (ii) spin current Josephson effect which shows interference between two condensates; (iii) spin current vortex – a topological defect which is an analog of a quantized vortex in superfluids, of an Abrikosov vortex in superconductors, and cosmic strings in relativistic theories;

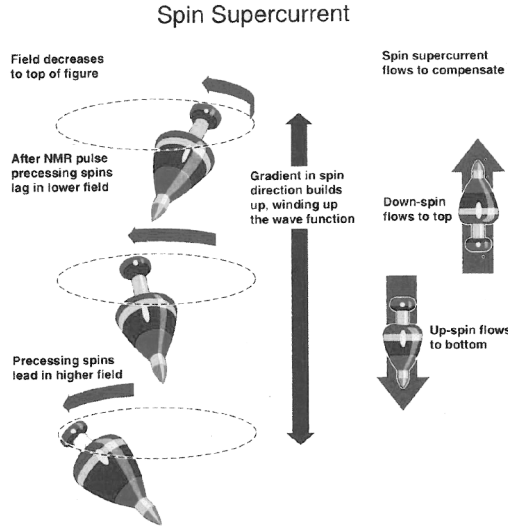


Fig. 1. After an NMR pulse, the nuclear spins precess around the steady magnetic field direction. Spins precess more slowly at the top and the variation in precession rates gradually establishes a gradient in the spin direction. This winds up the wave function and a vertical counterflow of upspin and dawn-spin is induced to compensate.

(iv) Goldstone modes related to the broken $U(1)$ symmetry – phonons in the spin-superfluid magnon gas. The BEC of magnons have been observed later in several magnetic systems, including the chiral and polar phases of superfluid ^3He , solid antiferromagnets and ferrites etc. We also touch the topic of spin supercurrent in general including spin Hall and intrinsic quantum spin Hall effects. The connections to the other areas of physics will also be discussed. The spin superfluidity of the magnon BEC type may have important applications in spintronic and magnonics. While for superconductivity we still need the low temperature, in solid state magnets the coherent spin precession may be achieved at room temperature.

1. Borovik-Romanov A.S., Bunkov Yu.M., Dmitriev V.V., Mukharskiy Yu.M.: JETP Letters **40**, 1033, (1984)
2. Bunkov Yu.M., Volovik G.E.: “Spin superfluidity and magnon BEC”, Chapter IV of the book “Novel Superfluids” (K. H. Bennemann, J. B. Ketterson, eds.) Oxford University press 2013. arXiv:1003.4889v3
3. Bunkov Yu.M., Alakshin E.M., Gazizulin R.R., Klochkov A.V., Kuzmin V.V., L'vov V.S., Tagirov M.S.: Phys. Rev. Lett. **108**, 177002 (2012)

Magnetic Moments in Topological Insulators Studied by EPR

V. Sakhin¹, A. Kiyamov², E. Kukovitsky¹, N. Garifyanov¹, R. Khasanov³,
Yu. Talanov¹, G. Teitel'baum¹

¹Zavoisky Physical-Technical Institute, FRC Kazan Scientific Center of RAS, Kazan 420029,
Russian Federation, sahin@kfti.knc.ru

²Kazan Federal University, Kazan 420008, Russian Federation

³Paul Scherrer Institute, Villigen 5232, Switzerland

Local magnetic moments embedded in the structure of topological insulators (TI) may dramatically change the physical properties of the system. The driving force of these changes is a time-reversal symmetry (TRS) breaking, that take place upon the magnetic ordering [1]. But the role of the local magnetic moments origin in such changes remains unclear. Using methods of SQUID-magnetometry and EPR spectroscopy we investigated two cases: a) local moments represent a doped magnetic ions; b) magnetic moments are intrinsic and originate from nonmagnetic structure defects.

The impact of doped magnetic ions was studied on Bi_2Te_3 TI single crystals, doped with Mn ions. Here the spins of introduced ions undergo ferromagnetic (FM) ordering due to strong indirect Ruderman-Kittel-Kasuya-Iosida (RKKY) exchange. RKKY is also responsible for eliminating fine structure of EPR spectra, which shows the features typical for FM-coupled system [2]. More than that, temperature dependence of EPR signal integral intensity is in consistence with SQUID-magnetometry data. This implies that in our system the transition to “diluted ferromagnet” phase takes place.

The specifics of intrinsic moments in TI was studied using the $\text{Bi}_{1.08}\text{Sn}_{0.02}\text{Sb}_{0.9}\text{Te}_2\text{S}$ single crystals [3]. Local magnetic moments in this compound originate from anti-site substitution defects in the central layer of quintuple layer structure. We show that intrinsic moments form superparamagnetic phase that consists of single-domain FM nanoinclusions imbedded into the perfect TI structure. The net magnetization of the entire array of such nanoparticles equals zero due to the random orientations of anisotropy fields for different nanoparticles.

In summary, we found that magnetic state of TI, corresponding to the presence of local magnetic moments, is determined by their origin, concentration and distribution.

1. Hor Y.S. *et al.*: Phys. Rev. B. **81**, 195203 (2010)
2. Sakhin V.O. *et al.*: JMMM **459**, 90–294 (2018)
3. Sakhin V.O. *et al.*: J. Supercond. Nov. Magn. **30**, 63–67 (2017)

SECTION 9

ELECTRON SPIN BASED METHODS FOR ELECTRONIC AND SPATIAL STRUCTURE DETERMINATION IN PHYSICS, CHEMISTRY AND BIOLOGY

Cu²⁺-Ion as an ESR Probe of Protein Structure

S. K. Saxena

Department of Chemistry, University of Pittsburgh, Pittsburgh, PA-15260,
sksaxena@pitt.edu

Pulsed-ESR techniques that reliably measure interspin separations in the order of 1.5–10 nm – even in non-crystalline samples – to ultimately provide an “amino-acid-level” picture of structure and structural transitions, have impacted biophysical research. The talk will discuss our efforts in developing Cu²⁺-ion based pulsed-ESR distance methods and illustrate how they were used to understand structure-function relationships of a DNA modifying protein. Finally, the talk will describe recent efforts to bind Cu²⁺-ions site selectively in proteins and in DNA. In proteins, the spin probe is assembled *in situ* from natural amino acid residues and a metal salt, and requires no post-expression synthetic modification. Initial results show that the resultant Cu²⁺-probe potentially provides distance distributions that are *five times narrower* than the common protein spin label – the approach, thus, potentially overcomes the inherent limitation of the current technology, which relies on a spin label with a highly flexible side-chain. In DNA Cu²⁺-based distance measurements directly measure the most-probable backbone distance.

Analytical Solution of the PELDOR Inverse Problem Using the Integral Mellin Transform

A. G. Matveeva^{1,2}, V. M. Nekrasov^{1,2}, A. G. Maryasov¹

¹ Voevodsky Institute of Chemical Kinetics & Combustion, SB RAS,
Novosibirsk 630090, Russian Federation, maryasov@kinetics.nsc.ru

² Novosibirsk State University, Novosibirsk 630090, Russian Federation

The PELDOR technique (also known as DEER) is widely used for molecular structure investigations since its invention [1]. The method allows distance measurements between spin labels which either naturally exist or are specially attached to the object under study. The most popular application is the distance measurements between unpaired electrons in double labeled macromolecules. The typical situation is that such a system consists of molecules in different conformations thus providing distance distribution between the pair of spin labels. Determination of this distance distribution function from experimentally measured PELDOR signal is ill posed mathematical problem, it is usually solved numerically by fitting experimental data using some regularizing assumptions. In this contribution we present analytical solution of the inverse problem [2].

The signal measured may be presented as $v(T) = \int_0^\infty f(r)K(r,T)dr$, with $K(r,T) = \int_0^1 \cos(T(1-3X^2)\gamma^2\hbar/r^3)dX$, where $f(r)$ is the distance distribution function to be obtained, γ is gyromagnetic ratio of electron spin, \hbar is Plank constant, and $X = \cos(\theta)$ with θ being the angle between vector r and external magnetic field direction. The above equation is a special case of Fredholm integral equation of the first kind. It is suitable to rewrite the equation in the form of

$$v(T) = \int_0^\infty p(w)\varphi(wT)dw, \quad (1)$$

where $w = \gamma\hbar/r^2$. Analytical form of φ was obtained long ago, it is $\varphi(Y) = \sqrt{\pi/6Y}[\cos(Y)C(\sqrt{6Y/\pi}) + \sin(Y)S(\sqrt{6Y/\pi})]$, here $C(x)$ and $S(x)$ are Fresnel functions. The equation kernel φ is a function of product of variables, wT , this allows to solve the equation using integral Mellin transform, which is defined as $Y(S) = \int_0^\infty y(x)x^{s-1}dx$, where s is a complex dimensionless variable. The real part of s is kept constant, it is chosen to make inverse transformation possible. Mellin transformation is closely related to widely used Fourier and Laplace transforms. Applying Mellin transform to the both sides of Eq. (1), one can get after some algebra $V(s) = P(1-s)\Phi(s)$, here capital letters mean Mellin transform of the respective quantities. The Mellin image of the distance distribution function is

$$P(s) = V(1-s)\Phi(1-s), \quad (2)$$

The desired distance distribution function is the inverse Mellin transformation of Eq. (2), $p(w) = \frac{1}{2\pi i} \int_{C-i\infty}^{C+i\infty} P(s)w^{-s}ds$. The kernel φ doesn't look simple,

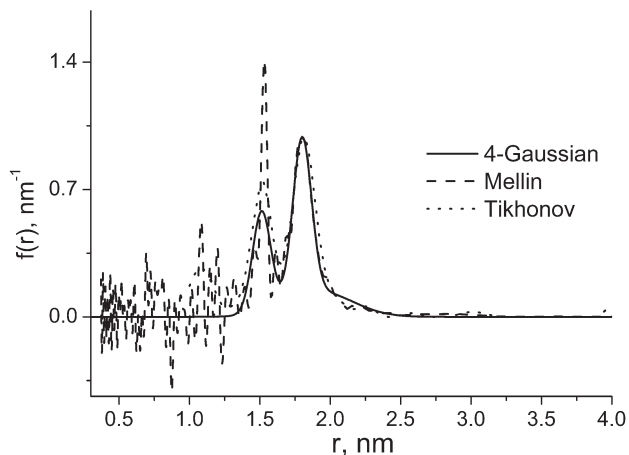


Fig. 1. Comparison of different techniques of treatment of real data obtained by PELDOR method [3]. Mellin transform is linear with respect to the input data. The feature of Mellin transform is that noise is mapped onto low distance part of the distribution function.

but its Mellin image may be calculated analytically thus making calculations much easier, it is too bulky to be presented here.

Different sources of errors and distortions are analyzed including noise level, sampling rate, signal windowing, etc.

The financial support of the Russian Science Foundation is gratefully acknowledged, A. G. Matveeva thanks project # 15-15-00021.

1. Milov A.D., Salikhov K.M., Shirov M.D.: *Fizika tverdogo tela* **23**, 975 (1981)
2. Matveeva A.G., Nekrasov V.M., Maryasov A.G.: *Phys. Chem. Chem. Phys.* **19**, 32381 (2017)
3. Matveeva A.G., Yushkova Y.V., Morozov S.V., Grygor'ev I.A., Dzuba S.A.: *Z. Phys. Chem.* **231**, 671 (2017)

Effective Method of Level Anti-Crossing Spectra of NV Centers in Diamond Calculation

S. V. Anishchik¹, K. L. Ivanov²

¹ Voevodsky Institute of Chemical Kinetics and Combustion SB RAS, Novosibirsk 630090, Russian Federation, svan@kinetics.nsc.ru

² International Tomography Center SB RAS, Novosibirsk 630090, Russian Federation, ivanov@tomo.nsc.ru

The negatively charged nitrogen-vacancy defect center (NV⁻ center) in diamond is of great interest due to its unique properties. The ground state of NV⁻ centers is a triplet state; the splitting of the energy level of the triplet depends on the spin projection on the symmetry axis. In an NV⁻ center, a selective intersystem crossing takes place from the excited triplet state to the excited singlet state, as well as from the singlet state to the ground triplet state. The rate of these processes depends on M_S , which is the spin projection on the NV⁻ symmetry axis. First, inter-system crossing leads to a much higher quantum yield of luminescence when light excitation occurs from the $M_S = 0$ state rather than from the states with $M_S = +1$ or $M_S = -1$. Second, inter-system crossing gives rise to a non-equilibrium state of the NV⁻ center after multiple cycles of light absorption and emission, with the population of the $M_S = 0$ state much higher than those of the states with $M_S = +1$ or $M_S = -1$. This effect is commonly referred to as optically induced spin polarization. Such a spin polarization, which is long-lived, enables various applications of NV⁻ centers.

Due to the magnetic dipole-dipole interactions between NV⁻ centers and other paramagnetic defects in the crystal spin polarization exchange can occur. Such a polarization transfer is of relevance for many applications. An informative method for studying such polarization transfer processes is given by the Level Anti-Crossing (LAC) spectroscopy. At LACs, there is no energy barrier for polarization transfer; consequently, coupled spins can efficiently exchange polarization. LACs give rise to sharp lines in the magnetic field dependence of the photoluminescence intensity of the NV⁻ center. The most pronounced line is observed at 1024 G, which comes from an LAC of the triplet levels in the NV⁻ center in its ground state. Other lines are termed, perhaps, misleadingly, cross-relaxation lines. In reality, all these lines are due to the coherent spin dynamics caused by spin polarization exchange at LACs of the entire spin system of interacting defect centers. Thus, it is reasonable to term the observed magnetic field dependences “LAC spectra”. For studying such LAC-lines we used sensitive lock-in detection to measure the photoluminescence intensity. This experimental technique allows us to obtain new LAC lines. Additionally, a remarkably strong dependence of the LAC-lines on the modulation frequency was found. Specifically, upon decrease of the modulation frequency from 12 kHz to 17 Hz the amplitude of the LAC-lines increases by approximately two orders of magnitude [1]. The experimental method was described in detail in previous publications [1, 2].

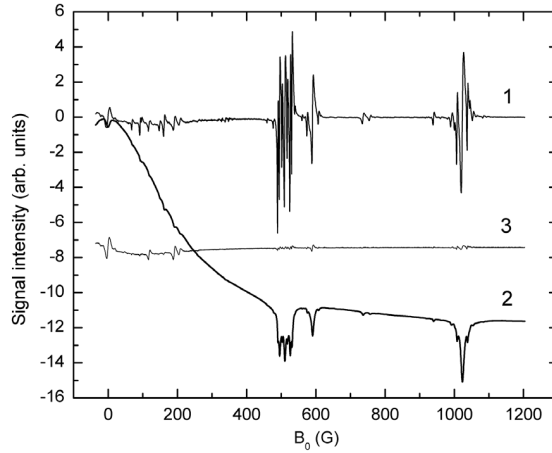


Fig. 1. Experimental LAC spectra of NV^- centers in a diamond single crystal. Lock-in signals (curves 1 and 3) and integrated spectrum 1 (curve 2). The laser light polarization vector \mathbf{E} is perpendicular to the magnetic field vector \mathbf{B}_0 (curve 1) or parallel to \mathbf{B}_0 (curve 3). Here $[111] \parallel \mathbf{B}_0$; the modulation frequency was 17 Hz. The modulation amplitude was 0.5 G.

In this work, we used our previously published experimental data [1]. In Fig. 1 we show the experimental LAC lines for a diamond single crystal with a very precise alignment of the crystal so that its $[111]$ axis is parallel to the external magnetic field (with an accuracy of a few angular minutes). Only one line in the LAC spectrum (the one at 1024 G) corresponds to the LAC in a single NV^- center in its ground state. All other lines correspond to LACs in coupled systems of NV^- center and other paramagnetic defects in the diamond crystal.

For understanding the nature of different lines in LAC spectrum we made use of a model, developed previously [3] for simulating coherent polarization transfer phenomena. In this model, we assume that light irradiation continuously generates electron spin polarization of the NV^- center. We neglect the spin evolution occurring during light excitation and relaxation to the ground state, thereby assuming that such processes are much faster than spin polarization transfer. Hence, we consider only polarization from the ground state of the NV^- centers; polarization transfer in the excited state can be treated in a similar manner.

For two interacting centers in the magnetic field \mathbf{B}_0 the Hamiltonian takes the form:

$$\begin{aligned}
 H = & \beta \mathbf{B}_0 g_1 \mathbf{S}_1 + D_1 [S_{1z}^2 - S_1(S_1 + 1)/3] + E_1 (S_{1x}^2 - S_{1y}^2) + \sum \mathbf{S}_1 A_i \mathbf{I}_i + \\
 & \sum P_i [I_{iz}^2 - I_i(I_i + 1)/3] + \beta \mathbf{B}_0 g_2 \mathbf{S}_2 + D_2 [S_{2z}^2 - S_2(S_2 + 1)/3] + E_2 (S_{2x}^2 - S_{2y}^2) + \\
 & \sum \mathbf{S}_2 A_j \mathbf{I}_j + \sum P_j [I_{jz}^2 - I_j(I_j + 1)/3] + D_{\text{dd}} [3(\mathbf{S}_1 \cdot \mathbf{n}_{12})(\mathbf{S}_2 \cdot \mathbf{n}_{12}) - \mathbf{S}_1 \cdot \mathbf{S}_2], \quad (1)
 \end{aligned}$$

Here β is the Bohr magneton, \mathbf{S}_1 and \mathbf{S}_2 are the electron spin operators of NV^- center and of the second paramagnetic center, as well as g_1 and g_2 are theirs

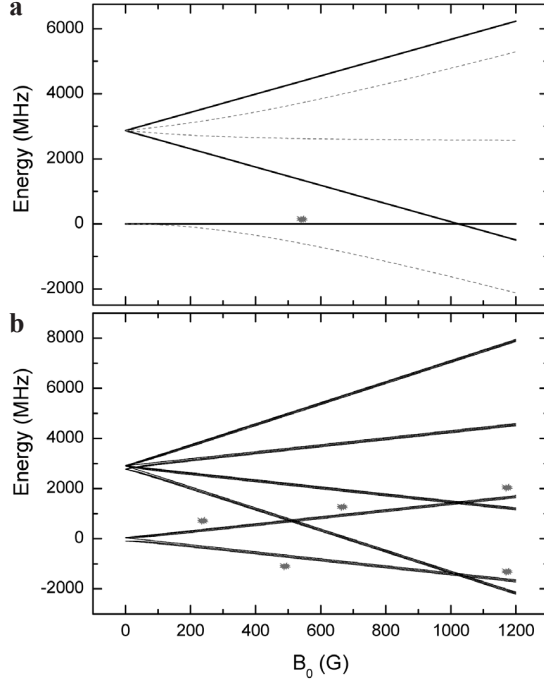


Fig. 2. Energy levels of a single NV^- center (a) and of coupled NV^- center and P1 center (b). The “bright” $M_S = 0$ states of the NV^- center are highlighted.

g -tensors, \mathbf{I}_i and \mathbf{I}_j are the nuclear spin operators associated with NV^- center and with the second paramagnetic center, A_i and A_j are appropriate HFI tensors, D and E are the zero-field splitting parameters, P is the nuclear quadrupolar interaction, D_{dd} is the dipolar interaction between the two centers, which depends on the distance between them, $D_{dd} \propto \mathbf{r}_{12}^{-3}$, where \mathbf{r}_{12} is the vector connecting the two defect centers and $\mathbf{n}_{12} = \mathbf{r}_{12}/r_{12}$ is unity length vector parallel to \mathbf{r}_{12} .

As an example, in Fig. 2 we show the energy levels in magnetic field B_0 of the single NV^- center oriented along B_0 (solid lines) and with B_0 along the tetrahedral angle 109.47° (dashed lines) and of the coupled NV^- center and P1 center (neutral nitrogen atom, replacing carbon in the diamond lattice). Interaction NV^- center with another paramagnetic defect center gives rise to additional LACs, as shown in Fig. 2.

Polarization generated by light excitation is given by the following density matrix:

$$\rho = \rho_{NV} \times \rho_{eq}, \quad (2)$$

Hence, the density matrix of the entire coupled system ρ is the direct product of the individual spin density matrices. Here ρ_{NV} is a matrix having only one non-zero element, which corresponds to population of the $M_S = 0$ state; ρ_{eq} describes the spin density matrices at equilibrium conditions.

To calculate the LAC spectrum we go through the following steps. First, we calculate ρ in the eigen-basis of the Hamiltonian (1). Second, we remove all off-

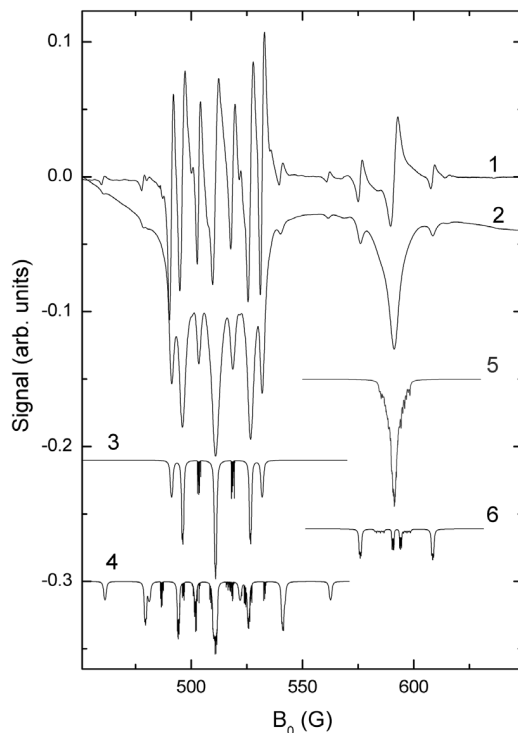


Fig. 3. Experimental LAC spectrum in the range 450–650 G (curve 1). Integrated experimental LAC spectrum (curve 2). Theoretically calculated LAC spectrum for coupled NV⁻ center and P1 center (curve 3) and for coupled NV⁻ center and P1 center with a ¹³C nucleus in the first coordinate sphere of P1 (curve 4). Theoretically calculated LAC spectrum for two coupled NV⁻ centers (curve 5) and for two coupled NV⁻ centers with a ¹³C nucleus in the first coordinate sphere of the second center (curve 6).

diagonal elements (coherences) of the density matrix thus assuming that they are washed out during the spin evolution over an extended irradiation period. Finally, we calculate the luminescence intensity as the total population of the $M_S = 0$ state, ρ_{00} , since this is the state, which provides bright luminescence upon irradiation when no spin mixing occurs.

In Fig. 3 we present the experimental LAC spectrum in the range 450–650 G and calculation results obtained using the outlined theoretical model. In all calculations the first NV⁻ center was aligned with \mathbf{B}_0 and the spectrum was averaged over four possible orientations of the partners. We used EPR parameters of the defect centers from literature in our calculations. It is safe to say that the model gives us not only positions of lines in the LAC spectrum but also relative line intensities.

The financial support of the Foundation for Basic Research (grants No. 16-03-00672 and 17-03-00932) is gratefully acknowledged.

1. Anishchik S.V., Ivanov K.L.: Phys. Rev. B. **96**, 115142 (2017)
2. Anishchik S.V., Vins V.G., Yelisseyev A.P., Lukzen N.N., Lavrik N.L., Bagryansky V. A.: New J. Phys. **17**, 023040 (2015)
3. Ivanov K.L., Yurkovskaya A.V., Vieth H.-M.: J. Chem. Phys. **128**, 154701 (2008)

Interaction of Native Protons with the Intrinsic Stable Radicals in Crude Oil as Revealed by ENDOR and DNP Measurements

**M. Gafurov¹, B. Gizatullin², A. Rodionov¹, G. Mamin¹,
C. Mattea², S. Stapf², S. Orlinskii¹**

¹ Kazan Federal University, Kazan 420008, Russian Federation, marat.gafurov@kpfu.ru

² Institute of Physics of Ilmenau Technical University, Ilmenau 98693, Germany,
Bulat.Gizatullin@tu-ilmenau.de

The most part of paramagnetic centers in crude oil [1] are concentrated preferably in asphaltenes and resins, and they frequently exist in the form of stable carbonaceous “free” radicals – unpaired electrons delocalized over many conjugated or aromatic chemical bonds. However, the nature and structure of the intrinsic paramagnetic centres in oil disperse systems remains unclear due to the complexity of the investigated material and the different forms of aggregation of its larger constituents.

In this work we present a study of electron/nuclear interaction in some crude oils, their fractions and solutions by continuous-wave and pulsed EPR, electron-nuclear double resonance (ENDOR) at X- (9 GHz), W-band (94 GHz) and fast field-cycling dynamic nuclear polarization (FFC-DNP) at X-band. A perceptible solid effect is found at room temperature as a result of the polarization transfer from the oil “free” radicals to the ¹H nuclei with different dynamics. Based on the analysis of the longitudinal nuclear relaxation times, three dynamical components described by different electron-proton coupling parameter were found, which in combination with ENDOR provides information about the distribution of the radicals in the high-molecular oil components. The obtained values of distances between radicals and protons evaluated from ENDOR measurements are in good agreement with the distribution of radicals in asphaltene aggregates reported in literature [2].

The work was partially supported by the Program of the competitive growth of Kazan Federal University among the World Leading Centers.

1. O'Reilly D.E.: J. Chem. Phys. **29**, 1188–1189 (1958)
2. Galtsev V.E., Ametov I.M., Grinberg O.Y.: Fuel **74**, 670–673 (1995)

Microwave-Assisted Cross-Polarization of Nuclear Spin Ensembles from Optically-Pumped Nitrogen-Vacancy Centers in Diamond

**F. Shagieva¹, S. Zaiser¹, P. Neumann¹, D. B. R. Dasari¹, R. Stöhr¹,
A. Denisenko¹, R. Reuter¹, C. A. Meriles², J. Wrachtrup¹**

¹ 3rd Institute of Physics, Stuttgart University, Stuttgart 70569, Germany,
f.shagieva@physik.uni-stuttgart.de

² Department of Physics, (CUNY) – City College of New York, New York 10031, USA

Nuclear magnetic resonance (NMR) is one of the most powerful techniques used in physics and life sciences. But for the on hand, it is limited by microscopic sample dimensions, and on the other, the size and cost of high-field spectrometers impede its extensive application. These factors motivate the developers to create high-resolution NMR systems that are smaller, cheaper, more robust and portable. Most recently, the shallow nitrogen-vacancy centres in diamond started to be used to perform nanoscale NMR imaging and spectroscopy of nuclear species under ambient conditions [1]. These multifunctional quantum sensors provide the noninvasive methods to not only get the chemical composition [2] of the molecules but also study the system dynamics in the nanoscopic volume above the diamond surface [3]. Despite a remarkable progress in this area, potential applications are often limited by low sensitivity. Hyperpolarisation techniques have the potential to overcome this limitation and revolutionise the use of compact NMR [4].

Several techniques to realise the (DNP) dynamic nuclear polarization using NV centres as an electron spin system have been demonstrated for internal diamond spins [5–7]. In this work we demonstrate the transfer of polarization from the NV's electron to the external nuclear spins and study the polarization dynamics.

1. Staudacher T. *et al.*: Science **339**, 561 (2013)
2. Aslam N. *et al.*: Science **357**, 67 (2017)
3. Staudacher T. *et al.*: Nat. Comm. **6**, 8521 (2015)
4. Halse M.E.: Trends Analyt. Chem. **83**, 76 (2016)
5. London P. *et al.*: PRL **111**, 067601 (2013)
6. Schwartz I. *et al.*: arXiv:1710.01508
7. Poggiali F. *et al.*: Phys. Rev. B **95**, 195308 (2017)

SECTION 10

OTHER APPLICATIONS OF MAGNETIC
RESONANCE

Ionic and Molecular Transport in Solid Electrolytes on Magnetic Resonance Data

V. I. Volkov

Institute of Problems of Chemical Physics RAS, Chernogolovka 1142432, Russian Federation;
Science Center in Chernogolovka RAS, Chernogolovka 142432, Russian Federation,
vitwolf@mail.ru

Ion-exchange membranes and polymer electrolytes for lithium cells attract keen attention of scientists in view of the development of modern environmentally clean and energy efficient technologies. The design of highly efficient materials requires fundamental scientific knowledge of the mechanisms of ion and molecular transport at the microscopic level. Of most interest is the relationship between the following fundamentally important characteristics that determine the ion and molecular transport.

1. The nanoscale structure of ion transport channels because these structural units form transport path for ion transfer by macroscopic distances

2. The type of interaction of mobile ions with functional groups and solvating molecules (water, organic compounds) and the state of solvent molecules in the polymer electrolyte.

3. The elementary steps of diffusion of ions and molecules, which can be characterized by the lifetime of a species, the time of translational displacement and the partial diffusion coefficient on various spatial scales.

Highly attractive methods that allow the mentioned information to be acquired are the magnetic resonance techniques, particularly, NMR. The following possibilities of the most popular magnetic resonance techniques are:

Electron paramagnetic resonance (EPR) provides information on the composition and structure of the first coordination sphere of paramagnetic ions, their mobility and local concentrations [1].

The method of electron-nuclear double resonance (ENDOR) makes it possible to selectively study the structure and dynamics of the environment of a paramagnetic centre in the range from 0.3 ± 0.5 to 1.5 nm [1, 2].

The main methods used in studying the state and mobility of ions in polymer electrolytes are NMR spectroscopy and pulsed NMR techniques, in particular, the NMR relaxation and pulsed field gradient NMR.

NMR spectroscopy. The most popular method is ^1H NMR, which was used to study hydration processes in ion exchange membranes. Information on hydration of ionic channels in membranes is of fundamental importance for understanding the mechanism of migration of cations and water molecules. NMR studies of cations in membranes and in gel and solid electrolytes for lithium cells reported [1]. The possibility of recording ^7Li , ^{23}Na and ^{133}Cs

NMR spectra for these systems have been demonstrated. The analysis of concentration dependences of chemical shifts and the shapes of NMR lines for

these nuclei provided information on the mechanisms of interaction of alkali metal ions with ionogenic groups and on the cation mobility.

NMR relaxation. The NMR relaxation methods provide unique information on the mobility of ions and molecules [3, 4]. Unfortunately, the quantitative treatment of experimental data was difficult due to the wide distribution of the correlation times of the ionic and molecular motion and the presence of paramagnetic impurities in these systems.

The pulsed field gradient NMR method, which makes it possible to directly measure the ionic and molecular self-diffusion is free from these drawbacks.

The NMR methods are especially attractive for acquiring detailed information on the ion and molecular transport in polymer electrolytes. The proposal presentation is demonstrating the potential of NMR methods in studying the formation of transport channels, the mechanisms of ion-polymer matrix interaction, the mobility and diffusion of ions and molecules in polymer electrolytes are analyzed and generalized. The translational mobilities of ions measured by pulsed field gradient NMR are compared with the data on ionic conductivity acquired by impedance spectroscopy methods [4, 5]. Attention is focused on the possibilities of NMR methods in studying the state of ions and molecules in electrolytes and also their diffusion mobility on different spatial scales. Based on the NMR data, the mechanisms of ion transport in ion-exchange perfluorinated membranes are proposed.

This work was supported by Russian Foundation for Basic Research (projects No. 18-08-00423 A).

1. Volkov V.I., Marinin A.A.: Russian Chemical Reviews **82** (3), 248 (2013)
2. Volkov V.I., Pukhov K.K., Choh S.H., Park I.-W., Volkov E.V.: Appl. Magn. Reson. **24**, 177 (2003)
3. Volkov V.I., Vasilyak S.L., Park I.-W., Kim H.J., Ju H., Volkov E.V., Choh S.H.: Appl. Magn. Reson. **25**, 43 (2003)
4. Chernyak A.V., Volkov V.I.: Appl. Magn Res. **45**, 287 (2014)
5. Volkov V.I., Dobrovolsky Yu.A., Nurmiev M.S., Sanginov E.A., Volkov E.V., Pisareva A.V.: Solid State Ionics. **179**, 148 (2008)

Electrodynamics of Superconductor/Ferromagnet Hybrids

S. V. Mironov

¹ Institute for Physics of Microstructures, Nizhny Novgorod 603087, Russian Federation, svmironov@ipmras.ru

The talk is devoted to the exotic electrodynamic phenomena originating at the interfaces between superconductors (S) and ferromagnets (F) due to the proximity effect, i.e. exchange of electrons between these two types of materials. First, we show that the spread of the Cooper pairs from the superconductor to the ferromagnet causes a strong inverse electromagnetic phenomenon, namely, the long-range transfer of the magnetic field from the ferromagnet to the superconductor [1]. Contrary to the previously investigated inverse proximity effect resulting from the spin polarization of superconducting surface layer, the characteristic length of the above inverse electrodynamic effect is of the order of the London penetration depth, which usually much larger than the superconducting coherence length. Remarkably, this spontaneous currents appear even in the absence of the stray field of the ferromagnet.

Another origin of the spontaneous current flowing along the S/F interfaces is the strong spin-orbit coupling arising due to the local breaking of the inversion symmetry. Such current creates a magnetic field near the superconductor surface, generates a stray magnetic field outside the sample edges, changes the slope of the temperature dependence of the critical field H_{c3} , and may generate the spontaneous Abrikosov vortices near the interface [2].

Finally, we show that a wide class of layered S/F hybrids demonstrates the emergence of the in-plane Fulde-Ferrell-Larkin-Ovchinnikov (FFLO) phase [3]. By decreasing the temperature, one can switch the system from uniform to the FFLO state which is accompanied by the damping of the diamagnetic Meissner response down to zero and also by the sign change in the curvature of the current-velocity dependence.

The work was supported by the Russian Science Foundation (grant 15-12-10020).

1. Mironov S., Mel'nikov A. S., Buzdin A.: *Appl. Phys. Lett.* **113**, 022601 (2018)
2. Mironov S., Buzdin A.: *Phys. Rev. Lett.* **118**, 077001 (2017)
3. Mironov S.V., Vodolazov D.Yu., Yerin Y., Samokhvalov A.V., Mel'nikov A.S., Buzdin A.: *Phys. Rev. Lett.* **121**, 077002 (2018)

Applications of Magnetic Resonance and Microwave Techniques for Identification of Liquid Materials

B. Rameev^{1,2}, G. Mozzhukhin², S. Tarapov³, İ. Ünal⁴

¹ Zavoisky Physical-Technical Institute, FRC Kazan Scientific Center of RAS, Kazan 420029, Russian Federation, rameev@gtu.edu.tr

² Gebze Technical University, Gebze/Kocaeli 41400, Turkey

³ O. Ya. Usikov Institute for Radiophysics and Electronics of NASU, Department of Radiospectroscopy, Kharkiv, 61085, Ukraine

⁴ TÜBİTAK, Marmara Research Center, MILTAL, Kocaeli 41470, Turkey

Identification of various liquid substances is very important problem both with respect security [1–4] and industrial applications [5]. The techniques, which provide a possibility of the chemical-specific identification of various materials, looks prospective for these applications. Among various techniques of liquid identification, the time-domain nuclear magnetic resonance (TD-NMR) is considered as very promising for detection of energetic, flammable, and other dangerous liquids [6]. TD NMR looks very attractive because of its high selectivity as well as relatively low price and maintenance expenses. However, for a reliable discrimination in a *large number* of various substances there is a need to obtain additional parameters for discriminations (e.g., the real and imaginary permittivities by dielectric spectroscopy, the ^{14}N NMR signal, diffusion constant or T_1/T_2 relaxation times distribution).

In this work, we review possible approaches in TD NMR as well as in MW dielectric spectroscopy to probe additional information about liquid content and to shorten the scanning time. Fast protocol based on the detection of ^{14}N NMR signal has been studied. It has been shown that the methods of MW dielectric spectroscopy may be used in the combinations with methods of TD NMR to obtain additional information on the tested liquids.

The work was supported by NATO Science for Peace and Security Programme (NATO SPS grant No. 985005 [G5005]). Authors also acknowledge a partial support by East Marmara Development Agency (MARKA, project No. TR42/16/ÜRETİM/0013) and by Research Fund of Gebze Technical University (grants No. BAP 2017-A-105-44).

1. Miller J.B., Barrall G.A.: Explosives Detection with Nuclear Quadrupole Resonance: American Scientist **93**, no. 1, 50–57 (2005)
2. Fraissard J., Lapina O., eds.: Explosives Detection using Magnetic and Nuclear Resonance Techniques, NATO Science for Peace and Security Series B: Physics and Biophysics. Dordrecht, Netherlands: Springer, 2009.
3. Rameev B.Z., Mozzhukhin G.V., Aktas B., eds.: Magnetic Resonance Detection of Explosives and Illicit Materials, Appl. Magn. Reson. **43**, no. 4, 463–467 (2012)
4. Apih T., Rameev B., Mozzhukhin G., Barras J., eds.: Explosives Detection using Magnetic and Nuclear Resonance Techniques, NATO Science for Peace and Security Series B: Physics and Biophysics, Dordrecht, Netherlands: Springer, 2014.
5. Blümich B.: Introduction to compact NMR: A review of methods, Trends in Analytical Chemistry **83**, 2–11 (2016)
6. Burnett L.J.: Liquid Explosives Detection, Proc. SPIE **2092**, 208-217 (1994)

Magnetic Resonance Study of $\text{BaAg}_2\text{Cu}[\text{VO}_4]_2$ Quantum Magnet

**Y. Krupskaya¹, M. Schäpers¹, A. U. B. Wolter¹, H.-J. Grafe¹,
E. Vavilova^{1,2}, A. Möller³, B. Büchner^{1,4}, V. Kataev¹**

¹ Leibniz Institute for Solid State and Materials Research IFW Dresden, Dresden 01069, Germany,
y.krupskaya@ifw-dresden.de

² Zavoisky Physical-Technical Institute, FRC Kazan Scientific Center of RAS, Kazan 420029,
Russian Federation

³ Institute of Inorganic Chemistry and Analytical Chemistry, Johannes Gutenberg University Mainz,
Mainz 55128, Germany

⁴ Institute of Solid State and Materials Physics, Technical University Dresden,
Dresden 01062, Germany

$\text{BaAg}_2\text{Cu}[\text{VO}_4]_2$ contains Cu(II) ions with $S = 1/2$ in a distorted two-dimensional triangular lattice interconnected via non-magnetic $[\text{VO}_4]$ tetrahedral units. The theoretical analysis showed that the magnetism of this compound is determined by a superposition of ferromagnetic (FM) and antiferromagnetic (AFM) spin-1/2 chains, which was fully supported by the static magnetization measurements [1]. In order to locally probe the magnetic properties we have studied the $\text{BaAg}_2\text{Cu}[\text{VO}_4]_2$ compound by means of High-Field/Frequency Electron Spin Resonance (HF-ESR) and Nuclear Magnetic Resonance (NMR) spectroscopies. The HF-ESR measurements, reveals an anisotropic ESR spectrum typical for the Cu(II) ions and determines the g -tensor, $g_{\text{parall.}} = 2.38$ and $g_{\text{perp.}} = 2.06$. Moreover, a substantial change in the spectral shape of the ESR lines at low temperatures characteristic for the presence of short range magnetic correlations is observed. The detailed analysis shows that the shape of the low-temperature ESR spectrum is defined by the development of the anisotropic internal fields corresponding to FM and AFM correlations in the respective Cu spin chains. The NMR study has revealed the presence of ^{51}V nuclei signals in the two types of chains, which strongly supports the ESR results. Altogether, the HF-ESR and NMR results experimentally confirm theoretical predictions of the superposition of FM and AFM Cu(II) spin-1/2 chains in $\text{BaAg}_2\text{Cu}[\text{VO}_4]_2$ [2].

This work was supported by the DFG through KA1694/8-1, WO1532/3-2, SU229/10-2 and by the Russian Foundation for Basic Research through RFBR 14-02-01194.

1. Tsirlin A. *et al.*: Phys. Rev. B **85**, 014401 (2012)
2. Krupskaya Y. *et al.*: Z. Phys. Chem. **231**, 759 (2017)

NMR Investigation of ^{14}N Quadrupole Coupling Interactions in Liquids

**G. V. Mozzhukhin¹, G. S. Kupriyanova², A. Maraşlı¹,
S. Mamadazizov², B. Z. Rameev^{1,3}**

¹ Gebze Technical University, 41400 Gebze/Kocaeli, Turkey, mgeorge@yandex.ru

² Baltic Federal University by Immanuel Kant, 236041 Kaliningrad, Russian Federation

³ Zavoisky Physical-Technical Institute, FRC Kazan Scientific Center of RAS, Kazan 420029, Russian Federation

For ^{14}N NMR relaxation the main interaction is the quadrupole interaction, i.e. the interaction of nucleus quadrupole moment with the electric field gradient (EFG) of surrounding electrons[1]. In liquids the components of the quadrupole interaction tensor fluctuate randomly with time providing the quadrupole mechanism. The quadrupole relaxation mechanism dominates for nitrogen compounds in ^{14}N NMR. There are different types of molecular motion that cause the fluctuation of electric field gradient on nucleus. In the case of isotropic stochastic rotational movement the correlation function is defined by one exponential dependence with characteristic time of correlation τ_c [2]. The relaxation studies based on the following approximations: i) fast movement (narrowing) limit $(\omega_0\tau_c)^2 \ll 1$ is working in our liquids; ii) the substances have isotropic molecular reorientation. In this case, the transverse and longitudinal relaxation are equal to each other and the quadrupole contribution is given by the following expression:

$$\left(\frac{1}{T_1}\right)_Q = \left(\frac{1}{T_2}\right)_Q = \frac{3}{8} \left(1 + \frac{\eta^2}{3}\right) \left(\frac{e^2 Q q_{zz}}{\hbar}\right)^2 \tau_c, \quad (1)$$

where $(T_1)_Q$ and $(T_2)_Q$ are longitudinal and transverse relaxation times correspondently, $I = 1$ is a spin quantum number, ω_I is the Larmor frequency of nuclei, τ_c is the effective correlation time, $e^2 Q q_{zz}$ is a quadrupole coupling constant (QCC), η is asymmetry parameter. Thus we may calculate QCC for liquids if we know T_1 and correlation time. However formula (1) doesn't provide needed information for the calculation of QCC C_q or correlation time τ_c . There were some attempts to calculate QCC in liquids nitrogen compounds with use τ_c , calculated on the base of Stokes-Einstein-Debye and Lamb [3, 4]) models. In these works the asymmetry parameter η was neglected that produces error of calculation within 10%.

We studied in low field of 575 mT 3 groups of nitrogen liquids including flammable liquids, some toxic liquids and water solutions of electrolytes. Our measurements of T_1 and linewidth were used for calculations of QCC in these liquids. The definition of QCC was carried out by use calculation of τ_c with use Lamb model. In group of solutions we will apply the use of microviscosity concept from [5].

The work was supported by NATO Science for Peace and Security Programme (NATO SPS grant No. 985005 [G5005]) and, TUBITAK grant under the Programme 2221 for Visiting Scientist (G. S. Kupriyanova). Authors also acknowledge a partial support by East Marmara Development Agency (MARKA, project No. TR42/16/ÜRETİM/0013) and by Research Fund of Gebze Technical University (grants No. BAP 2017-A-105-44).

1. Witanovski M.: Nitrogen NMR. Spectroscopy, *Pure and Applied Chemistry* **37**, 225–233 (1974)
2. Abragam A.: *The Principles of Nuclear Magnetism*, 314 p. Oxford: The Clarendon Press 1961.
3. Jenks G.J.: NMR Investigation of the Nitrogen Quadrupole Coupling Constant in Liquid Samples, *J. Chem. Phys.* **54**(2), 658–663 (1971)
4. Moniz W.B., Gutowsky H.S.: Nuclear Relaxation of N-14 by Quadrupole Interactions in Molecular Liquids, *J. Chem. Phys.* **38**, 1155–1162 (1963)
5. Boere R.T., Kidd R.G.: Webb G.A. (ed.), *Annual Reports on NMR Spectroscopy*, vol. 13, 319 p. New York: Academic Press 1982.

Ferromagnet/Superconductor Hybridization for Magnonic Applications

**I. A. Golovchanskiy^{1,2}, N. N. Abramov², V. S. Stolyarov^{1,3,4},
V. V. Bolginov^{2,3,5}, V. V. Ryazanov^{2,3,4}, A. A. Golubov^{1,6}, A. V. Ustinov^{2,7}**

¹ Moscow Institute of Physics and Technology, Dolgoprudny 141700, Russian Federation

² National University of Science and Technology MISIS, Moscow 119049, Russian Federation

³ Institute of Solid State Physics (ISSP RAS), Chernogolovka 142432, Russian Federation

⁴ Kazan Federal University, Kazan 420008, Russian Federation

⁵ Skobeltsyn Institute of Nuclear Physics, Lomonosov Moscow State University
Moscow 119991, Russian Federation

⁶ Faculty of Science and Technology and MESA+ Institute for Nanotechnology,
University of Twente, 7500 AE Enschede, The Netherlands

⁷ Physikalisches Institut, Karlsruhe Institute of Technology, Karlsruhe 76131, Germany

Magnonics is a promising field for operation with microwave signals via spin waves. A number of advantages favor development of magnonics towards information transfer and processing, including quantum information, for engineering of spin wave logic devices, and periodic magnonic band gap structures. The basics of magnonics is well laid out in refs. [1–3]. A good overview of modern trends in magnonics can be found in the Special Issue on Magnonics, Journal of Physics D: Applied Physics 2017.

With this work we propose to consider coupling of spin waves with a superconductor for development of magnonic applications with modified dispersion law. As was recently demonstrated experimentally [4], ferromagnetic resonance (FMR) spectrum of the magnetostatically coupled permalloy/niobium bilayer reveals standing magnetostatic surface spin wave (MSSW) resonances with enhanced phase velocity (Fig. 1a). The enhanced phase velocity originates from screening of the alternating magnetostatic stray fields of precessing magnetic moments in the ferromagnetic layer by the superconducting surface in the ideal diamagnetic Meissner state, which in turn enhances the actual magnetostatic fields acting on magnetic moments.

Behavior of spin waves coupled with a superconducting surface can be captured by micromagnetic simulations where the magnetostatic interaction is represented by the method of images (see Fig. 1b). Micromagnetic simulations allow to derive dispersion laws for all in-plane spin wave geometries. For instance, in MSSW geometry (Fig. 1b) the coupling not only enhances the phase velocity but also promotes a heavy nonreciprocity: the frequency band for wave numbers of one sign is enhanced approximately by a factor of 2 as compared with the band for opposite-sign wave numbers. Coupling of spin waves with a superconductor and its micromagnetic representation open unexplored opportunities for application in magnonics.

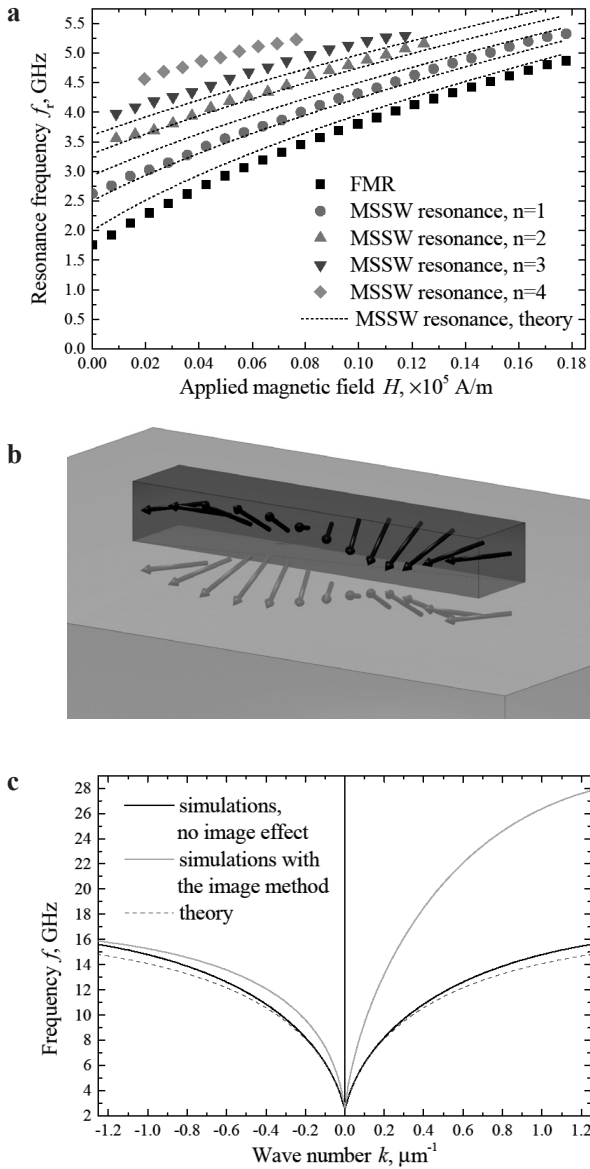


Fig. 1. Interaction of a spin wave with a superconductor. **a** Dotted data show the experimental dependencies of FMR and MSSW resonance frequencies f_r on magnetic field H for 90 nm thick and 130 μm wide permalloy rectangles placed on top of superconducting Nb transmission line. Dashed lines show the theoretical $f_r(H)$ dependencies for the same MSSW modes n . The mismatch between experimental and theoretical curves indicates enhanced phase velocity of MSSW coupled to a superconductor. **b** Illustration of the method of images. A ferromagnet is placed on the surface of a superconductor. Coupling of magnetic spins (dark arrows) with superconductor is equivalent to their interaction with the mirrored-image spins in respect to the superconducting surface (grey arrows). **c** Dispersion laws of MSSWs for a 100 nm permalloy film at magnetic field $H = 3.1 \cdot 10^3$ A/m. Dashed lines 3 show the theoretical dispersion. Black solid lines show the micromagnetic simulated dispersion in absence of superconducting screening. Grey solid lines show the micromagnetic simulated dispersion in presence of superconducting screening.

This work was supported by the Ministry of Education and Science of the Russian Federation (Megagrant project No. 14.Y26.31.0007), by the Russian Science Foundation (grant No. 18-72-00224), and by the Russian Foundation for Basic Research (grants No. 16-02-00418 and No. 17-02-01270).

1. Stancil D.: Theory of Magnetostatic Waves. Springer-Verlag New York, Inc., 1993.
2. Gurevich A. G., Melkov G. A.: Magnetization Oscillations and Waves. CRC Press, 1996.
3. Demokritov S. O., Slavin A. N.: Magnonics: From Fundamentals to Applications. Springer-Verlag Berlin Heidelberg, 2013.
4. Golovchanskiy I.A. *et al.*: Adv. Func. Mater. 1802375 (2018)

EPR of Gd^{3+} Centers in $Pb_{1-x}Gd_xS$ Narrow Gap Semiconductor Crystals: Observation of “Reversed” Dyson Profiles of the EPR Lines

V. A. Ulanov^{1, 2}, I. V. Yatsyk², R. R. Zainullin², A. M. Sinicin¹

¹ Kazan State Power Engineering University, Kazan 420034, Russian Federation, ulvlad@inbox.ru

² Zavoisky Physical-Technical Institute, FRC Kazan Scientific Center of RAS, Kazan 420029, Russian Federation

The PbS compound belongs to the group of lead chalcogenides (PbS, PbSe, and PbTe) which are direct narrow-gap semiconductors with a NaCl-type lattices. These compounds are used for producing the electronic and optoelectronic devices that operate in the mid-infrared range. At present the behavior of foreign magnetic impurities in lead chalcogenides is a subject of considerable interest because their highly tunable magnetic properties are suited for adding spintronic functionalities to semiconductor technologies. The presence of magnetic ions in volumes of the lead chalcogenide compounds and exchange interactions between magnetic impurities and carriers results in a number of new effects. These are the carrier concentration induced paramagnet-ferromagnet and ferromagnet-spin glass transitions [1], optical switching of magnetization [2], ultrafast spin transfer between magnetic impurities and carriers [3], and so on. Mechanisms of carrier-impurity spin transfer are very diverse and have not been fully studied to the present day.

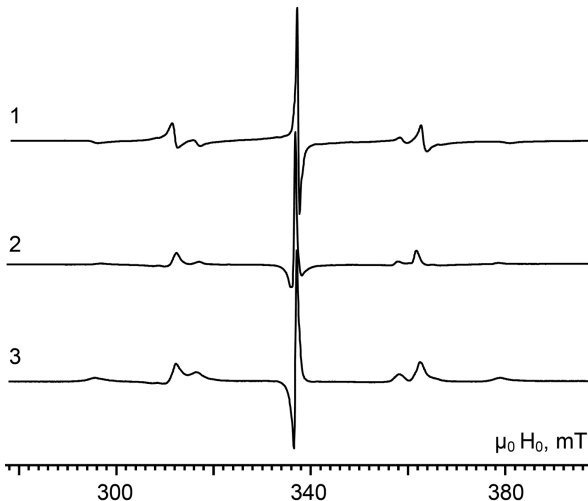


Fig. 1. EPR spectra of crystalline $Pb_{1-x}Gd_xS$ samples ($H_0 \parallel \langle 001 \rangle$; $T = 5$ K; $f_{EPR} = 9.41$ GHz; 1: $x = 1.1 \cdot 10^{-3}$; 2: $x = 4.3 \cdot 10^{-3}$; 3: $x = 6.5 \cdot 10^{-3}$).

For a number of reasons, the relaxation processes realized in lead sulphides and associated with interactions of electron spin moments of magnetic impurities with spin moments of charge carriers are, until now, poorly understood. Therefore, the purpose of this study was to obtain new experimental facts that could fill this gap. EPR was chosen as the experimental method and gadolinium as the magnetic impurity. It was previously established [4] that gadolinium replaces lead in a lead sulphide crystal and is in the Gd^{3+} state. As it was found, Gd^{3+} formed in the PbS crystals the paramagnetic centers with cubic symmetry. The EPR spectra of these centers could be described by well-known spin-Hamiltonian (SH)

$$H_s = \beta_e g H \cdot S + (1/60)b_4(O_4^0 + 5O_4^4) + (1/1260)b_6(O_6^0 - 21O_6^4).$$

The SH parameters determined at 5 K and $f_{EPR} = 9.41$ GHz were following: $g = 1.9904 \pm 0.0002$; $b_4 = 59.14 \pm 0.05$; $b_6 = -0.12 \pm 0.05$ (b_4 and b_6 in MHz). They were not sensitive to the concentration of gadolinium, but depended on temperature. It was found for $Pb_{1-x}Gd_xS$ monocrystalline samples that the EPR line shapes of Gd^{3+} centers were dependent on value of x (see Fig 1).

As it can be seen the spectrum number 1 consists of 7 lines having the classical Dysonian profiles usually described by asymmetry parameter A/B (the ratio between the maximum and minimum of the first derivative of a resonance line). Lines of spectrum 3 have inversed profiles and lines of spectrum 2 can be simulated by superposition of the spectra 1 and 3. The reasons of the observed unusual experimental facts are discussed.

1. Story T.: Acta Phys. Pol. A. **91**, 173 (1997)
2. Kapetanakis M.D., Wang J., Perakis I.E.: J. Opt. Soc. Am. B. **29**, A95 (2012)
3. Cygorek M., Axt V.M.: Semicond. Sci. Technol. **30**, 085011 (2015)
4. Bacskey G.B., Fensham P.J., Ritchie I.M., Ruff R.: J. Phys. Chem. Solids. **30**, 713 (1969)

Spectral Hole Burning Spectroscopy of Silicon Vacancy-Related Centers in SiC

**V. Soltamov^{1,2}, C. Kasper¹, G. V. Astakhov¹, S. A. Tarasenko²,
A. V. Poshakinskiy², A. N. Anisimov², P. G. Baranov², V. Dyakonov¹**

¹ Julius Maximilian University of Würzburg, Experimental Physics VI, Würzburg 97074, Germany, victrosoltamov@gmail.com

² Ioffe Institute, St. Petersburg 194021, Russian Federation

Negatively charged silicon vacancy-related centers (V_{Si^-}) in Silicon Carbide (SiC) has been attracting growing attention due to their prospective to use in quantum sensing, masers and quantum networks [1, 2]. These applications become possible because the ground spin state ($S = 3/2$) of the V_{Si^-} is already split in zero-magnetic field into two Kramers doublets by crystal field. These doublets can be optically polarized through an electron spin-dependent intersystem-crossing pathway and readout by means of optically detected magnetic resonance (ODMR) technique. The bottleneck of all mentioned above applications is inhomogeneous broadening of the V_{Si^-} energy levels. While classical spectroscopic tools such as EPR and ENDOR are perfect for determining the line broadening induced by hyperfine interactions, information on other sources of broadening is difficult to extract using these methods.

We overcome this obstacle by studying the broadening of the V_{Si^-} ODMR signal in zero magnetic field by means of Spectral Hole Burning (SHB) technique in a radio-frequency domain [3]. In this technique, ODMR spectrum is obtained as relative change of the V_{Si^-} photoluminescence while sweeping the probe rf-frequency. Application of a second rf-field was found to induce SHB. Studying a spectral dependence of “holes” on magnetic field and frequency, we found that local variations of strain fields in the SiC crystal are the main source of the V_{Si^-} resonance line broadening. Our results allow deeper understanding of the V_{Si^-} ground state properties and to propose new measurement protocols for quantum sensing.

V.A.S. was supported by the Alexander von Humboldt-Foundation.

1. Tarasenko S.A., Poshakinskiy A.V., Simin D., Soltamov V.A., Mokhov E.N., Baranov P.G., Dyakonov V., Astakhov G.V.: *Phys. Stat. Sol. (b)* **255**, 1700258 (2018)
2. Soykal Ö.O., Dev P., Sophia E.: *Economou Phys. Rev. A* **9**, 034022 (2018)
3. Kehayias P., Mrózek M., Acosta V.M., Jarmola A., Rudnicki D.S., Folman R., Gawlik W., Budker D.: *Phys. Rev. B* **89**, 245202 (2014)

SECTION 11

MEDICAL PHYSICS

Interaction of Statins with Different Model Membranes Studied by NMR Spectroscopy

**L. Galiullina¹, G. Musabirova¹, A. Aganov¹, V. Klochkov¹,
H. A. Scheidt², D. Huster²**

¹ Physics Department, Kazan Federal University, Kazan 420008, Russian Federation, lgaliull@kpfu.ru

² Institute for Medical Physics and Biophysics, Leipzig University, Leipzig D-04107, Germany

Hydroxy-methyl-glutaryl-coenzyme A (HMG-CoA) reductase inhibitors or statins reduce amount of low-density lipoprotein (LDL) cholesterol, which is known as a well-established risk factor for atherosclerosis. Despite the fact that statins have a common pharmacologic target, which is essential to sterol biosynthesis, their efficiency, safety, and potential non-LDL actions differ considerably depending on their chemical structure. Origins of these differences are not well investigated. There is a hypothesis that metabolism and safety of statins depend on their location in the cell membrane [1], but to the present day there is a lack of information in literature on interactions of statins with the surface of the cellular membrane.

The interactions of atorvastatin, cerivastatin, fluvastatin, rosuvastatin, lovastatin, simvastatin and pravastatin with model membranes were studied. Dodecylphosphocholine (DPC) and sodium dodecylsulfate micelles (SDS) were used as model cellular membranes in liquid state investigations and 1-palmitoyl-2-oleoyl-*sn*-glycero-3-phosphocholine (POPC) bilayers were used for solid-state studies. The results of NMR experiments allowed determining average locations of different statins in model membranes. It was shown that in all model systems cerivastatin has the deepest location in the membrane, pravastatin weakly or just partially interacts with membrane surface and other statins share intermediate locations in model membranes. However, it was found that the depth of intercalation in the membrane depends on used model system.

Analysis of obtained data showed that location of statins in model membranes correlate with their pharmacological features. It has been suggested that a deeper penetration of statins into a membrane is associated with more effective LDL cholesterol-lowering action, but at the same time with higher risk of rhabdomyolysis.

The work was supported by Russian Science Foundation (grant №17-75-10124).

Spectra Convolution for Quantitative Analysis in EPR Spectroscopy

S. V. Kuzin, N. A. Chumakova, E. N. Golubeva, A. A. Korotkevich

Chemistry Department, Lomonosov Moscow State University, Moscow 119234, Russian Federation,
ser.12.08@yandex.ru

The report is devoted to application of convolution technique for obtaining of quantitative information from EPR spectra. Common method, which is based on double integration of an EPR spectrum, has a low accuracy when noise is significant. Another possibility is to measure spectrum amplitude and to compare it with amplitude of another spectrum (is referred here to as *standard spectrum*). The standard spectrum should be recorded for a sample with known number of paramagnetic particles and also this spectrum should to have high signal-to-noise ratio (*SNR*). When the last method is applied only two points of experimental spectrum are used to obtain quantitative information. Besides, procedure of measurement of highly noisy spectrum amplitude cannot give accurate results.

In this work another approach to quantitative treatment of EPR spectra based on a convolution with standard spectrum is proposed. Accuracy of convolution technique was studied in series of numerical experiments using artificially distorted EPR spectra. Very low sensitivity of the proposed method to the presence of noise was demonstrated (error is less than 5% up to $SNR = 2$).

The developed method was applied to study nitroxide radicals release to buffer media from biodegradable polymer matrices. Experimental EPR spectra of spin probes in PBS with low *SNR* (total amount of spins $\sim 10^{13}$) were treated by convolution with standard spectra of corresponding radicals. For the standard spectra recording the samples containing $\sim 10^{16}$ spins were prepared. Quantitative results were compared with those obtained using conventional ways such as double integration and measuring of amplitudes. It was shown that the novel method allows observing of reproducible fine features of release processes. Using obtained information the diffusion kinetics based mathematical model was developed.

The work was supported by Russian Foundation for Basic Research (grants 16-03-00333, 17-02-00445).

Living Systems Can Produce Magnetic Iron Oxide Crystals. EPR Spectroscopy Data

S. Yurtaeva

Zavoisky Physical-Technical Institute, FRC Kazan Scientific Center of RAS, Kazan 420029,
Russian Federation, s.yurtaeva@kfti.knc.ru

Presently it is well known about the processes of spontaneous biomineralisation in living organisms. Iron biomineralisation results in formation of iron oxide biominerals. The iron is accumulated mostly in ferrihydrite form ($5\text{Fe}_2\text{O}_3 \cdot 9\text{H}_2\text{O}$) within ferritin mineral core and magnetite/maghemite ($\text{Fe}_3\text{O}_4/\gamma\text{Fe}_2\text{O}_3$) forms. These crystals play an important part in functioning of living systems as provide the organism with the iron store and protect cells from radicals. The excess amount of them may be observed in different pathologies, such as pathologies of brain, tumors and others.

Such crystalline particles cause the appearance of magnetic properties in biological tissues and may be detected by the EPR technique. The signal is due to Electron Magnetic Resonance (EMR) of iron oxide nanoparticles. The nature of the signal and characteristics are still the subject of interest.

The characteristics of EMR signals in different biological tissues (tissues of laboratory rats with different pathologies, cancer tumor tissues, rat tissues after the effect of hypogravitation, nerve tissues) were investigated. The general characteristics of EMR signals were determined: non-monotonic temperature

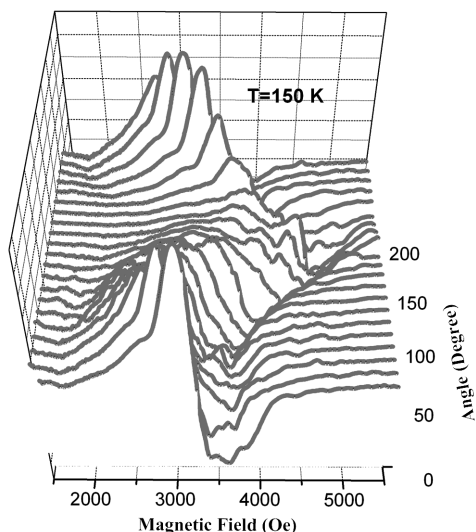


Fig. 1. Angular dependence of EMR signal in injured spin cord.

behavior of resonance field (H_{res}), linewidth (ΔH) and integrated intensity, axial and cubic components in H_{res} anisotropy. Verwey phase transition, character for magnetite crystal structure was detected. The characteristics indicate that there are magnetite crystals in tissues. The different types of anisotropic behavior of signals were detected. It was determined, that they characterize the different types of geometry of crystalline inclusions. Magnetic resonance investigation of EMR signals in biological tissues and blood is suggested to use as the method of detection of anomalous accumulation of tissue iron in the forms of iron oxide nanocrystals (magnetite and ferritin).

POSTERS

NMR Investigation of Sodium Gluconate

M. M. Akhmetov, G. G. Gumarov, V. Yu. Petukhov, M. Yu. Volkov

Zavoisky Physical-Technical Institute, FRC Kazan Scientific Center of RAS, Kazan 420029,
Russian Federation, mansik86@mail.ru

Practically all biochemical processes are accompanied by conformational changes, i.e. the nature of the interaction and the structure of the reaction products formed are determined by the spatial structure and the possibilities of mutual adjustment (including conformational) of the participating molecules. There are a number of papers devoted to the study of conformations of aldonic acids using the NMR method, in particular, gluconic acid in aqueous solution [1]. However, publications on the study of the conformational structure of sodium gluconate in aqueous solution have not been found in the available literature. In this paper, we present the results of studies of the conformational changes in sodium gluconate in aqueous solution as a function of the concentration by using NMR on ^1H and ^{13}C nuclei.

NMR spectra were recorded on the AVANCE 400 BRUKER spectrometer in a magnetic field of 9.395 Tesla. Resonance on ^1H and ^{13}C nuclei for solutions of calcium gluconate was observed at a frequency of 400 and 100 MHz, respectively. To establish the binding between individual nuclei of the molecule, a pulse sequence of 2D correlation spectroscopy, ^1H - ^{13}C , was used.

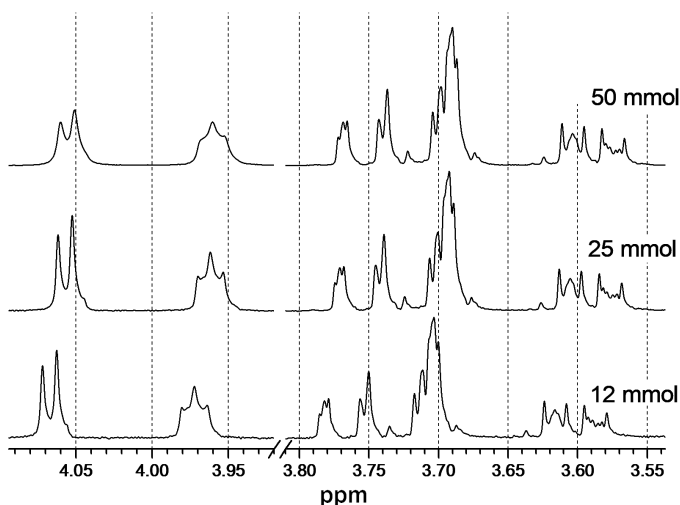


Fig. 1. ^1H NMR spectra of sodium gluconate solution.

The structure of sodium gluconate in the crystalline state is given in [2]. In the ^1H NMR spectra of solutions of sodium gluconate in D_2O , displacement of some lines as a function of concentration was detected (Fig. 1). This, as we know, indicates the presence of intermolecular hydrogen bonds [3]. The most noticeable shift is observed for the H2 and H3 lines corresponding to the protons closest to the sodium atom in the structure of the sodium gluconate molecule.

1. Horton D., Walaszek Z., Ekiel I.: *Carbohydrate Research* **119**, 263–268 (1983)
2. Lis T.: *Carbohydrate Research* **122**, 23–29 (1983)
3. March J.: *Organic chemistry*. New York: A Wiley-Interscience Publication John Wiley and Sons 1985.

^3He NMR in Contact with Nanoparticles

**E. M. Alakshin¹, E. I. Kondratyeva¹, V. V. Kuzmin¹,
K. R. Safullin^{1,2}, A. A. Stanislavovas¹, A. V. Savinkov¹,
A. V. Klochkov¹, M. S. Tagirov^{1,2}**

¹ Institute of Physics, Kazan Federal University, Kazan 420008, Russian Federation,
alakshin@gmail.com

² Institute of Applied Research, Academy of Sciences of the Republic of Tatarstan, Kazan 420111,
Russian Federation, murat.tagirov@gmail.com

The resonance magnetic coupling between ^{169}Tm and ^3He nuclei at the solid (thulium ethyl sulfate) – liquid interface manifested by cross-relaxation processes was observed for the first time in 1984 [1]. Later on, the resonance magnetic coupling of the nuclei of liquid ^3He with the ^{141}Pr nuclei of a PrF_3 van Vleck paramagnetic fine powder was discovered by pulsed nuclear magnetic resonance (NMR) methods [2]. In addition, a series of works on the NMR study of ^3He in contact with PrF_3 and LaF_3 nanopowders was carried out [3–4]. The only one observation of the effect of the magnetic phase transition of a solid substrate on the magnetic relaxation of ^3He nuclei was reported [5].

The spin kinetics of ^3He in contact with a mixture of LaF_3 and DyF_3 micro-powders at temperatures of 1.5–3 K has been studied by pulsed nuclear magnetic resonance. The DyF_3 is a dipolar dielectric ferromagnet with the phase transition temperature 2.55 K, whereas the diamagnetic fluoride LaF_3 is a diluting substance for the optimal observation conditions of ^3He NMR in powder pores. The magnetic phase transition in DyF_3 is accompanied by a considerable change in the character of fluctuations of the magnetic moments of dysprosium ions, which affect the spin kinetics of ^3He in contact with the substrate. Significant changes in the relaxations rates of the longitudinal and transverse magnetizations of ^3He have been discovered in the region of magnetic ordering of the solid matrix. This work was supported by the Russian Foundation for Basic Research, project no. 16-32-60155 mol_a_dk.

1. Egorov A.V., Aukhadeev F.L., Tagirov M.S.: JETP Lett. **39**, 584 (1984)
2. Egorov A.V., Irisov D.S., Klochkov A.V.: JETP Lett. **86**, 416 (2007)
3. Tagirov M.S., Alakshin E.M., Gazizulin R.R.: J. Low Temp. Phys. **162**, 645 (2011)
4. Alakshin E.M., Gazizulin R.R., Gazizulina A.M.: Low Temp. Phys. **41**, 47 (2015)
5. Saito S.: Phys. Rev. Lett. **36**, 975 (1976)

Low-Frequency RYDMR in Mechanical Properties of Crystals

V. I. Alshits, E. V. Darinskaya, M. V. Koldaeva, E. A. Petrzhik

Shubnikov Institute of Crystallography of FSRC “Crystallography and Photonics” RAS,
Moscow 119333, Russian Federation, mkoldaeva@ns.crys.ras.ru

The sensitivity of mechanical properties of nonmagnetic crystals to the magnetic field is now a well-established phenomenon known as magnetoplastic effect (MPE). Its physical origin is related to transformations of structure of impurity complexes due to magnetoinduced spin transitions eliminating a quantum exclusion of some electron transitions. The effect of the magnetic field on a crystal manifests itself in dislocation displacements, changes of macroplastic characteristics or microhardness, etc [1]. MPE is observed both under a constant magnetic field and in the scheme of electron paramagnetic resonance (EPR). In the latter case one deals with the Reaction Yield Detected Magnetic Resonance (RYDMR). In our case we detect dislocation paths in NaCl crystals and microhardness of ZnO, triglycine sulfate, and potassium hydrogen phthalate crystals. The main specific feature of our experiments is using the ultralow magnetic fields (and accordingly frequencies) with the Earth’s magnetic field 50 μT and other fields in the range of 26–261 μT as the static field [2, 3].

The low-frequency RYDMR of dislocation path in NaCl crystals manifests very anisotropic properties, for instance, a strong dependence of the resonance frequency ν_r on the sample orientation in the static magnetic field [2, 3]. This frequency changes when the sample turns about the selected crystallographic direction by an angle θ to the Earth’s magnetic field as $\nu_r = \nu_0 \cos\theta$, where ν_0 is the resonance frequency at $\theta = 0$. Different structural positions of impurities in a distorted lattice of the dislocation core are characterized by a discrete set of angles $\theta \rightarrow \theta + \Delta\theta_i$ which leads to a frequency spectrum of dislocation paths.

In fact, an anisotropy of RIDMR is not specific for the motion of dislocations only. That is a common property of resonance effects in ultralow fields. Resonance changes have been detected in the microhardness of ZnO, triglycine sulfate, and potassium hydrogen phthalate crystals after their exposure in the Earth’s magnetic field in the same EPR scheme. It has been shown that the preliminary exposure of ZnO, triglycine sulfate, and potassium hydrogen phthalate crystals to ultralow crossed magnetic fields – the Earth’s magnetic field and ac pump field – leads to a resonance change in their microhardness. The resonance frequency of microhardness peaks is determined by the classical condition of electron paramagnetic resonance only at certain orientations of the crystals with respect to the Earth’s magnetic field. Turns of all samples with respect to the direction B_{Earth} by angle θ reduce the resonance frequency in proportion to $\cos\theta$ like in the case of dislocation motion. The observed giant anisotropy of the resonance is attributed to the presence of own local magnetic fields $B_{\text{loc}} \gg B_{\text{Earth}}$ in the crystals.

RYDMR spectra including numerous peaks of dislocation paths at low pump frequencies beginning with 10 kHz [4], as well as the quartet of equidistant peaks [5] related to $\theta = 0$, have been measured in NaCl crystals. In the static magnetic field $B = (26\text{--}261) \mu\text{T}$ the frequencies of the RYDMR peaks correspond to the Zeeman splitting of the levels with four g -factors 1.79, 1.88, 1.97 and 2.06. The difference of the neighboring values $\Delta g = 0.09$ does not depend on B . The equidistance is violated only at the lowest fields, $B \gg 26 \mu\text{T}$, and frequencies $\nu \sim 0.7 \text{ MHz}$.

1. Alshits V.I., Darinskaya E.V., Koldaeva M.V., Petrzhhik E.A. in: Dislocations in Solids (J. P. Hirth, ed.). Amsterdam: Elsevier 2008.
2. Alshits V.I., Darinskaya E.V., Koldaeva M.V., Petrzhhik E.A.: JETP Lett. **104**, 353 (2016)
3. Alshits V.I., Koldaeva M.V., Petrzhhik E.A.: JETP Lett. **107**, 618 (2018)
4. Alshits V.I. *et al.*: JETP Lett. **99**, 82 (2014)
5. Alshits *et al.*: JETP Lett. **98**, 28 (2013)

EPR Spectra in CaF_2 Crystals Doped with CeO_2

L. K. Aminov, I. N. Kurkin, A. V. Lovchev, R. M. Rakhmatullin

Institute of Physics, Kazan Federal University, Kazan 420008, Russian Federation,
rafail.rakhmatullin@kpfu.ru

The variation of EPR spectra is observed in CaF_2 crystals depending on the content of CeO_2 and methods of the crystal growth. In this study the content of CeO_2 has been increased gradually from 0.5 wt% CeO_2 up to 15 wt% CeO_2 . The research is partly motivated by previous EPR studies of mixed fluorite crystals with general formula $(\text{MeF}_2)_{1-x-y}(\text{REF}_3)_x(\text{RF}_3)_y$; Me = Ca, Sr, Ba; R = Y, La, Lu; RE – paramagnetic trivalent rare-earth ions [1]. A high concentration of R and RE ions in fluorite crystals leads to the appearance of variety of paramagnetic centers and to formation of clusters.

CaF_2 single crystals were grown by Bridgman–Stockbarger (BS) and temperature gradient techniques (TGT) in argon atmosphere. EPR measurements were made at X-band cw Bruker ESP 300 spectrometer at low (helium) temperatures. For samples grown by the BS technique with 0.5 wt% CeO_2 and 2 wt% CeO_2 the “usual” tetragonal centers with g -values $g_{\parallel} = 3.05 \pm 0.01$, $g_{\perp} = 1.39 \pm 0.01$ predominate. For samples grown by the TGT method with approximately the same content of CeO_2 , with 0.5 wt% CeO_2 and 3 wt% CeO_2 the trigonal centers with g -values $g_{\parallel} = 3.67$ and $g_{\perp} < 0.3$ are observed. For the sample grown by the BS technique with 5 wt% CeO_2 the “new” tetragonal center with $g_{\parallel} \sim 0.73$, $g_{\perp} = 2.38$ has been detected (Fig. 1). These values are close to the tetragonal centers with $g_{\parallel} = 0.725 \pm 0.001$ and $g_{\perp} = 2.402 \pm 0.002$ observed earlier in [2] in CaF_2 doped with CeF_3 and co-doped with sodium. Such center was recently detected [3] in mixed $\text{Ba}_{1-x}\text{La}_x\text{F}_{2+x}$ crystals doped with 0.1 at% Ce^{3+} ions. The structure of the center is a controversial issue. It was supposed in [3] that this

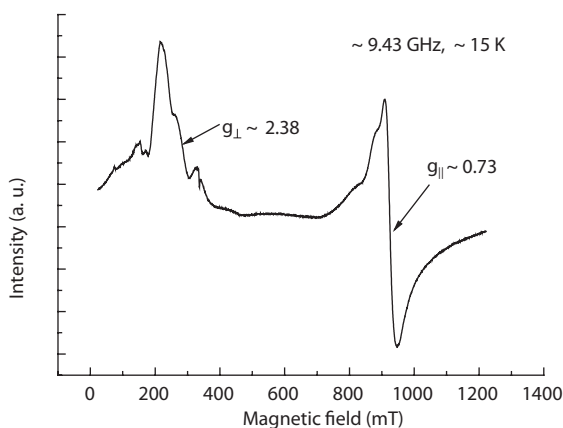


Fig. 1. EPR spectrum of $\text{CaF}_2+5\text{wt}\%\text{CeO}_2$.

tetragonal center is due to cubooctahedral cluster $\text{CeLa}_5\text{F}_{37}$. However, it has been found later that similar center is observed in BaF_2 doped only with CeF_3 [4]. Therefore it has been proposed that this tetragonal center may be due to the chain $\text{Ce}^{3+} - \square - \text{Ce}^{3+}$ elongated along the fourfold axis, where \square is a vacancy at the Ca position. Note that the concentration of the “new” tetragonal center had a maximum at 1% of CeF_3 in BaF_2 and it does not dominate over the “usual” tetragonal center. Fig. 1 shows that the “new” tetragonal center in this work is the main type of paramagnetic center in CaF_2 at 5% of CeO_2 .

The further increase of CeO_2 content from 10wt% to 15%wt of CeO_2 leads to the broad EPR line extended over all available ranges of magnetic fields.

This work was funded by the subsidy allocated to Kazan Federal University for the state assignment in the sphere of scientific activities [numbers 3.1156.2017/4.6]. EPR measurements were done using the equipment of the Federal Center of Shared Equipment of Kazan Federal University. The authors are grateful to A.A. Rodionov for the help with EPR measurements.

1. Aminov L.K., Gafurov M.R., Kurkin I.N., Rodionov A.A.: *Appl. Magn. Reson.* **45**, 1147 (2014)
2. McLaughlan S.D.: *Phys. Rev.* **160**, 287 (1967)
3. Aminov L.K., Kurkin I.N., Kurzin S.P., Gromov I.A., Mamin G.V., Rakhmatullin R.M.: *Phys. Solid State* **49**, 2086 (2007)
4. Aminov L.K., Kurkin I.N.: *Phys. Solid State* **55**, 123 (2013)

Influence of Magnetic Field on the Luminescence from X-irradiated Diamonds

**S. V. Anishchik¹, V. I. Borovkov¹, A. R. Melnikov¹, V. G. Vins²,
D. G. Bagryantsev², A. P. Yelisseyev³**

¹ Voevodsky Institute of Chemical Kinetics and Combustion SB RAS, Novosibirsk 630090,
Russian Federation, svan@kinetics.nsc.ru

² VELMAN Ltd., Novosibirsk 630060, Russian Federation

³ V. S. Sobolev Institute of Geology and Mineralogy SB RAS, Novosibirsk 630090,
Russian Federation

Investigation of magnetic field effects provides information about primary spin-dependent processes under irradiation. We detected for the first time such effects in luminescence from samples of synthetic diamond.

We studied the magnetic field effects in the luminescence from diamonds under X-irradiation. Two types of experiments were performed. In the first type we used CW irradiation from a Mo anode X-ray tube and varied the detection wavelength and external magnetic field B [1]. In the second type the sample was irradiated with about one nanosecond long X-ray pulses and the kinetics of luminescence was measured with and without external magnetic field alternately with the method of single photon counting [2].

In most of the tested diamond samples we observed a magnetic field insensitive long lived (time range of minutes) luminescence after the X-ray pulse. In these samples it is impossible to study the nanosecond time scale magnetic field

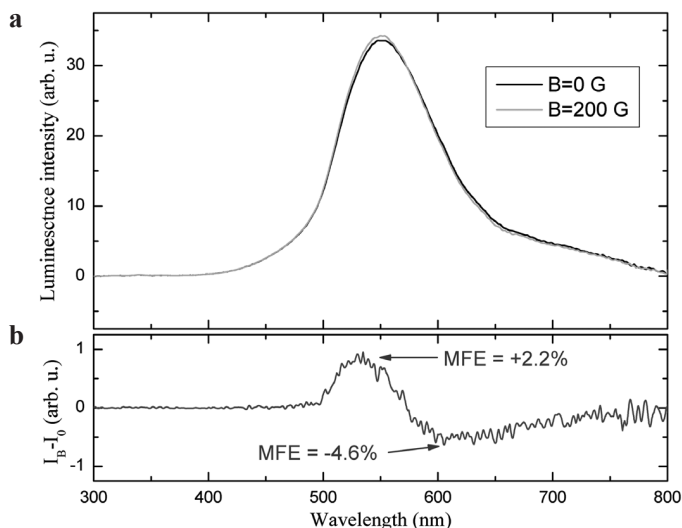


Fig. 1. The stationary magnetic field effect on the intensity of luminescence from single crystal of Ib type diamond with about 50% of ^{13}C under continuous X-ray irradiation.

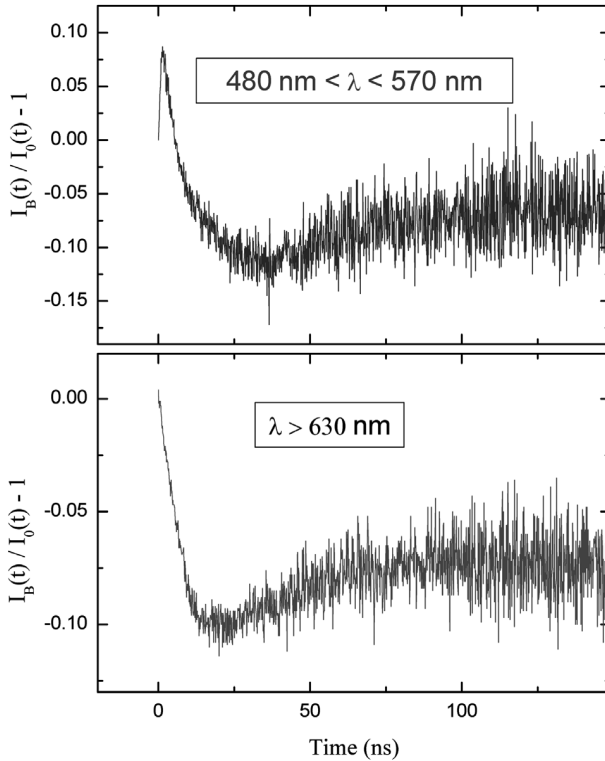


Fig. 2. The time-resolved magnetic field effect on the intensity of luminescence from single crystal of Ib type diamond with about 50% of ^{13}C under pulse X-ray irradiation.

effects in the luminescence. Although the nanosecond time scale luminescence kinetics could be detected in the first seconds of measurements, so short a measurement time is not enough to obtain sufficient signal to noise ratio. The CW magnetic field effects were also not detected in these samples.

But in several diamond samples the long lived luminescence was not so intense. In these samples we detected CW and time-resolved magnetic field effects. The shapes of the effects are different in different samples. As an example Figures 1 and 2 show the CW and time-resolved effects from isotope substituted diamond sample of type Ib with about 50% of ^{13}C . Currently we consider possible models to account for the observed effects.

The financial support of the Foundation for Basic Research (grant 16-03-00672) is gratefully acknowledged.

1. Kalneus E.V., Melnikov A.R., Korolev V.V., Ivannikov V.I., Stass D.V.: *Appl. Magn. Res.* **44**, 81–96 (2013)
2. Anishchik S.V., Grigiryants V.M., Shebolaev I.V., Chernousov Yu.D., Anisimov O.A., Molin Yu.N., *Instruments and Experimental Techniques* **32**, 813–815 (1989)

The Application of the Clinical MR Scanner for Multinuclear Research

N. V. Anisimov¹, A. G. Agafonnikova²

¹ Faculty of Fundamental Medicine, Lomonosov Moscow State University, Moscow 119991, Russian Federation, anisimovnv@mail.ru

² Faculty of Physics, Lomonosov Moscow State University, Moscow 119991, Russian Federation

It is reported the use of 0.5 T clinical MR scanner Bruker Tomikon S50 not only in biomedical research, but also for technological applications. For this purpose, NMR signals were registered from nuclei other than protons. Typical MRI equipment only works on protons. We carried out technical work that allowed us to register nuclei different from protons.

The ¹⁹F NMR signal was recorded during the perfluorocarbon compounds (PFC) research. Particular attention was paid to the preparation Perftoran®, well-known as blood substitute. We experimented with animals (rats), which were intravenously injected with this drug. In addition, by the ¹⁹F MRI method, the human gastrointestinal tract was studied, for which the volunteer swallowed capsules, filled with PFCs – perfluorodecalin and perfluorotributylamine. In all cases, at a specified time interval, the localization of the drug was monitored by MRI, and by NMR its transformation and the dynamics of excretion from the organism were monitored.

Studies were also carried out using test samples (phantoms) to optimize the parameters of the ¹⁹F MRI scanning of specific PFCs – perfluorodecalin and octafluorocyclobutane in the gas phase. The latter drug is a potential contrast agent for lung research.

In the process of multinuclear research, NMR spectra and MR images from ³¹P, ¹¹B, ²³Na nuclei were obtained at natural abundance, and for ¹³C, ²H – for isotope enrichment. For isotopically unenriched samples of ¹⁷O, ²⁹Si and ¹⁴N, only NMR spectra, (but not MRI) have so far been reliably recorded. In addition, outside the magnetic field, the nuclear quadrupole resonance spectra of ³⁵Cl (28.1 MHz) were successfully detected from powdered potassium chlorate. For ²³Na, NMR spectra and MR images of various parts of the human body, including the brain, were obtained.

We successfully recorded ¹³C signals using the polarization transfer methods – the Overhauser effect and the DEPT and INEPT techniques. We obtained NMR spectra using these methods not only by rf excitation of protons, but also fluorine nuclei. We used these techniques when recording the ¹³C signal from perfluorodecalin. It is hydrocarbon compound in which the hydrogen atoms are replaced by fluorine.

We conducted experiments on the simultaneous recording of NMR signals from two types of nuclei with close gyromagnetic ratios. The pairs ¹H/¹⁹F (isoflurane – C₃F₅HClO) and ¹³C/²³Na (sodium bicarbonate – NaHCO₃) were chosen. The excitation of signals for both nuclei of pair was carried out simultaneously – by

a short single pulse or by a sequential selective RF excitation of each nucleus from the selected pair. The reference frequency of the phase detector was set equal to the half-sum of their Larmor frequencies. The speed of digitization of the signal was less than their difference, and the filtering of the signal (digital and analog) was disabled. A useful result – the spectrum on which NMR lines from both nuclei from the selected pair are represented, was achieved due to a multiple spectral “aliasing” of both signals relative to the reference frequency of the phase detector – the undersampling effect [1].

Multinuclear resources of the scanner were also used for technological applications – non-invasive identification of alcohol-containing products. It was assumed on the basis of measuring the amplitudes of ^1H , ^2H , ^{13}C , ^{17}O NMR spectra and relaxation times for each of the branded samples with a volume of 0.5 liters and a 40% strength, to reveal their possible differences. The reason for the differences was that the products were made from different raw materials and brought from different geographical regions [2]. The spectra of all the above mentioned nuclei were obtained. Due to the large volume of the sample, they are obtained with a high signal-to-noise ratio at an acceptable time (~10 min).

It was noted that the difference in the T_2 values is most clearly seen on the ^{17}O NMR spectra. This difference is well revealed by the linewidth. On the spectra of ^2H , this difference is less pronounced, and for protons – it is not detected at all. It is due to the fact that the ^{17}O NMR lines are very wide, and the contribution of the inhomogeneous broadening is very small, in contrast to the ^1H NMR lines.

The clinical scanner can be successfully used for multinuclear applications – both medical-biological and technological. The ability to examine large samples in it creates favorable opportunities for recording nuclei with a low natural abundance and a small gyromagnetic ratio. To increase the sensitivity to signals from such nuclei, it is also useful to implement the double resonance methods.

1. Anisimov N.V., Pavlova O.S.: *Appl. Magn. Reson.* **49**(5), 523 (2018)
2. Martin M.L., Martin G.J.: *NMR Basic Principles and Progress* **23** (1990)

NMR Study of Magnetic Properties of New Triangle-Lattice Compound A_2MnTeO_6

**E. Anisimova^{1,4}, D. Gafurov^{1,4}, G. Raganyan², E. Zvereva²,
V. Nalbandyan³, A. Vasiliev², E. Vavilova¹**

¹ Zavoisky Physical-Technical Institute, FRC Kazan Scientific Center of RAS, Kazan 420029, Russian Federation, jenia.vavilova@gmail.com

² MSU, Moscow 119991, Russian Federation

³ SFU, Rostov-na-Donu 344090, Russian Federation

⁴ KPhU, Kazan 420019, Russian Federation

As it was shown by magnetometry and ESR measurements a new family of A_2MnTeO_6 ($A = Li, Na$) demonstrates a nontrivial effect of hidden magnetic order. It's static and dynamic magnetic properties indicate a strong frustration on the triangular lattice and a two-dimensional character of magnetism. Our NMR studies make it possible to clarify the picture of the establishment of the magnetic order for different values of the external magnetic field. The data on nuclear magnetic relaxation and transformation of the shape of the spectrum prove a presence of the magnetic order, even in small external fields, where the static magnetometry data does not demonstrate any features on the temperature dependence of the magnetic susceptibility.

The work was supported by grant RFBR 18-02-00664

CW Saturation of Nitroxyl Radicals in Liquids

**M. M. Bakirov¹, K. M. Salikhov^{1,2}, R. T. Galeev¹,
I. T. Khairuzhdinov¹, B. Bales³**

¹ Zavoiyskiy Physical-Technical Institute, FRC Kazan Scientific Center of RAS, Kazan 420029, Russian Federation, pinas1@yandex.ru

² Kazan Federal University, Kazan 420008, Russian Federation

³ Western Institute of Nanoelectronics, University of California, Los Angeles 18111, USA

The shape of the CW saturation line of the spin probes depends on T_1 and T_2 relaxation times, the spin decoherence and spin coherence transfer between probes. These parameters depends on the different interactions: spin exchange interaction, dipole-dipole interaction and the hyperfine interaction of the unpaired electrons with magnetic nuclei. This gives the way to study these interactions. We carried out an experimental and theoretical study of the possibilities of this approach to the determination of relaxation parameters that depend on the exchange and dipole-dipole interactions.

EPR Measurements of 4-Hydroxy-2,2,6,6-tetramethylpiperidine-1-¹⁵N-oxyl, (TEMPOL-¹⁵N) and 4-Hydroxy-2,2,6,6-tetramethylpiperidine-d₁₇-1-¹⁵N -oxyl, (TEMPOL-¹⁵N-d₁₇) in 60% water glycerol solution were carried out at different mw power. Experiment was performed at temperature range from 273 to 340 (K) and concentrations from 10⁻⁴ to about 30 · 10⁻² mole/l. T_1 , T_2 relaxation times were measured for each temperature. Heisenberg spin exchange and Dipole-Dipole constants were obtained for this samples in our previous work [1, 2]. Some saturation curves for EPR spectra of nitroxyl radicals have been shown on Fig. 1.

1. Salikhov K.M., Bakirov M.M., Galeev R.T.: Appl. Magn. Reson. **47**, 1095-1122 (2016)
2. Bales B.L., Bakirov M.M., Galeev R.T., Kirilyuk I.A., Salikhov K.M.: Appl. Magn. Reson. **48**, 1399-1445 (2017)

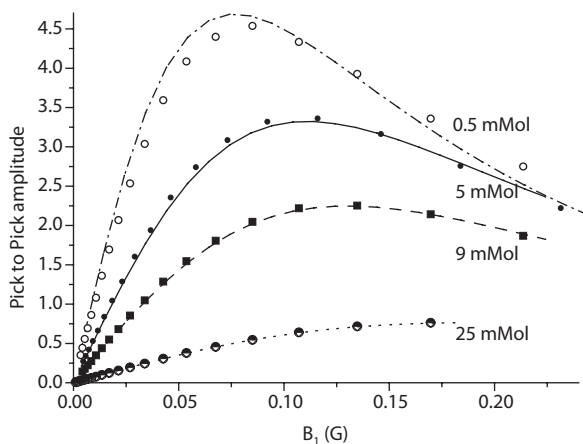


Fig. 1. Saturation curves Tempol N15D at 298 K (points – experimental data, lines – model values).

Receiving and Transmitting System for a Specialized Small-Sized Magnetic Resonance Scanner with a 0.4 Tesla Field

**A. A. Bayazitov¹, Ya. V. Fattakhov¹, V. E. Khundiryakov²,
A. R. Fakhrutdinov¹, V. A. Shagalov¹, R. Sh. Khabipov¹**

¹ Zavoisky Physical-Technical Institute, FRC Kazan Scientific Center of RAS, Kazan 420029, Russian Federation, bayazitov.alfis@kfti.knc.ru

² Kazan Federal University, Kazan 420008, Russian Federation

The work is devoted to the receiving-transmitting system for a small-sized specialized traumatological magnetic resonance scanner with 0.4 T magnetic field induction. At the heart of the scanner is a permanent magnet, which makes it possible to use a less expensive means of cooling. Also the scanner has compact dimensions and can be installed in mobile specialized transport. The dimensions of the working area of the scanner along the field direction are 210 mm. Small workspace area of the scanner, imposing some restrictions on the size of the receiving and transmitting system. The transmitting circuit and the receiving coil are located at a distance of 5 mm, for this reason, a small inductive coupling is shown in both circuits. To reduce the coupling, we rotated the receiving sensor relative to the transmitting circuit.

In the work, mathematical modeling of a receiving sensor of various designs was carried out to obtain a sensor with a homogeneous signal distribution in the field of interest. When modeling the coil, parameters such as X_1 , X_2 , R_z , R_y and the number of loops were changed. X_1 and X_2 is the distance between the loops, and R_z , R_y is the half-axis of the ellipse. It was assumed that the maximum deviation of the field from the mean value should be less than 10%. The area of homogeneity estimation is $150 \times 100 \times 60$ mm, respectively along the X , Y and Z axes.

Taking into account the simulation results, several prototypes were manufactured and their characteristics were measured. The magnitude of the received signal of the NMR-imaging response along the main axis of the prototypes was measured. The first prototype corresponds to a sample of 4 parallel loops. The second prototype corresponds to a sample of 6 loops connected in parallel. Double extreme loops have a width of 20 mm, two internal ones have a width of 10 mm. The third prototype reflects the variant corresponds to the sample of 6 loops: internal double loops are connected in series with each other with a loop width of 20 mm, the last one in loop is connected in parallel, the width of the loop is 10 mm. We settled on the second variant of the test sample with 6 loops, since it has a large signal amplitude for reception.

Spatial Structure of YRFK Peptides with Triphenylphosphonium Moiety by NMR Spectroscopy

D. S. Blokhin^{1,2}, R. Garifullin¹, T. I. Abdullin¹, V. V. Klochkov²

¹ Institute of Fundamental Medicine and Biology, Kazan Federal University, Kazan 420008, Russian Federation, dblohin@kpu.ru

² Institute of Physics, Kazan Federal University, Kazan 420008, Russian Federation

Chemical conjugation of oligopeptides with artificial compounds, including amino acid analogues, is an established way of increasing stability and improving pharmacokinetic properties of oligopeptides without substantial disruption of their natural structure and functions. For this purpose, terminal and/or side group modification of peptides with alkyl/lipid or polymeric moieties are routinely used [1]. Phosphorus-containing compounds are poorly investigated peptide modifiers which however have a great potential for modulation of physicochemical/transport properties of oligopeptides. Their properties are directly related to their spatial structure.

NMR spectroscopy is one of the most powerful techniques for characterization of spatial structure of peptides. In this paper, we determined the spatial structures of a series of modified TPP oligopeptides (Fig. 1) by NMR spectroscopy in H₂O/D₂O mixed solution supplemented with DPC micelles. Micelle-forming deuterated surfactants are commonly used to assist the NMR analysis of peptide molecules in aqueous solution. DPC micelles are utilized to decrease mobility of small peptide molecules, thus increasing informativeness of their NMR spectra [2].

NMR assignments for oligopeptides were obtained from 2D ¹H-¹H TOCSY and ¹H-¹H NOESY spectra on a 500 MHz NMR spectrometer (Bruker, AVANCE II-500) at 298 K. For structural calculations, the ensemble was subjected to restrained molecular dynamics using the XPLOR-NIH software.

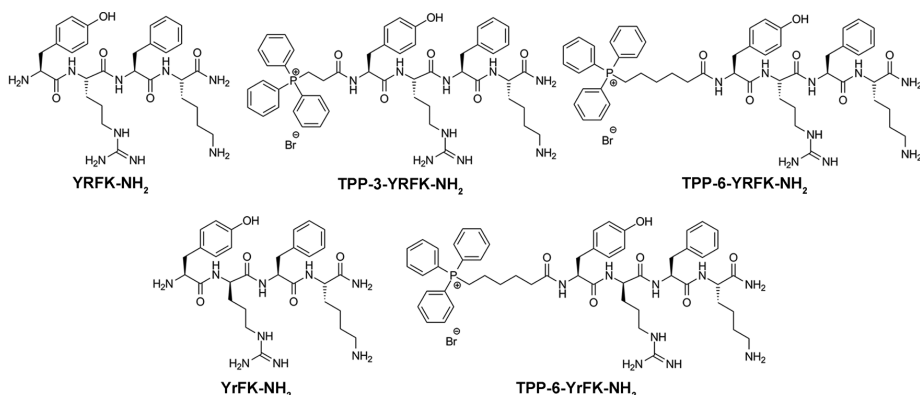


Fig. 1. Structure of tetrapeptides based on YRFK motif and their triphenylphosphonium derivatives (R – L-arginine; r – D-arginine).

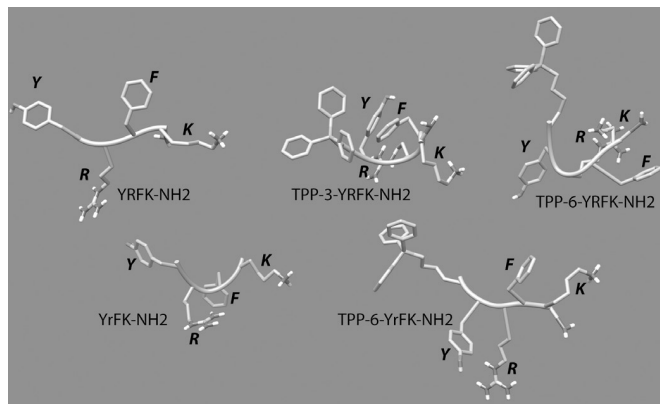


Fig. 2. Three-dimensional minimum energy structures of YRFK-NH₂, TPP-3-YRFK-NH₂, YrFK-NH₂ and TPP-6-YrFK-NH₂.

The structures of oligopeptides are shown in Fig. 2. The backbone RMSD values for Arg-Lys fragment were 0.56 ± 0.18 Å (YRFK-NH₂) and 0.55 ± 0.22 Å (YrFK-NH₂). The analogous values for Tyr-Lys fragment were 0.05 ± 0.03 Å (TPP-3-YRFK-NH₂), 0.20 ± 0.12 Å (TPP-6-YRFK-NH₂) and 0.09 ± 0.06 Å (TPP-6-YrFK-NH₂). From the analysis of the obtained spatial structures and RMSD, it can be concluded that the presence of TPP-tailings stabilizes the oligopeptide molecules.

This work was performed according to the Russian Government Program of Competitive Growth of the Kazan Federal University.

1. Shiba K.: Chem. Soc. Rev. **39**(1), 117 (2010)
2. Warschawski D.E., Arnold A.A., Beaugrand M., Gravel A., Chartrand É., Marcotte I.: Biochim Biophys Acta (BBA), Biomembranes **1808**(8), 1957 (2011)

Peculiarities of Low Temperature FMR in Ion Beam Synthesized Co Silicide Films

V. V. Chirkov¹, G. G. Gumarov¹, V. Yu. Petukhov¹, M. M. Bakirov¹

¹ Zavoisky Physical-Technical Institute, FRC Kazan Scientific Center of RAS, Kazan 420029, Russian Federation, chirkov672@gmail.com

Thin ferromagnetic films with the uniaxial magnetic anisotropy were synthesized by Co^+ implantation into single-crystal silicon in the external magnetic field [1]. It was concluded that the formation of the induced magnetic anisotropy is due to the directional atomic pair ordering (the Neel-Taniguchi model). The linear temperature dependence of the magnetic anisotropy constant for synthesized films was revealed in the temperature range from 100 to 300 K that is not described by the Callen-Callen model. The obtained dependence can be explained by the difference in the coefficients of thermal expansion of the Si (111) substrate and the ion-beam-synthesized cobalt silicide films. The aim of this work is to study the peculiarities of FMR at temperatures below 100 K.

The samples of thin films of cobalt silicides obtained by ion-beam synthesis in the external magnetic field at energy of 40 keV were studied. FMR spectra were recorded on an EMXplus X-band EPR spectrometer at in-plane geometry. The set of oscillating peaks are observed in the spectra in the temperature range from 40 to 80 K (see Fig. 1). The period of oscillations increases with the temperature rise and depends on the power of the microwave radiation in a complex manner.

We believe that observed oscillations in the FMR spectra are the spectrum of spin-wave resonance in a tangentially magnetized thin film [2].

1. Chirkov V.V., Gumarov G.G., Petukhov V.Yu. *et al.*: Appl. Magn. Reson. **49**, 381 (2018)
2. Vasilevskaya T.M., Sementsov D.I.: J. Solid State **49**, 1913 (2007)

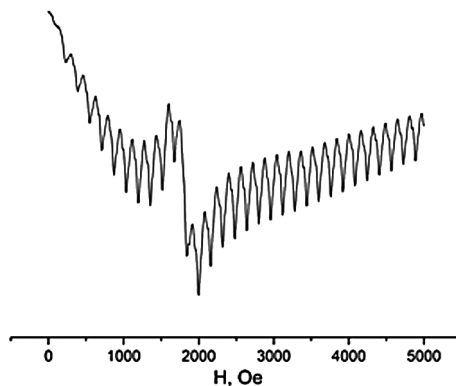


Fig. 1. FMR spectra for a sample at a temperature of 40 K.

Fe^{3+} -Cytochromes Signals in EPR Spectra of Sportsmen's Serum Blood

**A. I. Chushnikov¹, M. I. Ibragimova¹, G. V. Cherepnev²,
V. Yu. Petukhov¹, I. V. Yatsyk¹**

¹ Zavoisky Physical-Technical Institute, FRC Kazan Scientific Center of RAS, Kazan 420029,
Russian Federation

² Tatarstan Republic Clinical Hospital №2, Kazan, 420043, Russian Federation

Monitoring the health of professional athletes is very important in sports medicine because any metabolic disorders can adversely affect the professional qualities of sportsmen. Usually examining the status of athletes include hematological and biochemical analysis but these tests do not provide information about a protein such as cytochrome C. At the same time, for example EPR can detect signals from the paramagnetic centers of iron and copper incorporated into the composition of the cytochromes. The blood levels of such proteins in athlete's blood may also provide useful information for a more correct assessment of the status of the athlete. Therefore, the aim of this work was to analyze the signals in the EPR serum spectra from the paramagnetic centers of iron in cytochromes.

EPR spectra were recorded from equal volume (0.5 ml) of serum on a Bruker EMX Plus spectrometer at 9.38 GHz with a microwave power of 2 mW, a modulation frequency of 100 kHz, a modulation amplitude of 5 G at a temperature of $T = 5\text{--}77$ K. A study group consisted of 57 professional athletes from the Continental Hockey League.

At a liquid nitrogen temperature the EPR spectra from blood serum usually contain 3 signals: with $g \sim 4.3$ from Fe^{3+} ($S = 5/2$) incorporated into the com-

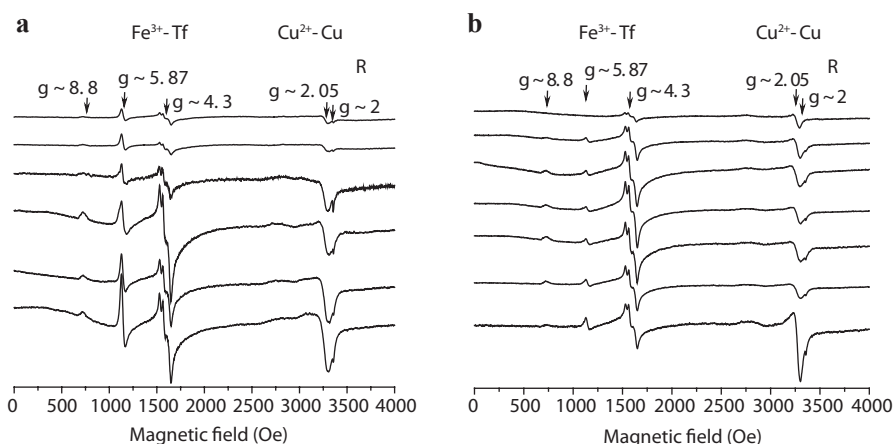


Fig. 1. Spectra from the samples of the athlete's serum recorded at $T = 5$ K. Spectra in Figs. 1a and b demonstrate the different levels of Fe^{3+} -cytochrome C.

position of the transferrin – plasma iron-glycoprotein; with $g \sim 2.05$ from Cu^{2+} ions incorporated into the composition of the ceruloplasmin – copper-containing plasma protein and signal with $g \sim 2$ from free radicals. The nature of the last has not yet fully established. At helium temperatures, the signals with g -factors 5.87 and 8.8 are presented along with the three above mentioned signals. These signals with high probability can be identified as a signal of high-spin heme iron (Fe^{3+}) in the composition of cytochromes. This assumption was based on the fact that signals from cytochromes are recorded only in the temperature range $T = 5\text{--}40$ K [1]. In particular, the signal with $g = 5.87$ with high probability can be identified as a signal from Fe^{3+} in cytochrome C. The type of another cytochrome with g -factor 8.8 is not yet uniquely identified.

A feature of the spectra is that for 14% of athletes at $T = 5$ K the line intensity with $g \sim 5.87$ is practically comparable with the intensity of the Fe^{3+} -transferrin line with $g \sim 4.3$ (Fig. 1a). Spectra with a relatively low intensity of the line with $g \sim 5.87$ were recorded for 86% of athletes (Fig. 1b). The presence of highly intensive absorption line from cytochrome C in the EPR spectra of serum is possibly due to the usage of various metabolically active preparations, for example, the permitted preparation of cytochrome C. This assumption requires further additional studies.

It should be noted that biochemical analyzes do not provide data on the content of cytochrome C in the blood serum, therefore the EPR method can be useful in routine testing in order to clarify the assessment of the athlete's status.

1. Harbitz E., Andersson K.K.: Cytochrome *c-554* from *Methylosinus trichosporium* OB3b; a protein that belongs to cytochrome c2 family and exhibits a HALS-type EPR signal: PloS One, e22014, 6 (7) (2011)

The Study of Protein Ligand Interaction by Water LOGSY NMR

A. G. Danilova^{1,2}, A. N. Turanov³, B. I. Khairutdinov^{1,2}, Yu. F. Zuev¹

¹ Kazan Institute of Biochemistry and Biophysics, FRC Kazan Scientific Center of RAS,
Kazan 420111, Russian Federation, khairutdinov@kibb.knc.ru

² Kazan Federal University, Kazan 420008, Russian Federation

³ Zavoisky Physical-Technical Institute, FRC Kazan Scientific Center of RAS, Kazan 420029,
Russian Federation

The protein ligand interaction plays a key role in structural biology. Such interactions depend both on the specific interactions in the binding site as well as the non-specific forces outside the binding pocket. Computational modeling such process widely used in modern science together with experimental measurements by physical methods. One of the promising approaches to study of protein ligand interaction is application WaterLOGSY NMR experiment [1]. This experiment allows to measure dissociation constant for the system of low molecular weighted ligands that bind protein.

Thus in this work dissociation constants of interaction ceftriaxonum, warfarin and rutin with human serum albumin or bovine serum albumin have been measured. The formation of complexes of the studied ligands with albumin is shown experimentally.

1. Dalvit C., Fogliatto G., Stewart A. *et al.*: J. Biomol. NMR **21**, 349 (2001)

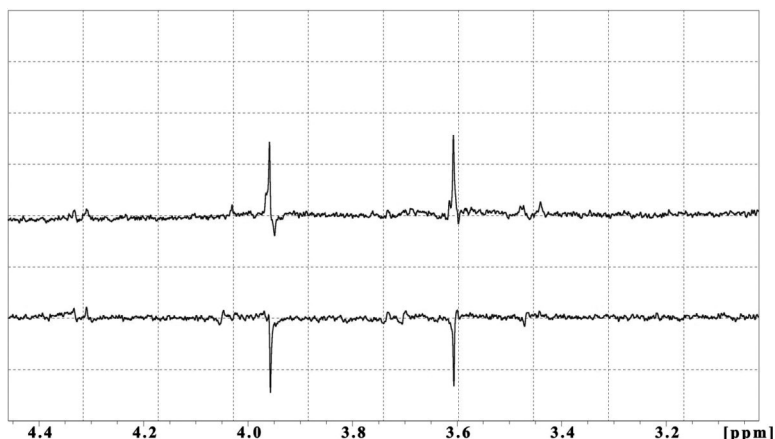


Fig. 1. Fragment of WaterLogsy spectra for water solution of 800 μM free warfarin (bottom) and 800 μM warfarin with 10 μM bovine serum albumin (upper). Changing of the phase NMR signals of the warfarin indicate formation protein ligand complex.

Electron Spin Resonance Study of $\text{Sm}_{1-x}\text{Eu}_x\text{B}_6$ Solid Solutions

S. V. Demishev^{1,2,3}, M. I. Gilmanov², A. N. Samarin¹, A. V. Semeno^{1,2},
N. E. Sluchanko^{1,2}, N. Yu. Shitsevalova⁴, V. B. Filipov⁴, V. V. Glushkov^{1,2,3}

¹ Prokhorov General Physics Institute of RAS, Moscow 119991, Russian Federation,
gilmanov@lt.gpi.ru

² Moscow Institute of Physics and Technology, Dolgoprudny 141700, Moscow region,
Russian Federation

³ National Research University Higher School of Economics, Moscow 101000, Russian Federation

⁴ Institute for Problems of Materials Science of NASU, Kiev 03680, Ukraine

Topological Kondo insulator candidate SmB_6 was recently investigated by the means of electron spin resonance (ESR) [1]. A possible magnetic phase transition was reported on the (110) sample surface at the temperature $T_c \approx 5.35$ K. In this regard, the study of an influence of different magnetic impurities on ESR and magnetic order formation could be quite valuable. First results of such examination performed on high frequency (60 GHz) ESR spectrometer for the case of Eu doping are reported in the present work.

A series of solid solutions $\text{Sm}_{1-x}\text{Eu}_x\text{B}_6$ with $x = 0.005, 0.02, 0.05$ have been studied. It is found out that even the smallest Eu concentration drastically changes the ESR spectrum at low temperatures (Fig. 1). At temperatures $T > 7-8$ K the only one narrow line with $g \approx 2$ is observed for every concentration as should be expected for the case of isolated Eu^{3+} magnetic ion in $^8\text{S}_{7/2}$ state. Below $T^* \sim 7$ K the ESR line intensity starts to grow significantly and the spectrum structure becomes much more complicated. The most striking feature of the observed behavior is that the value of $T^* \sim 7$ K is very close to characteristic temperature T_c corresponding to the transition in undoped SmB_6 single crystal

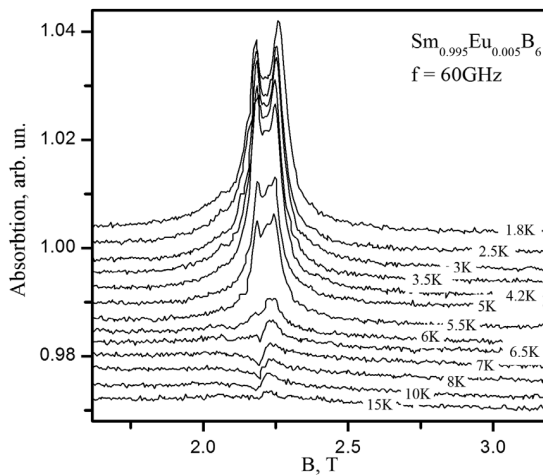


Fig. 1. Temperature dependence of $\text{Sm}_{1-x}\text{Eu}_x\text{B}_6$ ESR spectra for $x = 0.005$.

and almost coincides for different compositions. It is worth noting that even 10 times change in Eu^{3+} concentration leads to relatively small shift in T^* value about $\sim 1\text{--}2$ K.

The ESR parameters analysis in $\text{Sm}_{1-x}\text{Eu}_x\text{B}_6$ line shape analysis is difficult due to complicated line shape, which dramatically changes with Eu concentration. This problem may require future additional study of transport and magnetic properties which together with ESR data may shed more light on the effects of Eu doping of strongly correlated topological Kondo insulator SmB_6 .

This work was supported by programmes of Russian Academy of Sciences “Electron spin resonance, spin-dependent electronic effects and spin technologies”, “Electron correlations in strongly interacting systems” and by RFBR grant 17-02-00127 A.

1. Demishev S.V., Gilmanov M.I., Samarin A.N., Semeno A.V., Sluchanko N.E., Samarin N.A., Bogach A.V., Shitsevalova N.Yu., Filipov V.B., Karasev M.S., Glushkov V.V.: *Sci. Rep.* **8**, 7125 (2018)

The Nature of Electron Spin Resonance in CeB_6

S. V. Demishev^{1,2,3}, M. I. Gilmanov², A. N. Samarin¹, A. V. Semeno^{1,2},
N. E. Sluchanko^{1,2}, N. Yu. Shitsevalova⁴, V. B. Filipov⁴, V. V. Glushkov^{1,2,3}

¹ Prokhorov General Physics Institute of RAS, Moscow 119991, Russian Federation,
gilmanov@lt.gpi.ru

² Moscow Institute of Physics and Technology, Dolgoprudny 141700, Russian Federation

³ National Research University Higher School of Economics, Moscow 101000, Russian Federation

⁴ Institute for Problems of Materials Science of NASU, Kiev 03680, Ukraine

In our recent study angular dependencies of electron spin resonance (ESR) line parameters in CeB_6 were reported [1]. Significant discrepancies with the model of ESR in antiferroquadrupolar (AFQ) phase of CeB_6 developed by Shlottmann [2] were found. For example, g -factor predicted in [2] turned out to be $\sim 25\%$ larger than the theoretical expectation. Moreover, theory [2] fails to describe satisfactorily symmetry of experimental angular dependencies of the g -factor. Another observation which could not be at the time explained by the model [2] is considerable anomalies in temperature behavior of g -factor, line width and oscillating magnetization in [100] direction. These results were disputed in recent publication [3], which suggests that theory [2] may be used for description of the ESR in CeB_6 . Here we are aimed to compare these two different interpretations in order to elucidate physics of the ESR in this strongly correlated metal.

Although it seems that with some presumptions model [3] actually allows fitting g -factor data, it still faces problems of accounting for an antiferromagnetic fluctuations, which are essential for the explanation of the observed anomalies of ESR parameters for [100] direction. Even more importantly, the only reason for the ESR signal to become observable offered by models [2, 3] is the narrowing of the resonance line due to ferromagnetic correlations in the AFQ phase. However, close to the phase boundary along with broadening of the ESR line its intensity tends to zero, which does not taken into consideration in [2,3]. Moreover, phase transition inside the AFQ was reported recently [4] from the transport data. In fact, ESR line is observable only below the transition which occurs around $T \approx 3.8$ K at the resonance field. Thereby the physical picture of the aforementioned theoretical models [2, 3] is also should be reconsidered. This work is supported by the Russian Scientific Foundation, Grant №17-12-01426.

1. Semeno A.V., Gilmanov M.I., Bogach A.V., Krasnorussky V.N., Samarin A.N., Samarin N.A., Sluchanko N.E., Shitsevalova N.Yu., Filipov V.B., Glushkov V.V., Demishev S.V.: Scientific Reports **6**, 39196, (2016)
2. Shlottmann P.: Appl. Phys. J. **113**, 17E109 (2013)
3. Shlottmann P.: Magnetochemistry, **4**, 27 (2018)
4. Demishev S.V., Krasnorussky V.N., Bogach A.V., Voronov V.V., Shitsevalova N.Yu., Filipov V.B., Glushkov V.V., Sluchanko N.E.: Scientific Reports **7**, 17430 (2017)

Structural Model of the Yb³⁺ Ion in the LiCaAlF₆ Single Crystal

**M. L. Falin¹, V. A. Latypov¹, A. M. Leushin², G. M. Safiullin¹,
A. A. Shakirov², A. A. Shavelev²**

¹ Zavoisky Physical-Technical Institute, FRC Kazan Scientific Center of RAS, Kazan 420029, Russian Federation, falin@kfti.knc.ru

² Kazan Federal University, Kazan 420008, Russian Federation

Lithium calcium hexafluoroaluminate LiCaAlF₆ (LiCAF) is a colquirite-type fluoride with the hexagonal structure belonging to the D_{3d}² (P $\bar{3}1c$) space group (group number 163). It is an optically uniaxial crystal with two formula units per unit cell. Six fluorine (F) atoms surround a lithium (Li), calcium (Ca), or aluminum (Al) atom. Each Li, Ca, and Al cation occupies a deformed octahedral site with C_{3v} symmetry as shown in Fig. 1 [1]. The lattice constants are $a = 4.996$ Å and $c = 9.636$ Å. The LiCAF crystals when doped with rare-earth (RE) ions (Ce³⁺, Nd³⁺, Er³⁺, Tm³⁺) are used in photonic devices because they are good hosts for optically active cations. Recent examples of applications include the use of Nd³⁺-LiCAF in photolithography [2] and Ce³⁺-LiCAF in ultraviolet (UV) chirped-pulse application [3]. In addition, Ce³⁺-doped LiCAF has been reported as a leading candidate for a tunable solid-state laser in the UV region [4].

The optical spectra due to f-d transitions between the ground and excited configurations of RE ions were investigated in the majority of studies devoted to doped LiCAF crystals. Electron paramagnetic resonance (EPR) spectra of Ce³⁺, Dy³⁺, Er³⁺, Yb³⁺ ions were observed in [4, 5]. However, the study of EPR spectra and optical spectra of RE ions which are due to the configuration f-f transitions, provides information about the magnetic properties of the RE³⁺-doped LiCAF and the local structure of the RE ion site in such crystals.

This report is devoted to the detailed study of impurity RE paramagnetic centers formed by Yb³⁺ ions in the LiCAF single crystal by EPR and optical f-f spectroscopy methods.

The LiCAF crystals were grown using the Bridgman technique in the fluorinating atmosphere. Their melting point is about 810 °C. We used an Ar:CF₄ gaseous mixture with the volume ratio of 7:4 to fill the chamber after its evacuation to 10⁻⁴ mbar. Components of the charge of LiCAF to be grown were taken in ratios correspondent strongly to the stoichiometric composition. The measured temperature gradient was about 70 °C/cm. The achieved temperature gradient was sufficient for the LiCAF compound which melts congruently to crystallize with relatively high rates. The pulling rate of the crucible in our experiments was 4 mm/h. The LiCAF crystals were grown on seed crystals with the orientation of the specified optical c -axis perpendicular to the boule.

The results of these experiments made it possible to conclude that Yb³⁺ ions replace host cation sites Ca²⁺ forming one type of the paramagnetic center with trigonal symmetry (C_{3v}) without any charge compensators in its immediate

neighborhood. The positions of lines in optical spectra were specified for this center. The Stark level energies of the Yb^{3+} multiplets were determined from optical spectra. The crystal field parameters of this center were determined from the scheme of energy levels and g -factors of the ground Kramers doublet. The crystal-field potential of the Yb^{3+} center made it possible to judge, at least qualitatively, about the nearest surrounding of the Yb^{3+} ion.

This work was supported by the program of the Presidium of the Russian Academy of Sciences no. 5 “Electron spin resonance, spin-dependent electron effects and spin technologies” and by the subsidy of the Russian Government (agreement No.02.A03.21.0002) to support the Program of Competitive Growth of Kazan Federal University and optical spectroscopy experiments were funded by the Russian Foundation for Basic Research (project no. 18-32-00936). AML was funded by the subsidy allocated to Kazan Federal University for the state assignment in the sphere of scientific activities (project 3.672.2017/8.9).

1. Viebahn V.W.: *Z. Anorg. Allg. Chem.* **386**, 335 (1971)
2. Sarantopoulou E., Kollia Z., Cefalas A.C.: *Microelectron. Eng.* **53**, 105 (2000)
3. Liu Z., Kozeki T., Suzuki Y., Sarukura N.: *Opt. Lett.* **26**, 301 (2001)
4. Dubinskii M.A., Semashko V.V., Naumov A.K., Abdulsabirov R.Y., Korableva S.L.: *Laser Phys.* **3**, 216 (1993)
5. Kurkin I.N., Sedov L.L., Yagudin Sh.I.: *Solid State Physics* **32**, 2779 (1991).
6. Yamaga M., Lee D., Henderson B., Hant T.P.J., Gallagher H.G., Yosida T.: *J. Phys.: Condens. Matter* **10**, 3223 (1998)

New Fe(III) Complexes with Tetradentate Schiff Bases and Photosensitive Ligands

**E. Frolova, O. Turanova, M. Volkov, L. Mingalieva, L. Gafiyatullin,
I. Ovchinnikov, A. Turanov**

Zavoisky Physical-Technical Institute, FRC Kazan Scientific Center of RAS, Kazan 420029,
Russian Federation, fro-e@yandex.ru

As a result of the search for new materials with a photoactive channel for controlling magnetic properties, a series of Fe (III) coordination compounds of general formula $[\text{FeL}(\text{Sp})_2]\text{BPh}_4 \times \text{MeOH}$ (where Sp is a photosensitive monodentate ligand, such as salen, bzacen, acen) was synthesized, characterized and studied by EPR, NMR, and UV-spectroscopy.

The effect of the chemical structure of the equatorial ligand on the spin state of the Fe (III) ion was proved by EPR and NMR both in solid state and in CH_2Cl_2 solutions. For complexes with two aromatic groups in L (salen), the high-spin state of Fe (III) ions is observed ($S = 5/2$, $D > h\nu$, $E/D \sim 1/3$). For compounds with the presence of two methyl groups and the absence of aromatic rings in L (acen), a spin transition was observed in the temperature range 160–340 K. The combination of aromatic and aliphatic groups in L (bzacen) leads to extending the temperature range of the spin transition.

Finally, the variation of structural fragments in tetradentate ligands leads to a change in the electronic environment of the coordination node, the geometry of the molecules, and, correspondingly, the spin state.

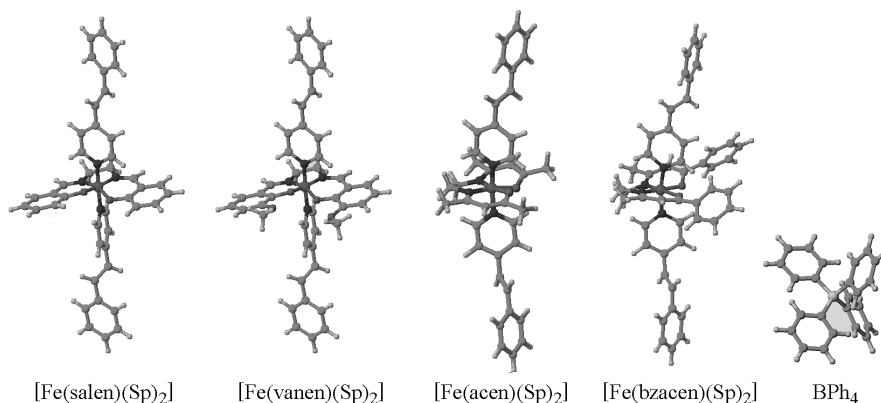


Fig. 1. The structure illustration of the studied Fe (III) complexes.

Study of the Conformation of γ -Irradiated Calcium Gluconate by the ESR Method

A. R. Gafarova, G. G. Gumarov, I. A. Goenko

Zavoisky Physical-Technical Institute, FRC Kazan Scientific Center of RAS, Kazan 420029,
Russian Federation, albina-gafarova@mail.ru

One of the most popular drugs used in disorders of calcium metabolism in the body is calcium gluconate (GC). The new mechanically activated modified nano-dispersed amorphous form of calcium gluconate (MACG) significantly increases the bioavailability and efficacy of treatment [1, 2]. When attempting to study the changes in the stereochemical structure of a molecule by mechanical activation, it became clear that accurate data on the structure including the initial GC are still lacking, since classical methods proved to be inapplicable. In this paper we consider the possibility of using the ESR method to determine the conformation of calcium gluconate. Since the initial GC does not have a resolved ESR signal, then to obtain information about the system, it is possible to introduce artificial defects into it, for this we used ionizing radiation in our work. We used samples of tableted calcium gluconate, as well as pure laboratory GC Sigma Aldrich. The samples were irradiated with photons on the gamma-therapeutic system Rokus, after which they were investigated by ESR.

The spectra were analyzed using the Easy Spin program. The spectra are multicomponent, with a clearly pronounced hyperfine structure. The components of the model spectra correspond to different radicals. The data obtained with the help of modeling can be used to calculate torsion angles corresponding to the hyperfine coupling constants [3]. Thus, in the study of GC samples, exact values of the torsion angles between the C-H bond and the axis of the orbital of the unpaired electron were obtained. The position of the paramagnetic centers on different carbon atoms with the components of the spectrum is compared. As a result, two possible conformations of the calcium gluconate molecule were revealed.

1. Patent of Russia № 2373185 (2009)
2. Konygin G.N. *et al.*: Experimental substantiation of calcium gluconate production. Materials of conf. "Actual Issues of Pediatric Surgery", p. 56–59. Izhevsk, 2003.
3. Sosulin I.S., Sosulin V.I., Shiryayeva E.S., Feldman V.I.: Radiation Physics and Chemistry, 178–183 (2015)

Study of γ -Irradiated Calcium Gluconate by X- and Q-EPR

**A. R. Gafarova, G. G. Gumarov, I. A. Goenko, M. M. Bakirov,
R. B. Zaripov, V. Yu. Petukhov**

Zavoisky Physical-Technical Institute, FRC Kazan Scientific Center of RAS, Kazan 420029,
Russian Federation, albina-gafarova@mail.ru

One of the most popular drugs used in disorders of calcium metabolism in the body is calcium gluconate (GC). The new mechanically activated modified nano-dispersed amorphous form of calcium gluconate (MACG) significantly increases the bioavailability and efficacy of treatment [1, 2]. When attempting to study the changes in the stereochemical structure of a molecule by mechanical activation, it became clear that accurate data on the structure including the initial GC are still lacking, since classical methods proved to be inapplicable. In this paper we consider the possibility of using the ESR method to determine the conformation of calcium gluconate. Since the initial GC does not have a resolved ESR signal, then to obtain information about the system, it is possible to introduce artificial defects into it, for this we used ionizing radiation in our work. We used samples of tableted calcium gluconate, as well as pure laboratory GC Sigma Aldrich. The samples were irradiated with photons on the gamma-therapeutic system Rokus, after which they were investigated by ESR.

The spectra were analyzed using the Easy Spin program. The data obtained with the help of modeling can be used to calculate torsion angles corresponding to the hyperfine coupling constants [3]. Thus, in the study of GC samples, exact values of the torsion angles between the C-H bonds and the axis of the orbital of the unpaired electron were obtained. The position of the paramagnetic centers on different carbon atoms with the components of the spectrum was compared. As a result, two possible conformations of the calcium gluconate molecule were revealed. The reliability of the results of conformational analysis is confirmed by EPR studies in two frequency bands (X- and Q-bands).

1. Konygin G.N. *et al.*: Patent of Russia № 2373185 (2009)
2. Konygin G.N. *et al.*: Materials of conf. "Actual issues of Pediatric Surgery", **56** (2003)
3. Sosulin I. S., Shiryayeva E.S., Feldman V.I.: Radiation Physics and Chemistry. **117**, 178 (2015)

Proximity Effect in Superconducting Triplet Spin-Valve F2/S2/F1/S1 Structure

**R. R. Gaifullin¹, V. N. Kushnir², R. G. Deminov¹, L. R. Tagirov^{1,3},
M. Yu. Kupriyanov^{1,4,5}, A. A. Golubov^{5,6}**

¹ Institute of Physics, Kazan Federal University, Kazan 420008, Russian Federation,
gaifullin.rashid@gmail.com

² Theoretical Physics Department, Belorussian State University, Minsk 220030,
Republic of Belarus

³ Zavoisky Physical-Technical Institute, FRC Kazan Scientific Center of RAS, Kazan 420029,
Russian Federation

⁴ Skobeltsyn Institute of Nuclear Physics, Moscow State University, Moscow 119992,
Russian Federation

⁵ Moscow Institute of Physics and Technology, Dolgoprudny 141701, Russian Federation

⁶ Faculty of Science and Technology and MESA+ Institute of Nanotechnology, University of Twente,
P.O. Box 217, 7500 AE Enschede, The Netherlands

We investigate the critical temperature T_c of F2/S2/F1/S1 structure (Si is a singlet superconductor, Fi is a ferromagnetic metal), where the long-range triplet superconducting component is generated at canted magnetizations of the F layers [1]. Previously it was demonstrated that transition temperature T_c in F2/F1/S [2] and F2/N/F1/S [3] structures (N is a normal metal) can be a non-monotonic function of the angle α between magnetizations of the two F layers, against the monotonic $T_c(\alpha)$ behavior obtained for the F2/S/F1 trilayers [4].

Matrix method [5] is employed to calculate T_c as a function of the spin-valve parameters. We study the impact of an additional layer S2 on different spin-valve effect modes – the standard switching effect, the triplet spin-valve effect, the inverse switching effect – by variation of the interfaces transparencies, the exchange splitting energies, and the layers thicknesses. We examine the conditions under which superconductivity in an additional S2 layer is suppressed and it plays the role of a normal layer, and conditions under which the superconductivity is conserved and affects on the superconducting T_c .

The support in part by RFBR (grants No. 16-02-01171-a, 15-32-20362-bel_aved) is gratefully acknowledged.

1. Bergeret F.S., Volkov A.F., Efetov K.B.: Rev. Mod. Phys. **77**, 1321 (2005)
2. Fominov Ya.V., Golubov A.A., Karminskaya T.Yu., Kupriyanov M.Yu., Deminov R.G., Tagirov L.R.: JETP Lett. **91**, 308 (2010)
3. Deminov R.G., Tagirov L.R., Gaifullin R.R., Kupriyanov M.Yu., Fominov Ya.V., Golubov A.A., to be submitted
4. Fominov Ya.V., Golubov A.A., Kupriyanov M.Yu.: JETP Lett. **77**, 510 (2003)
5. Kushnir V.N.: Superconductivity of the Layered Structures. Minsk: Belarus National Technical University 2010.

Nitric Oxide Production in the Rat Hippocampus in Acute Phase of Ischemic and Hemorrhagic Insult: Participation of NO-synthase

**Kh. L. Gainutdinov^{1,2}, V. V. Andrianov^{1,2}, G. G. Yafarova^{1,2},
S. G. Pashkevich³, M. O. Dosina³, Y. P. Stukach³, T. Kh. Bogodvid²,
V. S. Iyudin¹, A. A. Denisov³, V. A. Kulchitchky³**

¹ Zavoisky Physical-Technical Institute, FRC Kazan Scientific Center of RAS, Kazan 420029, Russian Federation

² Institute of Fundamental Medicine and Biology, Kazan Federal University, Kazan 420008, Russian Federation

³ Institute of Physiology of Nat. Acad. of Sci. of Belarus, Minsk 220072, Belarus, kh_gainutdinov@mail.ru

System of nitric oxide (NO) is one of the most studied systems of the organism [1, 2]. Its role is documented for the central and autonomous nervous systems, for cardiovascular function and blood supply to the brain and the heart, where deviations in NO level may incur risks of stroke and infarction [1, 3, 4, 5]. The NO system participate in reactions of oxidative stress, glutamate-calcium cascade, and inflammation [2]. In present time the development of cerebral ischemia and following stroke is associated with impaired cerebral blood flow, as well as violations of its regulation by the NO system [6]. No doubt that the role of NO system in the pathogenesis of a number of diseases associated with vascular disorders is defining [6, 7]. Previously, by the methods of EPR spectroscopy our team has evaluated effect of ischemic stroke on the intensity of NO production in the tissues of the brain, heart and liver of rats in vivo [8]. It was shown that in 5 hours after modelling of ischemia double reduction of NO production was observed in the tissues of the hippocampus, heart and liver. This investigation continues the previous research, and its main purpose is to study the processes of NO-synthase involvement in the control of NO levels in the hippocampus of rats after modelling both ischemic and haemorrhagic stroke.

Modeling of ischemic and hemorrhagic stroke was produced on rats according to [8]. After 5, 24 and 72 hours it was carried out fence of the hippocampus. A similar extraction of tissue samples were also produced from control animals. In all series, on the day of the experiment, rats were anesthetized by intraperitoneal injection of a mixture of ketamine-chloralose-acepromazine (55.6 mg, 5.5 mg and 1.1 mg/kg, respectively). The components of the spin trap NO (DETC-Na, FeSO₄, sodium citrate) was injected 30 minutes before the extraction of studied tissue. The studies of the effect of non-selective blocker of NO-synthase (NOS) on the NO production in the modeling of ischemic and hemorrhagic stroke were carried out to estimate of the contribution of different sources of NO. The L-NAME in dose of 10 mg/kg, which was administered intraperitoneally 60 minutes previously to decapitation. The measurements of the spectra of the complex (DETC)₂-Fe²⁺-NO were performed on the spectrometer ER 200 SRC Bruker in the X band (9.50 GHz). The amplitude of the EPR spectra was always

normalized to the weight of the sample (details of the EPR signal measurement technique described earlier [5, 8].

Based on direct measurements of NO by EPR spectroscopy it was shown that in 5 hours after the onset of symptoms ischemic and hemorrhagic stroke the formation of NO in the hippocampus was reduced by 2-3 times and this reduction was maintained for 24 and 72 hours. The results show that a systemic character of decreasing in the intensity of NO production during the modelling of ischemic events in the brain reflects the effects of central dysregulation of the functions at the level of the whole organism that it is appropriate to consider under implementing the correction of the vital systems of the body in stroke. It has indicated that nonselective NO-synthase blocker L-NAME reduced the low level of NO production in 3 times by its administration in 72 hours after post-ischemic and hemorrhagic stroke. But it was discovered that L-NAME returns the level of NO production to baseline (control) by its administration in 5 hours after ischemia.

Supported by RFBR (Grant No. 18-515-00003) and by Belarusian Republican Foundation for Fundamental Research (Grant B16R-166).

1. Vanin A.F.: *Biohimia* (in Russian) **63**, 924–938 (1998)
2. Terpolilli N.A., Moskowitz M.A., Plesnila N.: *J. Cereb. Blood Flow Metab.* **32**, no. 7, 1332–1346 (2012)
3. Andrianov V.V., Sitdikov F.G., Gainutdinov Kh.L. *et al.*: *Ontogenez* (in Russian) **39**, no. 6, 437–442 (2008)
4. Reutov V.P., Okhotin V.E., Shuklin A.V. *et al.*: *Uspekhi Physiol. Nauk* (in Russian) **38**, no. 4, 39–58 (2011)
5. Gainutdinov Kh.L., Gavrilova S.A., Iyudin V.S. *et al.*: *Appl. Magn. Reson.* **40**, no. 3, 267–278 (2011)
6. Pacher P., Beckman J.S., Liaudet L.: *Physiol. Rev.* **87**, 315–427 (2007)
7. Godinez-Rubi M., Rojas-Mayorquin A.E., Ortuno-Sahagun D.: *Oxidative Medicine and Cellular Longevity* 2013:1–16 (2013)
8. Andrianov V.V., Pashkevich S.G., Yafarova G.G. *et al.*: *Appl. Magn. Reson.* **47**, no. 9, 965–976 (2016)

Spin-Spin Interactions in AFM Dirac Semimetals: Diluted and Enriched Cases

Yu. V. Goryunov¹, A. N. Nateprov²

¹ Zavoisky Physical-Technical Institute, FRC Kazan Scientific Center of RAS, Kazan 420029,
Russian Federation, goryunov@kfti.knc.ru

² Institute of Applied Physics of the ASM, Chisinau 2028, Moldova

A very short time has elapsed since the discovery [1, 2] of the 3D analog of graphene, the Dirac semimetal of cadmium arsenide Cd_3As_2 . From that moment, other substances of this class were discovered. Particularly of particular interest is the Dirac semimetal in which, in the composition of Cd_3As_2 , one cadmium atom is replaced by an europium atom, i.e. EuCd_2As_2 . This semimetal belongs to the class of antiferromagnetic (AFM) Dirac semimetals [3]. Many exotic topological states can be derived from such AFM Dirac semimetals by means breaking certain symmetry, thereby providing an model system for investigation of topological phase transitions.

Very effective method for investigation of magnetic and spin states is the electron spin resonance. We performed the X band ESR measurements in the temperature range 10–300 K of two pnictides: EuCd_2As_2 (structural type CaAl_2Si_2 , space group P3m1) and $\text{Eu}_x\text{Cd}_{3-x}\text{As}_2$ (centrosymmetric fluorite type structure, space group I41/acd).

In the ESR for EuCd_2As_2 , it was observed almost symmetric Lorentzian resonance line. At high temperature g -factor for this compound was 2.03 and pic-to-pic linewidth was 900 Oe. The resonance linewidth and field depend on temperature as $(T-T_c)^{-1/2}$. This indicative of spin fluctuations associated with the phase transition temperature T_c . Also at high temperatures was observed Curie-like temperature dependence of the inverse the ESR intensity with positive temperature Curie Weiss $\theta_{\text{cw}} = 16$ K (high temperature approximation $\theta_{\text{cw}} \sim 25$ K, see figure) , which contradicts $T_c = T_N \sim +7$ K.

For the $\text{Eu}_x\text{Cd}_{3-x}\text{As}_2$, data on the magnetic susceptibility and ESR showed the presence of an Eu^{2+} ions additional AFM phase ordered at $T_{\text{AFM}} \sim 124$ K. Measurements of the ESR allow us to identify this phase (g -factor near 4.4) as it consisted of Eu^{2+} ions located in tetrahedral vacancies in fluorite type cell. Main phase ($g \sim 2.2$) consists of the Eu^{2+} ions in the positions substituting of the Cd^{2+} ions. Taking in attention, in normal cases $g \sim 2.0$, the ESR data for both compounds show anomalous large values of the g -factor of the Eu^{2+} ions. Analysis of the role of the RKKY interaction in this situation leads to the conclusion that the RKKY interaction in the classical view can not lead to change of a sign of interaction selectively in dependence on position types in the crystal lattice. Consequently, we are dealing with a new type of spin-spin interactions, associate with the local symmetry breakings of the crystal by magnetic ions. This interaction leads to the splitting of twice degenerate Dirac nodes on two Weyl nodes with different energies and to formation of different topological phase.

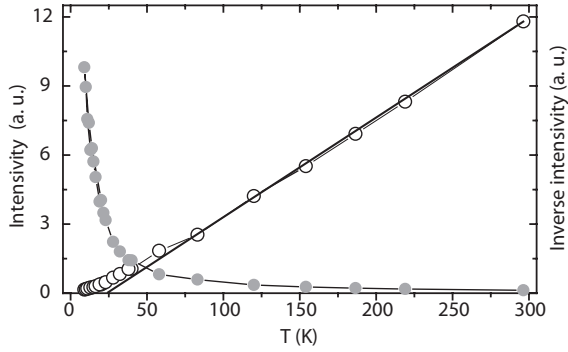


Fig. 1. The temperature dependence of the ESR line intensity and an inverse intensity in the EuCd_2As_2 .

We believe such observed behaviour of θ_{cw} , T_{N} , g -factors and linewidth are connected with critical spin fluctuations and these critical spin fluctuations are caused by the relevant topologic instability of electronic structures of these compounds.

1. Liu Z., Jiang J., Zhou B., Wang Z., Zhang Y., Weng H., Prabhakaran D., Mo S., Peng H., Dudin P., Kim T., Hoesch M., Fang Z., Dai X., Shen Z., Feng D., Hussain Z., Chen Y.: *Nature Materials* **13**, 677 (2014)
2. Madhab Neupane, Su-Yang Xu, Raman Sankar, Nasser Alidoust, Guang Bian, Chang Liu, Ilya Belopolski, Tay-Rong Chang, Horng-Tay Jeng, Hsin Lin, Arun Bansil, Fangcheng Chou, M. Zahid Hasan: Discovery of a three-dimensional topological Dirac semimetal phase in high-mobility Cd_3As_2 , arXiv:1309.7892v4 [cond-mat.mes-hall] 29 Jan 2015
3. Guiyuan Hua, Simin Nie, Zhida Song, Rui Yu, Gang Xu, Kailun Yao: Dirac semimetal in type IV magnetic space group, arXiv:1801.02806v1 [cond-mat.mtrl-sci] 9 Jan 2018

Magnetic Proximity Effects in $\text{CaCu}_3\text{Ti}_4\text{O}_{12}$ -Based Composites

**T. Gavrilova^{1,2}, A. Yagfarova², I. Gilmudtinov², J. A. Deeva³, I. Yatsyk^{1,2},
N. Lyadov^{1,2}, Y. Kabirov⁴, T. Chupakhina³, R. Eremina^{1,2}**

¹Zavoisky Physical-Technical Institute, FRC Kazan Scientific Center of RAS, Kazan 420029, Russian Federation, tatyana.gavrilova@gmail.com

²Institute of Physics, Kazan Federal University, Kazan 420008, Russian Federation

³Institute of Solid State Chemistry of the RAS (UB), Ekaterinburg 620990, Russian Federation

⁴Southern Federal University, Rostov-on-Don 344006, Russian Federation

Here we investigated the materials, which consist of two inorganic phases. One of the components of the composite material is $\text{CaCu}_3\text{Ti}_4\text{O}_{12}$ (CCTO), which dielectric behavior exhibits an extraordinary high dielectric constant and shows good thermal stability in a wide temperature range. As the second component of the composite material we chose two ferromagnetic materials: lanthanum-strontium manganite $\text{La}_{0.7}\text{Sr}_{0.3}\text{MnO}_3$ (LSMO) or strontium hexaferrite $\text{SrFe}_{12}\text{O}_{19}$ (SFO).

$\text{LSMO}_x\text{CCTO}_{1-x}$ ($0.01 \leq x \leq 0.3$) and $\text{SFO}_x\text{CCTO}_{1-x}$ ($0.01 \leq x \leq 0.1$) composites were synthesized using a solid state method, while the pre-synthesized ferromagnetic was added to the stoichiometric amount of CaO, CuO and TiO

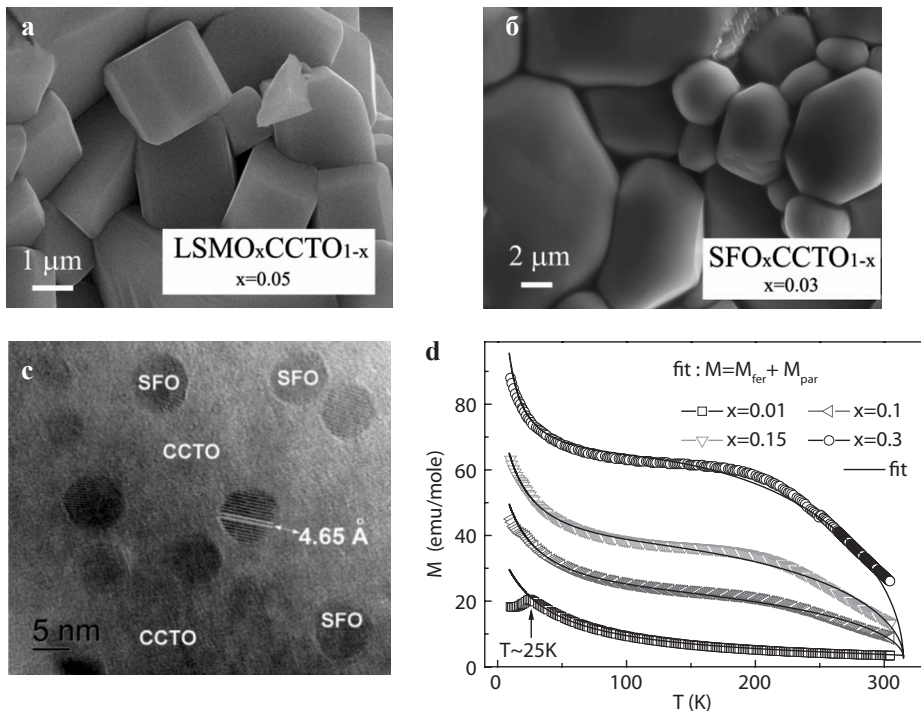


Fig. 1. SEM images: **a** $\text{LSMO}_{0.05}\text{CCTO}_{0.95}$; **b** $\text{SFO}_{0.03}\text{CCTO}_{0.97}$; **c** High-resolution transmission electron microscopy image of $\text{SFO}_{0.07}\text{CCTO}_{0.93}$; **d** Temperature dependencies of magnetization in $\text{LSMO}_x\text{CCTO}_{1-x}$

oxides to form the CCTO structure. The obtained composites had the granular structure (Fig. 1a, b). The intrinsic structure of the granules (ferromagnetic nanoinclusions inside CCTO matrix) is shown in Fig 1c.

The magnetization of investigated samples can be presented as the sum of the paramagnetic contribution $M_{\text{par}} = \chi \cdot H = C \cdot H / (T - \Theta)$ from CCTO component and ferromagnetic contribution $M_{\text{ferr}} = M_S \cdot \tanh(T_C M_{\text{ferr}} / T M_S)$ from LSMO or SFO component (see Fig. 1d). From the fitting of the temperature dependence of the magnetization we can see the mutual influence on the magnetic properties of both components: (i) decrease of the Curie temperature of the ferromagnetic phase; (ii) the Weiss constant θ and the effective magnetic moment of the paramagnetic phase has the strong concentration dependence. ESR measurements confirm mutual influence on the magnetic properties of both components to each other [1, 2]. The observed mutual influence on the magnetic properties of both components can be tentatively attributed to the interface exchange interactions between them, suggesting the presence of a possible magnetic proximity effect.

1. Gavrilova T.P., Eremina R.M., Yatsyk I.V. *et al.*: J. Alloys and Compounds **714**, 213 (2017)
2. Gavrilova T.P., Deeva J.A., Yatsyk I.V. *et al.*: Physica B: Cond. Matter **536**, 303 (2018)

Magnetoresistance of Magnetic NanoContact with Taking Account Gradients of Chemical Potentials

L. Gerasimova, N. Useinov

Institute of Physics, Kazan Federal University, Kazan 420008, Russian Federation,
lidia.gerasimova.96@mail.ru

A computer program for modeling a tunnel magnetoresistance (TMR) in magnetic nanocontacts (NC) ferromagnetic/insulator/ferromagnetic (FM^L/I/FM^R, where FM^L are left and FM^R right ferromagnetic metals) with taking account gradients of chemical potentials was created. The NC is simulated by a nanosized circular insulating disk of the radius made in a membrane, which divides the space on two half-spaces, occupied by single-domain ferromagnetic metals. The main program units are a module for calculating the TMR of the planar contact, based on the quasiclassical theory of spin-polarized conductivity [1]; a module that takes into account geometry of the contact [2]; and an original module taking account gradients of chemical potential. We develop a theory of spin-transport through magnetic NC's taking into account gradient terms in the series expansion of Green function. The theory covers ballistic $l > a$ and diffusive $l < a$ regimes (l is the mean free path, a is the radius of the contact) to explain the variety of observed experimental data. The basic mathematical background and calculation details can be found in article [3].

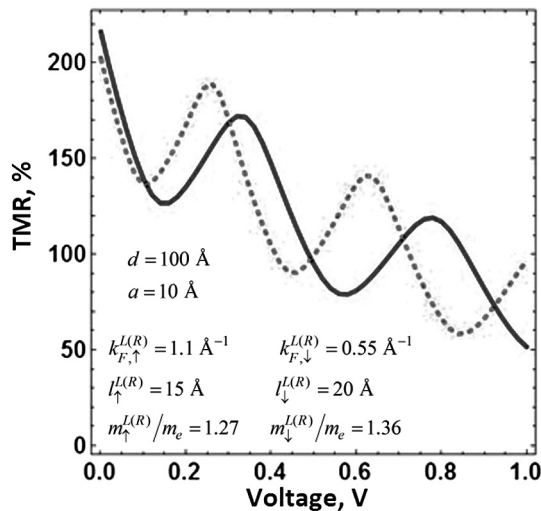


Fig. 1. The TMR dependence on the voltage applied to NC at room temperature. Solid line – without taking into account, dotted line – with taking into account the difference in effective masses in a ferromagnetic metal.

The quantitative model of spin-polarized conductance and TMR of point magnetic contacts is of great importance for determining the characteristic dimensions of a NC, and for explaining the large value of the TMR observed in experiments. At present time, great efforts have been made to create reliable nanocontacts with predictable properties, considering the interface matching of the nanowire connections between normal, semiconductor, ferromagnetic and superconducting materials in nanoscale spintronics devices.

The main goal of the present work is to study the effect that the chemical potential gradients can have on the tunnel characteristics in a magnetic NC, in particular, on spin-polarized conductance and TMR. A specific feature of the study is to take into account some distinction between in the effective masses of electrons with different spin orientations in the ferromagnetic metals.

Results of the TMR calculations for symmetric NC Fe/Al₂O₃/Fe are shown in Fig. 1. The tunnel barrier thickness between the magnetic domains is assumed to be equal $d = 100 \text{ \AA}$. The height of the energy potential above the Fermi energy is $U_b = 0.76 \text{ eV}$. The values of Fermi wave vectors $k_{F\alpha}^{L(R)}$, spin-polarized mean-free paths $l_{\alpha}^{L(R)}$ and effective mass in units of free electron mass $m_{\alpha}^{L(R)}/m_e$ for electrons of spin subbands in ferromagnetic layers are shown in the figure (where $\alpha = (\uparrow\downarrow)$ is the spin index).

In this work are shown dependences of TMR on the ratio of radius contact to mean free path of conduction electrons and dependences of TMR on voltage. It can be used for interpreting the experimental data on tunnel structures like of Fe/Al₂O₃/Fe or CoFeB/MgO/CoFe, NC's resistance of Fe-Co or Ni-Mumetall. The TMR effect may improve possible MRAM benefits, which can be fabricated as a system of uniform NC cells.

1. Tagirov L. *et al.*: Phys. Rev. B **63**(10), 104428 (2001)
2. Useinov A. *et al.*: J. Phys.: Condens. Matter. **19**(19), 196215 (2007)
3. Useinov N.: Theoretical and Mathematical Physics **183**(2), 705–714 (2015)

FMR Studies of Epitaxial Pd Films Implanted with Iron Ions

**A. I. Gumarov¹, I. V. Yanilkin¹, I. R. Vakhitov¹, B. M. Khaliulin¹,
A. A. Rodionov¹, R. V. Yusupov¹, M. N. Aliyev², L. R. Tagirov^{1,3,4},
V. I. Nuzhdin³, R. I. Khaibullin³**

¹ Institute of Physics, Kazan Federal University, Kazan 420008, Russian Federation,
amir@gumarov.ru

² Baku State University, AZ-1148 Baku, Azerbaijan

³ Zavoisky Physical-Technical Institute, FRC Kazan Scientific Center of RAS, Kazan 420029,
Russian Federation

⁴ Institute of Applied Research ASRT, Kazan 420111, Russian Federation

Metal alloys with a low concentration of magnetic impurities were studied for a long time [1, 2]. Palladium (Pd) films of nanoscale thickness with an admixture of iron (Fe) in the concentration range 1–10 at.% are of particular interest. Usually such films are obtained by magnetron sputtering [3] and molecular beam epitaxy (MBE) [4, 5]. However, ion implantation is a very promising method for alloying of palladium matrix with a magnetic impurity of iron [6], it can be used to produce new nanostructured materials with unique magnetic properties.

We implanted Fe⁺ ions with an energy of 40 keV and a different fluence ($0.5\text{--}3.0 \cdot 10^{16}$ ion/cm²) into Pd epitaxial films in order to induce ferromagnetism in them and to study its evolution depending on the nominal concentration of the iron impurity. The thickness of the Pd films was chosen to adjust the average projected range (Rp) of the iron ions with the middle of the film thickness for the each fluence. The crystal structure of the films was studied by low energy electron diffraction technique and X-ray diffraction analysis. Experimental profiles of iron depth distribution were obtained by X-ray photoelectron spectroscopy in combination with the argon ion etching technique. The magnetic properties were studied by methods of ferromagnetic resonance and vibrating sample magnetometry in a wide range of temperatures and various measurement geometries. The effect of the implanted iron fluence on Curie temperature was investigated. At the maximum fluence, the spinodal decomposition and formation of a multiphase magnetic system were detected by FMR technique. The effect of subsequent ultra-high vacuum annealing on the magnetic parameters and the magnetic phase composition of the Pd films with an implanted iron impurity was studied. A comparative analysis of magnetic properties of the samples obtained both by ion implantation and MBE methods is carried out.

The Program of Competitive Growth of Kazan Federal University supported by the Russian Government is gratefully acknowledged, as well as the partial support by RFBR projects No 18-32-01041 and 16-02-01171-a. Synthesis and analysis of the films were carried out at the PCR Federal Center of Shared Facilities of KFU.

1. Nieuwenhuys G.J.: *Adv. Phys.* **24**, 515 (1975)
2. Korenblit I.Y., Shender E.F.: *Soviet Phys. Uspekhi* **21**, 832 (1978)
3. Bol'ginov V.V. *et al.*: *JETP Letters* **105**, 169 (2017)
4. Garifullin I.A. *et al.*: *Appl. Magn. Reson.* **22**, 439 (2002)
5. Esmaeili A. *et al.*: *Appl. Magn. Reson.* **49**, 175 (2018)
6. Hitzfeld M. *et al.*: *Phys. Rev. B* **29**, 5023 (1984)

Signature of the Field Induced Quantum Phase Transition in the Low-Dimensional Magnet BiCoPO_5

**M. Iakovleva^{1,2}, E. Vavilova¹, H.-J. Grafe², A. Alfonsov², B. Büchner²,
Y. Skourski³, R. Nath⁴, V. Kataev²**

¹ Zavoisky Physical-Technical Institute, FRC Kazan Scientific Center of RAS, Kazan 420029,
Russian Federation

² Leibniz Institute for Solid State and Materials Research (IFW Dresden), Dresden 10069, Germany

³ Dresden High Magnetic Field Laboratory (HLD-EMFL), HZDR, Dresden 01328, Germany

⁴ Indian Institute of Science Education and Research-Thiruvananthapuram (IISER), Kerala 695016,
India

The frustrated dimeric chain compound BiCoPO_5 orders antiferromagnetically at $T_N = 11$ K at zero magnetic field. Application of an external magnetic field lowers the transition temperature towards zero at a field of $H_C \sim 15.3$ T [1] which, according to theory, could be a signature of a field-driven quantum phase transition [2]. In this work we present an investigation of the title compound by magnetometry and nuclear magnetic resonance (NMR) techniques. The high-field magnetization measurements show no saturation of the magnetic moment up to the highest magnetic field of 60 T. The ^{31}P NMR relaxation rates measured at 9 T exhibit a peak at $T = 8$ K corresponding to the AFM order. With increasing the field this peak shifts towards lower temperatures and is not seen any more down to 1.7 K at a field of 13 T. Remarkably, at a magnetic field of 15 T the T -dependence of the relaxation rates shows an opening of the gap that possibly indicates the emergence of a new quantum disordered phase of BiCoPO_5 with gapped spin excitations above H_C .

1. Mathews E., Ranjith K.M., Baenitz M., Nath R.: Solid State Commu. **154**, 56 (2013)
2. Rong-Gen Cai, Run-Qiu Yang, Kusmartsev F.V.: Phys. Rev. D **92**, 086001 (2015)

Time Features of the Magnetic Effect on the Luminescence of Poly(9,9-di-n-octylfluorenyl-2,7-diyl) Films with Additive of KI Salt

N. Ibrayev¹, D. Afanasyev^{1,2}

¹ Institute of Molecular Nanophotonics, Buketov Karaganda State University, Karaganda 100028, Kazakhstan, niazibrayev@mail.ru

² Institute of Applied Mathematics, Karaganda 100028, Kazakhstan, a_d_afanasyev@mail.ru

The optical properties of poly(9,9-di-n-octylfluorenyl-2,7-diyl) (PFO) films doped with potassium iodide (KI) are investigated. Adding an external heavy atoms into a semiconductor polymer can change not only the rate and efficiency of various photophysical reactions but also the probability of formation of free charge carriers in the polymer. Absorption and luminescence spectra, kinetics of fluorescence and delay luminescence of polymer films were studied. Investigations of the effect of an external magnetic field on the PFO luminescence over a wide time range was investigated.

A degree of ordering of the composite films is determined from an analysis of absorption spectra. It is found that the addition of potassium iodide leads to a drop in the degree of ordering of PFO films and decreases the fluorescence intensity and lifetime of the polymer. The kinetics of photoluminescence of PFO–KI films is studied in wide time range. Analysis of the experimental data on long-term luminescence using the percolation model showed that the addition of potassium iodide to the polymer increases the degree of disordering of the film. This disorder has a substantial effect on the time characteristics of annihilation delayed fluorescence and phosphorescence at recording times above 50 μs after laser photoexcitation.

Investigations of the effect of an external magnetic field on luminescence kinetic of the PFO in the range from 10^{-10} s to 10^{-3} s indicate a complex character of the time dependence of the magnetic effect. The changes in both the magnitude and sign of the magnetic effect are observed over the entire measured time range. In a pure PFO film, a magnetically sensitive photoprocess occurs in the ordered phase of the polymer at times below 1 ns. The magnetic effect is connected with the process of triplet-triplet annihilation of electronic excitations in a polymer at registration times of more than 1 μs .

Effect of Magnetic Field on the Recombination Luminescence of Polymer Semiconductor Composites

N. Ibrayev¹, D. Afanasyev^{1,2}, A. Nurmakhanova¹

¹ Institute of Molecular Nanophotonics, Buketov Karaganda State University, Karaganda 100028, Kazakhstan, niazibrayev@mail.ru

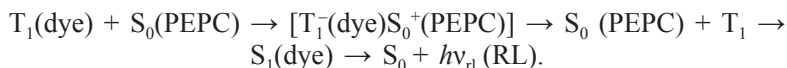
² Institute of Applied Mathematics, Karaganda 100028, Kazakhstan, a_d_afanasyev@mail.ru

An investigation of features of the generation and recombination of electron-hole pairs (EHP) in molecular semiconductor composites are receiving much attention in connection with the possibility of their practical use in electroluminescent and photovoltaic solar cells. A degree of participation of the triplet state in the processes of formation of EHP is one of the poorly studied questions. This work presents results of an investigation of the effect of an external magnetic field (EMF) on the kinetics of luminescence of polymeric composites of poly (N-epoxypropylcarbazole) (PEPC) derivatives with heavy atoms of different chemical nature doped with anionic polymethine dye (PD).

The investigation of delayed luminescence (DL) of PD in the range from 100 K to 300 K was carried out to determine the role of the triplet state in the formation and recombination of EHP. Samples were irradiated with the second harmonic of the neodymium laser LCS-DTL-374QT (532 nm). It led to the excitation of dye molecules in the absorption band $S_1 \rightarrow S_0$.

DL of dye consisting of two bands was recorded under pulse photoexcitation at temperature of $T = 100$ K of PEPC films. The short-wave band with a maximum at 600 nm coincides spectrally with the fluorescence spectrum under steady-state photoexcitation and is due to the radiative transition from the singlet-excited state S_1 to the ground state S_0 . DF spectrum exhibits a broad band in the region of 700–850 nm with a maximum of about 750 nm, which is a phosphorescence band of the dye.

Measurements of DL kinetics at the $\lambda_{\max} = 600$ nm have shown that emission decays more slowly in the PEPC matrix than in the polyvinyl butyral. The lifetime is equal to 0.5 ms for a PD in polyvinyl butyral, which is shorter than the lifetime of the dye luminescence in PEPC films. The difference in the luminescence duration of PD in these polymers is result of presence of a portion of the recombination luminescence (RL) in the total luminescence along with the delayed fluorescence (DF) $S_1 \rightarrow S_0$. The nature of DF is associated with the interconversion of dye molecules from T_1 state to the S_1 state. A slower RL is associated with the formation of EHP of the cation-radical of the carbazole fragment of PEPC and the electro-neutral radical of PD:



The value of magnetic effect ($g(B)$) falls in the series of PEPK – 2IPEPC – 3BrPEPC – PEPC + KI films. For the dye in PEPC matrix, a negative $g(B)$ was observed, and $g = 26\%$ for $B \sim 0.5$ T. The $g(B)$ is smaller in matrices of 2IPEPC and 3BrPEPC. The value of $g(B)$ decreases from 10 to 6% at a value of $B \sim 0.5$ T with increasing number of heavy atoms in the polymer unit. In PEPC film with the addition of an external heavy atom (KI salt), the magnitude of $g(B)$ was equal to 5%. In the time range after 0.2 ms the value of $g(B)$ decreases with a further increase in time for polymer films of 2IPEPC and 3BrPEPC. For the PEPC + KI film, the decrease in $g(B)$ occurs in a another time range – starting from 0.6 ms. The $g(B)$ becomes close to 0 at $t_{\text{reg}} \sim 1.2$ ms. Decrease in $g(B)$ was not registered in the accessible time range for PEPC–PD film.

The singlet-triplet (S-T) conversion of EHP is the magnetosensitive stage. A decrease in the intensity of RL in EMF shows that the formation of EHP mainly proceeds along the triplet channel ($S_1 \rightarrow T_1 \rightarrow T_{\text{EHP}}$). EMF reduces the probability of annihilation of triplet EHP and increases the probability of their dissociation into free charge carriers (CC). The CC (electron), remaining on the dye, is in a stationary state, while the hole can move along the polymer chain. When the Coulomb barrier is overcome by a hole, the bound EHP can form free CC. In the opposite case, there will be a recombination of EHP with subsequent emission of a light quantum. As shown by measurements of the time dependence of $g(B)$, the presence of a heavy atom in the polymer leads to a decrease in the lifetime of triplet EHP. In the case of the presence of an external heavy atom (PEPC + KI), the lifetime of triplet EHP is greater than in films of 2IPEPC and 3BrPEPC. The processes occurring in the polymer chain play a decisive role in the EHP lifetime.

The decrease in $g(B)$ with the addition of a heavy atom to the sample is due to the competing effect of spin-orbit interaction and EMF on spin-selective processes involving the excited triplet states of dye. A heavy atom leads to an increase in the concentration of triplets in the sample and increases the probability of both transitions from the singlet state to the triplet state and vice versa. This in turn reduces the degree of influence of the EMF on transitions of the EHP from one spin state to another. At times above 200 μs , a reduction in the concentration of the EHP and a decrease in the contribution of RL to the intensity of total luminescence may occur.

Study of Synthetic Hydroxyapatites by EPR

K. Iskhakova, A. Sorokina, A. Starshova

Institute of Physics, Kazan Federal University, Kazan 420008, Russian Federation,
kamilaiskh@gmail.com

Hydroxyapatites (HA) play an important role in biomaterial engineering, especially in mineralized tissue engineering like bone tissue and tooth enamel. Thus, HA and blood components based biocomposites can be used for rhinoplasty. HA ceramic foams are perfect for a treatment of defects of bone tissue and for increasement of osseointegration degree of metal prosthesis and soft tissues. There are some research on calcium phosphate paste for 3D print too.

As methods of synthesis and processing of HA based materials are improved, various techniques of analytical control of their chemical composition and morphology are required. We investigated HA samples, which were synthesized using CaCl_2 and CaNO_3 solutions and had a different purification levels. Samples were irradiated by X-ray for 30 minutes. The research was conducted by using electron paramagnetic resonance (EPR) method on X-band EPR spectrometer Bruker ESP300 at room temperature.

The received data was processed by using a spectra simulation in Matlab programming environment using special module EasySpin. As a result of the research, we identified range of EPR signals as CO_2^- , NO_3^{2-} , CO_3^- and estimated its spectroscopic parameters. We also tracked dynamics of signal intensity of irradiated paramagnetic centers. During the investigation it was revealed that EPR method is able to differ HA sampeles, which were synthesized by using different techniques.

The financial support of the Russian Foundation for Basic Research (grant 18-32-00337 mol_a) is gratefully acknowledged.

Resinous-Asphaltene Aggregates by NMR Analysis

D. Ivanov, V. Scirda

Institute of Physics, Kazan Federal University, Kazan 420008, Russian Federation

Resins and asphaltenes primarily make the greatest contribution to the formation of solid-state structures in oil. Resins and asphaltenes are very important fractions of crude oil, oil residues, and bitumen. The tendency of asphaltenes to aggregate distinguishes them from other components of oil. Aggregation of asphaltenes can cause complex nonlinear effects in the rheological processes characteristic of asphaltene-containing solutions, including oil and water-oil emulsions. In turn, the anomalies of the rheological properties of oil cause the latter to be classified as non-Newtonian fluids.

A promising approach for solving this problem is the use of the nuclear magnetic resonance (NMR) method [1]. The choice of NMR as a physical method for studying such complex systems as oil is not accidental and is due to a number of undeniable advantages: the method is non-destructive, sensitive to the component composition of the object under study, and the possibility of research directed at the site of the object under investigation [2, 3].

Summarizing the experimental results obtained in this paper, it can be concluded that the use of the NMR method makes it possible to characterize the state of asphaltene aggregates. It is shown that the size of a resinous-asphaltene coat directly depends on the size of aggregates of asphaltenes.

The work was supported by the scholarship program of British Petroleum in the promising areas of development of the oil and gas industry.

1. LaTorraca G.A.: *Magnetic Resonance Imaging* **16**, no. 5, 659–662 (1998)
2. Yang Z., Hirasaki G.J.: *J of Magn. Reson.* **192**, no. 2, 280–293 (2008)
3. Sun B.: *Magnetic Resonance Imaging* **25**, no. 4, 521–524 (2007)

NMR spectrum was significantly broadened at the temperature +2 °C and became narrow when the temperature was increased. We could not reach the region of slow exchange because of the limited temperature range of the solvent, thus the line shape analysis was not used. For measuring the thermodynamic parameters in fast exchange regime the CPMG (Carr-Purcell-Meiboom-Gill) technique was applied [1]. The CPMG NMR spectra were recorded for the temperature range from +2 to +16 °C. Then the values of chemical exchange rate were found for two groups of protons. The activation thermodynamic parameters (enthalpy, entropy) were obtained from the Eyring plot.

It was assumed that the exchange processes observed in the ^1H NMR spectra were related with the interconversion between pS- and pR-enantiomers. This exchange occurs because of the low energy barrier between pS- and pR-enantiomers due to rotation of the functionalized arene fragments.

The semiempirical quantum chemical method was used to analyze the structure and energy of pillar[5]arene **1** in the ground, intermediate and transition states and to estimate the energetic barrier of the transition between enantiomers.

This work was supported by the Russian Foundation for Basic Research (grant №17-03-00858).

1. Loria J.P., Palmer III A.G.: *J. Am. Chem. Soc. B.* **121**, 2331 (1999)

Heterointerfaces Composed of Complex Ferroelectric Oxides: an Experimental Insight

**A. Kamashev¹, R. Zagidullin¹, D. Pavlov¹, I. Piyanzina^{1,2},
D. Tayurskii², R. Mamin^{1,2}**

¹ Zavoiisky Physical-Technical Institute, FRC Kazan Scientific Center of RAS, Kazan 420029, Russian Federation

² Kazan Federal University, Kazan 420008, Russian Federation, i.piyanzina@gmail.com

For the paradigmatic oxide heterostructure with LaAlO₃ (LAO) thin films grown on SrTiO₃ (STO) substrates for LAO films with more than three layers and LaO termination towards the TiO₂ interface, a two dimensional electronic gas (2DEG) is formed in the STO layers next to the interface which becomes superconducting below a temperature of 300 mK [1, 2]. The superconducting state coexists with a magnetic state. It was concluded, that the primary mechanism responsible for the 2DEG formation is electronic and structural reconstructions.

2DEG has been later found in other non-magnetic dielectrics. But the common feature for all systems is that the creation of the 2DEG can be due to either the polar nature of one of components or due to defects or dopants. It has been shown that analogous to the ionic polar discontinuity, 2DEG may be created at an interface due to electric polarization discontinuity [3, 4]. An attractive materials for such a purpose are ferroelectrics. They have a wide range of different distinctive properties, which can expand the scope of application in nanoelectronics.

Recently, it has been theoretically predicted that q2DEG can be created at the interface of nonpolar oxides one of which is ferroelectric [3, 4]. And In the present work we experimentally test the possibility of such a switchable q2DEG realization. The thin film of epitaxial Ba_{0.8}Sr_{0.2}TiO₃ (BSTO) was sputtered on the top of single crystalline SrTiO₃ substrate using the magnetron sputtering technique. Conductivity measurements were performed by a four-point probe method. In our investigation we present electrical resistivity versus temperature measurements and results are still under consideration.

The reported study was funded by RFBR according to the research project № 18-32-00595.

1. Ohtomo A., Hwang H.: Nature **427**, 6973 (2004)
2. Reyren N., Thiel S., Caviglia A. *et al.*: Science **317**, 5842 (2007)
3. Niranjana M.K., Wang Y., Jaswal S.S., Tsymbal E.Y.: Phys. Rev. L **103**, 016804 (2009)
4. Fredrickson K.D., Demkov A.: Phys. Rev. B. **91**, 115126 (2015)

Rescaling of 2D ESEEM Data for Inverse Problem Solving

Yu. E. Kandrashkin, A. A. Sukhanov, V. F. Tarasov

Zavoisky Physical-Technical Institute, FRC Kazan Scientific Center of RAS, Kazan 420029,
Russian Federation, spinalgebra@gmail.com

An electron spin echo envelope modulation (ESEEM) spectroscopy has proven to be a useful technique for studying unresolved hyperfine interactions (HFI). However, solving the inverse problem in a one-dimensional ESEEM experiment in complex systems becomes a challenge due to overlapping signals from different sources. The rare earth ions often have magnetic nucleus which strongly interacts with the electron(s). This allows the multifrequency ESEEM methodology to be expanded for experiments with a single microwave frequency applied to different EPR transitions. Here we present the results of the rescaling transformation $(\omega/\Delta m)^2 - \omega_z^2$, where ω is the experimentally detected frequency, ω_z is the nuclear Larmor frequency and Δm is the order of the coherence, to the 2D ESEEM data. This procedure allows the ESEEM peaks to be tracked with the change of the magnetic field, and as a result, essentially simplifies the resolving of the HFI and nuclear quadrupole interaction (NQI) parameters even in the case of the complicated ESEEM data.

The rescaling procedure has been applied to spectra from crystals Y_2SiO_5 and YVO_4 doped by Neodymium ion (Nd^{3+}) [1]. The near-to-reflection symmetry of peaks allows to differentiate the HFI parameters from 8 nearby sites located in the range 0.35–0.55 nm around the ion doped in the crystal Y_2SiO_5 . The comparison of the crystal structure based on the X-ray diffraction data [2] from intact crystal and on the ESEEM data from doped by Nd ions crystals is discussed [1]. The crystal YVO_4 consist of Vanadium nuclei $I = 7/2$ with relatively strong NQI. In general, this interaction greatly increases the number of the detectable ESEEM frequencies, and the identification of the peaks becomes non-trivial. Nevertheless, the rescaling of the ESEEM data simplifies essentially the evaluation of the interaction parameters.

1. Kandrashkin Yu.E., Zavartsev Yu.D., Koutovoi S.A., Sukhanov A.A.: Appl. Magn. Reson., 2018, (accepted)
2. Maksimov B.A., Kharitonov Y.A., Ilyukhin V.V., Belov N.V.: Dokl. Akad. Nauk SSSR **183**(5), 1072–1075 (1968)

New Approach of Determination T_1 and T_2 Relaxation Times by Using the CPMG Pulse Sequence

I. Khairuzhdinov, R. Zaripov, K. Salikhov

Zavoisky Physical-Technical Institute, FRC Kazan Scientific Center of RAS, Kazan 420029, Russian Federation

The Carr-Purcell-Meiboom-Gill (CPMG) pulse sequence is useful to avoid some decoherence pathways into the spin system [1, 2]. Long train of echo signals enables efficient measurements of spin-spin relaxation time and the diffusion constant (Fig. 1). When the EPR spectrum line width is much less than the microwave field strength, so-called non-selective excitation, the refocusing pulses can be effectively de-phase of magnetization to refocus the magnetic field inhomogeneity at each echo time [3]. In selective excitation case the magnetization will be particularly on longitudinal direction. This leads to a large number of echo signals. Time decay of echo signals looks like exponential combination of relaxation times T_1 and T_2 in different proportions.

Analytical expressions for the first few echo signals within the spin density matrix formalism were obtained and analyzed. We performed numerical simulation of CPMG experiment for different relations between inter pulse delays and relaxation times values.

In this work we propose methods for more accurate determination of relaxation times by using CPMG sequence.

The reported study was funded by RFBR according to the research project № 18-32-00428.

1. Carr H.Y., Purcell E.M.: Phys. Rev. **94**, 630 (1954)
2. Meiboom S., Gill D.: Rev. Sci. Instrum. **29**, 688 (1958)
3. Song Y.-Q.: Journal of Magnetic Resonance **157**, 82–91 (2002)

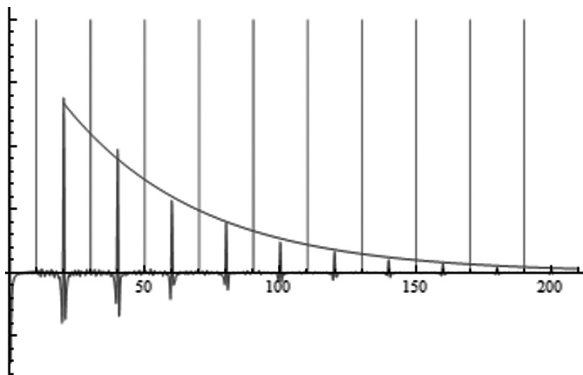


Fig. 1. Simulation of pulse train for CPMG sequence.

Strain-Induced Rotation of Magnetic Easy Axis in Permalloy Microparticles Studied by Ferromagnetic Resonance

**T. Khanipov¹, N. Nurgazizov¹, A. Zagitova², A. Bukharaev^{1,2},
L. R. Tagirov^{1,2}**

¹ Zavoisky Physical-Technical Institute, FRC Kazan Scientific Center of RAS, Kazan 420029, Russian Federation, timurkhanipov@gmail.com

² Kazan Federal University, Kazan 420008, Russian Federation

Influence of mechanical stress on magnetic properties of ferromagnets is of great interest nowadays. It's well known that creating of magnetic data storages and logical elements for micro- and nanoelectronics is available using stress-induced magnetic effect, and extremely low energy consumption is the special feature of these devices [1]. In this report it is shown that due to mechanical stress the magnetic easy axis of permalloy microparticle array can be rotated substantially. Also, using calculations, as it was demonstrated in [2], the anisotropy fields were evaluated for unstressed and stressed samples and compared with the earlier obtained values in work [3].

To fabricate stressed samples the glass substrate (10×4 mm² and 0.30 mm thick) was bent by fixing on a special holder with constant curvature radius (76 mm). On the next step, permalloy was deposited through the grid with 25×25 μm² mesh by electron beam evaporation in ultrahigh vacuum of Multiprobe P (Omicron) setup. After that, the sample was extracted from the holder, so that compressed permalloy particle array was created on the glass substrate. To fabricate unstressed sample, the same technology was utilized, however, without using special holder. Permalloy film thickness was adjusted to 30 nm.

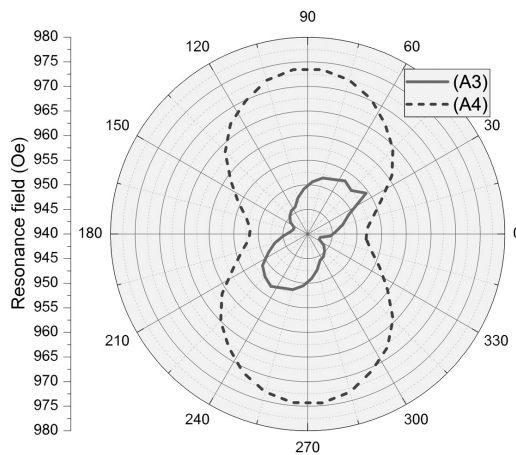


Fig. 1. Angular dependence of the FMR field for resonance: A3 – unstressed sample; A4 – stressed sample.

The magnetic anisotropy of the samples was studied using ferromagnetic resonance (FMR) technique. The FMR measurements were carried out on Bruker EMX Plus spectrometer with the external magnetic field (H_{ex}) up to 1.4 T and microwave field H_{mw} with the frequency $\omega = 9.8$ GHz perpendicular to H_{ex} . Spectra were recorder in the in-plane geometry in 0 to 360 angular degrees range with 10° step. Angular dependences of resonant field for unstressed and stressed samples are shown on figure 1.

As we can see from Fig. 1, the direction of the magnetization easy axis for the stressed sample (A4) appeared to be rotated about 35 angular degrees against the unstressed sample (A3). Taking into account that the deposition procedure was similar for the both samples, we conclude that rotation of the easy axis direction took place due to mechanical stress in stressed sample A4. It is main finding of the investigation presented in this report.

1. Roy K.: Appl. Phys. Lett. **103**, 173110 (2013)
2. Esmaeili A., Vakhitov I.R., Yanilkin I.V., Gumarov A.I., Khaliulin B.M., Gabbasov B.F., Aliyev M.N., Yusupov R.V., Tagirov L.R.: Applied Magnetic Resonance **49**, 175 (2018)
3. Bizyaev D., Bukharaev A., Kandrashkin U., Mingalieva L., Nurgazizov N., Khanipov T.: JETP **20**, 24 (2016)

Magnetic Properties of Antiferromagnetic Chain Ternary Chalcogenides TlFeS_2 and RbFeSe_2

**A. Kiiamov¹, F. Vagizov¹, L. R. Tagirov^{1,2}, T. Gavrilova², Z. Seidov³,
V. Tsurkan^{4,5}, I. Filipova⁴, D. Croitoro⁴, H.-A. Krug von Nidda⁵,
A. Günther⁵, A. Loidl⁵**

¹ Institute of Physics, Kazan Federal University, Kazan 420008, Russian Federation

² Zavoisky Physical-Technical Institute, FRC Kazan Scientific Center of RAS, Kazan 420029, Russian Federation, tatyana.gavrilova@gmail.com

³ Institute of Physics, Azerbaijan National Academy of Sciences, AZ-1143 Baku

⁴ Institute of Applied Physics, MD-20208 Chisinau

⁵ EP V, EKM, University of Augsburg, D-86135 Augsburg

We report on magnetic susceptibility, specific heat, Mössbauer and ESR experiments on single crystals of the covalent-chain antiferromagnetic compounds TlFeS_2 and RbFeSe_2 . Collinear magnetic order with strongly reduced moments sets in at $T_N = 196$ K for TlFeS_2 and at $T_N = 248$ K for RbFeSe_2 , respectively. The magnetic moments are oriented perpendicular to the chain direction. For RbFeSe_2 compound, the small anomaly in $C(T)$ and the corresponding low value of entropy at T_N indicate a significant spin reduction and the existence of AFM fluctuations even far above T_N . The specific heat measurements of TlFeS_2 do not show any anomaly at T_N [1]. Mössbauer parameters determined in the entire temperature range indicate that iron in TlFeS_2 [2] and RbFeSe_2 is in ferric (trivalent) state having strong covalent bonding to selenium ligands. The measured hyperfine fields are quite reduced as compared to that in high-spin ferric compounds corroborating the strong spin reduction of Fe^{3+} . High-temperature susceptibility and ESR measurements strongly suggest a one-dimensional metallic character of chains composed of edge-sharing $[\text{FeX}_4]$ tetrahedra (X is chalcogen).

This work was supported by the German Research Foundation (DFG) within the Transregional Collaborative Research Center TRR 80 “From Electronic Correlations to Functionality” (Augsburg-Munich-Stuttgart). Z. Seidov received financial support from German Academic Exchange Service (DAAD).

1. Aldzhanov M., Guseinov N., Sultanov G., Nadzafzade M.: Phys. Status Solidi B **159**, K107 (1990)
2. Welz D., Deppe P., Schaefer W., Sabrowsky H., Rosenberg M.: J. Phys. Chem. Solids **50**, 297 (1989)

Low Temperature Mössbauer Study and Magnetic State of $\text{Fe}_{1.05}\text{Se}_{0.3}\text{Te}_{0.7}$

**A. G. Kiiamov¹, F. G. Vagizov¹, D. A. Tayurskii¹, L. R. Tagirov^{1,2},
V. Tsurkan³, A. Loidl³**

¹ Institute of Physics, Kazan Federal University, Kazan 420008, Russian Federation,
AiratPhD@gmail.ru

² Zavoisky Physical-Technical Institute, FRC Kazan Scientific Center of RAS, Kazan 420029,
Russian Federation

³ Experimental Physics V, Centre for Electronic Correlations and Magnetism, University of Augsburg,
Augsburg 86159, Germany

$\text{Fe}_{(1+y)}\text{Se}_{(1-x)}\text{Te}_x$ system was actively investigated after discovering of superconductivity in iron selenide [1]. The interplay between magnetism and superconductivity in the systems is still unclear. It is well known that partial substitution of selenium by tellurium atoms leads to appearance of over-stoichiometric iron atoms. This feature is a consequence of structural instability of FeTe that could be considered as a parent compound for $\text{Fe}_{(1+y)}\text{Se}_{(1-x)}\text{Te}_x$ system at $x > 0.5$ [2–4]. It has been shown that such over-stoichiometry of iron atoms leads to the appearance of excess interlayer iron centers (Fe2) located between Fe-Te layers formed by Fe1 iron atoms [4, 5]. Multiple studies confirmed the significant influence of that excess iron atoms on the magnetic and electronic properties of the compound.

In the present study we focus on the influence of partial substitution of tellurium by selenium on magnetic properties of the iron telluride system. The single-crystalline $\text{Fe}_{1.05}\text{Se}_{0.3}\text{Te}_{0.7}$ sample was investigated utilizing Mössbauer spectroscopy. The analysis of the result correlatively with our previous Mössbauer studies of $\text{Fe}_{1.05}\text{Te}$ system [4] allowed to highlight the contribution of tellurium-selenium substitution effects, because the fraction of excess iron atoms is the same for the both samples according to our data.

The studied single-crystalline $\text{Fe}_{1.05}\text{Se}_{0.3}\text{Te}_{0.7}$ sample was grown by the Bridgman method. The structure and stoichiometry were measured and confirmed by the Rietveld analysis of the XRD patterns and wave-length-dispersive X-ray electron-probe microanalysis. The Mössbauer-effect measurements were carried out in a temperature range from 5 K to 297 K (RT), using a conventional constant-acceleration spectrometer (WissEl, Germany) with ^{57}Co as γ -radiation source. A set of numerous thin flakes packed with the surface orientation parallel to the cleavage plane (001) was used as a sample (absorber) for the Mössbauer-effect measurements. Low-temperature measurements were carried out with a continuous flow cryostat (model CFICEV from ICE Oxford, UK). The measurements were done for the zero angle between the crystallographic c -axis of the crystalline flakes and propagation direction of γ -radiation.

The Mössbauer spectra of $\text{Fe}_{1.05}\text{Se}_{0.3}\text{Te}_{0.7}$ single-crystalline sample obtained at low and room temperatures are presented in Fig. 1. Both of the spectra show only one asymmetric doublet line which is typical for $\text{Fe}_{(1+y)}\text{Se}_{(1-x)}\text{Te}_x$ system. It is

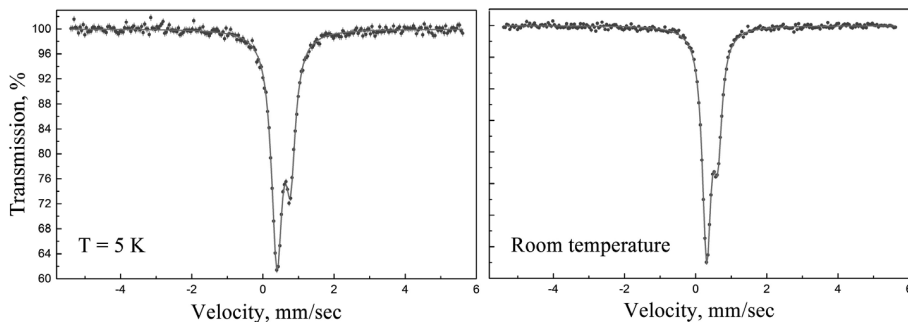


Fig. 1. The Mössbauer spectra of $\text{Fe}_{1.05}\text{Se}_{0.3}\text{Te}_{0.7}$ single-crystalline sample obtained at low and room temperatures.

notable that the low temperature spectrum does not show any traces of magnetic splitting of the doublet. This indicates an absence of any magnetic order in the sample. Nevertheless, it could not be deduced that selenium doping leads to suppression of magnetism in the system, because magnetic sextets were observed in $\text{FeSe}_{0.5}\text{Te}_{0.5}$ [6] compound with higher concentration of selenium atoms.

We expect that our *ab initio* calculations can shed light on the reasons for absence of magnetic order in $\text{Fe}_{1.05}\text{Se}_{0.3}\text{Te}_{0.7}$ system unlike that in $\text{Fe}_{1.05}\text{Te}$.

The reported study was funded by RFBR according to the research project № 18-32-00342. The measurements at KFU were carried out utilizing equipment of the PCR Federal Center of Shared Facilities.

1. Fang M., Pham H., Qian B. *et al.*: Phys. Rev. B **78**, 224503 (2008)
2. Martinelli A., Palenzona A., Tropeano M. *et al.*: Phys. Rev. B **81**, 094115 (2010)
3. Gronvold F., Haraldsen H., Vihovde J.: Acta Chemica Scand. **8**, 1927 (1954)
4. Kiiamov A.G., Vagizov V.G., Tagirov L.R. *et al.*: Annalen der Physik **529**, 1600241 (2017)
5. Zhang L., Singh D.J., Du M.H.: Phys. Rev. B **79**, 012506 (2009)
6. Szymański K., Olszewski W., Dobrzyński L. *et al.*: Supercond. Sci. Technol. **24**, 105010 (2011)

NMR Structural Elucidation of Indole-3-Carbaldehyde Phenylhydrazones

M. I. Kodess^{1,2}, M. A. Ezhikova¹, O. S. Ermakova², Y. A. Azev²

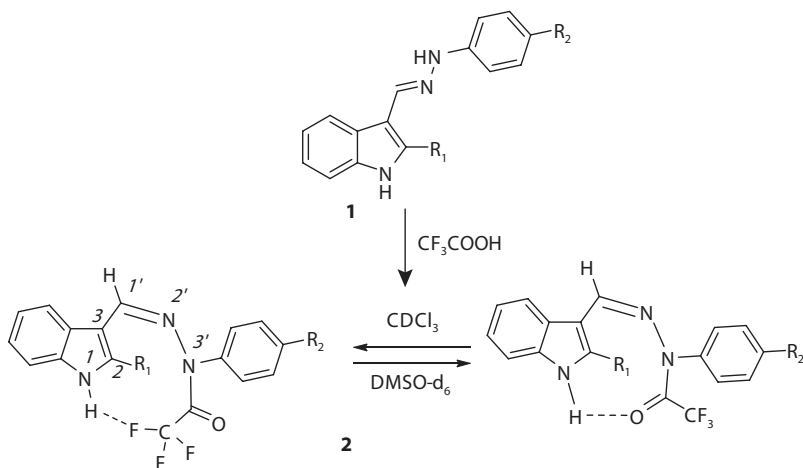
¹ Postovsky Institute of Organic Synthesis, Ural Branch, Russian Academy of Sciences, Yekaterinburg 620990, Russian Federation, nmr@ios.uran.ru

² Ural Federal University, Yekaterinburg 620002, Russian Federation, azulax@yandex.ru

Phenylhydrazones **1** obtained from indole-3-carboxaldehydes, as well as their previously unknown trifluoroacetyl derivatives **2** were characterized by the ¹H, ¹⁹F, ¹³C and ¹⁵N NMR spectroscopy. The full assignment of the NMR signals was carried out by 2D ¹H-¹³C and ¹H-¹⁵N HSQC/HMBC experiments.

According to the published data, in compounds with fixed geometry, both two-bond and three-bond nitrogen-proton couplings constants are larger in magnitude for the proton that lies closer in space to the lone-pair electrons on the nitrogen atom [1, 2]. To determine the configuration of C=N double bond in hydrazones, we performed 2D ¹H-¹⁵N HSQMBBC [3] experiments and measured coupling constants ⁿJ_{N,H} (n = 2, 3).

In the starting hydrazones **1**, the value of geminal coupling constants are ²J_{N,H} ≈ 3.0–3.5 Hz, which indicates the *E*-configuration, whereas the trifluoroacetyl derivatives **2** are formed as *Z*-isomers, ²J_{N,H} ≈ 12.0–13.0 Hz. The three-bond coupling constants in the *E/Z* isomers differ insignificantly, but they also depend on the double bond geometry: the vicinal constants are larger for *syn*-orientation of the proton relative to the lone-pair electrons on nitrogen.



Hydrazones **2** exist as *pseudo*-cyclic structures stabilized by an intramolecular hydrogen bond of the N-H...F-C type in chloroform, or N-H...O=C in dimethyl sulfoxide, which was confirmed by the observed coupling constants through hydrogen bond, $J_{(N)H-F} = 1.3$ Hz in $CDCl_3$ and $J_{(N)H-CO} = 3.8$ Hz in $DMSO-d_6$.

It should be noted that unusual long-range through space couplings between nitrogen N-3' and proton H-2 ($R_1 = H$) or protons of the methyl group at indole carbon C-2 ($R_1 = CH_3$) were observed.

1. Crepeaux D., Lehn J.M., Dean R.R.: *Molecular Phys.* **16**, 225 (1969)
2. Crepeaux D., Lehn J.M.: *Org. Magn. Reson.* **7**, 524 (1975)
3. Williamson R.T., Marquez B.L., Gerwick W.Y., Kover K.E.: *Magn. Reson. Chem.* **38**, 265 (2000)

Contrast Agents for Magnetic Resonance Imaging Based on Nanosized Rare Earth Fluorides

**E. I. Kondratyeva^{1,2}, E. M. Alakshin¹, A. V. Bogaychuk¹, A. V. Klochkov¹,
V. V. Kuzmin¹, M. S. Tagirov^{1,2}**

¹ Institute of Physics, Kazan Federal University, Kazan 420008, Russian Federation,
katarina.kondratyeva@gmail.com

² Institute of Applied Research, Academy of Sciences of the Republic of Tatarstan, Kazan 420111,
Russian Federation, murat.tagirov@gmail.com

Nanosized rare-earth fluorides such as TbF₃ and DyF₃ are perspective candidates for the use as contrast agents (CA) in high-field MRI due to their advantages. Lanthanides used as CA usually shortens the time T_1 , slightly, but have a significant effect on the relaxation time T_2 . The Dy³⁺ ion has a highest effective magnetic moment among of all lanthanides (10.63 μ_B). Although the magnetism is an intrinsic property of bulk materials, the magnetic properties of nanoparticles are significantly affected by their size, shape, and surface properties [1]. Zheng and coauthors [2] reports about TbF₃ nanoparticles coated with polyethylamine (PEI) as T_2 -contrast agents for strong field (>3 T) MRI. Due to strong paramagnetism, the TbF₃ nanoparticles showed excellent r_2 relaxivity (395.77 mM⁻¹s⁻¹) and negligible r_1 relaxivity in magnetic field 7 T. The authors of the article [3] proposed the use of HoF₃ and DyF₃ nanoparticles as contrast agents for high-field MRI. In this paper, ellipsoid-like and rhomboid-like HoF₃

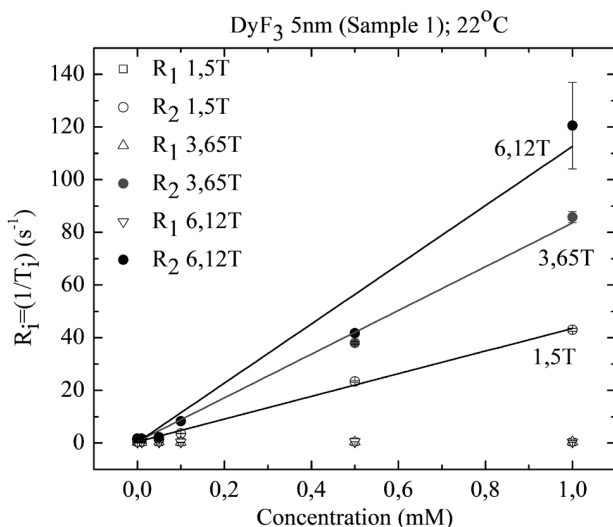


Fig. 1. The concentration dependences of the longitudinal and transverse relaxation rates of water protons in colloid solutions of DyF₃ (5 nm).

and DyF₃ nanoparticles with characteristic sizes of 50–100 nm were studied. The highest values of transverse relaxation at 9.4 T, described in the literature for this type of contrast agents, were found.

The samples of nanosized DyF₃ and TbF₃ were synthesized by a method of precipitation from a colloidal solution. NMR experiments were carried out on a unique pulsed home-built NMR spectrometer. All experiments were carried out at a temperature of 21.5 °C in magnetic fields of 1.5 T; 3.65 T; 6.12 T. The concentration dependences of the longitudinal and transverse relaxation rates of water protons in colloid solutions of DyF₃ (5nm) are shown in Figure for different magnetic fields.

This work has been supported by the Russian Scientific Foundation (project no 17-72-10198).

1. Vuong Q.L., Berret J.-F., Fresnais J., Gossuin Y., Sandre O.: *Adv. Healthcare Mater.* **1**, 502 (2012)
2. Zheng X., Wang Y., Sun L., Chen N., Li L., Shi S., Malaisamy S., Yan C.: *Nano Research* **9**, 1135 (2016)
3. Gonzalez-Mancebo D., Becerro A.I., Rojas T.C., Garcia-Martin M.L., de la Fuente J.M., Ocana M.: *Part. Part. Syst. Charact.* **34**, 1700116 (2017)

Self-Association of Disordered Protein Alpha-Casein According to PFG NMR Spectroscopy

A. M. Kusova, A. E. Sitnitsky, Yu. F. Zuev

Kazan Institute of Biochemistry and Biophysics, FRC Kazan Scientific Center of RAS,
Kazan 420111, Russian Federation, alexakusova@mail.ru, yufzuev@mail.ru

During last years the considerable attention has been given to the intrinsically disordered proteins for further understanding of protein functioning. In the present study we have chosen bovine α_s -casein (α_s -CN) from casein family of milk proteins. Conformation and aggregation of caseins are controlled by the balance of hydrogen bonds, hydrophobic interactions and electrostatic repulsion, which depend on temperature, pH and ionic strength of solution. Due to the lack of a rigid three-dimensional tertiary conformation, all caseins can reply directly on changes in protein environment.

Pulsed field gradient nuclear magnetic resonance (PFG-NMR) allows direct observation of translational mobility of molecules in mono and polydisperse systems. The self-diffusion coefficient can give information about the size and structure of the molecules, about the physical and chemical interactions. The study of the concentration dependences of self-diffusion coefficients macromolecules makes it possible to analyze the types and contributions of intermolecular interactions.

In this article, we have shown the great potential of the PFG-NMR application to study the behavior of protein with a disordered structure in a wide range of concentrations. Concentration dependence of the casein self-diffusion coefficient is analyzed in the frame work of known theoretical approach based on the Vinj's frictional formalism of non-equilibrium thermodynamics. Using this phenomenological approach, the concentration dependence of self-diffusion coefficient of casein was divided into two parts, corresponding to different sizes of diffusing particles. It is shown that at beyond the definite protein concentration in solutions the protein α_s -casein molecules interact with each other and form associates.

This work was supported by RFBR grant no. 18-415-160011.

1. Vink H.: J. Chem. Soc. Faraday Trans. I **81**, 1725 (1985)

Narrowing Behavior of Hyperfine Coupling Structure in CuEr Alloys

S. Lvov, E. Kukovitsky

Zavoisky Physical-Technical Institute, FRC Kazan Scientific Center of RAS, Kazan 420029, Russian Federation, lvov@kfti.knc.ru

The ESR spectrum of Er^{3+} in several binary copper-erbium alloys was studied. Erbium concentration was varied in the range 30–2500 ppm. Measurements were conducted in X-range at the temperature 1.7–4.2 K. The spectrum corresponds to the ion in crystal field of cubic symmetry with g -factor respected to the value for Γ_7 doublet. Alloys preparation method was reported earlier [1] and allows getting ESR spectrum with fully resolved hyperfine structure of odd erbium isotopes ^{167}Er . Presented measurements spread ESR observable erbium concentration range from tens of ppm to thousands ppm in copper-erbium system having zero-solubility scale. Hyperfine interaction constants values in wider concentration range support tendency of evident decreasing with erbium concentration increase previously found in very dilute area (Fig. 1).

The formation of an increasing number of erbium clusters and the onset of special erbium-copper phases take place in the transition from a dilute to a more concentrated area. Therefore found tendency is discussed from point of view strengthening role of the RKKY interaction between erbium spins. Experimental results evaluated in terms of extended Bloch-Hasegawa theory.

1. Kukovitsky E.F., Lvov S.G.: ESR Study of CuEr Dilute Alloys. PMM (in press).

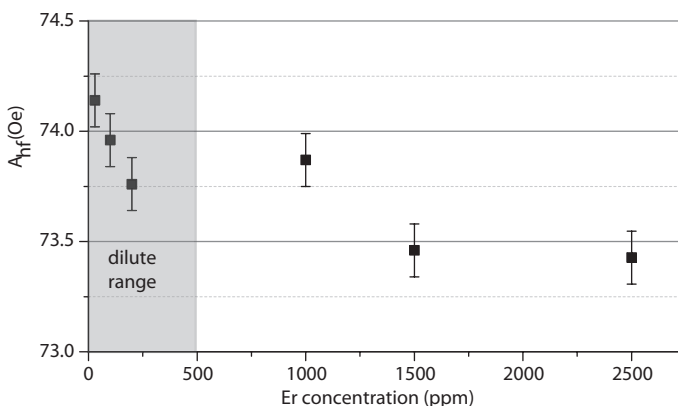


Fig. 1. Concentration dependence of hyperfine coupling constant of ^{167}Er in copper-erbium alloy.

Nuclear Quadrupole Resonance Study of Polymorphic Forms of Piracetam

S. Mamadazizov¹, G. Kupriyanova¹

¹ Institute of Physics and Mathematics, Immanuel Kant Baltic Federal University,
Kaliningrad 236016, Russian Federation, sultonazar.mamadazizov@mail.ru

In recent years, scientific community reveals a renewed interest to nuclear quadrupole resonance (NQR) spectroscopy. This method represents a very convenient tool for structural studies of different pharmaceutical compounds. It is non-destructive, does not demand special preparation of the sample or expensive equipment and, at the same time, it is very informative especially for identification of different polymorphic structures.

Piracetam is a nootropic drug, which has proven to be effective against several degenerative disorders, from cognitive deficits to Alzheimer's disease. In spite of its extensive use in medicine mechanisms underlying its pharmaceutical action are still far from being deeply understood. It is well-known that physical and chemical properties of the compounds depend on their polymorphic structure.

Table 1. Calculated ¹⁴N NQR frequencies of different piracetam polymorphic structures.

Form	N(i)	ν_{+} , MHz	ν_{-} , MHz	ν_0 , MHz
I	1	3.493	3.066	0.428
	2	2.044	2.945	0.099
II	1	0.987	0.661	0.326
	2	1.735	1.311	0.423
III	1	3.306	2.940	0.366
	2	2.961	2.595	0.365

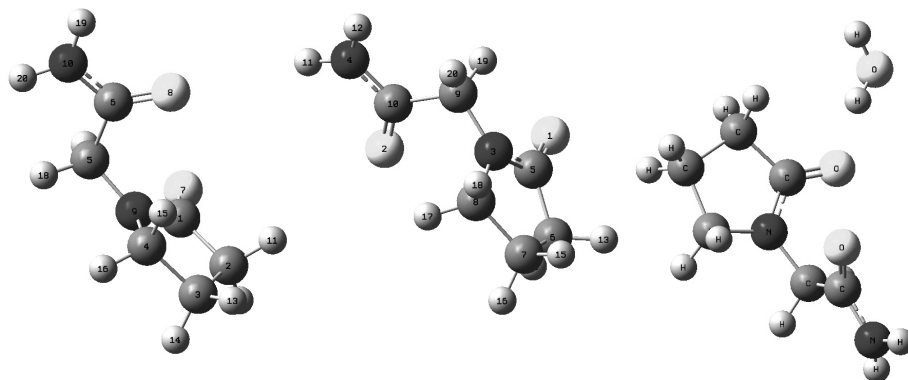


Fig. 1. Polymorphic forms of piracetam.

The purpose of this work to investigate polymorphic states of piracetam in order to understand the impact of slight difference in structure on ^{14}N NQR spectra and relaxation times. It was shown that density functional theory could be used for ^{14}N NQR lines assignments even in complex models [1]. NQR frequencies for nitrogen could be calculated:

$$\nu_{\pm} = \frac{Q_{cc}}{4}(3 \pm \eta); \quad \nu_0 = -\frac{Q_{cc}}{2}\eta.$$

Results of theoretical calculations on B3LYP/6-311++G(3df,3pd) level, with additional functions for hydrogen, shown on Table 1. Difference in spectra is obvious. The mechanism of hydrogen bonding formation and its influence on NQR data is discussed. NQR could be used for identification of polymorphic structures in piracetam based drugs. Experimental data will be published elsewhere.

1. Mamadazizov S., Shelyapina M.G., Kupriyanova G.S., Mozhukhin G.V.: Chem. Phys. **506**, 52–60 (2018)

Modelling NMR Spectra of Gallium Borate Glasses

D. Materka, M. Olszewski

Institute of Physics, University of Szczecin, 70-451 Szczecin, Poland,
daniel.materka@gmail.com; marcin.olszewski@usz.edu.pl

Currently, it is possible to obtain well theoretically predicted spectra of crystallite matter consisted of quadrupole nuclei [1]. However, for simulating a glassy state quadrupole nuclei NMR spectrum, it is needed to slightly scatter parameters of quadrupolar coupling. In order to compute a total spectrum, the numerical methods have to be employed in spite of the fact that the analytical representation of the spectrum at each point of the sample when summing on all of its orientations does not exist [2].

The method of computing the model is similar to the method used to analyze powders, but amongst others, additional parameters e.g asymmetry coefficient of the EFG (Electric field gradient) and quadrupolar coupling constant have been scattered to simulate a local disorder in the structure of the glass. Such a feature is not supported or partially supported by any other NMR modelling-related software so the separate computer program has been written for this particular need.

The family of borate glasses have the very interesting optic, magnetic, superionic conductivity properties related to possible applications in the optical engineering which come from uniqueness of its structure and chemical properties which has been taken into consideration. In order to obtain a very near and therefore an information-abundant spectrum the MAS (Magic-angle spinning) spectroscopy method has been used [3]. The comparison with the empirical data and results of the in-house software and the commonly used programs such as DMFit has been done in order to assess the accuracy of the model.

1. Seleznyowa K., Sergeev N.A., Olszewski M., Stępień P., Yagupov S.V. *et al.*: Fittin MAS NMR spectra in crystals with local disorder: Czjzek's vs. Maurer's model for 11B and 71 Ga in polycrystalline gallium borate. *Solid State Nuclear Magnetic Resonance* **85–86**, pp.12–18. Elsevier 2017.
2. Olszewski M., Stępień P.: *Journal of Education and Technical Sciences* **2**, iss. 1, 31–33 (2015)
3. Freude D.: Quadrupolar Nuclei in Solid-State Nuclear Magnetic Resonance, in: "Encyclopedia of Analytical Chemistry" (R. A. Meyers, ed.), p. 12188. 2000.

Towards an Alpha-Casein Translational Mobility by NMR

D. L. Melnikova¹, I. V. Nesmelova², V. D. Skirda¹

¹ Institute of Physics, Kazan Federal University, Kazan 420008, Russian Federation, melndaria@gmail.com

² Department of Physics and Optical Sciences, and Center for Biomedical Engineering and Science, University of North Carolina, Charlotte, NC 28223, USA, Irina.Nesmelova@uncc.edu

In the last decade it became known, that proteins have functional activity not only in globular condition, but in partly or whole disordered form [1]. The intrinsically disordered proteins functional role could be bound to the need of molecular plasticity for more effective identification by the partner-molecules [2, 3].

The degree of compactness of the polypeptide chain depends on the amino acid residue composition of a given protein and on environmental conditions, including the concentration of the protein itself and/or the crowders. Hence, there is a great interest to understand how the intrinsically disordered proteins (IDPs) behave in the wide range of concentrations, from dilute to highly concentrated solutions. In particular, understanding the translational diffusion of IDPs, which is the major mode of macromolecular transport in biological or chemical systems (e.g., the self-diffusion, hereafter denoted simply as diffusion), becomes important.

The purpose of current work was to study structural and dynamical features of translational mobility of the intrinsically disordered protein α – casein in water solutions in a wide range of concentrations by NMR with pulsed field gradient (PFG).

This work was supported by the Faculty Research Grant from the University of North Carolina to I.V.N. NMR measurement were carried out on the equipment of the Federal Centre of Shared Facilities at Kazan Federal University.

1. Uversky V.N., Gillispie J.R., Fink A.L.: *Proteins* **41**, 415–427 (2000)
2. Dunker A.K., Lawson D.J.: *J. Mol. Graphics and Modelling* **19**, 26–59 (2001)
3. Uversky V. N.: *J. Biomol. Struct. Dyn.* **21**, 211–234 (2003)

Optimization of Pulse RF Sequences Parameters for Contrast Enhancement of MR Images in the Presence of Magnetic Nanoparticles

A. V. Nikitina, Yu. V. Bogachev

Department of Physics, St.-Petersburg State Electrotechnical University,
St.-Petersburg 197376, Russian Federation, nastya_nikitina1996@mail.ru

Promising contrasting agents for MRI are multimodal negative agents based on magnetic nanoparticles (MNPs), which can perform not only diagnostic but also therapeutic functions [1]. In this case, the analysis and optimization of parameters of pulsed RF NMR sequences becomes relevant for MRI studies in the presence of MNPs.

In this regard, research was carried out on NMR relaxation of protons of biological liquids models in the presence of magnetic nanoparticles of different composition and with different shells. For the majority of the investigated MNPs, the dependence of the spin-lattice R_1 and spin-spin R_2 relaxation rates on the concentration of MNPs in water-holding model solutions was linear [2]. Found r_2 relaxation efficiency had a constant value, indicating the aggregation stability of the investigated MNPs.

For some of the studied MNPs, the dependence of the spin-spin R_2 relaxation rate on the MNPs concentration was nonlinear, their dynamic r_{2d} relaxation efficiency decreased when the MNPs concentration increased, indicating a significant aggregation of these MNPs in water-holding model solutions in the presence of the magnetic field. A method for assessing the aggregation stability of MNPs in water solutions has been developed.

There was also a difference in the values of R_1 rates of protons in different magnetic fields, that testified to the presence of frequency dispersion of the spin-lattice relaxation time, typical for heterogeneous media [3, 4].

Based on the obtained relaxation characteristics, a program was developed to optimize the parameters of pulse RF sequences for MRI studies both in the absence of MNPs and in the presence of MNPs (the working windows of the program are shown in Fig. 1a and 1b, respectively).

This program implements three sequences: “spin echo”, “inversion-recovery”, and “gradient sequence”. The program provides an opportunity to study graphs of the dependence of the intensity of the MR signal on the parameters of the sequence for white, gray matter and cerebrospinal fluid.

When using magnetic nanoparticles, a graph of the dependence of the MR signal intensity on the sequence parameter for five MNPs concentrations is also displayed. Also in the program window are simulated images showing the intensity of the signal on a scale of gray.

Using this program, the user can evaluate the impact of pulse sequence parameters on the contrast of MR images, choose the optimal sequence parameters

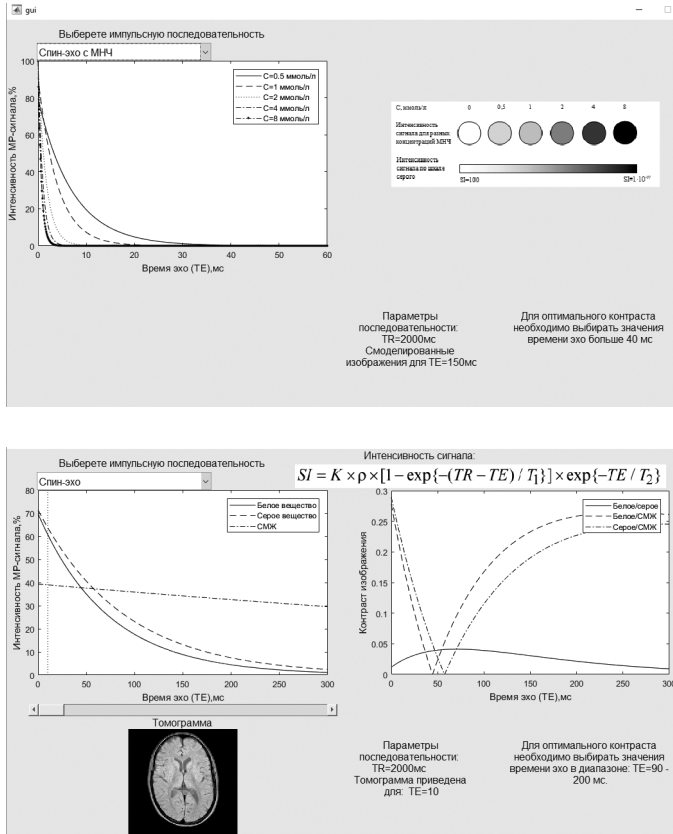


Fig. 1. The working windows of the program.

and determine the necessary concentration of MNPs to improve the contrast of MR images.

The developed program of control of parameters of pulse RF sequences can be used for training of students and medical personnel too.

The obtained results can be used for medical diagnostics with the use of new contrast agents based on magnetic nanoparticles in vivo and in vitro, and in the development of new methods for magnetic resonance theranostics.

1. Bogachev Yu.V., Knyazev M.N., Marchenko Ya.Yu. *et al.*: Diagnostic magnetic resonance. S.-Petersburg: Publishing house of SPbETU “LETI”, 212 p., 2013.
2. Bogachev Yu.V., Nikitina A.V. *et al.*: Appl. Magn. Reson. **48**, I,7, 715–722 (2017)
3. Chizhik V.I., Chernyshev Yu.S., Donets A.V. *et al.*: Magnetic Resonance and Its Applications. Switzerland: Springer International Publishing, 785 p., 2014.
4. Bogachev Yu.V., Drapkin V.Z., Knyazev M.N. *et al.*: Magnetic Resonance Imaging in a Weak Magnetic Field. SPb.: Publishing house of SPbETU “LETI”, 260 p., 2012.

Experimental Investigation of Magnetostriction in LiRF_4 ($R = \text{Ho, Dy}$) in Strong Magnetic Fields

**D. S. Nuzhina¹, S. Abe², A. G. Kiiamov¹, S. L. Korableva¹,
K. Matsumoto², I. V. Romanova¹, A. C. Semakin¹, M. S. Tagirov¹,
K. Ubukata²**

¹ Institute of Physics, Kazan Federal University, Kazan 420008, Russian Federation, nuzh.darya@gmail.com

² Physics Department, Kanazawa University, Kanazawa, 920-11, Japan

Due to excellent magnetic properties, double fluorides of rare earth elements have been the subject of intense research over the past four decades [1–4]. Nevertheless, the study of magnetic properties of LiRF_4 single crystals ($R = \text{rare earth}$) is an important problem for the development of the theory of magnetoelastic effects in magnetically concentrated crystals containing rare-earth ions. It was

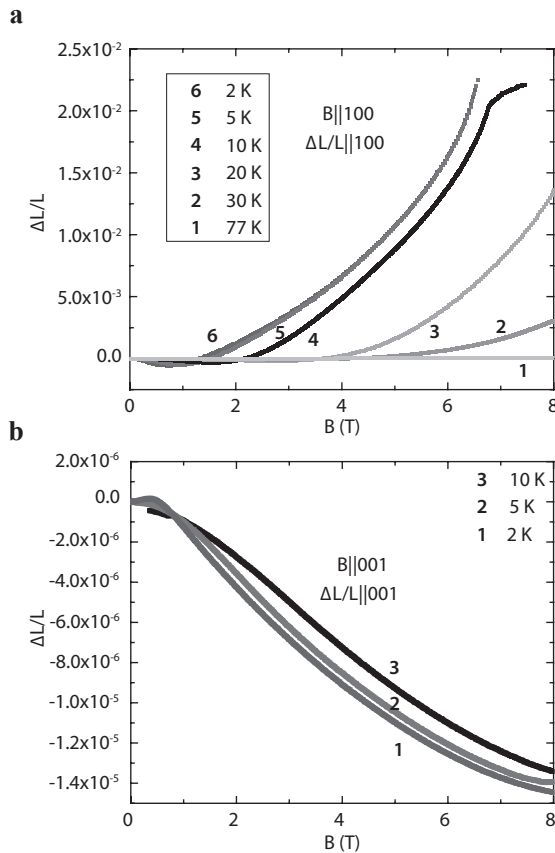


Fig. 1. Magnetostriction as a function of the magnetic field in **a** LiDyF_4 single crystal $B||100$, $T = 2, 5, 10, 20, 30, 77$ K; **b** LiHoF_4 single crystal $B||001$, $T = 2, 5, 10$ K.

previously found that external magnetic fields significantly affect the structure and elastic properties of the crystal lattice of rare-earth double fluorides [5–7]. However, for double fluorides crystals giant magnetostriction in high fields was not observed. Also, as shown in ref. [2], LiHoF₄ and LiDyF₄ crystals can be used as miniature devices for effective Faraday rotation of the radiation polarization plane in spectral ranges of visible, ultraviolet and vacuum ultraviolet radiation (with a wavelength of less than 200 nm).

Single crystals of LiHoF₄ and LiDyF₄ were grown by the Bridgman-Stockbarger method. The single crystal was oriented using an X-ray diffractometer Bruker D8 Advance and then shaped into a cube approximately 3 mm. Magnetostriction measurement of LiHoF₄, LiDyF₄ single crystals have been carried out on a capacitive dilatometer [8] in static magnetic fields in the range 0–8 T at temperatures of 2, 5, and 10 K (Fig. 1). Record values of magnetostriction in single crystals of LiDyF₄ ($\Delta L/L \cdot 10^{-2}$) were obtained for the first time. Also, the destruction of crystals was observed at $\mathbf{B} \approx 6$ T. Calculations of magnetostriction will be made in accordance with [9].

The work was supported by Russian Foundation for Basic Research (grant № 18-42-160012 p_a)

1. Aminov L.K. *et al.*: Handbook on the Physics and Chemistry of Rare Earths **22** (1996)
2. Hansen P.E., Nevald R.: Phys. Rev. B **16**, 146 (1977)
3. Vasyliov V. *et al.*: Optics Express **20**, 14460–14470 (2012)
4. Kjaer K. *et al.*: Journal of Physics: Condensed Matter **1**, 5743 (1989)
5. Al'tshuler S.A.: JETP Lett. **32**, 214–216 (1980)
6. Bumagina L.A. *et al.*: JETP **53**, 792–797 (1981)
7. Yu R., Abdulsabirov *et al.*: FTT **35**, 1876–1880 (1993)
8. Abe S. *et al.*: Cryogenics **52**, 10, 452–456 (2012)
9. Romanova I.V. *et al.*: Magnetic Resonance in Solids. Electronic Journal **18**, 2, 16205 (2016)

Soviet Serial EPR and NMR Spectrometers by the Mid-1980s

V. V. Ptushenko^{1,2}

¹ A. N. Belozersky Institute of Physico-Chemical Biology, M.V. Lomonosov Moscow State University, Moscow 199234, Russian Federation, ptush@belozersky.msu.ru

² N. M. Emanuel Institute of Biochemical Physics of Russian Academy of Sciences, Moscow 199334, Russian Federation

Thanks to the efforts of outstanding Soviet scientists and organizers of science, beginning with the head of the Soviet scientific school of chemical radiospectroscopy Academician V. V. Voevodsky, his disciples, and scientists of other scientific schools in Moscow, Leningrad, Kazan, Donetsk, Novosibirsk, Krasnoyarsk, Minsk, Tallinn and other scientific centers of the USSR, there was a serial production of devices for magnetic resonance by the 1980s in the USSR.

The scientific research and development works in the field of magnetic resonance methods were concentrated mainly in the institutes of the Academy of Sciences (AS) of the USSR, as well as in some industry-specific research institutes and universities. At the same time, the industrial production belonged mainly to the Ministry of Instrumentation, Automation and Control Systems of the USSR (Minpribor) since 1965. Scientific institutions often also possessed abilities to produce small series of the devices developed.

Two organizations of AS played a major role in coordinating the research and development works and manufacturing: the Council for Scientific Instrument Engineering headed by V. L. Talroze since 1965, and the Commission on Radiospectroscopy headed consecutively by V. V. Voevodsky (since foundation in 1959 to 1967), L. A. Blumenfeld (in 1967–1971), and E. I. Fedin (since 1971 until the end of the Soviet AS).

The main manufacturer of serial EPR and NMR spectrometers until 1982 in the USSR was the Smolensk Scientific Development and Production Center “Analitpribor” which produced up to 25 EPR and up to 20 NMR spectrometers annually by the early 1980s. The models RE-1306 (EPR), RYa-2305, RYa-2309, and RYa-2310 (NMR) were the main produced devices from mid-1970s till early 1980s. In addition, small series of magnetic resonance devices were also produced in a number of special design departments (SDD).

EPR of Calixarenes Dopped by Rare-Earth Metals Ions

**E. A. Razina¹, A. S. Ovsyannikov^{1,2}, S. E. Solovieva^{1,2}, I. S. Antipin^{1,2},
A. I. Konovalov¹, G. V. Mamin¹, M. R. Gafurov¹, M. S. Tagirov¹,
S. B. Orlinskii¹**

¹ Kazan Federal University, 420008, Russian Federation, Kazan, helenrazi@yandex.ru

² Arbutov Institute of Organic and Physical Chemistry, FRC Kazan Scientific Center of RAS, Kazan 420088, Russian Federation

The development of current computation technologies is closely related to creation of new type materials based on the application of quantum states such as metal-organic grids. Calixarenes dopped by rare-earth metal ions are a promising molecular platform for the realization of metal-organic grids, and accordingly have great potential for use as functional materials [1].

The investigated substances are $\text{BuS}_4\text{CH}_2\text{COOH}$ calixarenes dopped by ions of rare-earth metals Lu^{3+} , La^{3+} , Gd^{3+} , Yb^{3+} , Er^{3+} and $\text{S}_8\text{CH}_2\text{COOH}$ dopped by Tb^{3+} , Dy^{3+} . Samples were synthesized by the Antipin I.S. in Laboratory of Organic Chemistry at the Institute of Chemistry of KFU [2]. For the EPR studies calixarenes dopped by rare-earth ions Lu^{3+} , La^{3+} , Tb^{3+} , Gd^{3+} , Yb^{3+} , Er^{3+} and Dy^{3+} were grown in the form of crystals. Important, calixarenes dopped by rare-earth ions in during the growth of the molecules. The average size of the microcrystals of calixarenes is about $100 \times 100 \times 4 \mu\text{m}$.

The measurements were carried out using a Bruker spectrometer, W-band, at a temperature of 15–300 K.

The EPR spectra of calixarenes dopped by Lu^{3+} , La^{3+} , Tb^{3+} , Gd^{3+} , Yb^{3+} , Er^{3+} and Dy^{3+} ions are shown in Fig. 1. The approximation results are presented in figure 1 and colored blue. The parameters obtained as the result of the approximation are listed in table 1.

Comparing the g -factors of calixarenes dopped by rare-earth metal ions with the g -factors of free Gd^{3+} , Yb^{3+} , Er^{3+} and Dy^{3+} ions and g -factors of Gd^{3+} , Yb^{3+} , Er^{3+} and Dy^{3+} ions in CaWO_4 [3] indicates that the obtained g -factors values are closer to the values of the g -factors in CaWO_4 crystals and differ from g -factor

Table 1. Comparison of g -factors.

	S	g_{zz}	g_{yy}	g_{xx}	D (MHz)	g -factors of free ions	g -factors in CaWO_4 [3]
S8-Tb	3/2	–	–	–	–	1.5	17.7–17.8
S4-Gd	7/2	2.01(1)	1.98(1)	1.98(1)	880(9)	2	1.9915–1.9916
S4-Yb	1/2	4.70(5)	6.95(5)	7.50(5)	–	1.1	1.05–3.90
S4-Er	1/2	9.5(1)	13.0(1)	16.8(1)	–	1.2	1.25–8.38
S8-Dy	1/2	19.8(5)	16.5(5)	12.0(5)	–	1.3	5.5–7.5
		13.0(5)	5.7(5)	5.7(5)	–	–	

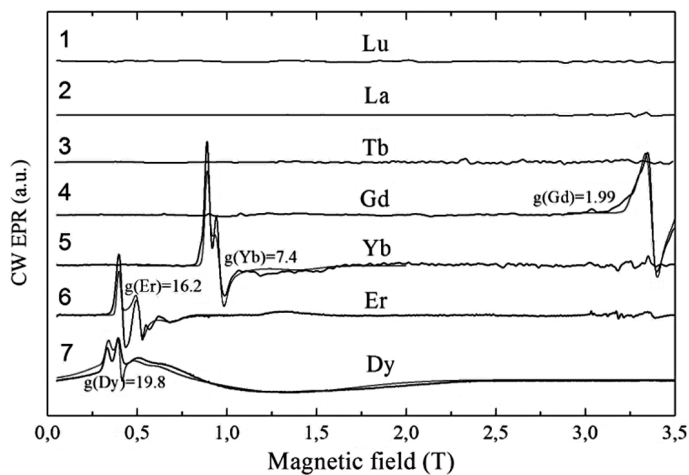


Fig. 1. Continues wave EPR spectra of 1: Lu^{3+} , 2: La^{3+} , 4: Gd^{3+} , 5: Yb^{3+} , 6: Er^{3+} ions in $\text{BuS}_4\text{CH}_2\text{COOH}$ and spectra of 3- Tb^{3+} and 7- Dy^{3+} ions in $\text{S}_8\text{CH}_2\text{COOH}$.

of free ions which indicates the electric crystal field of the surrounding atoms and shows the localization of ions in microcrystals .

However, the lines obtained in the study have a significant width (0.03–0.1 T). To reduce the spin interaction, and by extension the linewidth, the calixarenes containing paramagnetic and nonparamagnetic rare-earth ions must have a 1:100 ratio or less.

1. Furukawa H., Müller U., Yaghi O.M.: *Angewandte Chemie International Edition* **54**, iss. 11, 3417–343 (2015)
2. Antipin I., Burilov V., Valiyakhmetova A., Mironova D.L.: *RSC Advances* **6**, iss. 50, 44873–44877 (2015)
3. Kurkin I.N.: *Collected Paramagnetic Resonance* **5**, 31–73 (1969)

ESR and Luminescence Investigations on Quantum Dots Doped with Various Paramagnetic Ions

**D. O. Sagdeev¹, R. R. Shamilov¹, V. K. Voronkova², A. A. Sukhanov²,
Yu. G. Galyametdinov^{1,2}**

¹ Kazan National Research Technological University, Kazan, Russian Federation, demsagdi@yandex.ru

² Zavoisky Physical-Technical Institute, FRC Kazan Scientific Center of RAS, Kazan 420029, Russian Federation, ansukhanov@mail.ru

Quantum dots (QDs) doped with various paramagnetic ions are the perspective materials for optoelectronics, biomedicine and spintronics [1, 2]. At the least time, the most investigated paramagnetic QDs are doped with manganese ions. However, doping QDs with other paramagnetic ions is also interesting for the science and applications [3].

In that research we synthesized and studied luminescent and magnetic properties of paramagnetic quantum dots CdS doped with Mn²⁺, Cu²⁺, Eu²⁺, Gd³⁺ ions and analyze correlation between reaction conditions and paramagnetic shell of dopant ions using ESR method [4]. Also using the ESR technique we studied changing of Cu:CdS QDs luminescence wavelength on Cu ions oxidative state.

The europium (II) doped CdS QDs were studied by ESR for the first time. Also influence of doping CdS with europium and gadolinium paramagnetic ions on luminescence was investigated. CdS luminescence quenching by doping the Eu²⁺ ions was observed in comparison with pure CdS and Gd:CdS QDs synthesized by the same method.

This work was financially supported by the Russian Foundation for Basic Research (Project № 17-03-00258 A).

1. Jiang C., Shen Z., Luo C., Lin H., Huang R., Wang Y., Peng H.: *Talanta* **155**, 14–20 (2016)
2. Fainblat R., Barrows C.J., Hopmann E., Siebeneicher S., Vlaskin V.A., Gamelin D.R., Bacher G.: *Nano Lett.* **16** (10), 6371–6377 (2016)
3. Wuab P., Yan X.P.: *Chem. Soc. Rev.* **42**, 5489 (2013)
4. Galyametdinov Yu.G., Sagdeev D.O., Voronkova V.K., Sukhanov A.A., Shamilov R.R.: *Russ. Chem. Bull.* **67** (1), 172–175 (2018)

Excessive Oscillating Magnetization in CeD₆ and ESR Line Shape Analysis in Wölfle-Abrahams Theory

A. N. Samarin^{1,2}, M. I. Gilmanov^{1,2}, A. V. Semeno¹, S. V. Demishev^{1,2,3}

¹ Prokhorov General Physics Institute of RAS, Moscow 119991, Russian Federation

² Moscow Institute of Physics and Technology, Dolgoprudny 141701, Russian Federation

³ National Research University Higher School of Economics, Moscow 101000, Russian Federation

In our recent work [1] we presented results of high frequency (60 GHz) electron spin resonance (ESR) investigation of dense Kondo system cerium hexaboride, CeB₆. Experimental technique used allowed absolute calibration of the cavity absorption in the units of magnetic permeability [2]. Further line shape analysis within localized magnetic moments (LMMs) model [1, 2] allowed finding oscillating magnetization value M_0 , g -factor and ESR line width W . It was found that the oscillating magnetization $M_0(T)$ exceeded the static magnetization $M(T)$ by about 20% in the temperature range $T \sim 2.4\text{--}2.6$ K when magnetic field \mathbf{H} was aligned along the [100] crystallographic direction [1]. At the same time, for the cases $\mathbf{H}||[110]$ and $\mathbf{H}||[111]$, the oscillating magnetization was 20% less than static magnetization.

In the present work, we are aimed on explanation of observed anomalous $M_0(T)$ behavior with the help of Wölfle-Abrahams theory developed for the ESR description in dense Kondo systems [3]. In this approach, the ESR absorption line consists of three contributions: 4f LMMs contribution, contribution of itinerant electrons and cross-term describing interaction of free electrons and LMMs. The LMMs and itinerant electrons are characterized by different g -factors (g_f , g_c) and line widths (W_f , W_c) and dynamic susceptibility acquires the form

$$\chi \sim \mu_B^2 (g_f^2 \chi_{ff} + g_c^2 \chi_{cc} + 2g_c g_f \chi_{cf})$$

where χ_{ff} – denotes contribution from 4f LMMs, χ_{cc} – is the contribution from itinerant electrons and χ_{cf} – mark the term due to interaction between LMMs and itinerant electrons [3].

We show that Wölfle-Abrahams theory may describe experimental ESR line shape of CeB₆ assuming equal g -factors ($g_f = g_c$) and equal static and oscillating magnetizations ($M_0 = M$) thus eliminating the paradox discovered in [1]. Fig. 1 shows temperature dependencies of ESR line width $W_f(T)$ for magnetic field directions [100], [110] and [111]. Although our analysis gives an estimation of ESR line width $W_c(T)$, which is about 30–75 times larger than $W_f(T)$ (Fig. 1), the contribution of free electrons ccc and the cross-term ccf appear very important for correct description of the ESR line shape in the strongly considered case. To our

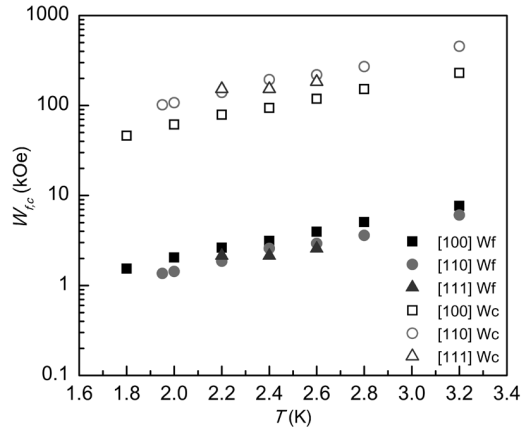


Fig. 1. Temperature dependencies of ESR line width for various CeB_6 directions. W_f – LMM contribution, W_c – itinerant electrons contribution.

best knowledge, this is first time when Wölfle-Abrahams theory [3] was applied just for detailed analysis of the ESR line shape in strongly correlated metals.

This work is supported by Programmes of Russian Academy of Sciences “Electron spin resonance, spin-dependent electronic effects and spin technologies” and “Electron correlations in systems with strongly interacting systems”.

1. Semeno A.V., Gilmanov M.I., Bogach A.V., Krasnorussky V.N., Samarin A.N., Samarin N.A., Sluchanko N.E., Shitsevalova N.Yu., Filipov V.B., Glushkov V.V., Demishev. S.V.: *Sci. Rep.* **6**, 39196 (2016)
2. Samarin A.N., Semeno A.V., Gilmanov M.I., Glushkov V.V., Lobanova I.I., Samarin N.A., Sluchanko N.E., Sannikov I.I., Chubova N.M., Dyadkin V.A., Grigoriev S.V.: *Physics Procedia* **71**, 337 (2015)
3. Abrahams E., Wölfle P.: *Phys. Rev. B* **78**, 104423 (2008)

Peculiar Features of the Spectrum Saturation Effect When the Spectral Diffusion Operates. System with Two Frequencies

K. M. Salikhov

Zavoisky Physical-Technical Institute, FRC Kazan Scientific Center of RAS, Kazan 420029,
Russian Federation

The saturation of the spins spectrum with two separated spectral lines is theoretically analyzed in the presence of the spectral diffusion. Surprising effects of circularly polarized magnetic field on the spectrum under saturation conditions were obtained. The alternating field pushes two lines while the spectral diffusion tends to shift the lines to the center of gravity. As a result the so called exchange narrowing of the spectrum occurs at a higher rate of spectral diffusion with an increase in the amplitude of the alternating field.

Theoretical Study of the EPR Spectrum Saturation Effect Taking Into Account Spectral Diffusion in a System with Gaussian Distribution of Resonance Frequencies of Spins

K. M. Salikhov, I. T. Khairuzhdinov

Zavoisky Physical-Technical Institute, FRC Kazan Scientific Center of RAS, Kazan 420029,
Russian Federation

The paper analyzes the saturation effect for the model situation when a set of resonant frequencies of spin packets is described by the Gaussian distribution and when there is spectral diffusion, which is a random process without correlation. The shape of the spectrum is obtained for arbitrary values of magnetic resonance parameters: relaxation times of the longitudinal and transverse components of the system magnetization vector, spectral diffusion rate and dispersion of the Gaussian distribution of resonance frequencies and magnetic induction of the microwave field. An analytical expression for the spectrum saturation curve is found. For the optimal case, when the frequency of the microwave field coincides with the center for the Gaussian distribution of resonant frequencies, a detailed analysis of the dependence of the saturation curve of the spectrum is presented. The value of the induction of the microwave field, at which the maximum of the saturation curve is achieved, is found for arbitrary values of the paramagnetic relaxation times, the spectral diffusion rate and the dispersion of the Gaussian distribution of spin frequencies. An algorithm for finding the spin-lattice relaxation time is formulated using the experimental value of the microwave field induction at which the saturation curve passes through the maximum.

NMR Study of Influence of the Defects to the Magnetic Interactions and Ground State of Honeycomb Compound $\text{Li}_3\text{M}_2\text{SbO}_6$ (where M is Cu and Ni)

T. Salikhov¹, E. Zvereva², V. Nalbandyan³, A. Vasiliev², E. Vavilova¹

¹ Zavoisky Physical-Technical Institute, FRC Kazan Scientific Center of RAS, Kazan 420029, Russian Federation, jenia.vavilova@gmail.com

² MSU, Moscow 119991, Russian Federation

³ SFU, Rostov-na-Donu 344090, Russian Federation

A new generation of layered antimonite $\text{A}_3\text{M}_2\text{SbO}_6$ (where A = Li, Na and M is transition metal) with honeycomb structure is in the focus of the attention of the investigation during last years. In these compounds ordered mixed-layers of magnetic cations M^{2+} and Sb^{6+} alternate with non-magnetic alkali metal layers. The crystal structures are very soft and even slight modification results in drastic changes in the magnetic properties. The non-stoichiometry and the non-magnetic defects in such systems are very important factors that allow adjusting their magnetic and electrical characteristics. Here we present the results of NMR study of $\text{Li}_3\text{M}_2\text{SbO}_6$ (where M is Cu and Ni) in presents of non-stoichiometry. We show that the lithium deficiency and the site inversion in these compounds lead to the transformation of interactions in a two-dimensional hexagonal lattice and change the ground state. Moreover, the appearance of vacancies at the position of lithium increases its mobility, which can be detected by NMR-relaxometry even in such a magnetically concentrated compound.

The work was supported by grant RFBR 18-02-00664

Anomalous Features of Antiferromagnetic Resonance in GdB_6

**A. V. Semeno¹, M. I. Gilmanov^{1,2}, N. E. Sluchanko, N. Yu. Shitsevalova³,
V. B. Filipov³, S. V. Demishev¹**

¹ Prokhorov General Physics Institute of RAS, Moscow 119991, Russian Federation, semeno@lt.gpi.ru

² Moscow Institute of Physics and Technology, Dolgoprudny 141701, Russian Federation

³ Frantsevich Institute for Problems of Materials Science NASU, Kiev, Ukraine

We report first measurements of electron spin resonance (ESR) performed as in paramagnetic (PM) and in antiferromagnetic (AFM) phases of the metallic antiferromagnet GdB_6 ($T_N = 15.5$ K). Single resonance line is observed above T_N . It is found that strong line broadening starts in PM below $T^* \sim 70$ K accompanied by the shift of g -factor from its high temperature value $g \approx 2$. The relation between g -factor and the linewidth ΔW in this range is: $\Delta W(T) \sim \Delta g(T)$. Such behavior is not typical for AFM metals and may be caused by the motion of Gd^{3+} ions in oversized boron cages. The transition to AFM phase manifests itself by abrupt shift of the line position (from $B_0 \sim 1.9$ T до $B_0 \sim 3.9$ T at $\nu = 60$ GHz) with further smooth evolution characterized by four-line structure formation shifting to lower fields. The dependence $\omega(B_0)$ in AFM phase is well described by the model of easy axis antiferromagnet $\omega/\gamma = (H_A H_E + H_0^2)^{1/2}$, where H_E is the exchange field and H_A is the anisotropy field, which allows us estimating the latter parameter as $H_A \approx 800$ Oe. The origin of H_A may be explained by dipole-dipole interaction induced by mutual shift of Gd^{3+} ions. In this case the value of H_A gives the upper limit of this shift as $\sim 10\%$.

This work was supported by RSF Grant No. 17-12-01426.

Influence of the Substrate Bias Voltage on the Structure Pd_{1-x}Fe_x Thin Films by Magnetron Sputtering

Sh. M. Shabakaev¹, I. V. Yanilkin¹, A. M. Rogov², R. V. Yusupov¹

¹ Institute of Physics, Kazan Federal University, Kazan 420008, Russian Federation

² Interdisciplinary Center for Analytical Microscopy, Kazan Federal University, Kazan 420008, Russian Federation, shshabakaev@gmail.com

Substrate bias voltage is one of the factors that affect the crystal structure and morphology of thin films deposited by magnetron sputtering [1]. Thus, in the case of Ni thin films bias voltage was used to control a type of a film texture [2]. In this work, we report on the results of studying the influence of bias voltage on the morphology and magnetic properties of thin Pd_{1-x}Fe_x thin films with low x values. The films of ~ 20 nm thickness were deposited to the n-type Si or R-cut Al₂O₃ substrates by DC magnetron sputtering from two separate Pd and Fe targets (99.98% purity) with the power adjusted for a desired film composition ($x = 0.04$). Substrate bias values were 0 V, -20 V, -50 V and -100 V.

In Fig. 1 we compare the morphologies of the Pd_{0.96}Fe_{0.04} films on Al₂O₃ deposited with 0 V and -100 V biases of the substrate. In both cases, films have the granular structure. Application of the bias to the substrate has led to a set of the morphology modifications. The shape of the grains has changed from elliptical to spherical and the lateral size of the grains has increased by $\sim 20\%$. Simultaneously the roughness of the film has decreased by a similar amount. We assume that the electric field due to the applied bias accelerates the ions of the Ar gas in the magnetron chamber as well as the ions of the target materials that create a pressure and make the film denser in the course of the deposition.

Deposited films were studied with ferromagnetic resonance (FMR) spectroscopy. In particular, we investigated temperature dependencies of the FMR

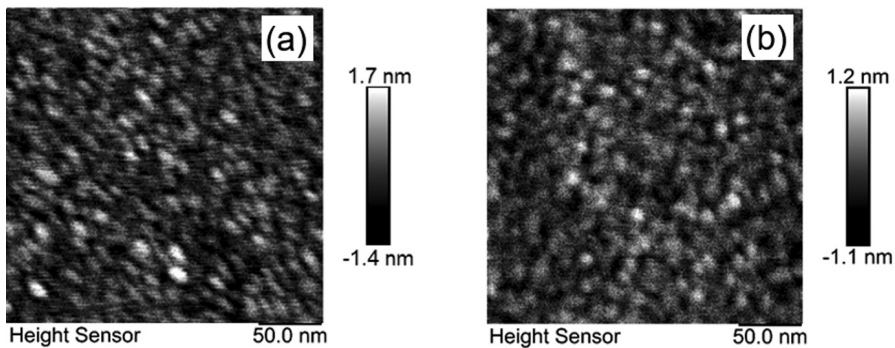


Fig. 1. AFM images of the Pd_{0.96}Fe_{0.04} films on Al₂O₃ substrate deposited with the substrate bias voltages of 0 V (a) and -100 V (b).

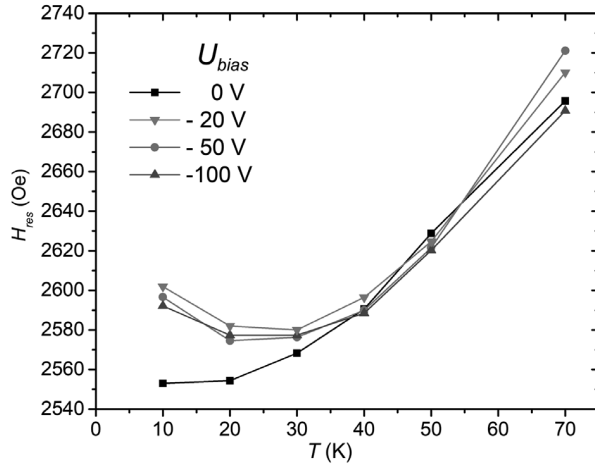


Fig. 2. Temperature dependencies of the FMR resonance field of the magnetron sputtered $\text{Pd}_{0.96}\text{Fe}_{0.04}$ 20 nm thick films on Si deposited with various substrate biases.

resonance fields for the films of the identical composition that differed only in the value of the substrate bias (Fig. 2).

Temperature variation of the FMR resonance field reveals a clear difference for the films deposited with and without the applied bias irrespective of the bias value. We note also that the character of the temperature dependencies for the films deposited with nonzero bias is closer to the dependence observed for epitaxial $\text{Pd}_{1-x}\text{Fe}_x$ films. This, in our opinion, indicates the improvement under bias application of the quality of $\text{Pd}_{1-x}\text{Fe}_x$ films deposited by magnetron sputtering technique.

1. Håkansson G., Sundgren J.E., McIntyre D., Greene J.E., Münz W.D.: *Thin Solid Films* **153**, 55 (1987)
2. Dzhumaliev A.S., Nikulin Yu.V., Filimonov Yu.A.: *Physics of the Solid State* **58**, 1247 (2016)

EPR Spectroscopy of Impurity Centers in Mixed Crystals $\text{LiSr}_x\text{Ca}_{1-x}\text{AlF}_6:\text{Ce}^{3+}$

**A. A. Shakirov, A. A. Shavelev, S. B. Orlinsky, D. G. Zverev,
A. A. Rodionov, A. S. Nizamutdinov, V. V. Semashko**

Institute of Physics, Kazan Federal University, Kazan 420008, Russian Federation,
shakirov_1995@mail.ru

Fluoride crystals with the colquirite structure LiCaAlF_6 (LiCAF) doped with Ce^{3+} ions are used as active media for obtaining laser radiation in the ultraviolet spectral range [1]. A significant vibrational broadening of the laser transitions of these ions causes a broad laser tuning range (282–312 nm), and due to wide band gap of the matrix, there is no photoinduced degradation of laser properties [2]. The disadvantage of this active medium is low isomorphic capacity with respect to Ce^{3+} ions, which leads to appearance of three types of impurity centers and the limitation of the differential efficiency on the one hand and the increase of defects quantity with increase of concentration of the activator ions on the other [3]. Thus, an increase of isomorphic capacity for a given active medium is an urgent task, especially in view of the possibilities of developing ultrashort pulse duration generators [4] and lasers with distributed feedback [5].

The purpose of this work is investigation of impurity centers of Ce^{3+} in mixed crystals $\text{LiSr}_x\text{Ca}_{1-x}\text{AlF}_6$ (with a step $x = 0,2$) grown by the Bridgman method.

The reported study was funded by RFBR according to the research project 18-32-00936.

1. Dubinskii M.A. *et.al.*: Journal of Modern Optics **40**, 1–5 (1993)
2. Fromzel V.A. *et.al.*: Advances in Optical and Photonic Devices 101–116 (2010)
3. Semashko V.V. *et.al.*: Laser Physics **5**, 69–72 (1995)
4. Sarukura N. *et.al.*: Optics Letters **22**, 994–996 (1997)
5. Schowalter S.J. *et.al.*: Optics Letters **37**, 4961–4963 (2012)

EPR-Spectroscopy and Spin-Lattice Relaxation NO_3^{2-} Complex and Mn^{2+} Ions in Synthetic Hydroxyapatite

D. V. Shurtakova, G. V. Mamin, M. R. Gafurov, S. B. Orlinskii

¹ Institute of Physics, Kazan Federal University, Kazan 420008, Russian Federation, darja-shurtakva@mail.ru

Hydroxyapatite $\text{Ca}_{10}(\text{PO}_4)_6(\text{OH})_2$ is used in medicine for various applications, including pain reduction and restoring functions of damaged body tissues, for creating implants, in orthopedics and maxillofacial surgery. Getting full information about synthetic materials based on hydroxyapatite is an important and urgent task.

The aim of work is to describe the temperature dependences of the spin-lattice relaxation of NO_3^{2-} complex and Mn^{2+} ions in synthetic hydroxyapatite. Sizes of the powder particles are 1000 nm and 30 nm.

Temperature dependence of the spin-lattice relaxation rate for the micrometer-sized particles has been described by phonon density function $\rho \sim \omega^2$. The Debye temperature obtained was $T_D = 328 \pm 10$ K. However, in work [1] the Debye temperature obtained from the heat capacity and was found to be $T_D = 389$ K. The next step was description of the spin-lattice relaxation rate by phonon density taken from [2]. In this case, the Debye temperature was $T_D = 378 \pm 10$ K and coincided within the error with the value $T_D = 389$ K.

Also description of the spin-lattice relaxation rate by the phonon density taken from [2] was made for nanoparticles and for the powder containing Mn^{2+} ions.

1. Slepko A.: Journal of Applied Physics **117**(7), 074701
2. Biktagirov T.B.: Journal of Low Temperature Physics **9**, no. 1, 1–6 (2015)

The Study of the Receptor Properties of Pillar[5]arene Binding to DNA by NMR Spectroscopy

P. Skvortsova¹, D. Shurpik², I. Stoykov², Yu. Zuev¹, B. Khairutdinov^{1,2}

¹ Kazan Institute of Biochemistry and Biophysics, FRC Kazan Scientific Center of RAS, Kazan 420111, Russian Federation, skvpolina@gmail.com

² Kazan Federal University, Kazan 420008, Russian Federation

The development of systems for the efficient transfer of genetic material is one of the greatest promise for the medical therapy and diagnostics. Such systems can be based on using the supramolecular platforms as the transfection agents. Pillar[5]arenes are a class of new macrocyclic compounds, which potentially can act as the universal platforms of creating transport systems for the delivery of the biologically active compounds as well as the plasmid DNA into the cell.

Thus in this work the complex of 4,8,14,18,23,26,28,31,32,35-decakis-[(N-(2',2',2'-triethylaminoethyl)-carbamoylmethoxy)-pillar[5]arene deca-iodide with the palindromic DNA decamer was investigated by high resolution NMR spectroscopy. The NMR spectra were completely assigned using homo- and heteronuclear correlation experiments: ¹H-¹H COSY, ¹H-¹H NOESY, ¹H-¹³C HSQC, ¹H-¹³C HMBC. The formation of the pillar[5]arene complex with the DNA was shown by two-dimensional NOESY spectroscopy and diffusion measurements.

The work was supported by the Russian Foundation for Basic Research No. 17-03-00858a.

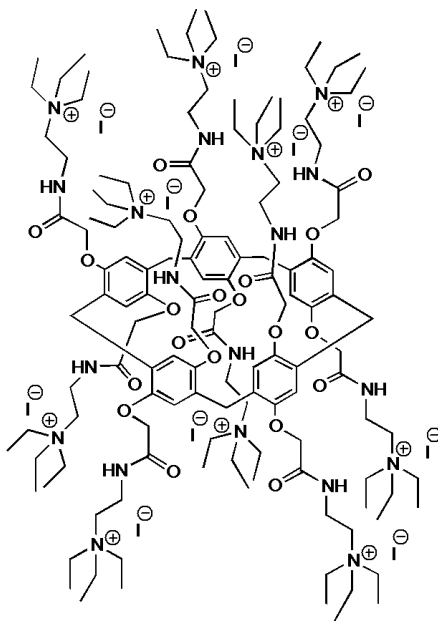


Fig. 1. Structure of the investigated pillar[5]arene.

Effect of Dimerization on the Photophysical Properties of Zinc Coproporphyrin I

A. A. Sukhanov¹, V. S. Tyurin², V. K. Voronkova¹

¹ Zavoisky Physical-Technical Institute, FRC Kazan Scientific Center of RAS, Kazan 420029, Russian Federation

² A. N. Frumkin Institute of Physical chemistry and Electrochemistry Russian Academy of Sciences, Moscow 119071, Russian Federation

The results of time-resolved electron paramagnetic resonance (TR EPR) of zinc complexes of coproporphyrin I tetraethyl ester (ZnCPP-1) in solvents: *o*-terphenyl, chloroform/isopropanol mixture and dichloromethane depending on the time after the laser pulse photo-excitation have been presented. The TR EPR spectra of the ZnCPP-1 complex in *o*-terphenyl indicate the presence of only one type of the photoexcited triplet state, while in the solution of the chloroform/isopropanol the TR EPR spectrum is a sum of two different triplet spectra. The triplet spectrum detected in *o*-terphenyl is described by the zero-field splitting (ZFS) parameters and the *aaa/eee* electron spin polarization (ESP) pattern characteristic of zinc porphyrin derivative triplets. This spectrum is assigned to the monomeric ZnCPP-1 complex. A new spectrum detected together with the monomer spectrum in the chloroform/isopropanol has a reverse ESP pattern. The new spectrum is especially clearly observed in the time interval of 1.4-3 μ s after the laser pulse, when the intensity of the spectrum from the monomer triplet is substantially reduced. In addition to the reverse ESP pattern, an increase in the ZFS parameters of the new spectrum is observed. The density functional theory (DFT) calculation of the monomer and dimer structures and their energies show that the dimer formation is energetically favorable. On the basis of the TR EPR data and DFT calculation, it is concluded that the ZnCPP-1 complex is dimerized in the solution of the chloroform and isopropanol mixture and the new spectrum is assigned to the dimer. The effect of the dimerization on the photoexcited triplet state of ZnCPP-1 is discussed.

This work was supported by the Russian Foundation for Basic Research (project No. 16-03-00586).

TR EPR of Compact Naphthalimide-Phenothiazine Dyads for Understanding of Photophysics of Thermally Activated Delayed Fluorescence

B. G. Tang¹, A. A. Sukhanov², X. Li³, W. Yang¹, Zh. Wang¹, F. Zhong¹, J. Zhao¹, V. K. Voronkova², G. Gurzadyan³

¹ State Key Laboratory of Fine Chemicals, School of Chemical Engineering, Dalian University of Technology, Dalian 116024, P. R. China, zhaojzh@dlut.edu.cn

² Zavoisky Physical-Technical Institute, FRC Kazan Scientific Center of RAS, Kazan 420029, Russian Federation, vio@kfti.knc.ru

³ Institute of Artificial Photosynthesis, State Key Laboratory of Fine Chemicals, Dalian116024, P. R. China, gurzadyan@dlut.edu.cn

Precise controlling of the electronic coupling between electron donor and acceptor units in a dyad is pivotal for development of novel organic materials, for instance, thermally-activated delayed fluorescence (TADF) materials. Knowing the underlying photophysics of TADF allows proper design of high efficiency organic light-emitting diodes. Herein we present the synthesis of two compact electron donor/acceptor dyads based on phenothiazine (PTZ, electron donor) and naphthalimide (NI, electron acceptor), and the study of the electronic coupling effect on the photophysical properties (C–N substitution in NI-N-PTZ and C–C substitution in NI-C-PTZ, respectively). Picosecond and nanosecond transient absorption spectra showed the formation of charge separated states in these dyads. TADF was only observed for NI-N-PTZ. The study of the triplet state with time-resolved electron paramagnetic resonance spectroscopy (TREPR) confirms significant difference in photophysical properties of NI-C-PTZ and NI-N-PTZ. The TR EPR spectra of NI-C-PTZ are typical for triplet state with $e a e/a e a$ electron spin polarization (ESP) pattern. The zero-field splitting (D and E) parameters which characterize the splitting of the triplet into sublevels in zero magnetic field were determined by computer simulation.

The shape of spectrum for NI-C-PTZ dyad remains unchanged within the detection interval of 0.6–3 μ s. In contrast to this the spectrum of NI-N-PTZ dyad changes with increasing observation time after laser flash. In addition, the shape of the spectrum and the ESP pattern differ significantly from those observed for NI-C-PTZ dyad.

The observed features of the TR EPR spectra for NI-N-PTZ are discussed from the point of view of their connection with the TADF properties.

This work was supported by the Russian Foundation for Basic Research (project No. 16-03-00586) and the Program of the Presidium of RAS №9.

Influence of the Tetradentate Schiff Base on the Spin-Variable Properties of [FeL(tpv)] BPh₄ Complexes According to EPR Data

**O. Turanova, E. Milordova, T. Ivanova, L. Mingalieva,
V. Shustov, L. Gafiyatullin, I. Ovchinnikov**

Zavoisky Physical-Technical Institute, FRC Kazan Scientific Center of RAS, Kazan 420029,
Russian Federation, alex@kfti.knc.ru

In connection with the search for new coordination spin-variable compounds, a series of Fe (III) polymer complexes [FeL (tpv)] BPh₄, where the equatorial ligands L = salen, bzacen, acen are the tetradentate Schiff N₂O₂ base of the donor type, has been synthesized, characterized and studied by the EPR method. The photosensitive bidentate ligand tpv = 1,2-di (4-pyridyl) ethylene was used as the axial bridging ligand.

In coordination compounds with two aromatic groups C₆H₅ in L ligand (salen), Fe (III) ions are in high-spin state ($S = 5/2$, $D > h\nu$, $E/D \sim 1/3$). In compounds with two aliphatic groups CH₃ in ligand L (acen), Fe(III) ions are in the low-spin state and form dimers with weak exchange interactions ($S_1 = S_2 = 1/2$, $g_{x(1)} = 1.945$, $g_{y(1)} = 2.135$, $g_{z(1)} = 2.380$, $g_{x(2)} = 2.100$, $g_{y(2)} = 1.945$, $g_{z(2)} = 2.380$, $J_{12} = 0.005 \text{ cm}^{-1}$). The combination of aromatic and aliphatic fragments in the ligand L = bzacen leads to the appearance of spin-variable properties. The influence of the crystallization time on the properties of the spin transition is revealed. When fast crystallization (1–4 hours) spin transition observed in the interval (240–320) K, when slow crystallization (24 hours) – in the interval (100–230) K. The difference of the structures formed in this cases is confirmed by the measurement of X-ray powder diffraction patterns and may be due to the presence of solvent molecules in the complex when fast crystallization.

The change of the spin state of the Fe (III) complexes with N₄O₂ donor environment is explained by the change of the crystal field strength and symmetry depending on the donor activity of the terminal fragments of the equatorial ligand.

The Study of Magnetic Properties of Fe(III) Complexes with Multidentate Schiff Bases in Dichloromethane by NMR, EPR, and UV-Spectroscopy

M. Volkov, E. Frolova, L. Mingalieva, L. Gafiyatullin, O. Turanova, E. Milordova, I. Ovchinnikov, A. Turanov

Zavoisky Physical-Technical Institute, FRC Kazan Scientific Center of RAS, Kazan 420029, Russian Federation, mihael-volkov@yandex.ru

Spin-crossover transitions are very sensitive to weak external influences (temperature, pressure, photo irradiation, etc.). Their study is important both for fundamental science and for the prospects of their practical applications. Most studies of magnetic properties of complexes have been performed for solids and much less attention is focused on their solutions, although the magnetic properties of complexes in solutions can vary widely.

In this work the magnetic properties of the solutions of three Fe(III) complexes [Fe(salten)Cl], [Fe(salten)(Pic)]BPh₄, and [Fe(acen)(Him)₂]BPh₄ were studied (in the temperature range of 185–295 K), where H₂salten = 4-azaheptamethylene-1,7-bis(salicylideneimine), H₂acen = NN'-ethylenebis(acetylacetylideneimine), Pic = 4-methylpyridine, Him = imidazole, BPh₄ = tetraphenyl borate. Each of these complexes was dissolved in dichloromethane, the first and the second at a concentration of 5.0 mmol/L, the third at 5.5 mmol/L. The magnetic susceptibility χ_v of the studied solutions was measured by a Bruker Avance 400 NMR spectrometer with using a spherocylindrical ampoule [1]. The paramagnetic contribution χ_{para} was determined as the difference of the volume magnetic susceptibility χ_{sol} of the complex solution and χ_{diam} of the pure solvent. The temperature dependences of μ_{eff} for the three solutions of the complexes were obtained. In the solution of the first complex only the high-spin state $S = 5/2$ is observed, while the solutions of the second and the third complexes demonstrate an incomplete spin-crossover between the low-spin $S = 1/2$ and the high-spin $S = 5/2$ states. It was revealed that in the solutions of the last two complexes the spin-crossover has a greater slope than in the solid state.

The EPR spectra of the above solutions were recorded by an Bruker EMX-plus EPR spectrometer (X-band, CW mode), the electronic spectra recording was carried out by a Varian Cary 100 spectrophotometer. The methods of EPR and spectrophotometry allow us qualitative to confirm the presence or absence of a spin-crossover in solutions.

Magnetic Properties of High-Spin Fe(III) Complexes with Schiff Based Photoactive Ligands

V. Vorobyeva¹, N. Domracheva¹, E. Zueva^{2,3}, M. Gruzdev⁴

¹ Zavoisky Physical-Technical Institute, FRC Kazan Scientific Center of RAS, Kazan 420029, Russian Federation, vvalerika@gmail.com

² Arbuzov Institute of Organic and Physical Chemistry, FRC Kazan Scientific Center of RAS, Kazan 420088, Russian Federation

³ Kazan Federal University, Kazan 420008, Russian Federation

⁴ G. A. Krestov Institute of Solution Chemistry, RAS, Ivanovo 153045, Russian Federation

The unusual magnetic behavior of two novel Fe(III) compounds of the formula $[\text{FeL}_2]\text{X}$ (where $\text{X} = \text{Cl}^-$ (**1**), NO_3^- (**2**), and L is a photoactive ligand, 4-bromobenzoyloxy-4-salicylidene-N'-ethyl-N-ethylenediamine) was examined by means of electron paramagnetic resonance and pulsed laser irradiation. EPR spectrum consists of two types of resonance lines and all Fe^{3+} ions are in a high-spin state. The I-type of resonance lines dominates at low temperatures (LT), while the II-type prevails at high temperatures (HT). A transition from the LT to HT spectrum with increasing temperature accompanied by a redistribution of the integrated intensity are observed. This behavior is typical for a structural phase transition with a double-minimum potential. The height of the barrier between the potential minima was determined from the EPR data and is 35 cm^{-1} . The redistribution of the number of Fe^{3+} centers between the LT and HT minima with changing the temperature calculated for compound **1** allowed to conclude that the sample, most likely, undergoes an order-disorder ferroelectric phase transition, and below $T_k = 100 \text{ K}$ (the phase transition temperature) a nonzero average electric dipole moment appears. To get an insight into molecular structure of Fe^{3+} centers and their supramolecular organization, a DFT calculations was performed. On the basis of our findings, the LT- and HT-phase structures were proposed for our compounds. It was also shown that photoexcitation in the UV region at 5 K converts cationic complexes into ligand-to-metal charge transfer (LMCT) states, in which the iron is ferrous, and the unpaired electron is located on the salicylidene moieties. The LMCT states decay back to the ferric one, and ferric complexes further form the most stable (LT) phase structure.

Time-Resolved EPR Study of TEMPO-Bodipy Dyad

K. Xu¹, J. Zhao¹, A. A. Sukhanov²,
V. K. Voronkova²

¹ State Key Laboratory of Fine Chemicals, School of Chemical Engineering, Dalian University of Technology, Dalian 116024, China

² Zavoisky Physical-Technical Institute, FRC Kazan Scientific Center of RAS, Kazan 420029, Russian Federation, ansukhanov@mail.ru

Boron Dipyrromethane (Bodipy) chromophores show high quantum yields, hydrophobicity, and large extinction coefficients [1–3]. Many chromophores covalently linked to or coordinated by stable nitroxide radicals have shown the ability to control the magnetic properties by photoexcitation of those systems [4–6]. Photoexcitation of chromophores initiates highly spin-polarized triplet states. Interaction between those triplet states and ground spin state of stable radical often leads to the spin polarization of the electron radical, which is a simple means for control the magnetic properties by photoexcitation. To observe those photoexcited states of such systems electron paramagnetic resonance (EPR) spectroscopy techniques are intensively used.

Laser flash induced spin-polarized transient electron paramagnetic resonance (TREPR) spectra for TEMPO-Bodipy dyad in isotropic and frozen solutions of liquid crystal 5CB are presented. Continuous wave TREPR measurements were carry out at X-bands. The TR EPR of the excited doublet state ($S = 1/2$) and quartet state ($S = 3/2$) of the dyad were observed. Mechanism of spin polarization as a result of triplet-radical interactions is discussed.

We are grateful to the Program of the Presidium of RAS №5 for partial financial support.

1. Ulrich G., Ziesel R., Harriman A.: *Angew. Chem. Int. Ed.* **47**, 1184 (2008)
2. Ziesel R., Harriman A.: *Chem. Commun.* **47**, 611 (2011)
3. Cakmak Y., Kolemen S., Duman S. *et al.*: *Angew. Chem. Int. Ed.* **50**, 11937 (2011)
4. Corvaja C., Maggini M., Prato M. *et al.*: *J. Am. Chem. Soc.* **117**, 8857 (1995)
5. Giacobbe E.M., Mi Q., Colvin M.T. *et al.*: *J. Am. Chem. Soc.* **131**, 3700 (2009)
6. Sukhanov A.A., Konov K.B., Salikhov K.M. *et al.*: *Appl Magn Reson* **46**, 1199 (2015)

EPR Investigation of Antioxidant Protection and Production of Nitric Oxide in Rat after Spinal Cord Injury

**G. G. Yafarova^{1,2,3}, I. I. Shaikhutdinov³, V. V. Andrianov^{1,2},
V. S. Iyudin¹, Kh. L. Gainutdinov^{1,2}**

¹ Zavoisky Physical-Technical Institute, FRC Kazan Scientific Center of RAS, Kazan 420029, Russian Federation

² Institute of Fundamental Medicine and Biology, Kazan Federal University, Kazan 420008, Russian Federation

³ Republican Clinical Hospital of the Tatarstan Republic, Kazan 420064, Russian Federation
gusadila@mail.ru

System of nitric oxide (NO) is one of the most studied systems of the organism [1, 2]. Its role is documented for the central and autonomous nervous systems, for cardiovascular function and blood supply to the brain and the heart, where deviations in NO level may incur risks of stroke and infarction [1, 3–5]. The NO system is also essential in adaptation to environmental changes and external conditions. In addition to vasodilation, NO participate in reactions of oxidative stress, glutamate-calcium cascade, and inflammation [2]. There is a debate about the role of NO in development of spinal cord injury (SCI), however research on dynamics of NO production at different stages of traumatic disease of the spinal cord (SC) is limited. In SCI processes leading to the accumulation of Ca^{2+} ions in the cell, energy deficiency, changes in active ion transport, glutamate excitotoxicity, and oxidative stress occur [6]. According to the literature, the activation of inducible NO-synthase in the SC is observed by 3 days after the injury [7]. According to other authors, a moderate increase in the level of NO (up to 0.5 μm) promotes cell survival or has a cytoprotective effect [7, 8]. Thus, NO, depending on the specific conditions, is characterized by both damaging and protective functions. Presumably, the role of NO depends on the concentration range, the cell type source and the environment in which it was received NO.

We used a model of SCI at the level of the first lumbar vertebra (L1) according to the modified method of A. Allen [8, 9]. We studied the tissue samples of the spinal cord, liver and heart in intact animals and in different periods of traumatic disease of the SC by EPR spectroscopy using the method of spin traps [1, 5, 10, 11]. As spin trap were applied the complex of Fe^{2+} with diethyldithiocarbamate $(\text{DETC})_2\text{-Fe}^{2+}\text{-NO}$. The records were carried out on EPR spectrometer X-band firm “Bruker” ER 200E SRC. In intact rats the production of NO in the SC was on average 1.3 $\text{nm/g}\times\text{hour}$ and in the heart of 5.2 $\text{nm/g}\times\text{hour}$. After 5 hours of SCI there is a decrease of NO production in the tested tissues and remains low up to 1 day. 3 days after SCI level of NO production in SC increases in 2.5 times. In a chronic period of SCI observed decrease in the level of NO production in the tissues of the heart, but in the SC levels of NO production in chronic period of traumatic disease was significantly more control level. We used the method of EPR spectroscopy also as method for estimation of the balance of systems $(\text{DETC})_2\text{-Cu}$ and $(\text{DETC})_2\text{-Fe}^{2+}\text{-NO}$ (NO/

Cu). The ratio of NO/Cu in SCI in intact rats averaged 1:80, which apparently helps to prevent the formation of peroxynitrite. It was found that 3 days after SCI, when the level of NO production in SC was on average 2.5 times more than in intact animals, also increases the concentration of (DETC)₂-Cu; and the ratio of NO/Cu in this period has averaged 1:50. In chronic period, the ratio NO/Cu was only 1:3. Thus, the dynamics of the intensity of formation of NO after SCI indicates its possible role as an inducer of apoptosis in the tissue of the damaged SC, and generalized activation of NO-ergic stress-limiting system in the early stages of SCI.

This work is supported by the Russian Science Foundation under grant № 17-04-01746 A.

1. Vanin A.F.: *Biohimia* (in Russian) **63**, 924–938 (1998)
2. Terpolilli N.A., Moskowitz M.A., Plesnila N.: *J. Cereb. Blood Flow Metab.* **32**, no 7, 1332–1346 (2012)
3. Andrianov V.V., Sitdikov F.G., Gainutdinov Kh.L. *et al.*: *Ontogenez* (in Russian) **39**, no 6, 437–442 (2008)
4. Reutov V.P., Okhotin V.E., Shuklin A.V. *et al.*: *Uspekhi Physiol. Nauk* (in Russian) **38**, no 4, 39–58 (2011)
5. Gainutdinov Kh.L., Gavrilova S.A., Iyudin V.S. *et al.*: *Appl. Magn. Reson.* **40**, no 3, 267–278 (2011)
6. Dumont R.J., Okonkwo D.O., Verma R.S. *et al.*: *Clin. Neuropharmacol.*, **24**, no 5, 254–264 (2001)
7. Kwak, E.K.: *Korean Med. Sci.* **20**, 663–669 (2005)
8. Yafarova G.G., Andrianov V.V., Yagudin R.Kh. *et al.*: *BioNanoScience* **6**, no 4, 332–334 (2016).
9. Yafarova G.G., Andrianov V.V., Yagudin R.Kh. *et al.*: *Bull. Experim. Biol. Med.* **162**, no 3, 316–319 (2017)
10. Mikoyan V.D., Kubrina L.N., Serezhenkov V.A. *et al.*: *Biochim. Biophys. Acta* **1336**, no 2, 225–234 (1997)
11. Gainutdinov Kh.L., Faisullina R.I., Andrianov V.V. *et al.*: *Bull. Experim. Biol. Med.* **154**, no 5, 635–637 (2013).

Magnetic Properties of $\text{CaCu}_3\text{Ti}_4\text{O}_{12}:\text{Fe}$ Solid Solutions

**A. Yagfarova¹, T. Gavrilova^{1,2}, I. Gilmudtinov¹, I. Yatsyk^{1,2}, J. A. Deeva³,
A. L. Zinnatullin¹, F. G. Vagizov¹, T. I. Chupakhina³, R. Eremina^{1,2}**

¹ Institute of Physics, Kazan Federal University, Kazan 420008, Russian Federation

² Zavoisky Physical-Technical Institute, FRC Kazan Scientific Center of RAS, Kazan 420029, Russian Federation, tatyana.gavrilova@gmail.com

³ Institute of Solid State Chemistry of the RAS (UB), Ekaterinburg 620990, Russian Federation

$\text{CaCu}_3\text{Ti}_4\text{O}_{12}:\text{Fe}$ solid solutions were synthesized using a solid state method from stoichiometric amounts of calcium carbonate (CaCO_3), iron (Fe) and copper and titanium oxides (CuO , TiO_2). The resulting mixture was annealed at the temperature $t = 1100^\circ\text{C}$ during 6 hours with an intermediate milling. However,

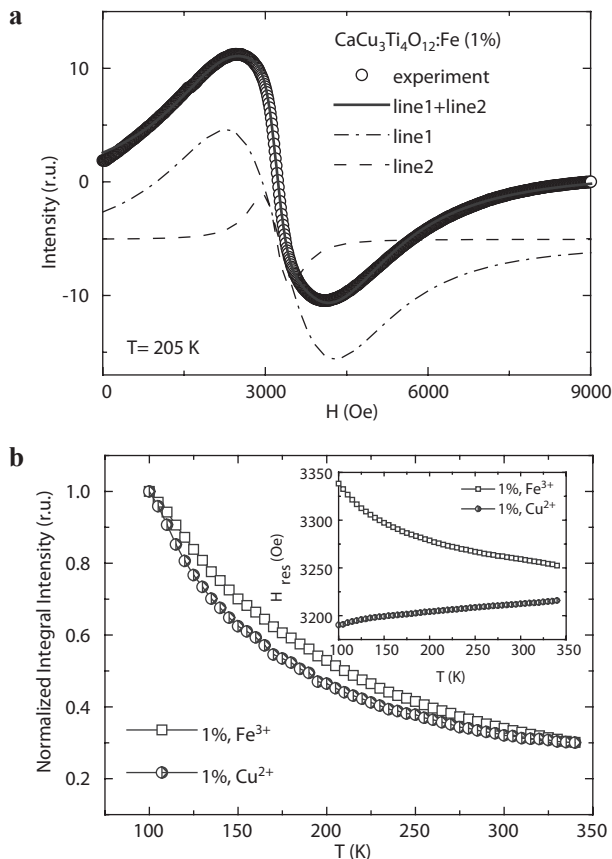


Fig. 1. a ESR spectrum of $\text{CaCu}_3\text{Ti}_4\text{O}_{12}:\text{Fe}$ (1%); **b** temperature dependence of parameters of ESR spectra of $\text{CaCu}_3\text{Ti}_4\text{O}_{12}:\text{Fe}$ (1%).

although the investigations of the dielectric properties of the $\text{CaCu}_3\text{Ti}_4\text{O}_{12}:\text{Fe}$ is presented in the literature, the data about the magnetic properties of these compositions are practically absent. The magnetic resonance investigations are presented only in [1] without the detailed analysis of the electron spin resonance (ESR) lineshape. The investigation $\text{CaCu}_3\text{Ti}_4\text{O}_{12}:\text{Fe}$ by the magnetometry and Mossbauer spectroscopy methods are presented in [2] and [3], respectively. Here we present the investigations of magnetic properties of $\text{CaCu}_3\text{Ti}_4\text{O}_{12}:\text{Fe}$ (1, 3, 7%) solid solutions by the magnetometry, magnetic resonance and Mossbauer spectroscopy methods.

The magnetization measurement showed the all investigated samples are in the paramagnetic state in the temperature range above 25 K, that corresponds to the Neel temperature of the pure $\text{CaCu}_3\text{Ti}_4\text{O}_{12}$. The investigation using the Mossbauer spectroscopy method showed: (i) Fe ions replace Cu, Ca and Ti ions in $\text{CaCu}_3\text{Ti}_4\text{O}_{12}$ crystal structure; (ii) iron ions are in a paramagnetic state and have a valence Fe^{2+} and Fe^{3+} .

ESR spectra of one of the investigated here solid solutions is presented in Fig. 1a. ESR lineshape of all investigated samples was fitted as the sum of two Lorentz lineshape (Fig. 1a). The temperature dependencies of parameters of the ESR spectra were obtained as the result of the fitting in the entire temperature range (Fig. 1b). The temperature dependence of the integral intensity of both components is closed to the paramagnetic Curie-Weiss law. The obtained values of resonance field correspond to g -factors 2.01–2.1, that typical for paramagnetic ions. The physical nature of these lines will be discussed.

1. Brizé V., Autret-Lambert C., Wolfman J. *et al.*: Solid State Sciences **11**, 875 (2009)
2. Grubbs R.K., Venturini E.L., Clem P.G. *et al.*: PRB **72**, 104111 (2005)
3. Pansara P.R., Raval P.Y., Vasoya N.H. *et al.*: Phys.Chem.Chem.Phys. **20**, 1914 (2018)

EPR, Magnetic Susceptibility Measurements, and Quantum-Chemical Calculations of Trinuclear Copper(II) Complexes Embedded in Functionalized Hyperbranched Polymer Boltorn H30

**S. Yurtaeva¹, R. Galeev¹, M. Kutyreva², N. Khafizov², I. Gilmutdinov³,
A. Rodionov³, R. Zaripov¹, O. Kadkin²**

¹ Zavoisky Physical-Technical Institute, FRC Kazan Scientific Center of RAS, Kazan 420029, Russian Federation, s.yurtaeva@kfti.knc.ru

² Butlerov Institute of Chemistry, Kazan Federal University, Kazan 420008, Russian Federation

³ Institute of Physics, Kazan Federal University, Kazan 420008, Russian Federation

Hyperbranched polymers and their functionalized forms can serve as a basis for the fabrication of various organic-inorganic hybrid materials combining the properties of both organic and inorganic constituents. Incorporation of transition metals into dendrimers and highly branched polymer architectures allows one to bring promising electrical, magnetic, optical, sensing, and catalytic properties to this kind of materials. Hyperbranched polymers with “imperfect” structure are more readily available as compared to their “perfect” dendrimer counterparts and exhibit, at the same time, comparable properties despite their random and polydisperse molecular composition. Metal centers in the dendritic environment can also serve as artificial models simulating biological systems, such as the metalloenzymes, thereby making it possible to study various biochemical reactions *in vitro*. Commercial hyperbranched polymers produced under the trademark Boltorn™ (Perstorp Specialty Chemicals AB, Sweden) can be functionalized with fumaric acid residues by the reaction with maleic anhydride. The resulting hyperbranched polymers contain a different number of free carboxyl groups per macromolecule depending on the ratio of reagents and are capable of coordinating transition metals. It was found that the structures and compositions of coordination adducts of the carboxyl-functionalized dendritic oligomer on the basis of third-generation hyperbranched polyester polyol Boltorn H30 are quite sensitive to variation of the degree of functionalization. Depending on the number of monofumaric ester groups per macromolecule, different types of complexes are formed even with the same metal ions. The ESR spectra of the synthesized copper(II) complexes with acid-functionalized Boltorn H30 containing six carboxylic acid groups per macromolecule in average indicated the formation of a trinuclear ferromagnetically-coupled cluster with a ground spin state of $S = 3/2$ in solid samples. The obtained copper(II) triads incorporated in the Boltorn H30 dendritic architecture potentially can mimic active centers of oxydase and oxygenase enzymes. Moreover, exchange-coupled systems are of special interest as magnetic materials for newly developing areas of molecular spintronics and quantum information technologies.

EPR spectroscopy and magnetic susceptibility measurements were performed. The EPR spectra of a powder sample of the synthesized copper(II) complex

demonstrated four resonance lines with different temperature behavior. To confirm the assumption about the ferromagnetically-coupled trinuclear copper(II) clusters, the temperature dependence of the total integrated intensity of the EPR lines was studied. The integrated intensity of the EPR spectrum sharply increases at temperatures below 8–9 K, which is consistent with the assumption of the presence of ferromagnetic exchange interactions in the studied complex. As follows from the temperature dependence of the inverse value of the integrated intensity, the interaction between the Cu(II) ions should be weakly ferromagnetic and the transition of the complex to the quartet ground state with $S = 3/2$ takes place at low temperatures.

To complement the EPR studies and to confirm conclusions made on the basis of the behavior of the EPR at low temperatures, magnetochemical measurements of the powder copper(II) complex were performed. The temperature dependence of the magnetic susceptibility shows that there is some deviation from the Curie-Weiss law below 10 K and indicate the transition to a ferromagnetically ordered state. This result may be explained by the presence of ferromagnetically coupled copper(II) triads, as well as chain structures formed by coordination of copper(II) in polymer species with substantially lower molecular weights in comparison with the hyperbranched polymer globule.

Despite the impossibility of unambiguous determination of the structure of the studied copper(II) complexes by the accessible physicochemical methods, the combination of the quantum-chemical approach and experimental studies of the magnetic properties by the methods of ESR and magnetic susceptibility measurements allowed us to gain insight into the feasible structure of the coordination sites in the synthesized copper(II) complex with functionalized hyperbranched polymer Boltorn H30. The theoretical magnetic curves are in good agreement with the experimental data. It should be noted that the only method to uncover the structure–property relationships in this sort of “vague” systems seems to be to simulate their structure using computational techniques and to analyze their magnetic states at a molecular level using the quantum-chemical methods.

Heterointerfaces Composed of Complex Ferroelectric Oxides

R. Zagidullin¹, I. Piyanzina^{1,2}, D. Tayurskii², R. Mamin^{1,2}

¹Zavoisky Physical-Technical Institute, FRC Kazan Scientific Center of RAS, Kazan 420029, Russian Federation

²Kazan Federal University, Kazan 420008, Russian Federation, i.piyanzina@gmail.com

In 2004 the astounding phenomenon was found at the interface between two nonmagnetic wide-band-gap insulative oxides LaAlO₃ (LAO) and SrTiO₃ (STO) [1]. A two-dimensional electronic system (2DES) is formed in the STO layers next to the interface which becomes superconducting below a temperature of 300 mK [1, 2]. Remarkably, this superconducting state coexists with a magnetic state being stable up to the room temperature. It was concluded, that the primary mechanism responsible for the 2DES formation is the electronic reconstruction followed by structural reconstruction.

Since then 2DES has been later found in other non-magnetic dielectrics. And all of them have in common is that the creation of 2DES is due to either the polar nature of one of components or due to defects or dopants. Latter, it has been shown that 2DES can be created at the interface of nonpolar oxides one of which is ferroelectric [3,4]. The main advantage of using ferroelectrics is a possibility to switch on and off the polarization and thus to control properties of the electron system.

In the present work based on first-principles band structure calculations, we theoretically investigate the interface between a ferroelectric film (KNbO₃, BaTiO₃, LiNbO₃, PbTiO₃) and a nonpolar insulating SrTiO₃ (and MgO) substrate. We demonstrate the possibility of a 2DES formation at the interface. We analyze an impact of ferroelectric polarization onto the 2DES conducting properties, as well as a possibility of switchable and controllable metal-insulator transition in considered types of heterostructures. We present comparative study of different combinations of components containing varying number of ferroelectric overlayers, as well as layer-resolved density of states.

The reported study was funded by RFBR according to the research project № 18-32-00595.

1. Ohtomo A., Hwang H.: Nature **427**, 6973 (2004)
2. Reyren N., Thiel S., Cavaglia A. *et al.*: Science **317**, 5842 (2007)
3. Niranjan M.K., Wang Y., Jaswal S.S., Tsymbal E.Y.: Phys. Rev. L **103**, 016804 (2009)
4. Fredrickson K.D., Demkov A.: Phys. Rev. B **91**, 115126 (2015)

Study of Substituent Rⁱ Influence on Photoisomerization R¹-N=N-R¹ and R²-CH=CH-R³ by UV and 2D NMR Spectroscopy

H. Zuhayri¹, L. G. Gafiyatullin², O. A. Turanova², A. N. Turanov²

¹ Kazan Federal University, Kazan 420008, Russian Federation, zuhayri.hala.1@gmail.com

² Zavoisky Physical-Technical Institute, FRC Kazan Scientific Center of RAS, Kazan 420029, Russian Federation, lingafury@gmail.com

Geometric isomers of molecules have the same chemical structure but differ in configuration. It creates a difference in their physical (melting and/or boiling points, dipole moment, etc.), chemical (reactivity) and biological (antitumor activity) properties. Photoisomerization is an additional channel for controlling the state of such systems. This allows them to be used in medicine and technology.

In this work *cis-trans*-isomerisation of ethylene series compounds with various substituents on unsaturated atoms (4-stilbene, 4-styrylpyridine, 1-(Pyridin-4-yl)-2-(*N*-methylpyrrol-2-yl)ethene) and diazene series compounds (azobenzene) have been studied in acetonitrile solution at room temperature by UV-VIS spectrophotometer Varian Cary 100 and NMR spectrometer Bruker AVANCE-III 700.

An influence of ligand substituents on photoisomerization under irradiation has been shown ($\lambda = 254$ and 365 nm). An unusual kinetics of *cis-trans*-transition for styrylpyridine has been detected.

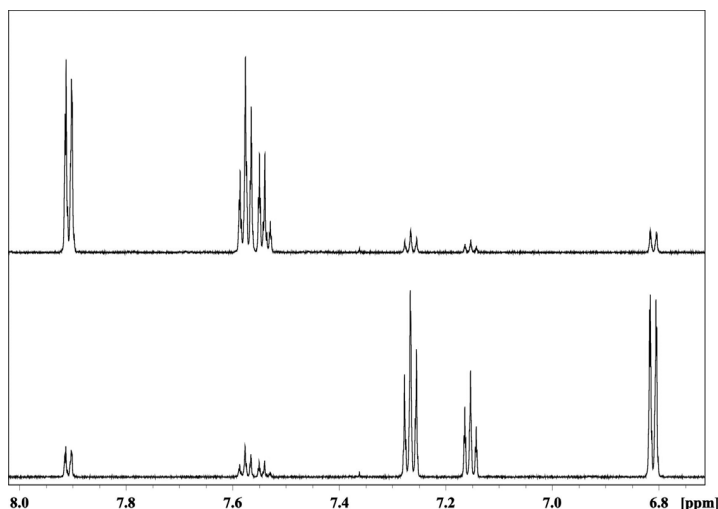


Fig. 1. ¹H NMR spectra of azobenzene before (upper) and after 110 minutes irradiation on 365 nm (bottom).

Influence of Temperature on the EPR Parameters of Electrically Conductive Compounds

A. M. Zyuzin, M. A. Bakulin, N. V. Yantsen, A. V. Ishaev

Mordovia State University, Saransk, 430005, Russian Federation, nkyancen@yandex.ru

Electrically conductive compounds have been increasingly used for the manufacture of shields for high voltage cables, self-regulating heating cables, and earthing conductors resistant to aggressive environments. Therefore, the study of the influence of temperature on the electrically conductive of compounds and the identification of the mechanisms of this influence is of great interest. In this paper, we present the results of studies of the temperature dependences of the EPR parameters of an electrically conductive peroxide-crosslinked compound EPC-35. The matrix of this compound was ethylene vinyl acetate, a filler providing electrical conductivity – carbon black with a mass fraction of about 34%. The EPR spectra were recorded at a frequency of 9.3 GHz on radiospectrometer PS 100X. A single absorption line with a g -factor of approximately equal to 2 was observed in the EPR spectrum.

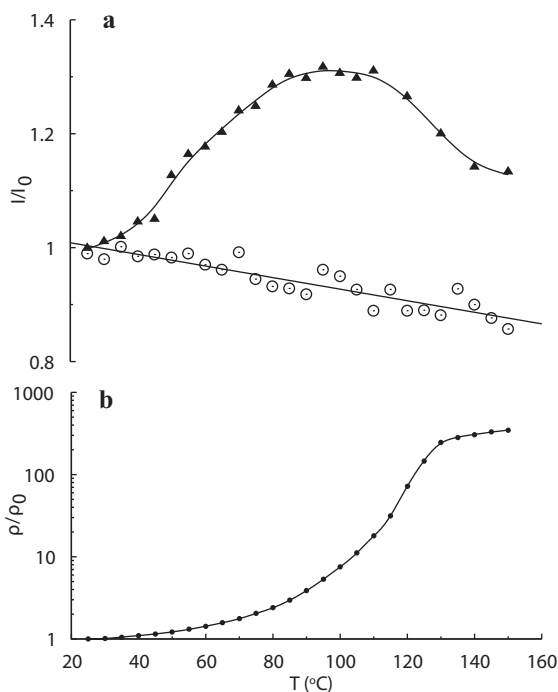


Fig. 1. Temperature dependence of the relative intensity of EPR ((a) triangles – compound, circles – carbon black) and electrical resistivity (b).

Fig. 1a shows the dependences of the intensity of the EPR line (the area under the curve of the absorption line) of an electrically conductive compound and pure technical carbon on temperature. It is seen that with increasing temperature the intensity of the absorption lines of the test compound significantly increases. At the same time, the resonance field and the width of the EPR line remained practically unchanged. Such a temperature dependence of the intensity of the EPR line indicates an increase in the concentration of paramagnetic centers in the sample electrically conductive compound. In the temperature range $\sim 90\text{--}110$ °C, the intensity of the EPR line reaches a maximum, and then its decrease is observed.

The observed dependence of the paramagnetic centers concentration with temperature increase can be explained by the formation of unpaired electrons due to the break of bonds in the conducting chains of carbon black. The chains break occurs due to higher value of the coefficient of thermal expansion of the matrix of ethylene vinyl acetate in comparison with the carbon black particles. The mechanism of formation of unpaired electrons in carbon black particles is described in [1, 2]. The partial destruction of the percolation grid in an electrically conductive compound is confirmed by the temperature dependence of the specific volume electrical resistance (Fig. 1b). It can be seen that this dependence correlates well with the temperature dependence of the intensity of the EPR absorption line.

At the same time, the intensity of the EPR line of pure carbon black used as the filler in the electrically conductive compound EPC-35 decreases smoothly with increasing temperature (Fig. 1a), similar to its behavior in paramagnets. This confirms the conclusion that the observed feature of the temperature dependence of the intensity of the EPR line of the conductive compound is due to the increase in the concentration of paramagnetic centers caused by the above-described mechanism of rupture of conducting chains formed by carbon black particles.

1. Kawamura K., Kimura S.: Bull. Chem. Soc. Jpn. **59**, 2991–2996 (1986)
2. Kashapov N.F., Nefed'ev E.S., Fahrutdinov I.M.: Bulletin of the Kazan Technological University, no. 6, 25–30 (2008)

AUTHOR INDEX

Abdullin, T. I.	116
Abe, S.	168
Abramov, N. N.	89
Adachi, T.	48
Afanasyev, D.	141, 142
Agafonnikova, A. G.	111
Aganov, A.	96
Akhmedzhanov, R. A.	20
Akhmetov, M. M.	102
Alakshin, E. M.	104, 158
Alfonsov, A.	140
Aliyev, M. N.	139
Alshits, V. I.	105
Aminov, L. K.	107
Andrianov, V. V.	131, 191
Anishchik, S. V.	75, 109
Anisimov, N. V.	111
Anisimov, A. N.	94
Anisimova, E.	113
Antipin, I. S.	171
Antonov, D.	34
Astakhov, G. V.	94
Azev, Y. A.	156
Babunts, R. A.	56
Badalyan, A. G.	56
Bagryantsev, D. G.	109
Bakirov, M. M.	53, 114, 118, 129
Bakulin, M. A.	199
Bales, B.	53, 114
Baranov, P. G.	56, 94
Bayazitov, A. A.	115
Beloborodov, I. S.	63
Bertaina, S.	45
Blokhin, D. S.	116
Bochkin, G.	26
Bogach, A. V.	4
Bogachev, Yu. V.	166

Bogaychuk, A. V.	158
Bogodvid, T. Kh.	131
Bolginov, V. V.	89
Borovkov, V. I.	109
Bowman, M. K.	33
Britt, R. D.	2, 52
Broderick, T.	27
Büchner, B.	45, 46, 86, 140
Bukharaev, A.	151
Bunkov, Yu. M.	67
Cherepanov, D. A.	31
Cherepnev, G. V.	119
Chirkov, V. V.	118
Chumakova, N. A.	97
Chupakhina, T. I.	135, 193
Chushnikov, A. I.	119
Croitori, D.	153
Danilova, A. G.	121
Darinskaya, E. V.	105
Dasari, D. B. R.	80
Deeva, J. A.	135, 193
Demidov, E. S.	63
Deminov, R. G.	130
Demishev, S. V.	4, 50, 122, 124, 174, 179
Denisenko, A.	80
Denisov, A. A.	131
Dietsche, W.	61
Dikanov, S. A.	6
Domracheva, N.	189
Dosina, M. O.	131
Dvinskikh, S. V.	42
Dyakonov, V.	94
Dzheparov, F. S.	54
Earle, K. A.	27
Eremina, R. M.	21, 135, 193
Ermakova, E. A.	146
Ermakova, O. S.	156
Ermolaeva, O. L.	63
Ezhikova, M. A.	156
Fakhrutdinov, A. R.	115
Falin, M. L.	125
Fattakhov, Ya. V.	115
Fel'dman, E.	26
Filipov, V. B.	4, 50, 122, 124, 179
Filipova, I.	153

Fine, B. V.	28
Fourmigué, M.	45
Fowler, B.	33
Fraerman, A. A.	63
Frolov, D. D.	61
Frolova, E.	127, 188
Gafarova, A. R.	128, 129
Gafiyatullin, L.	127, 187, 188, 198
Gafurov, D.	113
Gafurov, M. R.	79, 171, 183
Gaifullin, R. R.	130
Gainutdinov, Kh. L.	131, 191
Galeev, R. T.	53, 114, 195
Galeski, S.	58
Galiullina, L.	96
Galyametdinov, Yu. G.	173
Garifullin, R.	116
Garifyanov, N.	69
Gavrilova, T. P.	135, 193, 153
Gerasimova, L.	137
Gescheidt, G.	66
Gilmanov, M. I.	4, 50, 122, 124, 174, 179
Gilmutdinov, I.	135, 195, 193
Gimazov, I.	48
Gizatullin, B.	79
Glazkov, V.	58
Glushkov, V. V.	4, 122, 124
Goenko, I. A.	128, 129
Golbeck, J. H.	31
Golovchanskiy, I. A.	89
Golubeva, E. N.	97
Golubov, A. A.	89, 130
Gorev, R.	62
Gorka, M.	31
Goryunov, Yu. V.	133
Grafe, H.-J.	46, 86, 140
Griesinger, Ch.	14
Gruzdev, M.	189
Gulko, A. D.	54
Gumarov, A. I.	139
Gumarov, G. G.	102, 118, 128, 129
Günther, A.	153
Gurzadyan, G.	186
Gusev, N. S.	63
Gusev, S. A.	63

Gushchin, L. A.	20
Hagiwara, M.	9
Hara, S.	9
Heuveling, J.	38
Hiroi, Z.	9
Huster, D.	96
Iakovleva, M.	46, 140
Ibragimova, M. I.	119
Ibrayev, N.	141, 142
Ikeda, S.	9
Isaev, N.	38
Ishaev, A. V.	199
Iskhakova, K.	144
Ivanisenko, N.	38
Ivanov, D.	145
Ivanov, K. L.	17, 32, 75
Ivanova, A. V.	146
Ivanova, T.	187
Iyudin, V. S.	131, 191
Jeannin, O.	45
Kabanov, V. V.	44
Kabirov, Y.	135
Kadkin, O.	195
Kalachev, A. A.	8
Kamashev, A.	148
Kandrashkin, Yu. E.	149
Kasper, C.	94
Kataev, V.	45, 46, 86, 140
Khabipov, R. Sh.	115
Khafizov, N.	195
Khaibullin, R. I.	139
Khairutdinov, B. I.	121, 146, 184
Khairuzhdinov, I. T.	53, 114, 150, 177
Khaliulin, B. M.	139
Khaliullin, G.	11
Khanipov, T.	151
Khasanov, R.	69
Khundiryakov, V. E.	115
Kiiamov, A. G.	153, 154, 168
Kimura, F.	9
Kimura, T.	9
Kiryutin, A. S.	17, 32
Kitahara, Y.	9
Kiyamov, A.	69
Klochkov, A. V.	104, 158

Klochkov, V. V.	96, 116
Kodess, M. I.	156
Koldaeva, M. V.	105
Komarovskikh, A.	23
Kondratyeva, E. I.	104, 158
Konov, K. B.	21
Konovalov, A. I.	171
Korableva, S. L.	168
Korotkevich, A. A.	97
Kovaleva, E.	34
Krasnikova, Y.	58
Krug von Nidda, H.-A.	153
Krupskaya, Y.	86
Kukovitsky, E.	69, 161
Kukushkin, I. V.	61
Kulchitchky, V. A.	131
Kupriyanov, M. Yu.	130
Kupriyanova, G. S.	87, 162
Kupriyanov, I.	23
Kurashov, V.	31
Kurkin, I. N.	107
Kushnir, V. N.	130
Kusova, A. M.	160
Kusrayev, Yu. G.	15
Kutovoi, S. A.	21
Kutyreva, M.	195
Kuzin, S. V.	97
Kuzmin, V. V.	104, 158
Latypov, V. A.	125
Lazarev, I.	26
Lecaroz, J. A.	33
Leushin, A. M.	125
Li, X.	186
Likerov, R. F.	21
Likhtenshtein, G.	30
Lockart, M.	33
Loidl, A.	153, 154
Lovchev, A. V.	107
Lubitz, W.	12
Lvov, D. V.	54
Lvov, S.	161
Lyadov, N.	135
Mamadazizov, S.	87, 162
Mamin, G. V.	79, 171, 183
Mamin, R.	148, 197

Mannig, A.	60
Maraşlı, A.	87
Maryasov, A. G.	33, 73
Materka, D.	164
Matsumoto, K.	168
Mattea, C.	79
Matveeva, A. G.	33, 73
Melnikov, A. R.	109
Melnikova, D. L.	165
Meriles, C. A.	80
Milanovsky, G. E.	31
Milordova, E.	187, 188
Mingalieva, L.	127, 187, 188
Mironov, S. V.	84
Mironov, V.	62
Möbius, K.	7
Möller, A.	46, 86
Molochnikov, L.	34
Morozova, O.	17
Mozzhukhin, G. V.	85, 87
Musabirova, G.	96
Nadolinny, V.	23
Nalbandyan, V.	46, 113, 178
Nateprov, A. N.	133
Nath, R.	140
Nawa, K.	9
Nefyodov, Yu. A.	61
Nekrasov, V. M.	73
Nesmelova, I. V.	165
Neumann, P.	80
Nikitina, A. V.	166
Nizamutdinov, A. S.	182
Nizov, N. A.	20
Nizov, V. A.	20
Nurgazizov, N.	151
Nurmakhanova, A.	142
Nuzhdin, V. I.	139
Nuzhina, D. S.	168
Ohta, H.	9
Okamoto, Y.	9
Okubo, S.	9
Olszewski, M.	164
Orlinskii, S. B.	79, 171, 182, 183
Ovchinnikov, I.	127, 187, 188
Ovsyannikov, A. S.	171

Palyanov, Y.	23
Pashkevich, S. G.	131
Pavlov, D.	148
Petrzhik, E. A.	105
Petukhov, V. Yu.	102, 118, 119, 129
Pilone, O.	45
Piyanzina, I.	148, 197
Pomomaryov, A.	58
Poshakinskiy, A. V.	94
Povarov, K. Yu.	58, 60
Ptushenko, V. V.	170
Raganyan, G.	113
Rakhmatullin, R. M.	107
Rameev, B. Z.	85, 87
Razina, E. A.	171
Reichl, C.	61
Reuter, R.	80
Rodin, B. A.	32
Rodionov, A. A.	79, 139, 182, 195
Rogov, A. M.	180
Rogov, V. V.	63
Romanov, N. G.	56
Romanova, I. V.	168
Ryazanov, V. V.	89
Safiullin, G. M.	125
Safiullin, K. R.	104
Sagdeev, D. O.	173
Sagdeev, R. Z.	17
Sakhin, V.	69
Sakurai, T.	9
Sakurai, Y.	9
Salikhov, K. M.	53, 114, 150, 176, 177
Salikhov, T.	46, 178
Samarin, A. N.	4, 122, 124, 174
Samarin, N. A.	4
Samoilova, R. I.	37
Sapozhnikov, M.	62
Savinkov, A. V.	104
Saxena, S. K.	72
Schäpers, M.	86
Scheidt, H. A.	96
Schmidiger, D.	58
Schneider, E.	38
Scirda, V.	145
Seidov, Z.	153

Semakin, A. C.	168
Semashko, V. V.	182
Semeno, A. V.	4, 50, 122, 124, 174, 179
Semenov, A. Yu.	31
Sevastyanov, D. A.	146
Shabakaev, Sh. M.	180
Shagalov, V. A.	115
Shagieva, F.	80
Shaginyan, V. R.	47
Shaikhutdinov, I. I.	191
Shakirov, A. A.	125, 182
Shamilov, R. R.	173
Shavelev, A. A.	125, 182
Shchepetilnikov, A. V.	61
Sheberstov, K. F.	32
Shitsevalova, N. Yu.	50, 4, 122, 124, 179
Shurpik, D. N.	146, 184
Shurtakova, D. V.	183
Shustov, V.	187
Sinicin, A. M.	92
Sitnitsky, A. E.	160
Skirda, V. D.	165
Skorokhodov, E.	62
Skourski, Y.	140
Skvortsova, P.	184
Sluchanko, N. E.	50, 4, 122, 124 179,
Smirnov, A. I.	60
Sobgayda, D. A.	20
Soldatov, T. A.	60
Solovieva, S. E.	171
Soltamov, V.	94
Sorokina, A.	144
Stanislavovas, A. A.	104
Stapf, S.	79
Starshova, A.	144
Steinhoff, H.-J.	38
Stöhr, R.	80
Stoykov, I. I.	146, 184
Stolyarov, V. S.	89
Stukach, Y. P.	131
Sukhanov, A. A.	149, 173, 186, 185, 190
Tagirov, L. R.	130, 139, 153, 154, 151
Tagirov, M. S.	104, 158, 168, 171
Talanov, Yu.	48, 69
Tambasova, D.	34

Tang, B. G.	186
Tarapov, S.	85
Tarasenko, S. A.	94
Tarasov, V. F.	21, 149
Tatarsky, D. A.	63
Tayurskii, D.	148, 154, 197
Teitel'baum, G.	69
Tiemann, L.	61
Tormyshev, V. M.	33
Tsurkan, V.	153, 154
Turanov, A. N.	121, 146, 127, 188, 198
Turanova, O. A.	127, 187, 188, 198
Tyulyusov, A. N.	54
Tyurin, V. S.	185
Ubukata, K.	168
Udalov, O. G.	63
Ulanov, V. A.	92
Useinov, N.	137
Ustinov, A. V.	89
Ünal, İ.	85
Vagizov, F. G.	153, 154, 193
Vakhitov, I. R.	139
Vasil'ev, S.	26
Vasiliev, A.	46, 113, 178
Vavilova, E.	46, 86, 113, 140, 178
Vdovichev, S. N.	63
Veziñ, H.	45
Vieth, H.-M.	17
Vins, V. G.	109
Volkov, M. Yu.	102, 127, 188
Volkov, V. I.	26, 82
Vorobyeva, V.	189
Voronkova, V. K.	173, 185, 186, 190
Wang, Zh.	186
Wegscheider, W.	61
Wolter, A. U. B.	86
Wrachtrup, J.	80
Wulf, E.	60
Xu, K.	190
Yafarova, G. G.	131, 191
Yagfarova, A.	135, 193
Yang, W.	186
Yanilkin, I. V.	139, 180
Yantsen, N. V.	199
Yatsyk, I.V.	21, 92, 119, 135, 193

Yelisseyev, A. P.	109
Yoshizawa, D.	9
Yurkovskaya, A. V.	17, 32
Yurtaeva, S.	98, 195
Yusupov, R. V.	139, 180
Zagidullin, R.	148, 197
Zagitova, A.	151
Zainullin, R. R.	92
Zaiser, S.	80
Zaripov, R. B.	129, 150, 195
Zavartsev, Y. D.	21
Zeisner, J.	45
Zelensky, I. V.	20
Zhao, J.	186, 190
Zheludev, A.	58, 60
Zhong, F.	186
Zinnatullin, A. L.	193
Zuev, Yu. F.	121, 146, 160, 184
Zueva, E.	189
Zuhayri, H.	198
Zverev, D. G.	182
Zvereva, E.	46, 113, 178
Zvyagin, S.	58
Zyuzin, A. M.	199

© Федеральное государственное бюджетное учреждение науки
Казанский физико-технический институт имени Е. К. Завойского
ФИЦ КазНЦ РАН, 2018

Ответственный редактор: В. К. Воронкова; редакторы С. М. Ахмин, Л. В. Мосина; технический редактор
О. Б. Яндуганова. Издательство КФТИ КазНЦ РАН,
420029, Казань, Сибирский тракт, 10/7, лицензия № 0325 от 07.12.2000.

Отпечатано с оригиналов заказчика

АО "Информационно-издательский центр" · Казань, ул. Чехова 28, телефон +7 (843) 236 94 26



BENCH-TOP RESEARCH GRADE ELECTRON PARAMAGNETIC RESONANCE SPECTROMETER

SPINSCAN

Benefits

- ▶ Cavity Q-factor and MW power measurement
- ▶ Magnetic field modulation – 10 kHz-250 kHz
- ▶ Phase detection range – 0-360°
- ▶ First and second harmonics detection (in phase and out of phase)
- ▶ Amplitude resolution - 24 bit
- ▶ Broad signal channel dynamic range - digitization up to 140 dB per one scan
- ▶ High magnetic field resolution - up to 256 000 pts for any sweep range
- ▶ 2D, 3D - experiments (time, temperature, MW power, ampl. modulation vs magnetic field).
- ▶ Interface via Ethernet
- ▶ ADANI e-SPINOZA software - the new comprehensive user-focused software kit for data acquisition and processing
- ▶ Time- resolved EPR studies of radicals with pulsed laser, magnetic field, MW power triggering (time resolution – 2 μs; sample rate from 1 Hz)
- ▶ New ergonomic design

Sensitivity	8×10^{13} spins/T
Resolution	0,005 mT
Maximum magnetic field	0,7T
Sweep width	10^{-4} - 0,65 T
Operating Frequency	X-band
Microwave power	0,01 - 200mW

Microwave tuning	Automatic
Cavity	TE ₁₀₂
Q unloaded	5000
Amplitude resolution	24 bit
Dimensions	470 x 380 x 260 mm
Weight	45 kg

ADANI



<http://lab.adanisystems.com>
e-mail: info@adanisystems.com



